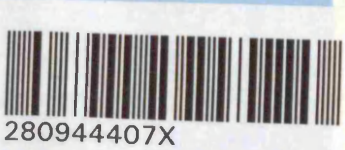

UNIVERSITY OF LONDON THESIS

Degree MD Year 2007 Name of Author DUNCAN RICHARD CASTELL SPALDING

An Investigation of Chemoresistance of Liver Cancers using the Comet Assay and Isolated Organ Perfusion Systems

DUNCAN RICHARD CASTELL SPALDING

BSc (Hons) FRCS (Eng) FRCS (Gen Surg)

Presented for the Degree of

MD

UNIVERSITY OF LONDON

2006

ProQuest LLC
789 East Eisenhower Parkway
P.O. Box 1346
Ann Arbor, MI 48106-1346

Abstract

Current approaches to selecting new chemotherapies are inadequate. *In vitro* tissue culture models ignore the tumour microenviroment whilst murine models do not mimic human cancers. The aim of this thesis was to develop an isolated, perfused and oxygenated human liver tumour model to investigate the short term effects of chemotherapeutic agents used in the treatment of liver cancer.

Expression of drug resistance transporter proteins was evaluated in hepatocellular carcinoma (HCC) and colorectal carcinoma (CRC) cell lines and did not correlate with drug resistance. P-glycoprotein (P-gp), when present, failed to demonstrate significant function. The comet assay demonstrated tumour DNA damage with chemotherapy and DNA-adduct repair with cisplatin.

An orthotopic model of human liver cancer in nude mice evaluated the topographic distribution of cisplatin DNA-adducts by the comet assay *in vivo*. This was correlated with the presence of tumour proliferation, hypoxia, vascularity and P-gp expression determined by immunohistochemistry. Rates of repair of DNA-adducts were both quantitatively and qualitatively different from *in vitro* data, and superficial tumour cells were more efficient at repair in comparison with deep cells.

An isolated, dual perfused liver cancer model was then developed in both the rat and human. In both models livers remained viable whilst on the perfusion circuit. Differences were observed in the timing of maximal DNA damage between drugs,

and DNA damage was dose dependent. Chemotherapy induced greater tumour DNA damage in superficial as compared to deep portions of the cancers.

This thesis has investigated the chemoresistance of liver cancers and developed a unique methodology for investigating human liver cancers using an *ex vivo* perfusion model. New insight into early DNA damage with chemotherapy has been demonstrated but more importantly the scientific basis established for a new approach to refining conventional therapies or evaluating new biological cancer therapies.

Statement of Originality

This thesis represents entirely my own original work and has not been submitted elsewhere for a degree.

Acknowledgements

I am most grateful to my supervisor Professor Brian Davidson at the Department of Surgery of the Royal Free Hospital and University College School of Medicine, who inspired this work and provided encouragement throughout. I owe him a great deal for his endless enthusiasm and energy, in particular his detailed discussions of experimental designs and results, and constructive criticism have been invaluable.

I am also indebted to Dr Daniel Hochhauser at the Department of Oncology of the Royal Free Hospital and University College School of Medicine, whose knowledge and limitless suggestions on how to interpret and expand the current work was an inspiration.

I would like to thank Professor John Hartley at the CRC Drug-DNA Interactions Research Group, who not only gave me valuable advice concerning the comet assay but also allowed me to perform the majority of this work in his laboratories. I am particularly grateful to his colleagues Janet Hartley and Victoria Spanswick for their generosity and patience in advising me on how to perform the laboratory work.

Dr Kanagasabai Ganeshaguru at the Department of Haematology of the Royal Free Hospital and University College School of Medicine gave an enormous amount of help regarding flow cytometry and western blotting, and was kind enough to allow me to perform this work in his laboratory.

Dr Barry Fuller and Dr Alex Seifalian at the Department of Surgery of the Royal Free Hospital and University College School of Medicine gave me a great deal of advice about isolated organ perfusion systems. Dr Richard Hodgkiss at the Gray Laboratory of the Cancer Research Campaign kindly donated the hypoxic probe NITP and provided help concerning its immunohistochemistry. Finally, Mahrokh Nohadani at the Department of Pathology of the Hammersmith Hospital gave me a large amount of help, advice and support in performing the immunohistochemistry in this work.

I would also like to thank the many other people, too numerous to mention, who at some stage have provided either advice or support. The number of names and Departments mentioned above reflects the enormous amount of co-operation, collaboration and generosity of spirit encountered during this work, all of which has made it extremely rewarding.

Contents

List of Figures

Chapter I

Chapter II

Chapter III

Chapter IV

Chapter V

Chapter VI

Chapter VII

Chapter VIII

Chapter IX

List of Tables

Chapter I

Chapter III

Chapter IV

Chapter V

Chapter VI

Chapter VII

Chapter VIII

Chapter IX

Abbreviations

5-FdUMP	5-fluorodeoxyuridine monophosphate
5-FdUTP	5- fluorodeoxyuridine triphosphate
5-FU	5-Fluorouracil
5-FUTP	5-fluorouridine triphosphate
ABC	ATP-binding cassette
AML	Acute myeloid leukaemia
AFB1	Aflatoxin B_1
ALT	Alanine aminotransferase
ANOVA	Analysis of variance
APC	Adenomatous polyposis coli
at-MDR	Atypical multidrug resistance
ATP	Adenosine triphosphate
BSO	DL-buthionine-(S,R)-sulfoxamine
CBU	Comparative Biology Unit
CEA	Carcinomoembryonic antigen
CRC	Colorectal cancer
CS	Cockayne's syndrome
CV	Coefficients of variation
$DiOC_2$	3,3'-diethyloxacarbocyanine iodide
Ds	Double strand
DTNB	5,5'-dithiobis-(2-nitrobenzoic acid)
ECM	Extracellular matrix
ERCC	Excision repair cross-complementing

FAP	Familial Adenomatous Polyposis
FACScan	Fluorescence-activated cell scanner
FCS	Foetal calf serum
FNA	Fine needle aspiration
FUDR	5-fluoro-2'deoxyuridine
GAG	Glycosaminoglycans
γ-GCS	γ-glutamylcysteine synthase
GDA	Gastroduodenal artery
GSH	Glutathione
GST	Glutathione S-transferase
HA	Hepatic artery
HBV	Hepatitis B virus
HCV	Hepatitis C virus
HCC	Hepatocellular carcinoma
HN_2	Mechlorethamine
HNPCC	Hereditary Non-Polyposis Colorectal Cancer
HMSH	human Mut S Homolog
IA	Intra-arterial
IC_{50}	Concentration of drug required to inhibit growth by 50%
ICL	Interstrand crosslinks
IDPRL	Isolated dual-perfused rat liver
IFN	Interferon
IL-2	Interleukin-2
i.p.	Intraperitoneal
IPRL	Isolated perfused rat liver

i.v.	Intravenously
LAK	Lymphokine-activated killer
LDF	Laser doppler flowmetry
LI	Labelling index
LRP	Lung resistance related protein
LTC_4	Leukotriene C_4
LV	Leucovorin
LVRT	Liver volume replaced by tumour
MA	Microwave ablation
MAb	Monoclonal antibody
MDR	Multidrug resistant phenotype
MEM	Minimum Essential Medium
MFI	Mean Fluorescence Index
MOAT	Multi-specific organic anion transporter
MRP	Multidrug resistance associated protein
MS	Median survival
MTX	Methotrexate
NER	Nucleotide excision repair
NITP	7-(4'-(2-nitroimidazol-1-yl)-theophylline
OLT	Orthotopic liver transplantation
OS	Overall survival
PBS	Phosphate-buffered saline
PCNA	Proliferating cell nuclear antigen
PFS	Progression free survival
P-gp	P-glycoprotein

Pt	Platinum
PV	Portal vein
PVI	Protracted venous infusion
RFA	Radiofrequency ablation
RF-C	Replication factor C
Rh 123	Rhodamine 123
RPA	Replication protein A
RR	Response rates
s.c.	Subcutaneous
SD	Standard deviation
Ss	Single strand
SRB	Sulforhodamine B
TACE	Transcatheter arterial chemoembolisation
TFIIH	Transcription factor IIH
TM	Tail moment
TNF	Tumour Necrosis Factor
Topo	Topoisomerase
TS	Thymidylate synthase
TTD	Trichothiodystrophy
VD	Vascular density
Vpm	Verapamil
XP	Xeroderma pigmentosum

CHAPTER I

INTRODUCTION

I. INTRODUCTION

1.1 Colorectal cancer (CRC) hepatic metastases

1.1.1 Incidence of colorectal cancer

In industrialised countries, colorectal cancer (CRC) is the third most common malignancy after lung and prostate cancer in men, and breast cancer in women. In Europe there were approximately 170,000 new cases in 1990 and over 90,000 deaths due to the disease (Esteve et al, 1993). It is a disease predominantly of older people, though it may occur at any age. Less than 5% of patients are under the age of 40 and more than half are over the age of 60, with a peak incidence between 70-80 years of age. There is no noticeable sex difference. High rates of CRC are characteristic of North America, the UK, New Zealand and Northern and Western Europe (Vogel and McPherson, 1989). The age standardised annual incidence rates in these countries are 10-32 per 100,000 population. The lowest rates are found in Asia, Latin America and Africa (< 10 per 100,000 annually), although regional differences in CRC incidence occur within each country.

Surgery is currently the first line treatment for CRC, although surgical cure is not possible in approximately 40% of patients owing to advanced stages of the disease (Gordon et al, 1993). If diagnosed at an early stage, CRC has an excellent prognosis following surgical resection. The 5-year survival rate for patients with tumours involving only the mucosa or submucosa is in excess of 90% (Cohen et al, 1993). For more advanced stages, adjuvant chemotherapy following curative resection has been shown to improve survival rates in patients with Dukes B_2 or C disease. Five-year survival rates of 89% and 65-69% respectively have been reported (Anonymous, 1995a; Francini et al, 1994; Moertel et al, 1995). Following potentially curative

surgery, 10-25% of patients subsequently develop local recurrence. Although recurrent disease can often be resected, ultimately dissemination of disease makes cure impossible.

The liver is the first organ reached by venous blood draining from the gastrointestinal tract and hence cancer cells via haematogenous spread have a high likelihood of lodging within the liver sinusoids. In one series of 1314 patients with advanced colon carcinoma, 77% had hepatic metastases (Bengtsson et al, 1981). In addition, at laparotomy for primary colon resection, 25% of patients demonstrate synchronous liver metastases (Bengmark and Hafstrom, 1969), and 20-30% develop metachronous liver metastases on follow up (Huylesk et al, 1989; Niederhuber and Ensminger, 1983).

1.1.2 Pathogenesis of CRC

Most CRC's develop through the sequence from normal colonic epithelium, to hyperplasia, to small adenoma, to intermediate adenoma, to dysplastic adenoma on to a carcinoma in situ (Bresailer and Kim, 1993). Adenomas are classified by histological architecture as tubular, tubulovillous and villous. Villous change is associated with a higher malignant potential, as are large adenomas (25% are > 1 cm in diameter) and high-grade epithelial dysplasia (severe dysplasia is found in 5-10% of adenomatous polyps). About 5% of adenomatous polyps are estimated to become malignant usually over a 5-10 year time course.

Relative risk factors of CRC include environmental factors, such as a diet low in fibre, folate and vegetables and high in alcohol, fat and red meat. A sedentary occupation

and cigarette smoking are also associated. The recognition of the genetic component of CRC continues to grow. There are two main inherited predisposition syndromes: Familial Adenomatous Polyposis (FAP) and Hereditary Non-Polyposis Colorectal Cancer (HNPCC), whilst the remaining cases are the result of sporadic colorectal cancer.

1.1.2.1 Familial Adenomatous Polyposis (FAP)

FAP is an autosomal dominant disorder in which multiple adenomatous polyps develop in the colon during the second and third decades of life. Individually each polyp has little risk of malignant transformation. However, the numbers are so great that the risk of CRC is almost 100% by 40 years of age (Cawkwell and Quirke, 1996). The gene that causes FAP (the adenomatous polyposis coli [*APC*] gene) encodes a 300 kDa cytoplasmic protein and most of the mutations seen, result via loss of expression or truncation of the protein. Although the precise function of the wild-type *APC* gene product has yet to be characterised it does bind to β-catenin, which in turn binds cadherins and suggests a role in cell to cell interactions, adhesion and metastasis (Kemler, 1993). Clinical studies have also been done of phenotypes of specific mutations. Families that do not demonstrate congenital hypertrophy of the retinal pigment as a clinical marker of FAP, have a mutation 5* to exon 9 of the *APC* gene (Olschwang et al, 1993). Less severe forms of FAP are associated with mutations of the extreme ends of the gene. By contrast, profuse FAP has been localised to exon 15, codons 1255-1467 (Nagase et al, 1992).

1.1.2.2 Hereditary Non-Polyposis Colorectal Cancer (HNPCC)

HNPCC is also an autosomal dominant disorder, which accounts for up to 6% of CRC cases. It is associated with other tumours including endometrium, ovary and hepatobiliary tract, usually involving the right side of the colon and produces poorly differentiated mucinous tumours, which are invasive. The gene responsible for 60% of HNPCC cases is human Mut S Homolog (*hMSH*$_2$) (Fishel et al, 1993). The other genes that have been identified are *hMLH1* (3p), *hPMS1* (2q) and *hPMS2* (7p) which account for 30%, 5% and 5% of cases respectively (Bronner et al, 1994; Nicolaides et al, 1994). All these genes encode enzymes involved in DNA surveillance; if any are defective, mismatched bases in replication are not repaired and genome-wide mutations follow.

Mutated mismatch repair genes produce microsatellite instability, short-repeat DNA sequences that are susceptible to mispairing during replication, which creates DNA loops. Normally these loops are repaired, with dysfunctional repair genes, however, they are undetected and new alleles occur. Evidence suggests that mismatch repair deficits cause cancer by inhibition of growth of colonic epithelium by the tumour growth factor β family and direct induction of apoptotic cell death, with the tumour growth factor β receptor (RII) acting as a tumour-suppressor gene in colon cells. Inactivation of RII mutations is present in more than 90% of patients with microsatellite instability (Grady et al, 1997).

1.1.2.3 Sporadic CRC

A multistep model for the genetic events in the progression of sporadic CRC has been proposed (Vogelstein et al, 1988). CRC occurs mainly in the elderly, which is

consistent with the theory that a cell must accumulate a combination of 4 or 5 defects, involving mutational activation of oncogenes and inactivation of tumour suppressor genes, to undergo full malignant transformation. If one or more of these defects are present at birth, fewer further mutations are required to complete transformation and CRC appears earlier. The most studied genetic changes in sporadic CRC are shown in Table 1.1.

1.1.3 Natural history of CRC metastases

Reported survival with untreated liver metastases from CRC varies. Most patients die within 2 years of diagnosis, Palmer and colleagues (Palmer et al, 1989) reported a mean survival of 12 months in untreated patients, whereas other groups have shown a median survival of only 4.5 months in patients discovered to have synchronous liver metastases at the time of primary surgery (Moertel and Reitemeyar, 1969). An analysis of 484 untreated patients by Stangl et al (Stangl et al, 1994), showed a median survival of 7.5 months from time of diagnosis. Six factors proved to be independently significant for survival. (i) Percentage liver volume replaced by tumour (LVRT), was the most important single factor (< 25% confirmed a clear outcome advantage and all patients with a LVRT of > 25% died within 3 years); (ii) the number of metastases, and unilateral versus bilateral distribution of metastases exerted a highly significant influence on survival; followed by (iii) grade of primary tumour; (iv) presence of extrahepatic disease and mesenteric lymph node involvement; (v) carcinomoembryonic antigen (CEA) (< 39) and (vi) age (< 59).

Genetic modification	Position	Frequency	Molecular function	Postulated stage in adenoma to carcinoma sequence
Oncogenes				
K-Ras	Chromosome 12	40%	Mutant ras-p21 is stable in active signal transmitting state, allowing cell proliferation and loss of adhesion	Intermediate, small to large adenoma
MYC		Low	Induces cell proliferation	N/K
Tumour-suppressor genes				
APC	Chromosome 5	>60%	Mutant protein binds Wt, causing loss of adhesion and possible transformation	Early adenoma formation
MCC (mutated in CRC)	Chromosome 5	60%	N/K	N/K
p53	Chromosome 17	75%	Mutation prevents apoptosis and GI arrest (disallowing DNA repair)	Late, adenoma to carcinoma
DCC (deleted in CRC)	Chromosome 18	30%	Loss of WT causes loss of normal adhesion	Intermediate, small to large adenoma and adenoma to carcinoma
NF1 GAP	Chromosome 17	14%	Loss of WT allows increase in the active GTP-bound ras-p21	Intermediate
Metastasis genes				
NM23		Low	N/K	Very late, metastases
Hypomethylation	Across genome	N/K	Allows overexpression of oncogenes	Early, adenoma formation

Table 1.1. Most commonly studied genetic changes in sporadic colorectal cancer. N/K = not known; WT = wild-type; GI = gastrointestinal; CRC = colorectal cancer.

1.1.4 Treatment of CRC hepatic metastases

1.1.4.1 Surgical resection

Surgical resection for isolated hepatic metastases from CRC has gained acceptance as a safe and potentially curative treatment. Several studies have demonstrated that resection of as much of 80% of the liver can be performed with an associated surgical mortality rate of < 5% (Gayowski et al, 1994; Scheele et al, 1995). Reported 5-year survival rates after curative resection of hepatic metastases range from 25 to 35% (Fong et al, 1997; Gayowski et al, 1994; Rosen et al, 1992; Scheele et al, 1995), and a further 10% survive between 5 and 9 years, despite relapse with irresectable cancer, thereby indicating substantial palliation (Scheele et al, 1990). Approximately 50% of all patients with CRC present at some stage with hepatic metastases, and around 20-25% eventually become candidates for liver resection. Thus only a small fraction (< 12.5%) of all patients with CRC may benefit from surgical resection. Advances in imaging and surgical techniques now permit earlier detection of metastases and improved perioperative survival. Current data confirm a multifactorial determinant of long term outcome following hepatic resection, including patient demographics, primary tumour factors, presentation of metastatic disease and surgical findings.

1.1.4.1.1 Patient demographics

It is clear from many reports that age has no impact on survival (Cady et al, 1992; Fong et al, 1999). Gender has had a prognostic importance in only one study by Holm et al (Holm et al, 1989), who found a significant survival advantage for women undergoing liver resection compared with men.

1.1.4.1.2 Primary tumour characteristics

The site of the primary CRC does not seem to have prognostic significance (Cady et al, 1998; Fong et al, 1999). Tumour grade (ploidy or differentiation) has been shown to be a statistically significant prognostic indicator (Cady et al, 1992), although a subsequent study conflicted with this observation (Cady et al, 1998). However, it was suggested that the small sample size in the original study accounted for the discrepancy. Other authors have also shown no prognostic predictive value (Fong et al, 1999; McEntee et al, 1992). The predictive value of Dukes staging has been conflicting. Dukes B colon cancer has been shown to have significantly better 5-year survival rates (35%), compared to patients with Dukes C colon cancer (28%) (Hughes et al, 1989). These findings have also been reported by other groups' (Adson and van Heerden, 1980; Finan et al, 1985; Fong et al, 1999; Hughes et al, 1989). In contrast, many other studies have found no correlation between the stage of the primary tumour, the presence or absence of mesenteric lymph nodes and survival, after resection of liver metastases (Cady et al, 1992; Nakamura et al, 1992).

1.1.4.1.3 Synchronous versus metachronous lesions

In 25% of patients with CRC, liver metastases are present when the primary lesion is diagnosed (Bengmark and Hafstrom, 1969). According to a review of the literature by Ballantyre and Quinn (Ballantyne and Quin, 1993), 5-year post resection survival among 433 patients with synchronous lesions was 27%. This was only slightly worse than the 31% 5-year post treatment survival in 555 patients with metachronous lesions. However, Hughes et al (Hughes et al, 1989) found a disease free interval of more than 1 year from the initial colorectal resection, which conferred a survival advantage over patients with either synchronous lesions or a shorter disease free interval (40% *vs* 24 % and 28% respectively, $P < 0.05$). Presentation of liver metastases with a disease free interval of < 12 months has also been found to be predictive of an adverse outcome by other groups (Fong et al, 1999). It should be noted, however, that even when the presentation of liver tumours is synchronous or within 12 months of primary resection, the 5-year survival rate was still 30%.

1.1.4.1.4 Pathological features of liver tumours

Historically, increasing numbers of liver metastases were thought to be associated with a poor prognosis, with solitary lesions being significantly more favourable. It has become apparent, however, that survival after removal of 3 lesions is similar to that seen after resection of a solitary lesion. Cady et al (Cady et al, 1998), noted that no patient with more than 3 metastatic lesions was alive after 4 years, and there was no difference in disease free survival in patients with either 1, 2 or 3 lesions. This is in agreement with several other published studies that set 3 lesions as the cut off for considering surgery (Gayowski et al, 1994; Hughes et al, 1989; McEntee et al, 1992). Cobourn et al (Cobourn et al, 1987), stressed the importance of distinguishing true

multiple metastases from solitary lesions with satellites. They noted a 33% 5-year survival in patients with satellite lesions, compared to 0% 3-year survival with true multiple lesions. Although the number of hepatic metastases resected is of prognostic significance, it seems to be unimportant whether the lesions are bilobar or unilobar, as long as removal with adequate residual hepatic function can be achieved (Cady et al, 1992; Hughes et al, 1989). However, Fong et al (Fong et al, 1999) found bilobar disease to be a predictor of adverse outcome, the 5-year survival rate was 29% and thus sufficiently favourable to justify the risks of resection if it was the only positive predictor of outcome.

The size of liver metastases is also thought to be predictive of outcome. Nakamura et al (Nakamura et al, 1992), reported 100% 5-year survival in patients with tumours less than 3 cm, compared to a 38% 3-year survival in patients with larger lesions. Similarly Fong et al (Fong et al, 1999), found that if the size of the largest tumour was > 5 cm this was an independent predictor of adverse outcome. Despite this the 5-year survival rate was 40% with tumours > 5 cm, and thus sufficiently favourable to justify surgery.

1.1.4.1.5 Carcinoembryonic antigen (CEA)

CEA is used as a marker for recurrent disease following resection of primary CRC (Martin et al, 1993). Recurrence is not always associated with an elevated CEA, and thus a low CEA does not eliminate the presence of metastases (Verdi et al, 1993). In a report by Cady et al, a CEA level > 200 ng/ml was one of the most significant preoperative indicators of poor prognosis after hepatic resection. No patient with a CEA level > 200 ng/ml had a disease free survival of greater than 5 years, whereas the

5-year disease free survival for patients with a CEA level < 5 ng/ml was > 50% (Cady et al, 1992). A subsequent study confirmed this with no long-term disease free survivors in patients with CEA levels > 200 ng/ml (Cady et al, 1998). Similarly Fong et al (Fong et al. 1999), reported that a CEA level > 200 ng/ml was predictive of adverse outcome, but even so the 5-year actuarial survival rate with a CEA level > 200 ng/ml was 24%. Of the 85 patients with this preoperative level 12 survived beyond 5 years.

1.1.4.1.6 Surgical margins

The most important prognostic factor in many studies is the presence or absence of adequate resection margins. In a number of studies no patient with positive margins was disease free after 20 months, and 5-year survival was poor (0-18%) (Cady et al, 1992; Hughes et al, 1989; Hughes et al, 1986). Five-year survival in patients with margins of < 1 cm varied from 18-26% compared with 44-50% reported in patients with margins > 1 cm (Cady et al, 1992; Hughes et al, 1989; Hughes et al, 1986).

1.1.4.1.7 Extrahepatic disease and lymph node metastases

Extrahepatic disease (lung lesions or contiguous spread) is not a contraindication to resection, if the entire tumour can be removed surgically. Survival however is significantly poorer in this group. Fong et al (Fong et al, 1999), reported an 18% 5-year actuarial survival rate in 88 patients who underwent simultaneous resection for both hepatic and extrahepatic metastases. Positive coeliac or hepatic lymph nodes are generally considered a contraindication to surgical resection. Results of patients with lymph node metastases have been universally poor with no long-term survivors reported in one study (Adson et al, 1984). A systematic review recently analysed 15

series that provided data on 145 node-positive patients (Rodgers and McCall, 2000). Five patients were reported to have survived 5 years after liver resection: 1 was diseases free, 2 had recurrent disease, and 2 had undescribed disease status. However, 5 studies involving 83 patients specified a formal lymph node dissection as part of the surgical procedure, and 4 of the 5 node-positive 5-year survivors were in these studies. The authors of the review concluded that there are few 5-year survivors after liver resection, with or without lymph node dissection, for CRC hepatic metastases involving the hepatic lymph nodes.

1.1.4.1.8 Repeat resection of recurrent hepatic CRC metastases

In patients who develop recurrent disease, the recurrence is limited to the liver in 40-60% (Hughes et al, 1986). Hepatic recurrence after liver resection is still an uncommon indication for further resection, being performed in only 7-10% of patients undergoing initial resection (Griffith et al, 1990; Stone et al, 1990). Early reports indicated that the survival rate was lower after repeat resection than after initial resection for CRC metastases. A multi-institutional study on 170 patients from the Repeat Hepatic Resection Registry 1994 (Repat Hepatic Resection Registry, 1994), showed 3- and 5-year actuarial survival rates of 37 and 26% respectively. This suggests that the results of repeat resection are no different from those of initial hepatectomy.

1.1.4.2 Chemotherapy

1.1.4.2.1 Systemic chemotherapy

Only the role of chemotherapy in advanced CRC will be discussed in detail in this section. As far as neoadjuvant chemotherapy is concerned for primarily unresectable hepatic metastases, there have only been a limited number of non-randomised retrospective studies and case reports, that have described down-staging to resectability using chemotherapy. Elias et al (Elias et al, 1995), reported 14 patients (9 with CRC metastases) who became resectable after 6 or more courses of intra-arterial chemotherapy with 5-Fluorouracil (5-FU), combined with epirubicin or mitomycin C. These patients represented only 6% of the total number of patients treated for unresectable liver tumours. Three patients had the volume of the future remnant liver increased by preoperative portal vein embolisation. Five of the nine patients were alive at 5 years.

Bismuth et al (Bismuth et al, 1996), also described 53 patients who underwent neoadjuvant chemotherapy with systemic 5-FU, leucovorin (LV) and oxaliplatin. They represented 16% of the total number of patients treated for unresectable liver tumours. Mean duration of preoperative chemotherapy was 8 months and a number of other techniques were used to increase resectability rates, including portal vein embolisation (5 patients) and two stage hepatectomy (5 patients). A 5-year survival rate of 40% may have been influenced by repeat hepatectomy in 15 patients (28%) and resection of pulmonary metastases in 10 (19%) of the patients. The same group then reported the follow-up of 701 patients with CRC liver metastases, who were evaluated for liver resection and deemed unresectable. Following chemotherapy with 5-FU, LV and oxaliplatin, 95 patients (13.6%) subsequently underwent a potentially

curative liver resection. The acturarial 5-year survival in this group was 34% (Adam et al, 2001). In a smaller group, comprising 42 patients with unresectable liver only CRC metastases, Alberts et al (Alberts et al, 2005) reported a 60% response rate with the same regime, allowing surgical resection in 17 patients (40%).

Following hepatectomy for liver metastases 60-70% of patients develop recurrent disease, usually in the liver, indicating a possible role for post operative adjuvant chemotherapy. Early trials of systemic chemotherapy after liver resection for CRC metastases failed to demonstrate any benefit in terms of survival (Donato et al, 1994). Although no prospective randomised study has evaluated the role of adjuvant systemic chemotherapy in patients subjected to potentially curative liver resection, the role of adjuvant intra-arterial (IA) chemotherapy has been addressed. Initial results were encouraging (Curley et al, 1993) (Nonami et al, 1997), however, a large randomised study of resection alone *vs* resection plus hepatic arterial 5-FU performed by the German Cooperative on Liver Metastases was closed prematurely after the interim analysis showed a lower survival in the treatment group (Lorenz et al, 1998). One year later, two large prospective randomised studies renewed interest in adjuvant IA chemotherapy. In the first, 109 patients having undergone resection of up to 3 CRC liver metastases were randomised between no adjuvant treatment *vs* hepatic arterial floxuridine (5-fluoro-2'deoxyuridine; FUDR) plus systemic continuous infusion of 5-FU. Although the recurrence-free survival at 3 years was significantly higher with chemotherapy, an overall survival benefit was not demonstrated (Kemeny et al, 1999a). The second study compared hepatic artery FUDR and dexamethasone plus systemic 5-FU *vs* systemic 5-FU alone. Results from the analysis of 156 randomised patients showed an improvement of the overall survival at two years with

the combination of IA and systemic chemotherapy (86% *vs* 72%, respectively, $P < 0.05$) (Kemeny et al, 1999b).

The role of chemotherapy in the management of patients with advanced CRC has been well established in 3 trials comparing chemotherapy plus best supportive care to best supportive care alone. These trials are summarised in Table 1.2.

Trial	Randomisation	Patient No.	Results (median survival)
Nordic	Primary expectancy *vs* MTX 250 mg/m^2, 5-FU500 mg/m^2 (3+23 hours),LV15 mg po x3 days	183	9 months *vs* (P < 0.02) 14 months
Scheithauer *et al*	Best Supportive Care *vs* 5-FU 550 mg/m^2/day, LV 200 mg/m^2/day + Cisplatin 20 mg/m^2/day D1-4 4 weekly	40	5 months *vs* (P = 0.006) 11 months
Allen-Mersh *et al*	Best Supportive Care *vs* Hepatic artery infusional fluoxuridine 0.2 mg/kg/day, heparin 5000 u/day for 14 days, 4 weekly	100	226 days *vs* (P = 0.03) 405 days

Table 1.2. Critical trials of chemotherapy versus best supportive care in patients with metastatic CRC.

In the Nordic study, patients with asymptomatic advanced disease were randomised to receive either chemotherapy (methotrexate [MTX], 5-FU, and LV) or primary expectancy. Five months post randomisation 57% of the patients in the primary expectancy arm had developed symptoms and crossed over to receive chemotherapy (Anonymous, 1992a). The median overall survival (OS) and progression free survival (PFS) were significantly better for the patients treated initially with chemotherapy (OS: 14 months and 9 months respectively, $P < 0.02$; PFS: 8 months and 3 months respectively, $P < 0.001$). Scheithauer et al, randomised 40 patients with metastatic CRC, to receive either chemotherapy (LV, 5-FU, and cisplatin) or best supportive care (Scheithauer et al, 1993). Both median survival and median time to disease progression were improved in the patients who received chemotherapy ($P = 0.006$ and $P = 0.008$ respectively). In the third study, the role of hepatic artery infusion of FUDR was established in 100 patients with unresectable liver metastases secondary to CRC (Allen-Mersh et al, 1994). Patients were randomised to hepatic artery infusion of chemotherapy or best supportive care. The median survival of the patients receiving chemotherapy was significantly longer than the best supportive care patients (405 days and 226 days $P = 0.03$).

These trials clearly demonstrate a survival advantage from the use of palliative chemotherapy in patients with advanced CRC. In addition, the Nordic study confirms a benefit from the early use of chemotherapy for metastatic disease, rather than delaying treatment until the onset of symptoms.

5-FU is itself inactive and requires intracellular conversion to form active metabolites. Its major active metabolite is 5-fluorodeoxyuridine monophosphate (5-FdUMP),

which inhibits thymidylate synthase (TS), the key enzyme in the biosynthesis of deoxythymidine monophosphate, essential for DNA synthesis. Although the affinity of 5-FdUMP for TS is approximately 1000-fold higher than that of the natural substrate, deoxyuridine monophosphate, effective inhibition resulting in deoxythymidine triphosphate depletion requires formation of the ternary complex of TS, 5-FdUMP and the folate co-factor 5,10-methylene-tetrahydrofolate. Hence, cell killing by 5-FU only occurs when the cell contains adequate levels of LV. 5-FU is also converted to 5-fluorouridine triphosphate (5-FUTP) and 5- fluorodeoxyuridine triphosphate (5-FdUTP) which are incorporated directly into RNA and DNA respectively, resulting in the production of DNA single-strand breaks.

Single agent response rates for bolus 5-FU of around 20-35% quoted in the 1980s are probably misleading. Large phase III trials published since 1995 quote objective response rates below 20% and median progression-free survival under 6 months (Anonymous, 1995b; Labianca et al, 1997). Modulation with LV, which acts by increasing intracellular levels of reduced folates, thus enhancing the formation and retention of the 5-FdUMP/TS complex, has improved response rates in the order of 2-fold. A meta analysis of 9 trials comparing 5-FU alone to 5-FU plus LV in over 1500 patients, showed a significantly higher response rate in the 5-FU/LV group compared to the 5-FU alone group (23% *vs* 11%, odds ratio 0.45, $P < 10^{-7}$). There was no difference in the median survival times (11.5 and 11 months respectively). The large number of patients who did not respond to treatment in both groups, and cross-overs from 5-FU alone to 5-FU/LV were thought to be plausible explanations for the lack of a survival difference (Anonymous, 1992b).

The response rates of 5-FU can be improved not only by modulation, but also by different scheduling of administration. The mechanism by which 5-FU exerts its cytotoxic effect depends on the dose schedule, bolus injections of high doses exert cytotoxic activity predominantly via inhibition of RNA whilst prolonged exposure to low doses acts mainly via inhibition of TS. A meta analysis comparing protracted venous infusion 5-FU to bolus 5-FU showed significantly higher response rates and median survival in the continuous 5-FU arm (response rates: 22% *vs* 14% respectively, P = 0.0002; median survival 12.1 months *vs* 11.3 months respectively, P = 0.04) (Anonymous, 1998a). Toxicity was also significantly reduced in the continuous infusion arm.

The de Gramont regimen is commonly used in France and the United Kingdom. This regime combines bolus and infusional administration of 5-FU with LV (LV 200 mg/m^2/day as a 2-hour infusion, 5-FU 400 mg/m^2/day bolus and a 22-hour infusion of 600 mg/m^2/day for two consecutive days every 2 weeks). This regime was compared in a randomised study to the Mayo NCCTG regime (LV 20 mg/m^2 and 5-FU 425 mg/m^2 days 1-5 repeated every 4 weeks) (de Gramont et al, 1997a). Four hundred and forty eight patients were randomised. The overall response rate for the monthly treatment was 14.5% and for the bimonthly treatment 32.6%, (P = 0.0004). Progression free survival was also significantly longer in the bimonthly group (27.6 weeks *vs* 22 weeks, P = 0.001). Median survival was longer with the bimonthly regime although this did not reach statistical significance (62 weeks *vs* 56.8 weeks, P = 0.067).

An additional variation in administration of 5-FU and other drugs utilises the circadian variation in the activity of enzymes. Cell division in normal tissues, unlike that in malignant tumours, tends to 'sleep' at night. Circadian modulation of drugs therefore offers the possibility of decreased toxicity and increased dose intensity. Levi et al, published a randomised study in patients with chemonaive metastatic CRC comparing constant rate or chronomodulated oxaliplatin, 5-FU and LV (Levi et al, 1997). The study was terminated early as there were significantly higher response rates in the chronomodulated treatment arm and a correspondingly lower rate of toxicity. Mitomycin C has also been used as a single agent in the management of metastatic CRC with response rates of 0-33% being reported (Petrelli and Mittelman, 1984). The combination of protracted venous infusion (PVI) 5-FU and mitomycin C has been shown to have significantly improved response rates and disease free survival compared to PVI 5-FU alone (response rates: 54% and 38% respectively; disease free survival 7.9 months and 5.4 months respectively) (Ross et al, 1997). The same group explored the effect of dose intensification by circadian timing of 5-FU in this combination. Three hundred and twenty patients with advanced CRC were randomised to receive either PVI 5-FU 300 mg/m^2 daily or circadian-timed infusion (CTI) of 5-FU, beginning at 600 mg/m^2 and subsequently reduced to 450 mg/m^2. Both groups received mitomycin-C at a dose of 7 mg/m^2 given every 6 weeks. The overall response rate for the PVI 5-FU group was 38%, compared with 30.3% for the CTI group (P = 0.176). There was no statistically significant difference in terms of disease-free survival (8 months *vs* 9.9 months; P = 0.131) or OS (15.8 months *vs* 16.3 months; P = 0.275) between the treatment groups. This study thus confirmed the high response rate and overall survival figures for the combination of PVI 5-FU and mitomycin C in

CRC, but failed to support previous evidence for improved response or survival with dose intensification by circadian timing of 5-FU (Price et al, 2004).

1.1.4.2.2 New systemic treatment options for advanced CRC

Irinotecan (CPT11) is a semisynthetic water-soluble camptothecan. Its mechanism of action is via inhibition of the nuclear enzyme DNA topoisomerase (topo) I. Topo I allows relaxation of supercoiled double strand (ds) DNA to occur so that transcription and translation can proceed. Inhibition of the enzyme results in an accumulation of single strand (ss) DNA breaks in the cell with resultant cell death. CRC cells are known to have levels of topo 14-16 times higher than those of normal tissues (Giovanella et al, 1989). Irinotecan has been shown to be an active drug in CRC. Following publication of a randomised trial comparing irinotecan and best supportive care to best supportive care alone, which showed a clear survival benefit in the irinotecan group (36% *vs* 14% at 1 year), it is now established as an effective second line agent in 5-FU resistant disease (Cunningham et al, 1998).

Raltitrexed (Tomudex) is a direct and specific TS inhibitor. It is incorporated into the cell via the reduced folate membrane carrier system. Once raltitrexed is intracellular, it is polyglutamated to more potent forms. This has two benefits, firstly it extends the intracellular retention of the drug and secondly it prolongs TS inhibition. Consequently, it can be administered as a single dose 3 weekly. Studies to date show that raltitrexed has comparable response rates to a 5-FU/LV combination and in 2 out of 3 phase III trials, a similar survival time (Cunningham et al, 1996; Kerr, 1997). This, combined with the fact that raltitrexed has a simple dose schedule represents an advance in the management of CRC. Currently trials are underway looking at the role

of raltitrexed in combination with 5-FU, oxaliplatin and irinotecan, and in addition its role in the adjuvant setting is also being assessed.

Oxaliplatin is a third generation platinum (pt) compound whose major toxicities are peripheral sensory neuropathy and nausea. As a single agent, response rates in patients with 5-FU resistant disease are 10% (Levi et al, 1993; Machover et al, 1996), and for those receiving first line treatment 25% (Diaz-Rubio et al, 1996). Synergy between oxaliplatin and 5-FU has been demonstrated both preclinically and clinically. De Gramont et al, demonstrated this phenomenon in 46 patients who had progressed on 5-FU/LV for metastatic disease or who had relapsed within 6 months of adjuvant treatment, by proceeding with the same schedule of 5-FU/LV on progression of disease, with the addition of oxaliplatin (de Gramont et al, 1995; Garufi et al, 1995). Rather than the expected response rate of 10%, the observed response rate in this trial was 46%. Two large Phase III trials have assessed the role of oxaliplatin in addition to 5-FU and LV as first line treatment for advanced CRC. In one, 420 patients were randomised to receive a regime of LV and 5-FU bolus plus a 24 hour infusion on 2 consecutive days every 2 weeks plus or minus 85 mg/m^2 oxaliplatin on D1 every 2 weeks. The median PFS was superior in the Oxaliplatin arm (39.6 weeks *vs* 27.8 weeks, P = 0.0001). An interim analysis was performed on 200 patients and response rates of 57% for oxaliplatin/5-FU/LV *vs* 26% for 5-FU/LV alone, were observed (de Gramont et al, 1997b). The second study assessed the role of oxaliplatin in addition to chronomodulated 5-FU/LV. Two hundred patients were randomised to receive chronomodulated 5-FU (700 mg/m^2/day x5) and LV (300 mg/m^2/day x5) with peaks at 04:00am, with or without oxaliplatin (125 mg/m^2 D1). The median PFS was 7.9 months in the oxaliplatin arm and 4.3 months in the control arm (P = 0.05). There was

no significant difference in the median OS between the arms (17.6 months oxaliplatin; 19.4 months control; P = 0.82) (Giachetti et al, 1997). An analysis of the use of second line chemotherapy and surgery for metastases in the two arms showed that the incidence of both of these modalities of treatment was more frequently employed in the control group. This may account for the lack of a significant survival benefit in the oxaliplatin arm (Giacchetti et al, 1998).

1.1.4.2.3 Intra-arterial hepatic chemotherapy for isolated liver metastases

Surgical excision should be considered in all patients with metastatic disease isolated to the liver. However, approximately 75-80% of patients have disease that is unresectable. Intra-arterial chemotherapy is based on the principle that CRC metastases derive most of their blood supply from the hepatic artery (once the lesion is approximately 1 mm), lower drug doses are required, lower toxicity is produced (because the liver eliminates 80% of the infused drug), and higher concentrations of drug in tumour tissues are achieved. FUDR has a higher concentration than 5-FU, when given via the hepatic artery (Ensminger and Gyves, 1983).

Phase II trials of intra-arterial hepatic chemotherapy using 5-FU and external pumps gave encouraging results with response rates between 30-80%. With the development of implantable pumps and the use of FUDR, response rates in the order of 30-60% have been reported (Dworkin and Allen-Mersh, 1991; Kemeny et al, 1990). Five randomised trials have been published comparing hepatic arterial infusion of chemotherapy with intravenous chemotherapy (FUDR via hepatic artery, FUDR intravenously or 5-FU bolus regimes intravenously). Two further trials compared hepatic arterial chemotherapy with no treatment. The majority of these trials

confirmed improved response rates with chemotherapy administered via the hepatic artery. However, the impact on survival was not consistently established in the individual trials. A meta analysis was therefore reported using data from the 654 patients included in these seven trials (Anonymous, 1996). For the 5 trials (391 patients) comparing intra-arterial hepatic with intravenous chemotherapy response rates of 41% *vs* 14% were reported and this improvement, in favour of hepatic artery chemotherapy, was highly statistically significant, ($P < 10^{-10}$). This translated into a median survival of 16 months *vs* 12.2 months in the two groups respectively which was not statistically significant ($P = 0.14$). A survival benefit for hepatic arterial chemotherapy was clearly demonstrated in the two trials in which the control arm was best supportive care. However, there are problems in interpreting these results, namely that the systemic treatment arm involves fluoropyrimidine treatment alone, without biochemical modulation, which is not the standard systemic treatment for metastatic CRC. Another potential influencing factor on the results is that in some of the trials there was a crossover from intravenous to intra-arterial hepatic chemotherapy and this may have had some bearing on the lack of survival benefit, despite improved response rates.

A major concern associated with hepatic artery infusional chemotherapy is its potential toxicity. Whilst this route of administration reduces the systemic toxicity associated with the fluoropyrimidines, it is associated with an increased risk of chemical hepatitis and sclerosing cholangitis, duodenal ulceration and hepatic artery thrombosis (Rougier et al, 1992). In an attempt to overcome these problems, short infusions of 5-FU have been used with some success.

These results demonstrate a possible role for intra-arterial hepatic chemotherapy in patients with unresectable isolated liver metastases. Future developments are being focused on the combined modality of intra-arterial hepatic and systemic chemotherapy, but the results of randomised trials are awaited to establish if this approach is superior to either treatment alone.

1.1.4.3 Direct ablation

Several interstitial ablative techniques have shown promising results as an alternative to systemic chemotherapy in the palliative treatment of CRC liver metastases. Cryoablation is the use of low temperatures to achieve cellular destruction. Most published series of CRC liver metastases treated by cryoablation have a short follow up, with only 5 studies following patients for more than 24 months (Ravikumar et al, 1991a; Ravikumar et al, 1991b; Dilley et al, 1993; Weaver et al, 1998; Ruers et al, 2001). Although it is difficult to infer valid long-term results, 2-year survival rates of up to 62% have been reported. Median survival times following cryoablation are generally greater than 24 months (range 8-30 months) (Seifert et al, 1998). With a median follow up of 14-30 months, the percentage of patients that are alive and disease free ranges from 10-50%.

Thermal ablative techniques use heat to destroy tissue through coagulative necrosis, which is irreversible if the temperature reaches 60-100°C. Several sources have been used to generate heat including radiofrequency ablation (RFA), which employs a high-frequency alternating current (350-500 KHz) that produces ionic agitation and results in frictional heat. Solbiati et al reported an overall survival of 100, 94 and 89% at 6, 12 and 18 months respectively in a series of 29 patients with 44 liver metastases

of different origins (22 patients with CRC). The disease-free survival rate was 50% at 12 months (Solbiati et al, 1997). Although experience is still limited, interstitial laser photocoagulation, whereby light at optical or near-infrared wavelengths scatters within tissue and is converted into heat, has reports of local tumour control rates ranging from 40-75%. Nolsoe et al used the Nd YAG laser in 11 patients with 16 CRC liver metastases and achieved complete necrosis in 12 of 16 tumours (Nolsoe et al, 1993). Mean diameter of the tumours was 2.4 cm, compared with 3.4 cm for tumours that were not completely destroyed. Finally, microwave ablation (MA) uses alternating ultrahigh-speed (2450 MHz) waves to induce rotation of water molecules and thus generate heat. Shibata et al recently randomised 30 patients with multiple espectable CRC liver metastases to either resection (16 patients) or intraoperative MA (14 patients); the mean disease-free survival time was 11.3 and 13.3 months respectively, with estimated 1, 2 and 3-year survival rates of 69, 56 and 23% for surgery, and of 71, 57 and 14% for MA respectively (Shibata et al, 2000). This suggests palliative benefit as with the other forms of local ablation.

1.1.4.4 Biological therapy

1.1.4.4.1 Immunotherapy

A number of tumour associated antigens have been identified on CRC cells: CEA, Cathepsin B, 17-1, Ca19-9 and TAG-72. Monoclonal antibodies (mAb) targeting these antigens result in antibody dependent cell-mediated cytotoxicity (ADCC). Monoclonal antibody 17-1A is a murine IgG class 2A immunoglobulin that detects tumour-associated antigen CO17-1A. Trials have been performed using mAb 17-1A in patients with advanced CRC. They have reported response rates in the order of 5% but this has not been statistically significant (Mellstedt et al, 1991; Wadler, 1991).

However, Riethmuller et al have shown a 30% reduction in mortality with mAb being used in the adjuvant setting for patients with Dukes C CRC (Riethmuller et al, 1998), although these results have not been reproduced by other groups. Other mAb are currently being investigated in advanced and adjuvant trials.

1.1.4.4.2 Cytokines

Cytokines with potential antitumour activity include Interleukin – 2 (IL-2), Interferon alpha (IFNα), Interferon beta (IFNβ), and Tumour Necrosis Factor (TNF). Cytokines are produced by lymphocytes in response to antigenic recognition by T cells. They induce an immune reaction, which can lead to rejection of cancer cells. The use of IL-2 and IFNα, β or χ alone or in combination have not been shown to be effective in the management of advanced disease and in addition to this they are associated with significant toxicity.

There is convincing *in vitro* data suggesting biomodulation of 5- FU with IFN (Chu et al, 1990; Wadler and Schwartz, 1990). Additionally, *in vitro* the modulation of 5-FU by LV plus IFN has been shown to be synergistic (Houghton et al, 1991). Randomised trials have been performed to assess the role of IFN as a lone modulator of 5-FU (Anonymous, 1995b; Greco et al, 1996) or in addition to LV (Kohne et al, 1998; Seymour et al, 1996). None of these trials have demonstrated any benefits from the clinical use of IFN in this situation.

1.1.4.4.3 Gene therapy

Gene therapy involves the insertion of genes into cells with the intent of correcting an inborn genetic error or creating a new cellular function. The molecular basis of CRC

is being extensively investigated and much is known about the numerous genes involved in the carcinogenesis in this disease. Gene therapy does not necessarily constitute the replacement of a mutated gene; there are a number of different approaches:

- Enzyme or prodrug systems (gene directed enzyme prodrug therapy – GDEPT). In this situation the transferred gene converts a non-toxic prodrug to an active cytotoxic agent. This can be a tumour specific action if the gene or prodrug is targeted to the tumour cells.
- Tumour suppressor gene replacement with wild type *p53*.
- Immune gene therapy e.g. a polynucleotide tumour vaccine of CEA cDNA.

Phase I and II clinical trials have been conducted using a variety of genes. Results have shown that, although gene therapy is well tolerated and has low toxicity, the clinical benefit is marginal (Havlik et al, 2002). Gene therapy as a definitive treatment for liver metastases remains limited, but it may be useful as an adjuvant treatment in combination with radiotherapy, chemotherapy and surgery to achieve disease-free survival.

1.2 Hepatocellular carcinoma

1.2.1 Epidemiology

Hepatocellular carcinoma (HCC) is the seventh commonest malignant neoplasm world-wide in men and the ninth in women. It is responsible for more than 4% of all cancer cases and is the third commonest cause of death from cancer throughout the world (315,000 deaths per year). It has an estimated annual incidence between 250,000 and over 1 million cases world-wide (Wands and Blum, 1991). HCC is more frequent in men than women with ratios between 3:1 to 8:1 reported. There are world-wide differences in incidence due to various aetiological factors prevalent in different geographical regions.

In Africa, HCC is frequently observed in Mozambique, Nigeria and South Africa, whereas in the Asiatic continent, China, Taiwan and Korea carry the highest incidence. In these countries the incidence ranges between 20 and 150 cases per 100,000 per year (Rustgi, 1987). In Western countries the rate is 10 times lower but progressively increasing. In the United States the incidence of histologically proven HCC increased from 1.4 per 100,000 population for the period from 1976-1980 to 2.4 per 100,000 for the period from 1991-1995 (El-Serag and Mason, 1999).

1.2.2 Risk factors

The two main aetiological factors for HCC are cirrhosis and viral hepatitis. Although cirrhosis is considered a major risk factor, it is not an absolute prerequisite for the development of HCC as shown by the occurrence of HCC's both in non-cirrhotic chronic liver diseases and in apparently normal liver. Numerous epidemiological and

experimental evidence indicates that HCC is of multifactorial aetiology. The relative roles of risk factors in HCC vary considerably among populations (Table 1.3).

	Prevalence (%)				
Risk Factor	**South Africa**	**China and Taiwan**	**Japan**	**USA**	**Southern Europe**
Hepatitis B virus	50	60-90	20	15	5-10
Hepatitis C virus	30	30	70	30-60	60-80
Alcohol	<10	<10	<10	<15	15-30

Table 1.3. Prevalence of risk factors in HCC patients: geographical differences.

1.2.2.1 Cirrhosis

Cirrhosis is a premalignant condition, irrespective of the aetiology, secondary to nodular hyperplasia progressing to carcinoma. About 70-90% of HCCs develop on a background of cirrhosis whilst 20% of patients who die of cirrhosis are noted to have HCC at autopsy (Okuda, 1992). Non alcoholic cirrhosis is more frequently associated with HCC than alcoholic cirrhosis. In patients with cirrhosis, the annual incidence of HCC is 2-7% (Liaw et al, 1986; Okuda et al, 1982).

1.2.2.2 Hepatitis B Virus

Hepatitis B virus (HBV) is an enveloped virus with a compact incomplete ds DNA genome. Chronic infection tends to occur after perinatal infection by a carrier mother, infections in very young children and in 10-15% of acute HBV infection in adults. World-wide chronic HBV infection correlates with the frequency of HCC, for example in Taiwan the carrier rate for HbsAg in the general population is 10%, but 80% in individuals with HCC (Tong et al, 1971). In a prospective study following over 20,000 Chinese males the risk of developing HCC in HbsAg carriers was 100 times that of HbsAg negative males (Beesley RP, 1987). The carriers at the highest risk of developing HCC are those with actively replicating infection (HbeAg positive) and those with cirrhosis.

The mechanism by which HBV contributes to hepatocarcinogenesis can be either direct or indirect. A direct mechanism is viral genome integration into the host chromosomal DNA (often at multiple sites). This either causes or contributes to genomic instability secondary to point mutation, inversion, translocation and deletion (Brechot et al, 1980). HBV integration can trigger large cellular deletions in cellular DNA (Rogler et al, 1985) resulting in the loss of tumour suppressor genes. Some viral gene products, such as HBX protein, activate transcription and may increase the expression of growth regulating genes involved in the malignant transformation of hepatocytes. As an indirect mechanism, persistent HBV infection (but not HBV itself) predisposes the hepatocyte to genetic changes resulting from other causes. The virus continuously replicates and causes recurrent episodes of hepatitis. The liver responds to persistent inflammation with continuous regeneration and fibrosis that eventually results in cirrhosis.

1.2.2.3 Hepatitis C Virus

Hepatitis C virus (HCV) is an RNA virus and may be more important than HBV in the aetiology of HCC. In most epidemiological studies, HCV has been diagnosed by the presence of antibodies to the virus, which unlike antibodies to Hepatitis A and B virus are not protective. There is a 4-fold higher incidence of HCC with the presence of anti HCV antibodies than among HBV carriers, this is particularly important in Japan, Italy and Spain and the United States (Sherlock S and Dooley J, 1993). Evidence suggests that the relationship between viral acquisition and the development of HCC is prolonged, taking approximately 30 years, with chronic active hepatitis occurring during the first 10 years, and cirrhosis after 20 years (Kijosawa K et al, 1990).

Eighty percent of anti-HCV positive (HbsAg negative) HCC patients have cirrhosis (Hasan et al, 1990), whilst HCC develops in 18% of patients with HCV associated cirrhosis within 2 years, and in 75% of patients within 15 years (Foster et al, 1997). The presence of both HCV and HBV increases the risk of HCC, as does the use of alcohol.

The mechanism by which HCV contributes to hepatocarcinogenesis in unknown. As an RNA virus, without the enzyme reverse transcriptase, there is no mechanism for it to be incorporated into the host DNA, nor is there any evidence to indicate the activation of protooncogenes or inactivation of tumour suppressor genes. Continuous viral replication with associated inflammation and hepatocyte cell death appears to contribute to HCV related hepatocarcinogenesis.

1.2.2.4 Miscellaneous factors

Aflatoxins probably increase the risk of HCC. These are produced by the fungi Aspergillus flavium and parasitium and are divided into two chemical groups, aflatoxin B_1 (AFB1) and its derivatives and aflatoxin G_1 and its series. AFB1 contaminates foods such as corn, groundnuts, rice and sorghum in tropical areas. AFB1 is a potent hepatocarcinogen in experimental animals being converted to its reactive 2,3-oxide by liver microsomes and subsequently trapped as an RNA adduct. This AFB1 epoxide reacts with the guanine residues of the DNA molecule forming a covalent bond. It causes a specific mutation, transversion of guanine to thymine in codon 249 of the *p53* tumour suppressor gene. A linear relationship between the risk of HCC and AFB1 content in diet has been established (Yeh et al, 1989).

Alcohol is a risk factor for HCC, particularly in older age groups. In London, where the incidence of HBV infection is low, HCC was seen in 30% of alcoholics with cirrhosis, compared with 4% of non-alcoholics with cirrhosis (Lee, 1966). The 10-year cumulative occurrence of HCC in patients with alcoholic cirrhosis is 18.5% (Yamauchi et al, 1993). Several mechanisms have been postulated to explain the role of alcohol in promoting the development of HCC: direct hepatocellular injury, activation of chemical carcinogens via the induction of the microsomal P450-dependent biotransformation system, suppression of the immune system and reduced activity of the enzymes involved in the repair of carcinogen-mediated DNA alkylation.

In HbsAg negative patient's cigarette smoking is a dose dependent risk factor for HCC (Kaklamani et al, 1991). Case controlled studies in developed countries show a 2 to 5-fold increased risk of HCC with oral contraceptive use (Schlesselman, 1995). Other disease processes which have a high incidence of HCC include autoimmune chronic active hepatitis, Wilson's disease, haemochromatosis, type I glycogen storage disease and porphyria cutanea tarda. HCC may also complicate immunosuppressive therapy following organ transplantation and clonorchiasis, shistosomiasis and membranous obstruction of the inferior vena cava are important factors in some endemic areas.

1.2.3 Natural history of HCC

The natural history of HCC is variable. Most patients die within 3-6 months after the onset of symptoms (Paraskevopoulos, 1994), but 3-year survivals of 50% have been reported (Llovet et al, 1999a). The progression of HCC depends largely on the size and number of tumours, growth rate, together with histological grade and the degree of cirrhotic changes. In 73 untreated patients with Child's A cirrhosis and a single HCC smaller than 5 cm in diameter, the 3-year survival was 26%, compared with 13% for 43 patients with Child's B cirrhosis (Livraghi et al, 1995). Approximately 20% of all nodules less than 1 cm in diameter when first detected already show microscopic signs of intrahepatic metastases, the number of tumours showing microscopic metastases increases with increasing tumour size and reaches 80% for nodules larger than 3 cm (Ebara et al, 1986).

1.2.4 Treatment of HCC

1.2.4.1 Surgical resection

Surgical resection appears to be the only potential curative treatment for HCC. Advances in diagnostic imaging techniques and the introduction and popularisation of ultrasound guided fine needle biopsy have led to the early detection of smaller HCC's. Despite this, only 5-15% of HCC patients are suitable for surgical resection due to the presence of cirrhosis, anatomically unresectable disease or extrahepatic and vascular spread. Resectability in cirrhotic patients is also limited by diminished functional reserve of the cirrhotic liver, with the associated risks of intraoperative bleeding and postoperative liver failure. In the absence of cirrhosis hepatic resection for HCC can be undertaken with low morbidity and mortality rates (Iwatsuki and Starzl, 1988; Nagorney et al, 1989), and are associated with 5-year survival of over 30% (Farmer et al, 1994; Zibari et al, 1998), and as high as 68% in one study (Nagasue et al, 1986).

The surgical approach in patients with cirrhosis is less clearly defined. European and Japanese centers using highly selective criteria have reported 5-year survival rates of 60-70% (Bruix et al, 1996; Llovet et al, 1999b). In Western countries, where liver cancer typically develops in the setting of well established cirrhosis, fewer than 5% of HCC patients meet these criteria and even in carefully selected patients the rate of tumour recurrence is 50% after 3 years (Anonymous, 1994; Llovet et al, 1999b).

As previously mentioned most HCCs develop on a background of cirrhosis and are frequently multifocal (Bhattacharya et al, 1997). The underlying cirrhosis poses a constant threat of *de novo* emergence of HCC after resection of the original tumour. HCCs that appear in the liver remnant could result from incomplete removal of

tumour, pre-existing intrahepatic metastases or undetected synchronous tumours. Less than 27% of recurrences occur near the resection site, suggesting that incomplete removal of the tumour is responsible for only a minority (Chen et al, 1994). An early recurrence of multiple lesions probably represents undetected synchronous lesions (Chen et al, 1994). Late recurrence (3-6 years after resection) is unlikely to be due to the presence of occult intrahepatic metastases but to non-synchronous mutlifocal tumourigenesis (Ouchi et al, 1993).

Most hepatologists now favour orthotopic liver transplantation (OLT) as the preferred option for early HCC. In one study 34 patients underwent liver resection and 30 patients had OLT for HCC with cirrhosis (Gugenheim et al, 1997). After resection there was a 5-year survival of 13% and 5-year recurrence of 92.6%, with the diameter of nodules being a predictive factor for outcome. In the transplanted group, 5-year survival was 32.6%, 5-year recurrence 40.9% and the predictive factor for outcome was the number of nodules. Two groups of patients were identified, those with large HCC (> 5 cm and/or > 3 nodules) and those with small HCC (≤ 5 cm and ≤ 3 nodules). It was concluded that OLT was the best treatment for small HCC because of the lower recurrence rate (11% *vs* 82.6%) but both treatments had a high recurrence rate in large HCCs (72.3% resection, 100% transplantation) (Gugenheim et al, 1997). OLT removes the entire process and can be applied to patients with end-stage liver disease. Recent data have shown that the restriction of OLT to patients with single tumours less than 5 cm or with 3 nodules, each less than 3 cm, will result in 5-year survival rates of approximately 70% (Bismuth et al, 1999; Llovet et al, 1998).

1.2.4.2 Chemotherapy

1.2.4.2.1 Systemic chemotherapy

The majority of patients with HCC present at an inoperable stage. There have been few randomised-controlled trials of systemic chemotherapy, and as such, its use tends to be limited to study groups. Many of these studies have enrolled patients with poor prognostic factors (impaired liver function, ascites, jaundice) thus it is not surprising that reported response rates are less than 20%, with a median survival of 2-6 months (Colleoni et al, 1994; Falkson et al, 1978; Nerenstone et al, 1988).

The first chemotherapeutic agent used was 5-FU (Brennan M et al, 1964; Nerenstone et al, 1988), which produced response rates of 0-10% and a median survival of 3-5 months. Combination with high dose folinic acid did not show any improvement in outcome (Zaniboni et al, 1988). Doxorubicin has been commonly used, but the objective response rate from 13 published trials was < 20% and the median survival only 4 months (Nerenstone et al, 1988). Other active single agents include 4'-epidoxorubicin (Hochster et al, 1985) – response rate 17% and cisplatin (Falkson et al.) – response rate 17%. Combination regimens have been more promising, such as the combination of systemic cisplatin, doxorubicin, 5-FU and IFNα in patients with advanced unresectable HCC (Leung et al, 1999) producing a 26% partial response rate in 13 patients. Four of 9 patients who underwent surgical resection after partial response revealed no visible tumour cells on histological examination. There was however significant toxicity (2 treatment related deaths due to neutropenic sepsis). Other cytotoxic drugs used have included mitomycin, vinblastine, fludarabine and doxifluridine. None of these agents either alone or in combination have produced a

significant improvement in survival. In addition, toxicity and multidrug resistance have proved to be major problems.

1.2.4.2.2 Intra-arterial chemotherapy

Intra-arterial chemotherapy is based on the principles that HCCs derive most of their blood supply from the hepatic artery, lower drug doses are required, lower toxicity is produced and a higher concentration of drug in tumour tissues is achieved compared with systemic chemotherapy (Chen et al, 1994). Fluorouracil and anthracyclines have been used, the latter producing response rates of up to 42% (Doci et al, 1988). When used in combination with floxuridine, LV and cisplatin, Patt et al reported a 64% response rate to the anthracycline doxorubicin, but with significant toxicity (3 treatment related deaths) (Patt et al.,1994). Other drugs used include mitomycin C, cisplatin and mitoxantrone, yielding response rates of 50%, 55% and 25% respectively (Kinami et al, 1985; Onohara et al, 1988; Shepherd et al, 1987).

1.2.4.2.3 Transcatheter arterial chemoembolisation (TACE)

Transcatheter arterial chemoembolisation (TACE) is a combination of chemotherapy and arterial embolisation that has both selective ischaemic and chemotherapeutic effects on HCC. It can be used only in the absence of major portal vein thrombosis. As there is no standard protocol, a large number of combinations have been used. Ryder et al reported a $\geq$ 50% reduction in tumour size in 10 of 18 patients with small tumours (< 4 cm) and a response in 5 of 49 patients with large or multifocal tumours, using doxorubicin and lipiodol (Ryder et al, 1996). Survival ranged between 3 days and 4 years with a median survival of 36 weeks. Despite encouraging figures for small tumours, several randomised trials have shown no significant improvement in survival

with TACE treatment over best supportive care (1-year survival 24% and 31% respectively) (Pelletier et al, 1990), (1-year survival 62% and 43.3% respectively) (Anonymous, 1995c).

1.2.4.3 Direct ablation

Cryoablation has reported 2-year survival rates of 30-63% (Crews et al, 1997; Adam et al, 1997; Wong et al, 1998) and RFA survival rates of 94, 86, 68 and 40% at 1, 2, 3 and 5 years respectively (Rossi et al, 1996). Percutaneous ethanol injection, however, is still considered to be the most effective form of direct ablative therapy for HCC. It is suitable for HCCs less than 3 cm in size and fewer than 3 in number. Absolute alcohol induces cellular dehydration, coagulative necrosis and vascular thrombosis, causing destruction of the tumour cells. Though 3 year survival rates of 55-70% have been reported, more than half of these patients develop recurrent tumour within 2 years (Castells et al, 1993; Isobe et al, 1994).

1.2.4.4 Hormonal therapy

The use of hormonal agents, in particular tamoxifen, is a convenient treatment modality for advanced HCC. Results, however, from small randomised trials on tamoxifen in the treatment of HCC are conflicting. Some prospective randomised studies have demonstrated significant prolongation of survival in the tamoxifen group with 1 year survival of 35-49% compared to 0-9% in the control group (Farinati et al, 1992; Martinez et al, 1994). However, randomised controlled studies showed that tamoxifen is not effective in prolonging survival in patients with cirrhosis and HCC (Anonymous, 1998b).

1.2.4.5 Immunotherapy

Immunologically active agents should theoretically be of use in the treatment of HCC, as the activity of lymphokine-activated killer (LAK) cells is often reduced in HCC patients (Son et al, 1982). Interferons, proteins produced by cells in response to viral infection and foreign antigens, play a role in viral reproduction and have immunomodulatory and antiproliferative effects on tumour cells. IFNα has been used as a single agent to treat advanced HCC and produced a response rate of 31.4% and a small improvement in survival (Lai et al, 1993). It has also been used in combination with doxorubicin to little effect (Kardinal et al, 1993) and with 5-FU with a documented response rate of 18% (Patt et al, 1993). More recently the combination of cisplatin, doxorubicn, 5-FU and IFNα given systemically produced a 26% partial response (Leung et al, 1999). Whilst combined therapy consisting of intra-arterial cisplatin infusion and systemic IFNα showed a partial response and 1 year survival significantly higher than a comparative group that received intra-arterial cisplatin only (33% *vs* 14%, $P < 0.05$ and 27% *vs* 9%, $P < 0.05$) (Chung et al, 2000). Other strategies have included the use of IFNα, IFNβ, LAK, interleukins and antibodies against α-fetoprotein and ferritin, all with no significant improvement in survival.

1.3 Chemotherapy – classes of anticancer drugs

The first use of drugs in cancer therapy stemmed from the observation of the myelosuppressive effects of sulphur mustard in men exposed to mustard gas during the First World War. This led to the use of nitrogen mustard and related compounds in the treatment of leukaemia and lymphoma (Priestman, 1989). The nitrogen mustards are thus the oldest effective cancer chemotherapeutics, many members of this group still remain in clinical use. Cytotoxic drugs can be classified according to their mechanism of action and biochemistry. The three main categories of anticancer agents are the alkylating agents, natural products and antimetabolites (Table 1.4).

Drug Family	Examples
I Alkylating agents	Nitrogen mustards eg melphalan, mechlorethamine hydrochloride, chlorambucil
	Cisplatin
II Natural products	Vinca alkaloids eg vincristine, etoposide
	Anthracyclines eg doxorubicin
	Non-anthracycline antibiotics eg actinomycin
III Antimetabolites	Methotrexate, 5-fluorouracil

Table 1.4. Examples of the three main categories of anticancer agents.

1.3.1 Cisplatin and alkylating agents

Cisplatin and classical alkylating agents such as the nitrogen mustards are agents commonly used in the treatment of solid tumours eg. cisplatin in testicular and ovarian malignancies (Reed and Kohn, 1990) and haematological malignancies eg melphalan for acute and chronic leukaemia (Colvin and Chabner , 1990). They act by binding covalently to DNA, and as they possess two functional groups can form mono- and diadducts, the former modifying only a single base, the latter including intra- and interstrand crosslinks (Lawley and Phillips, 1996) (Figure 1.1).

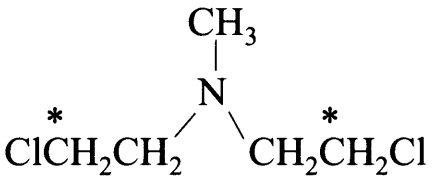

Mechlorethamine

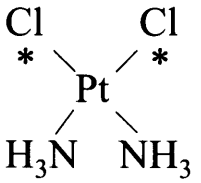

Cisplatin

Figure 1.1. Structures of the nitrogen mustard mechlorethamine (HN_2) and cisplatin. Functional groups are marked*.

Intrastrand crosslinks are formed by the drug binding to two nucleotides within the same strand of the DNA double helix, whilst interstrand crosslinks (ICLs) involve drugs binding to a nucleotide in each of the two DNA strands.

Cisplatin binds preferentially to the N^7 atom of guanine (G) and to a lesser extent the N^7 atom of adenine (A) residues. Cisplatin forms a variety of DNA adducts, the most prevalent (> 90%) of which is the 1,2 intrastrand crosslink. Other platinum DNA adducts include monofunctional 1,3 and longer range intrastrand, interstrand and protein DNA crosslinks (Figure 1.2). Because of their abundance and their ability to block DNA synthesis (Heiger-Bernays et al, 1990; Pinto and Lippard, 1985), intrastrand diadducts are considered to be the primary cytotoxic lesions caused by most platinum compounds. However, some studies have suggested that ICLs may also play a role in determining the cytotoxicity of platinum compounds (Fram et al, 1990; Osmak, 1992).

1,2-d(GpG) intrastrand crosslink	TCTAGGCCTTCT AGATCCGGAAGA
1,2-d(ApG) intrastrand crosslink	TCTTAGTTCTCT AGAATCAAGAGA
1,3-d(GpTpG) intrastrand crosslink	TCTGTGCACTCT AGACACGTGAGA
d(GpC)d(GpC) interstrand crosslink	TCCTTGCTCTCC AGGAACGAGAGG

Figure 1.2. Schematic representation of cisplatin adducts. The platinated nucleosides are underlined.

The nitrogen mustard mechlorethamine (HN_2) also binds preferentially to N^7 G. Although the majority of adducts are monoadducts, a total of 4-7% of the lesions are GZG ICLs, and these are thought to be the primary cytotoxic lesions (Chaney and Sancar, 1996).

The mechanism by which intra- and interstrand crosslinks induce cytotoxicity are unknown, however both block DNA polymerase I, preventing DNA synthesis and cell division. ICLs appear to be more cytotoxic because they are more difficult to process, and attempts to repair or replicate past such damage leads to highly cytotoxic ds breaks (Chaney and Sancar, 1996; Vock et al, 1998).

1.3.2 Natural products

The natural products include the vinca alkaloids, such as vincristine which exert their effects by binding to tubulin and thus inhibiting spindle formation and blocking mitosis. Etoposide, a semisynthetic derivative of podophylotoxin, produces ds DNA breaks by interacting with DNA and the enzyme topoisomerase (topo) II. This enzyme produces temporary enzyme associated DNA strand interruptions in ds DNA, to allow the relaxation of supercoiled DNA during replication. The presence of etoposide results in stabilisation of topo II induced DNA cleavable complexes, with production of ds breaks and a subsequent cascade of effects that culminate in cell death (Takano et al, 1992).

1.3.3 Anti-metabolites

5-FU was first synthesised in 1957 and has been the major cytotoxic agent used in the management of CRC since. 5-FU itself is inactive and requires intracellular conversion to form active metabolites. Its 3 major active metabolites are:

1. 5-fluorodeoxyuridylate (5-FdUMP), which inhibits thymidylate synthase (TS), the rate limiting step of DNA synthesis.
2. 5-fluorouridine triphosphate (5-FUTP), which incorporates into RNA and causes alteration in its processing.
3. 5-fluorodeoxyuridine triphosphate (5-FdUTP), which incorporates into DNA instead of deoxythymidine triphosphate (DTTP), the usual substrate for DNA polymerase.

5-FU degradation is rate limited by the enzyme dihydropyrimidine dehydrogenase (DPD), within 24 hours of a bolus injection up to 80% of the drug is metabolised.

1.4 Drug resistance

The objective of cancer treatment is to eradicate all cancer cells. The functional cell kill hypothesis states that a given drug concentration applied for a defined time period will kill a constant fraction of the cell population. Thus, the concentration, number and frequency of drug treatments are vital. Toxicity also has to be considered, therefore time intervals between cycles of treatment are designed to allow normal cell populations, in particular bone marrow, time to recover before repetition of therapy (Kaufmen and Chabner , 1996).

A chemotherapeutic agent that is effective in cell culture and animal models, although frequently applied successfully in human leukaemia and lymphoma, is often unsuccessful in eliminating solid tumours in adults. Heterogeneity in drug delivery and distribution; heterogeneity of the tumour microenviromental characteristics such as interstitial pH, partial pressure of oxygen (pO_2) and cell proliferation; and intrinsic or acquired drug resistance by the cancer cells themselves often means some tumour cells receive sublethal drug concentrations with subsequent treatment failure.

1.4.1 Heterogeneity of drug delivery and distribution

The efficacy of chemotherapy is limited by its inability to reach target cells *in vivo* in adequate quantities (Jain, 1996). A solid tumour *in vivo* consists of cancer cells, which often occupy < 50% of the total volume, and two extracellular components: vascular, occupying 1-10% of the total volume and interstitial, composed primarily of an abundant collagen rich matrix that surrounds cancer cells and separates them from the vasculature. Since no blood-borne molecules can reach cancer cells without passing through these compartments, there are therefore at least three physiological barriers to delivery (i) heterogeneous blood supply and blood flow in tumours, (ii) heterogeneous permeability of tumour vessels, and (iii) physico-chemical properties and hypertension of the interstitium.

1.4.1.1 Heterogeneous blood supply

In normal organs blood vessels are arranged in a predictable fashion and supply blood to cells areas of the constituent tissue. Although tumour vessels originate from well-organised host vessels, they are disorganised in their growth, structure and function. Consequently, some areas of the tumour may be hypervascular whereas others may be

hypo- or avascular (Jain, 1996). Furthermore, secondary to the irregular vasculature, there is often noticeable slowing of blood flow, exacerbated by the high viscosity of blood within tumours. Thus tumour blood flow tends to be spatially and temporally heterogeneous contributing a specific barrier to drug delivery.

Normal hepatic vasculature consists of flow into liver sinusoids as a singular confluence of arterial and venous blood. Structurally, the sinusoid is classified as a discontinuous capillary with endothelial gaps and no basement membrane (Martinez-Hernandez and Martinez, 1991). The vascularity of experimental liver metastases is dependent on size and growth of the tumours and appears to be a continually changing phenomenon. Ackerman et al, found that small tumours (< 1 mm) had no evidence of newly developed circulation, whilst tumours between 1-2 mm in diameter had neovascularisation encircling the tumour derived from either the arterial or portal circulation or from both. Tumours between 3-7 mm had well developed arterial circulations, whilst larger tumours ranging from 7-33 mm in size, developed a wide variety of vascular patterns ranging from predominantly arterial to predominantly portal as well as a combination of both (Ackerman, 1974). Lin et al performed an autopsy study on a total of 13 human livers with 101 metastases measuring < 1 cm in diameter (Lin et al, 1984). Of these 83 were injected with microfil via both the hepatic artery and portal vein, exclusive perfusion via the hepatic artery was seen in 12 tumours, no tumour had exclusive perfusion via the portal vein, the remaining 71 had a combination of both. With increasing size, the number of tumour vessels decreased in the centre of the tumour.

Angiographic studies have led to the classification of hepatic metastases according to their degree of vascularity. Kim et al, found that vascularity of hepatic metastases from CRC in 21 patients was the same or less than that of surrounding hepatic tissue (Grade I) in 38% of cases, slightly greater (Grade II) in 48% and much greater (Grade III) in 14% (Kim et al, 1977). Survival prolongation after devascularisation and IA chemotherapy was directly proportional to vascularity, with a median survival being 4, 10.5 and 11 months for Grades I, II and III respectively. They suggested that the portal vein may be more important than the hepatic artery in hypovascular tumours, indeed Honjo et al reported a good response following portal vein ligation in the treatment of hepatic tumours of various origins (Honjo et al, 1975).

The sinusoids of normally functioning liver acini change as cirrhosis is established and the microvasculature becomes composed of vessels resembling systemic capillaries. Similarly HCC shows a diffuse uniform pattern of capillarisation (Haratake and Scheuer, 1990). Small HCCs (< 3 cm) are surrounded by a vascular plexus consisting of hepatic arterial and portal venous branches that feed into tumour capillaries (Kita et al, 1991). Although portal blood supply to HCCs has been noted in a number of studies (Saitoh et al, 1994; Taniguchi et al, 1993), HCC blood supply is mainly arterial. Borderline nodules (regenerative nodules with focal areas of change suggesting HCC) have a dual portal and hepatic arterial supply. There is progressively more arterial supply in small HCCs (< 2.5 cm) compared with borderline nodules (Tanaka et al, 1992), and in higher-grade HCCs compared to well-differentiated HCCs and borderline lesions (Matsui et al, 1991).

Arterialisation in HCCs is usually accompanied by hypervascularity (increased blood flow compared to adjacent liver tissue). Reduction of portal flow appears to precede the increase in arterial flow, and early, well-differentiated HCCs may be hypo- or isovascular (Takayasu et al, 1986). Hypervascularity is usually present in higher-grade tumours greater than 2 cm in diameter, and establishing this condition from the low-flow state takes approximately a year (Ikeda et al, 1993). Since diagnostic arteriography relies on this aspect of HCC vascularity, its sensitivity depends on the size of the tumour. Arteriography is ineffective in tumours less than 1 cm in diameter; tumours 3 to 5 cm in diameter are detected with a sensitivity of 82 to 89%; and almost all larger tumours can be identified (Pavone et al, 1992).

1.4.1.2 Heterogenous permeability of tumour vessels

One of the major barriers to drug delivery is the tumour microvessel wall. In general, vascular permeability is much higher in tumours that in host tissues. However, the permeability of the wall to molecules is heterogeneous in tumours, in some regions tumour vessels are nearly impermeable whilst other regions are much more leaky than normal vessels (Yuan et al, 1994). The large pores in the vascular endothelium (Yuan et al, 1995) and discontinuity in the basement membrane (Bosman et al, 1985), presumably cause the leakiness of tumour vessels. These physiological properties of a tumour depend on its local environment. Tumours that are grown in a subcutaneous microenvironment have a tumour-dependent functional pore cut-off size ranging from 200 nm to 1.2 μm, which is dramatically reduced when the tumour is grown in a cranial microenvironment (Hobbs et al, 1998). In addition to size selectivity, the transvascular transport is influenced by the charge of molecules. Dellian et al, have demonstrated that positively charged molecules extravasate faster in solid tumours

compared to similar sized compounds with neutral or negative charges (Dellian et al, 2000).

1.4.1.3 Physico-chemical properties and hypertension of interstitium

The interstitial compartment presents a third barrier. The movement of molecules and particles depends on their size, charge and conformation and the physico-chemical properties of the interstitium. Movement through this compartment occurs by diffusion and convection. Unlike diffusion, which is unaffected by pressure gradients, convection is governed by them: fluid flows from areas of high pressure to areas of low pressure, carrying molecules with it. Small molecules such as oxygen and conventional chemotherapeutic agents (with a MW < 2000) migrate mainly by diffusion, whilst large molecules (with a MW > 5000), move mainly by convection. Diffusion coefficient (D) decreases with increasing MW of drug ($D \sim MW^{-n}$, $n \geq 1$). Thus, high MW drugs penetrate the interstitium slowly (Jain, 1999). The net transport of small molecules by diffusion may be further retarded as a result of binding to relatively large molecules that move at a much slower speed (Morrison et al, 1991).

The extracellular matrix (ECM) contributes to the drug resistance of a solid tumour. Tumour and stromal cells produce and assemble a matrix of collagens, proteoglycans (eg glycosaminoglycans [GAG]), and other molecules that hinder the transport of molecules. In normal tissues, resistance to water and solute transport is attributed to the amount of hydrophilic ground substance, predominantly GAG (Auckland and Nicalaynes, 1981; Comper and Laurent, 1978). Tumour tissue, however, possesses unique characteristics with extensive synthesis of ECM (Ronnov-Jessen et al, 1996), which leads to substantial differences in composition and assembly compared with the

host tissue. Recently, functional properties of ECM have been found to be correlated with total tissue content of collagen rather than GAG as previously thought (Netti et al, 2000). An extended collagen network was observed in the more penetration-resistant tumours studied.

Solid tumours also exhibit interstitial hypertension. In normal tissues, the pressure is approximately 0 mmHg, but in solid tumours it is uniformly higher, except at the periphery where it remains close to normal (Jain, 1996). A lack of functional lymphatics is a key contributor to interstitial hypertension. This has two effects: it reduces convection across the wall of tumour vessels and leads to steep pressure gradients from the tumour periphery to the surrounding host tissue. These gradients cause tumours to lose interstitial fluid, and along with it, therapeutic drugs, into the surrounding tissue.

1.4.2 Heterogeneity of tumour microenviromental characteristics

For chemotherapy to be successful it must be effective in the *in vivo* microenvironment. By the time a tumour has reached a detectable size, the cancer cells and their local microenvironments often become heterogeneous. Many microenviromental changes are the result of inefficient vascular function within the tumour, with subsequent gradients of critical metabolites such as oxygen (O_2), glucose, lactate and H^+ ions. Because of the selective pressure of the heterogeneous environments and the instability of the malignant genome, new and diverse cell phenotypes emerge with diverse responses to chemotherapeutic agents (Sutherland, 1988). Tumour growth is characterised by a phase of exponential cell proliferation followed by a phase of decreased growth rate associated with an increase in

nonproliferating (quiescent) cells and necrotic cells. Proliferating cells are usually located adjacent to functional blood vessels, whilst quiescent and necrotic cells are located at progressively greater radial distances from the vessels. The fraction of stem cells in human tumours is variable, but usually small (< 1%). These stem cells are targets for therapy, and from these cells resistant variants can emerge. Cloned stem cell lines from the same tumour often express a variety of cytotoxic sensitivities (Weichselbaum et al, 1986) (Figure 1.3).

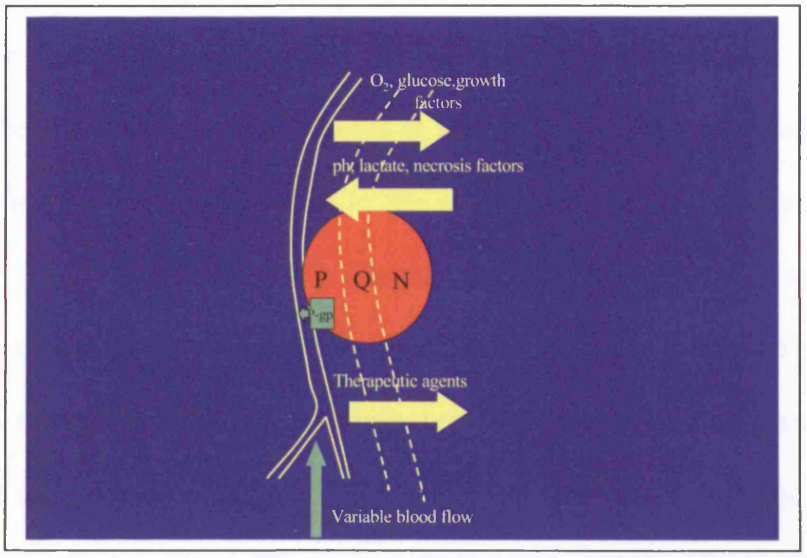

Figure 1.3. Factors contributing to the development of heterogeneous microenvironments and cells.

P, proliferating cells; Q, quiescent cells; N, necrotic cells; P-gp, P-glycoprotein.

Oxygen and pH are key microenviromental factors in the development and growth of tumours including their response to chemotherapy, their levels affecting tumour cell metabolism, glucose and O_2 consumption rates and tumour cell proliferation and viability (Casciari et al, 1992; Vaupel et al, 1989). Hypoxia can stimulate angiogenesis (Shweiki et al, 1992) as well as induce tumour cell apoptosis (Shimizu et al, 1996), thereby affecting tumour growth. The selective microenviromental characteristics displayed by tumours, such as interstitial acidity or hypoxia, can be either advantageous or unfavourable for cancer treatment depending on which modality is considered. The situation is even further complicated by intra- and intertumour variations in interstitial pH and pO_2. Hypoxic tumour cells are well known to be radiation resistant (Hockel et al, 1993). During chemotherapy, hypoxia can either aid cytotoxicity such as in the case of bioreductive drugs (Chaplin and Acker, 1987) and alkylating agent's (Skarsgard et al, 1995), or inhibit cytotoxicity, as with bleomycin or actinomycin D (Teicher et al, 1981). Similarly, acidic pH potentiates the cytotoxicity of alkylating agents (Jahde et al, 1989) and weak acids (Gerweck and Seetharaman, 1996) and decreases the cytotoxicity of other chemotherapeutic drugs (ie. adriamycin and bleomycin) (Wike-Hooley et al, 1984).

1.4.3 Intrinsic and acquired drug resistance

At a cellular level, CRC and HCC are often intrinsically resistant to multiple chemotherapeutic agent's (Kaufmen and Chabner, 1996; Nerenstone et al, 1988). Frequently they respond to initial treatment but acquire chemoresistance. A classic example occurs during the treatment of CRC with 5-FU in which first line treatment usually gives a 23% response rate, but second line therapy only achieves 7% response. The mechanism of resistance to this antimetabolite is known to be increased levels of

TS enzyme, the drug target, and 7-dihydrofoloate reductase, which is involved in metabolising the drug (Cole and Tannock, 2004).

The mechanisms of drug resistance are not fully understood. Undoubtedly, most resistant tumours have acquired a number of overlapping mechanisms for avoiding the toxic effects of chemotherapy. The most widely accepted hypothesis for development of acquired drug resistance is that cancer cells accumulate random spontaneous mutations and positive selection of these resistant cells carries clinical drug resistance (Kaufmen and Chabner, 1996).

It has long been recognised that simultaneous resistance to many seemingly structurally and functionally unrelated compounds can occur. These drugs are predominantly natural, or semisynthetic lipophilic, relatively large, heterogenous molecules including the *vinca* alkaloids (vincristine and vinblatine), epipodophyllotoxins (etoposide and teniposide), anthracyclines (doxorubicin and daunomycin), colchicine and taxols. Such cells are referred to as displaying a multidrug resistant phenotype (MDR) (Gottesman and Pastan, 1993). The term MDR covers a number of different mechanisms, including interference with the apoptotic pathway – such as inactivation of p53, expression of energy-dependent pump systems-such as P-glycoprotein (P-gp) or multidrug resistance associated protein (MRP), alteration in topos, or a combination of these (Figure 1.4).

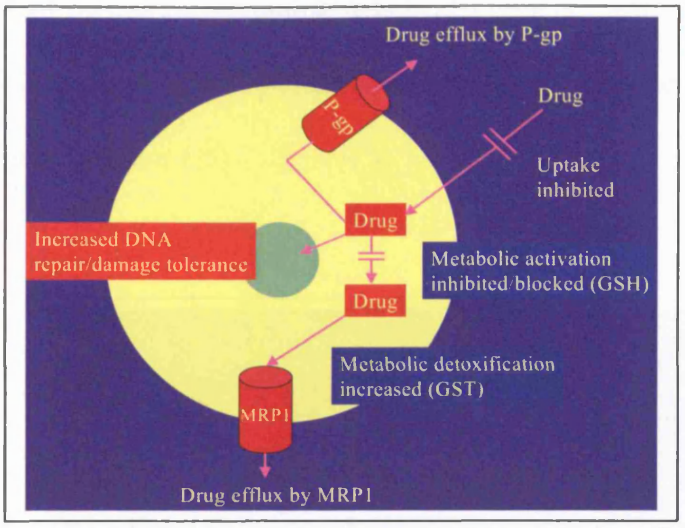

Figure 1.4. Summary of the major mechanisms of multidrug resistance.

1.4.3.1 P-glycoprotein (P-gp)

The best characterised form of drug resistance to date, usually referred to as classical MDR, is that mediated by the *MDR-1* gene. The protein product of *MDR-1* is P-gp which belongs to a super family of adenosine triphosphate (ATP)-binding cassette (ABC) transport proteins (Gottesman et al, 1996). As a result of P-gp expression, tumour cells exhibit an increased efflux of many cytotoxic agents with subsequent reduced intracellular accumulation resulting in insufficient drug levels for adequate anti tumour activity to occur (Kiehntopf et al, 1994).

There are two MDR genes identified in humans *MDR-1* and *MDR-2*, and three in mice. Only the product of *MDR-1* (P-gp) is associated with drug resistance (Cole and Tannock, 2004). P-gp is a cell surface glycoprotein of 170 kDa, which is located primarily in the plasma membrane. The molecule consists of two homologous transmembrane domains connected by a short joining section. Each domain consists

of three pairs of membrane-spanning α-helical segments, with the N- and C-termini on the cytoplasmic side of the membrane and three extracellular and two intracellular loops per domain (Figure 1.5).

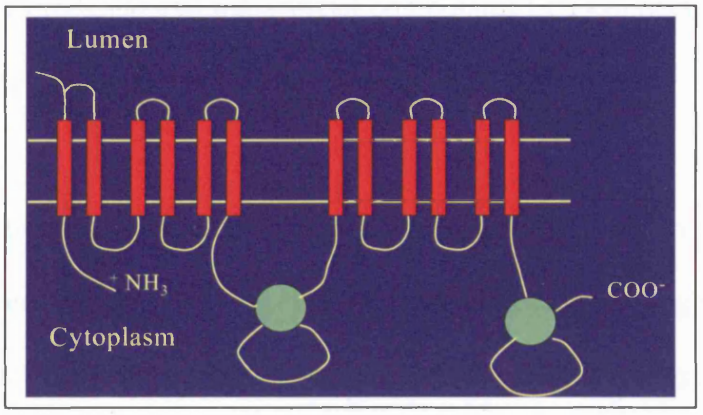

Figure 1.5. Proposed structure of P-gp.

Although there is considerable evidence that P-gp is involved in removal of chemotherapeutic drugs from the cell, the exact mechanism by which this occurs is unknown. The most prevailing hypothesis is that P-gp functions as a pore-forming protein, which acts in an energy dependent manner to export compounds. The identification of ATPase activity associated with P-gp provides a mechanism by which energy may be transduced for active drug efflux. This hypothesis, however, leaves a number of aspects not fully explained, such as the broad substrate specificity observed for P-gp, and the inability to correlate the initial rate of transport with the P-gp concentration. It has also been proposed that P-gp acts as a 'hydrophobic vacuum cleaner' by removal of compounds directly from the plasma membrane before they reach the cytosol (Gottesman et al, 1996). Under this model the primary determinant of substrate specificity would be the ability of a compound to interact with the lipid

bilayer and the secondary determinant would be its ability to interact with the binding site of the transporter. This is consistent with the observation that substrates for P-gp are lipophilic and that the major determinant of a particular substrate to be transported by P-gp is its relative hydrophobicity. Photoaffinity labelling, mutational analysis and inhibitor studies indicate that transport of compounds by P-gp occurs through a single barrel of the transporter (Figure 1.6).

Direct correlation has been found between the content of P-gp in the cell membrane and the degree of resistance to the selecting drug, with high levels found in chemoresistant CRC and HCC's (Cole and Tannock, 2004). P-gp overexpression in human tumour cells results in resistance to antracyclines, such as doxorubicin, to epipodophyllotoxins, such as etoposide, and to vinca alkaloids, taxoids, topotecan, and actinomycin D, but not to many of the other clinically important drugs, such as alkylating agents, cisplatin, methotrexate (MTX), and purine and pyrimidine analogues. Kiehntopf et al, reported a hammerhead ribozyme specifically recognising and cleaving the *MDR-1* mRNA (Kiehntopf et al, 1994). Liposome-mediated transfer of the ribozymes into MDR cell lines resulted in significantly reduced expression of the *MDR-1* gene, and reversed the multidrug resistance phenotype, restoring sensitivity to cytotoxics. Many drugs including verapamil (vpm), quinine, cyclosporin A and its non-immunosupressive analogue PSC-833, inhibit P-gp mediated drug efflux in cancer cell lines (Ford and Hait, 1990; Gottesman and Pastan, 1993). These chemosensitising agents act as competitive inhibitors and correct accumulation defects thus restoring drug sensitivity in MDR cell lines.

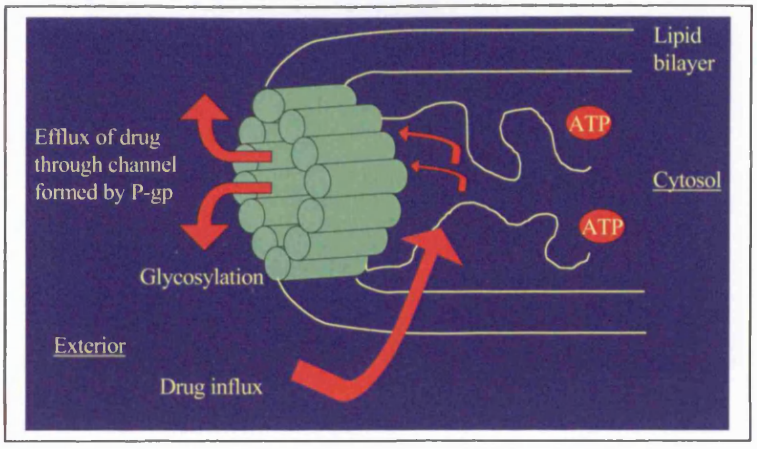

Figure 1.6. Schematic diagram of the proposed structure of P-gp, which functions as an energy-dependent drug efflux pump.

1.4.3.2 Multidrug resistance associated protein (MRP)

The MRPs are also members of the ABC superfamily of transport proteins. The *MRP* gene has been mapped to chromosome 16 at band p13.13-13.12, and is amplified relatively frequently in drug-selected human cell lines that over-express *MRP* mRNA. *MRP* is now known to be one of six genes that make up a family of multi-specific organic anion transporters (MOAT) (Lee et al, 1998). MRP1 now designates the original 190 kDa glycoprotein MRP, while both MRP2 (canalicular MOAT [cMOAT]) and MRP3 (MOAT-D) have been cloned and transfected into drug sensitive cells resulting in resistance to cisplatin, anthracyclines, etoposide, MTX; and vinca alkaloids, etoposide and MTX respectively (Ross, 2000). MRP1 is located at the basolateral side of epithelial cells and is believed to have an unusual arrangement of the membrane domains with five additional transmembrane domains at the N-terminus (Figure 1.7).

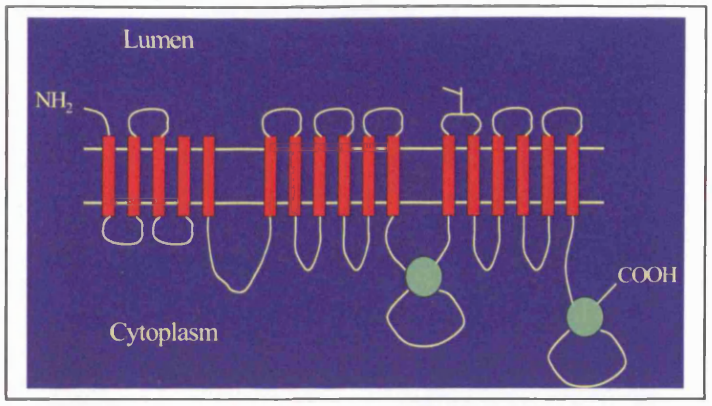

Figure 1.7. Proposed structure of MRP1.

It produces a similar range of resistance to that of P-gp, except to mitoxantrone (Futscher et al, 1994).

MRP transport relies on the presence of glutathione (GSH) with drug substrates being transported as either GSH conjugates or co-transported with GSH. Depletion of GSH with buthionine sulfoxamine (BSO) sensitises MRP over expressing cells to drugs that are transported by MRP (Lautier et al, 1996).

1.4.3.3 Lung resistance related protein (LRP)

A further protein, found in many MDR cells not overproducing P-gp, is LRP (Scheper et al, 1993), which has been identified as the human vault protein (Scheffer et al, 1995). Vaults are novel cellular organelles, broadly distributed and highly conserved among diverse erythropoeitic cells. They localise to nuclear pore complexes, thus are involved with intracellular transport (Figure 1.8).

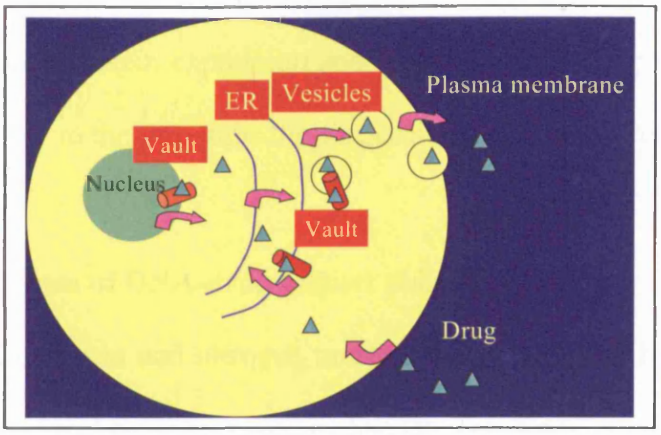

Figure 1.8. Hypothetical role of LRP in drug-resistance. LRP/vaults may mediate nucleocytoplasmic and vesicular transport of drugs. Through exocytotoxic vesicles the drugs would be extruded from the cell.
ER = endoplasmic reticulum.

The overexpression of LRP alone in transfected drug sensitive cells does not result in drug resistance (Scheffer et al, 1995), as this does not increase the number of intracellular vaults. The overexpression of vaults results in sequestration of therapeutic drugs within the vaults, preventing interaction with their targets. Conflicting reports exist as to the significance of overexpression of LRP in prognosis of haematological malignancies.

1.4.3.4 Atypical multidrug resistance (at-MDR)

At-MDR refers to cells with altered topo II activity (Beck, 1990). At-MDR cells show cross-resistance to topo II poisons and "pure" at-MDR cells are not resistant to vinca alkaloids, they have no change in P-gp expression or in drug accumulation, but show altered topo II activity by quantitative or qualitative means. Topo II alterations are complex, and numerous facets of the mechanisms involved remain unexplained

(Danks et al, 1993; Perrin et al, 1998). The main mechanisms of resistance are reduction in topo II protein expression and activity, both having the effect of limiting the target available to the drug thus limiting damage within the cell.

1.4.3.5 Mechanisms of DNA-drug adduct resistance

Mechanisms of cisplatin and nitrogen mustard resistance have been postulated to be associated with several different cellular changes including:

1.4.3.5.1 Reduced intracellular accumulation

The development of cisplatin resistance has been associated with decreases in intracellular accumulation. When decreases are observed they are usually modest, even if the level of resistance is high. To date, the search for a specific cisplatin membrane transport system has been inconclusive. Andrews and Howell (Andrews and Howell, 1990), noted that uptake was not saturable up to the solubility limit of cisplatin (3.3 mM), thus even if a transport system does exist it is either a low affinity site or very abundant.

1.4.3.5.2 Increased drug inactivation by intracellular thiols

Intracellular non-protein sulfhydryl GSH has multiple functions in catalysis, transport and reductive phenomena. Moreover, it reacts with toxic endogenous and exogenous substances, including free radicals and chemotherapeutic agents. These functions are important in drug resistance with agents such as nitrogen mustards (Arrick and Nathan, 1984) and cisplatin (Ishikawa and Ali-Osman, 1993).

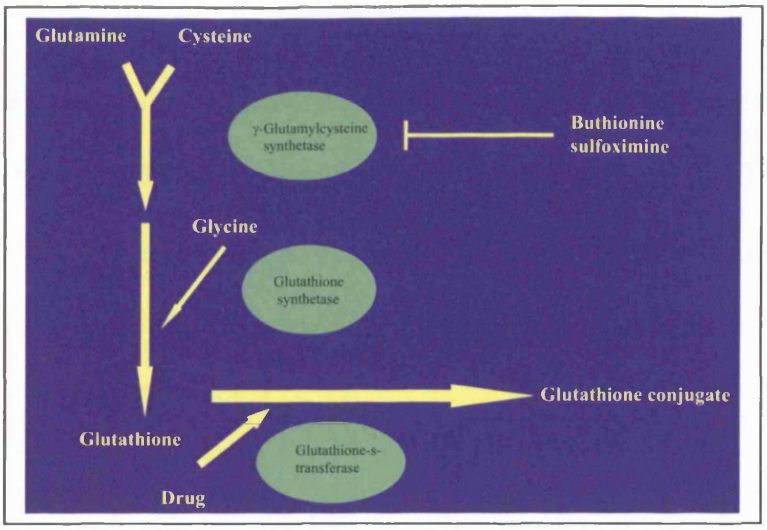

Figure 1.9. Simplified scheme of the glutathione synthesis pathway and conjugation of glutathione to drugs catalysed by glutathione-S-transferase.

GSH is a tripeptide of glycine, glutamic acid and cysteine which is synthetised intracellularly by two ATP-dependent catalytic reactions, involving γ-glutamylcysteine synthase (γ-GCS) and glutathione synthase. The rate-limiting step of GSH synthesis is catalysed by γ-GCS and is feedback inhibited by GSH (Figure 1.9).

As a potent nucleophile, GSH reacts with alkylating agents and evidence exists that the resulting GSH-S conjugate is then eliminated from the cell by an ATP-dependent GSH-S conjugate export pump (Ishikawa and Ali-Osman, 1993). GSH may protect cells by intercepting alkylating agents before they interact with DNA, certainly acquired resistance to alkylating agents is often accompanied by an elevation in GSH. Melphalan-resistant leukaemia cells have a 2 to 4-fold higher level of GSH than their sensitive parental cells (Somfai-Relle et al, 1984), whilst Ozols and his colleagues have demonstrated that ovarian cancer cell lines resistant to adriamycin, cisplatin and

other various alkylating agents have increased GSH levels (Behrens et al, 1987; Green et al, 1984; Rogan et al, 1984). Furthermore, lowering GSH levels by treatment with the γ-GCS inhibitor, BSO, can potentiate the activity of melphalan (Ozols et al, 1987) and cisplatin (Meijer et al, 1992). However, cisplatin is not invariably affected by BSO, suggesting there are other cellular mechanisms of resistance (Andrews et al, 1985).

1.4.3.5.3 Enhanced repair of DNA-drug adducts

DNA repair encompasses the molecular reactions that eliminate damaged or mismatched nucleotides from DNA. Five broad categories of DNA repair mechanisms exist:

1) Direct repair, using specific enzymes such as O^6-methylguanine-DNA methyl transferase (MGMT), to repair specific but directly reversible types of damage. The chemical bond linking the base to a substituent is broken leaving the base in situ in the DNA strand (Sancar, 1996).
2) Base excision repair, the single damaged nucleotide is removed in two steps. First, the modified base is released by a glycosylase, this cleaves the glycosylic bond linking the deoxyribose to the base, then the abasic sugar is released by a pair of apurinic or apyrimidinic (AP) endonucleases.
3) Nucleotide excision repair (NER), most DNA damage is repaired by the NER system which recognises DNA adducts induced by numerous chemical treatments (Wood, 1996). This mechanism, now well characterised, is known to consist of two distinct major steps: (i) the incision reaction involving damage recognition and excision of the damaged oligonucleotide or base, and (ii) repair synthesis of new DNA using the complementary strand as a template and its subsequent

ligation to restore strand continuity (Ma et al. 1995; Sancar, 1996; Wood, 1996). Human genetic defects in NER have been found in association with xeroderma pigmentosum (XP), Cockayne's syndrome (CS) and Trichothiodystrophy (TTD) (Ma et al, 1995; Sancar, 1996). In each of these diseases, several complementation groups have been defined from XPA to XPG, from TTD1 to TTD3, and CSA and CSB. These have been assigned to 11 complementation groups and so far have allowed the cloning of 6 human NER genes. Another class of laboratory-induced mammalian UV-sensitive NER-deficient mutants has been obtained from cultured rodent cells (Collins, 1993). These have been designated as excision repair cross-complementing genes (ERCC). Each of these genes and their corresponding proteins have been the subject of numerous studies aimed at describing NER at a molecular level (Sancar, 1996; Wood, 1995), this can be summarised as follows (Figure 1.10):

(i) The NER mechanism is initiated by XPA, which binds to the damaged site. XPE was also proposed as a protein involved in the recognition step. However, several studies have shown that XPE is not essential for this step (Sancar, 1996). The binding of XPA facilitates entry of the replication protein A (RPA) and forms a complex with it.

(ii) This complex then recruits transcription factor IIH (TFIIH) and ERCC1/XPF complexes.

(iii) The helicase activity of XPB and XPD contained in the TFIIH locally unwinds DNA. The structural modification(s) of DNA induced by this unwinding facilitates the 5' incision made by the ERCC1/XPF. Similarly, XPA/TFIIH recruits XPG which makes the 3' incision.

(iv) Repair synthesis is then carried out by the pol-δ and/or -ε which requires proliferating cell nuclear antigen (PCNA) and replication factor C (RF-C) to form a DNA synthesis complex as in DNA replication.

(v) Finally, the repair patch is sealed by a ligase, most likely ligase I.

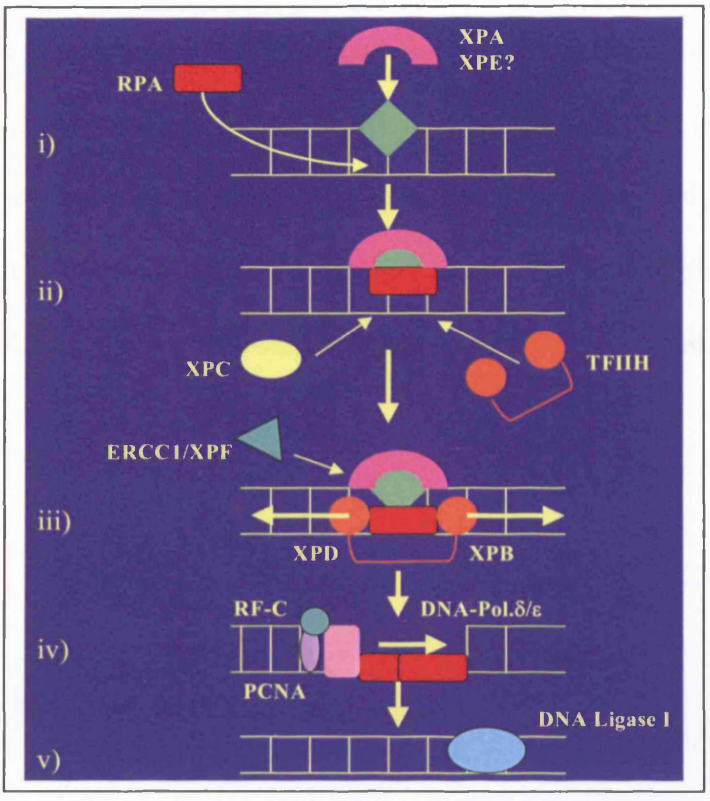

Figure 1.10. Model for human NER.

XPA-E, xeroderma pigmentosum A-E; RPA, replication protein A; TFIIH, transcription factor IIH; ERCC, excision repair cross-complementing gene; RF-C, replication factor C; PCNA, proliferating cell nuclear antigen.

4) Mismatch repair, this process detects and repairs mismatches in base pairing that disobey Watson-Crick rules, as occurs during recombination and replication events (Modrich, 1994). An ATP-dependent multisubunit nuclease removes the mismatch in the form of a mononucleotide. The resulting ss gap is filled by DNA polymerase δ or ε and closed by DNA ligase. The mismatch repair process was not thought to be involved in repair of DNA-drug adducts, however one compartment was found to bind to cisplatin intrastrand crosslinks (Duckett et al. 1996), implicating it in the repair of the lesion. Subsequently, it has been found this is due to the mechanism repairing mismatch lesions, rather than cisplatin adducts, that have occurred during replicative bypass (DNA replication occurring around cisplatin adducts without their removal) (Yamada et al. 1997) (Figure 1.11).

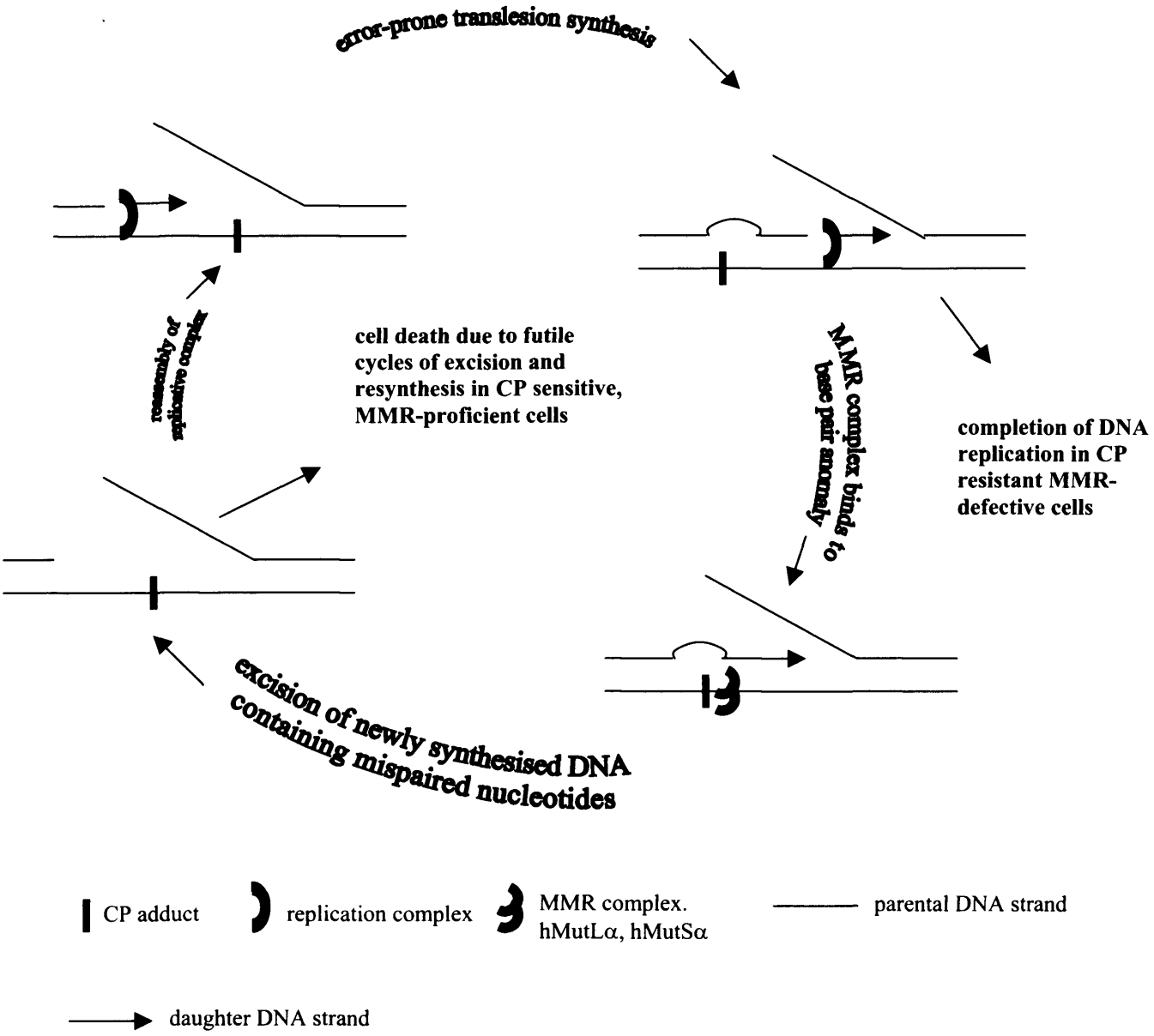

Figure 1.11. Proposed model for the contribution of mismatch repair activity to cisplatin cytotoxicity. DNA replication past cisplatin adduct results in imperfect base pairing. This anomaly is recognised by the hMutLα/hMutSα mismatch repair complex. Attempted mismatch repair fails because it is directed at the daughter strand. Thus, the newly synthesised strand is removed, and the lesion on the parental remains unexcised. The continued action of these futile replication/repair cycles results in the formation of gaps or strand breaks, which lead to cell death. An inability to initiate mismatch correction would be beneficial to the cell, because these futile repair attempts would be avoided.

5) Recombinational repair, this poorly understood mechanism is required for rejoining DNA ds breaks whilst preserving DNA fidelity. Double strand breaks can either be repaired with no check on integrity of the DNA code (non-homologous end joining), or be repaired accurately using information contained in homologous regions on another chromosome or sister chromatid for reference (homologous recombination) (Takata et al. 1998).

Many pt-resistant cell lines appear to have enhanced repair activity based on the rate of disappearance of pt-adducts (Masuda et al, 1990; Parker et al, 1991), and the rate of disappearance of ICLs (Chen G et al, 1992; Zhen et al, 1992). The pathway is capable of repairing both pt-monoadducts and pt-intrastrand diadducts in vitro, with a preference for the repair of monoadducts compared with intrastrand diadducts (Page et al, 1990; Szymkowski et al, 1992). The repair of pt-ICLs represents a specific challenge for DNA repair mechanisms. ICLs are large lesions, and as such are substrates for the NER mechanism. As both strands of DNA are damaged, however, NER alone cannot perform the process because excision of both strands would be required. At present, evidence points to a mechanism combining components of NER and homologous recombination. In rodent cells studied in vitro, this process has been shown to require the XPF-ERCC1 complex a heterodimer involved in NER (Thompson, 1996).

Since ICLs appear to be the major cytotoxic lesions for nitrogen mustards, it is logical that the NER and recombination pathways should be critical in repair of cytotoxic nitrogen mustard lesions. Cells lacking XPF-ERCC1 are hypersensitive to HN_2 (Hoy et al, 1985) and several pt-resistant cell lines characterised by an increase in the rate

of pt-adduct removal also show partial cross-resistance to melphalan and other nitrogen mustards (Kelland et al, 1992). Taken together these data suggest enhanced NER and/or recombination in resistance to nitrogen mustards has a role.

1.4.3.5.4 Increased platinum-DNA damage tolerance

Enhanced replicative bypass, defined as the ability of the replication complex of a cell to synthesise DNA past the site of DNA damage, has been suggested to have a potential role in cisplatin resistance (Mamenta et al, 1994), leading to increased DNA damage tolerance. Defects in mismatch repair are associated with cisplatin resistance (Fink et al, 1996). In an intact mismatch repair system futile cycles of translesion synthesis past cisplatin-DNA adducts followed by removal of the newly synthesised DNA eventually leads to cell death. Thus, an inability to initiate mismatch correction would be beneficial to the cell, because futile repair attempts would be avoided (Figure1.11). Five genes encode proteins required for mismatch repair, of these defects in hMLH1 or hMLH6 result in 1.5 to 4.8-fold increased cisplatin resistance and 2.5 to 6-fold increased replicative bypass of cisplatin adducts (Vaisman et al, 1998).

1.5 Models to study the effect of chemotherapy

Recent insights and discoveries in cancer biology have dramatically increased knowledge of this disease. The knowledge gained in the existence of tumour suppressor genes, critical genes and proteins involved in tumourogenesis and progression has led to a number of new strategies being developed to systemically treat metastatic disease. The resulting agents include monoclonal antibodies,

cytokines, antisense oligonucleotides and gene-specific targeted therapeutics (Brown et al, 2000). These strategies have been shown to produce a potent effect on cancer cells *in vitro* and in some *in vivo* tumour models, however, clinical results to date have been disappointing. For any therapy to be successful it must first reach target cells *in vivo* in optimal quantities and second, be effective in the *in vivo* microenvironment of the malignant phenotype (Jain, 1996).

1.5.1 *In vitro* models

Traditionally, the effect of chemotherapeutic agents is gained through the study of standard two dimensional monolayer cultures *in vitro*. Cells in tissue culture incubated with an agent in a well-controlled homogenous environment, however, are not adequate to describe damage produced in cells exposed in a solid environment. One approach to studying the biology of tumour micro-regions is to culture cancer cells in the form of three-dimensional multicell spheroids that simulate micrometastases or intervascular micro-regions of larger tumours (Olive et al, 1997). This tumour model is intermediate in complexity between standard two-dimensional monolayer cultures and tumours *in vivo*. Spheroids grown from tumour cell lines or directly from primary tumour specimens, show growth kinetics similar to tumours *in vivo*. As growth progresses, the number of cells that are proliferating decreases, and the proportion of non-proliferating (quiescent) cells increases. When cells become deprived of O_2, glucose, and other substrates, and when toxic metabolic waste products accumulate, there are steep gradients in these metabolites, and cell death and necrosis occurs in the centres of the spheroids. Over small distances of approximately 10-20 cell diameters (equivalent to the radial distance from small blood vessels in tumours) significant differences in cell microenvironment develop. Generally, most of

the proliferating cells in spheroids are located in the outer 3-5 cell layers. The quiescent cells are located more centrally and include a significant proportion of cells that are reproductively viable when removed from these environments. These cells can be recruited to repopulate the proliferating compartment. Sub-populations of cells from the peripheral or central regions of the spheroids can be isolated to study their biological properties and response to therapeutic agents. Major differences in sensitivity to drugs attributable to effects on accessibility and uptake as well as local microenvironments have been demonstrated in tumour cells grown as spheroids (Olive et al, 1997).

1.5.2 *In vivo* models

The National Cancer Institute (NCI) using three mouse tumours, a leukaemia, a sarcoma and a carcinoma created the first animal models (Gura, 1997). Agents that were effective against the mouse tumours, however, failed when used against equivalent human tumours. To overcome this, xenograft models were developed using implanted human tumours in Severe Combined Immunodeficiency (SCID) mice. Although these indicate the contribution of local microenvironment to chemotherapy distribution and response, they do not behave like naturally occurring human tumours. Often drugs effective in xenografts are ineffective in humans, whilst effective drugs are often missed. The NCI recently tested 12 chemotherapeutic agents currently used clinically against 48 human cancer xenografts, 30 of the tumours did not respond significantly (ie. > 50% reduction in tumour size) to any of the agents (Gura, 1997).

In order to create better models of cancer development in humans, similar genetic alterations (ie. activation of cancer promoting oncogenes or deletion of tumour

suppressor genes) have been produced in mice, with the intention of producing tumours that behave like human tumours. Results to date have been mixed. In humans the deletion of the retinoblastoma (*RB*) tumour suppressor gene produces cancer of the retina, and loss of the *BRCA1* gene causes human breast and ovarian cancer. Similar gene alterations in mice lead to pituitary gland tumours and no tumours respectively (Gura, 1997).

The above models usually rely on measuring changes in tumour size and survival secondary to chemotherapy. Drug concentration or gene expression is usually measured with techniques that have no spatial resolution to analyse the physico-chemical or physiological barriers that lead to heterogeneous drug delivery and cytotoxic effects in solid tumours, or require tumour removal thus missing the temporal dynamics. To obtain detailed insight into blood flow and distribution of drugs in a tumour, various modified versions of "window" techniques have been utilised (Jain, 1996). Tumour cells are implanted in either the ear of a rabbit, or the brain or dorsal skin of a rodent and covered with a glass cover slip, the resulting tumour grows against the glass and can be observed directly. The use of *in vivo* microscopy has been used to provide information on angiogenesis and blood flow (Jain et al, 1998; Leunig et al, 1992), vascular permeability (Yuan et al, 1996) and interstitial pH and pO_2 (Helmlinger et al, 1997) continuously and non-invasively.

In situ perfused solid tumour preparations were originally developed in rodents to study primarily rodent tumours by Gullino in 1961. Essentially each cancerous mass is connected to the circulatory system by a single artery and single vein, providing control over physiological, biochemical and pharmacological composition of the

arterial input and easy access to the venous output. This allows studies of transport and metabolism in solid tumours. This model has been adapted to the nude mouse allowing perfusion of human tumour xenografts implanted in ovarian fat pads (Kristjansen et al, 1994). It has been used to study tumour uptake of anthracyclines and subsequent clearance in human colon adenocarcinomas (Heijn et al, 1999), and the relationship between tumour physiology and the pharmokinetics of gemcitabine in human small cell cancer (Kristjansen et al, 1996).

1.5.3 Mathematical models

Biodistribution studies are expensive and difficult to carry out in humans, but such data can be easily obtained in rodents. Mathematical modelling uses physiological parameters such as organ volumes, blood flow rates and vascular permeabilities, the so-called compartments (organs) are connected anatomically. Such a physiologically based pharmokinetic model can be used for scaling up data from mice to humans. Baxter et al, devised a model for the biodistribution of mouse anti-bodies against CEA (Baxter et al, 1995). The model was found to be useful for optimisation of treatment parameters, such as dose and time interval for injections, binding affinities and choice of molecular carrier when tested with data obtained in human patients.

1.5.4 Methods to obtain data from human tumours

Drug resistance is considered to be the major obstacle to success in cancer chemotherapy, thus considerable effort has been made to identify tumours likely to be, or to become, resistant to the chemotherapy protocol of choice (Bellamy, 1992).

1.5.4.1 *In vitro* assays

Generally, such 'chemosensitivity testing' relies on comparative or quantitative estimates of cell growth in tissue culture, in the presence of a range of test concentrations of drugs of choice. The practical problems of processing tumour biopsies, waiting for assay results and planning therapy based on their results make most of these approaches difficult to use (Von Hoff, 1990). In addition, other considerations include whether a single biopsy is representative, whether response *in vitro* reflects that *in situ* and whether 'averaging' for the biopsied cell population overlooks small but resistant subpopulations.

1.5.4.2 **The comet assay** (The single-cell gel electrophoresis technique)

Unlike other approaches, the comet assay is single cell based and therefore provides information not only on the overall response of the sample (the mean or median response), but also on the heterogeneity inherent within each specimen thus indicating the presence of unusually resistant subpopulations (Olive et al, 1990; Olive et al, 1993). Multiple samples can be taken throughout therapy, and as only a few thousand cells are required, the assay can be performed with tumour cells obtained from procedures as minimally invasive as fine needle aspirate (FNA) biopsies. Olive et al, have quantified the hypoxic fraction in human breast cancers receiving radiotherapy using FNA biopsies only (Olive et al, 1993). The reduced sample size, however, potentially limits its representativeness. As the assay can be modified to detect DNA ss breaks, ds breaks and cross-links, it is applicable to a wide variety of chemotherapy agents (Fairbairn et al, 1995).

Hypoxic cells in solid tumours are resistant to killing by ionising radiation and some forms of chemotherapy. The use of the comet assay to detect hypoxic cells, is based on the fact that ionising radiation produces three times more DNA strand breaks in aerobic than hypoxic cells. Although subject to some limitations, intratumour oxygenation, modification of hypoxia by various means, and rates of re-oxygenation after treatment are important properties of solid tumours that can be addressed in specific patient populations using this method (Olive et al, 1993). Studies using the comet assay with multicell tumour spheroids and murine tumours, indicate that the extent of DNA damage caused by chemotherapeutic agents correlates with eventual tumour cell kill (Olive et al, 1996). Furthermore, tumour cells that have lost the ability to undergo rapid apoptosis are typically more resistant to killing by ionising radiation and other DNA damaging agents. The comet assay is able to detect apoptopic cells based on the appearance of the cell following lysis and electrophoresis. Apoptosis results in extensive fragmentation of DNA, thus most of the DNA is able to migrate. The appearance of apoptopic and necrotic cells are often similar using this method, however, titration with a DNA cross-linking agent can provide information on fragment size that can be useful in distinguishing between the two.

Up to 90% of solid tumour may be quiescent, and thus are resistant to anti-metabolites and mitotic spindle poisons. Measurement of the proportion of non-cycling cells in samples from solid tumours is possible by a brief *in vitro* exposure of tumour cells to the topo II inhibitor, etoposide. DNA breaks are produced by etoposide in proliferating cells, but not in quiescent cells (Olive and Banath, 1992).

1.5.5 *Ex vivo* isolated organ perfusion systems

The isolated perfused rat liver (IPRL) has been used for over 100 years to explore the physiology and pathophysiology of the liver (Miller, 1972). Its popularity is due to the fact that, in contrast to *in vivo* models, it allows repeated sampling of the perfusate and liver, permits easy exposure of the liver to different concentrations of test substances and is amenable to alterations in temperature that would not be tolerated *in vivo*. Furthermore, experiments can be done independent of the influence of other organ systems, plasma constituents and neural-hormonal effects. In contrast to the other *in vitro* models, hepatic architecture, cell polarity and bile flow are preserved in the IPRL. Normothermic extracorporeal perfusion of porcine livers have recently been shown to preserve liver function between 4 to 24 h and can reverse up to 1 h of warm ischaemic injury (Schon et al, 1993; St Peter et al, 2002).

Although chemotherapy has not been applied, primary human colorectal carcinomas have been perfused *ex vivo* in order to determine the geometric flow resistance (1-2 orders of magnitude higher than that observed in normal tissues) and microvascular network architecture of human tumours (Less et al, 1997). In addition, isolated perfused *ex-vivo* whole cirrhotic and normal human livers have been used to study hepatic micro-circulation and drug elimination (Villeneuve et al, 1990; Villeneuve et al, 1996a). More recently *MDR1* gene expression in pulmonary sarcoma metastases has been examined after acute *in situ* exposure (via isolated lung perfusion) to cytotoxic chemotherapy (Abolhoda et al, 1999).

Research Aims

To develop an isolated, perfused and oxygenated human liver tumour model to investigate the short term effects of chemotherapeutic agents used in the treatment of liver cancer by:

1. Assessing *in vitro* intrinsic drug resistance in HCC and CRC cell lines using first FACScan analysis to determine the expression of MDR related transporter proteins and P-gp function when present, second an enzymatic recycling procedure to evaluate the contribution of GSH and third the comet assay to examine the role of enhanced DNA repair.
2. Establishing an orthotopic model of human liver cancer in nude mice to evaluate the topographic distribution of cisplatin DNA-adducts by the comet assay *in vivo,* and correlating this with tumour proliferation, hypoxia, vascularity and P-gp expression determined using immunohistochemistry.
3. Creating an intrahepatic xenograft of human CRC in nude rats and developing an isolated dual-perfused rat liver model to assess the spatial and temporal pattern of drug induced DNA damage using the comet assay.
4. Developing an isolated, perfused and oxygenated human liver tumour model using liver specimens obtained from patients undergoing hemihepatectomy for either HCC or CRC and studying the spatial and temporal pattern of drug induced DNA damage using the comet assay.

CHAPTER II

MATERIALS AND METHODS

II. MATERIALS AND METHODS

2.1 Introduction

To assess *in vitro* intrinsic drug resistance in HCC and CRC cell lines, the Sulforhodamine B (SRB) assay provided a rapid and sensitive method for measuring drug-induced cytotoxicity in attached cell cultures. To examine the contribution of MDR related transporter proteins to drug resistance, fluorescence-activated cell scanner (FACScan) analysis enabled simultaneous quantitative determination of P-gp, MRP1 and LRP protein expression, quantitative assessment of active P-gp drug efflux, and the effect of known modulators of P-gp function. The comet assay allowed assessment of cytotoxic induced DNA damage on only a few thousand cells, thus it could be applied to both *in vitro* tumour cells, and cells obtained from procedures as minimally invasive as fine-needle aspirate (FNA) biopsies *in vivo*. As the assay could be modified to detect DNA single-strand breaks, double-strand breaks and crosslinks, it was applicable to a wide variety of chemotherapy agents.

2.2 Reagents and solutions

The details of the reagents and solutions used in the experiments are listed in Appendix 2.1. Most of the stock solutions used in this study were prepared according to the manufacturers' instructions, unless otherwise stated. The materials used in each experiment, whether cell culture or molecular biology techniques, were carefully selected to conform to standard laboratory safety procedures. The processes of cleansing or sterilisation either before or after *in vitro* or *in vivo* experiments were strictly adhered to according to the manufacturers' instructions and/or the local laboratory codes of practice.

2.3 Drugs

The details of the drugs used in the experiments are listed in Appendix 2.2. All aqueous stock solutions were prepared using ddH_2O. Multiple aliquots were stored between 15-25°C, with the exception of vincristine (stored between 2-8°C) and mechlorethamine (nitrogen mustard, [HN_2]) (stored at –20°C), to provide uniform samples for initial tests as well as retests, if required. Melphalan stock solution was prepared from freeze dried powder immediately prior to use due to its instability whilst stored. Drug solutions were prepared immediately prior to use by diluting the stock solution with serum-free Minimum Essential Medium, MEM (Gibco BRL, Life Technology, Paisley) to the required concentrations. Unused solutions and discarded supernatants were disposed of into alkali solution to inactivate any residual material.

2.4 Cell lines and cell culture

The human hepatic adenocarcinoma cell lines used were; HepG2, established from a 15-year-old Caucasian male; C3A, a clonal derivative of HepG2; SKHep-1, derived from ascitic fluid in a 52-year-old Caucasian male; Hep3B, derived from an 8-year-old Negro male and PLC/PRF/5. The human colonic adenocarcinoma cell lines used were; SW620, established from a lymph node of a 51-year-old Caucasian male; HT-29, isolated from a primary tumour in a 44-year old Caucasian female; CACO2, isolated from a primary tumour in a 72-year-old Caucasian male and WIDR derived from a primary rectosigmoid adenocarcinoma of a 78-year-old female. All cell lines were purchased from the European Collection of Cell Cultures, Salisbury, Wiltshire, UK. The human T-lymphoid multidrug resistant cell line, CEM/VLB_{100}, used as a P-gp positive control, was a gift from K.Ganeshaguru, Royal Free Hospital and University College School of Medicine, London, UK. Hep-G2, SKHep-1, Hep3B,

CACO2 and WIDR were cultured in EMEM (EBSS) with 2 mM L-glutamine and 1% non-essential amino acids (NEAA), C3A had 1 mM NaP added to the above. PLC/PRF/5 and CEM/VLB_{100} were cultured in Dulbeccos Modified Eagle Medium (DMEM) and 2 mM L-glutamine, SW620 in L-15 and 2mM L-glutamine and HT-29 in McCoy's 5a with 2 mM L-glutamine. All culture medium was supplemented with 10% heat-inactivated foetal calf serum (FCS), penicillin and streptomycin. All culture medium and reagents were obtained from Gibco-BRL, Life Technologies, UK.

To maintain healthy and contamination-free cultures, all procedures were carried out in a Class II laminar flow cabinet and all materials were sterile. Adherent cells were grown as monolayers in an atmosphere of 5% CO_2 in a 39°C humidified incubator and grown to confluence in plastic tissue culture flasks (Falcon, Becton Dickinson). Exhausted media, due to cell metabolism and spontaneous degradation of constituents needed to be changed periodically to ensure optimum growing conditions. Cells had to be subcultured into new flasks when they had either covered the surface available for growth or depleted the nutrients in the medium. Prior to subculturing, the medium was removed and cells washed once with Ca^{2+}/Mg^{2+}-free phosphate buffered saline (PBS). Cells were then detached from culture flasks using trypsin (0.05% w/v)-5 mM EDTA (Gibco-BRL, Life Technologies) solution, resuspended in fresh medium containing 10% FCS, and spun at 1500 g for 5 min. The supernatant was removed and the cells were resuspended in fresh medium. The appropriate volume of cells was replated in new tissue culture flasks containing fresh medium. Cell counts were performed using an Improved Neubauer haemocytometer and an inverted microscope. For storage, cells were trypsinised, pelleted and resuspended at approximately 5 x 10^6 cells/ml in FCS containing 10% v/v dimethylsulphoxide (AnalaR, BDH), the presence

of which prevented the formation of damaging ice crystals. One-millilitre aliquots were transferred to 1.5 ml Nunc cryotubes which were then frozen slowly and stored immersed in liquid nitrogen (-196°C). Recovery of cells from liquid nitrogen storage was performed by rapid thawing in a 37°C water bath. Thawed cells were washed in 10 ml of medium, harvested by centrifugation and were then transferred to 25 cm^2 flasks containing fresh culture medium.

2.4.1 Indirect Indicator test for *Mycoplasma* contamination

Cells were regularly screened for *Mycoplasma* contamination. Briefly, a 9 x 35 mm glass coverslip (Chance Propper, Scientific Lab Supplies Ltd) was placed into a Leighton tube (a tissue culture test tube with a flat bottom, Nunc). Four ml of DMEM/10% FCS was added and inoculated with 2 x 10^4 NIH 3T3 cells/tube, the cap was left loose and placed in a 39°C dry gassing incubator with 10% CO_2. After 24 h the tube was inoculated with 0.5 ml of supernatant from the culture to be tested. It was ensured the culture medium from the cells to be tested did not contain additives that would inhibit 3T3 growth, or antibiotics that might interfere with mycoplasma growth. Similarly, the medium was not harvested immediately after subculturing cells, or within 7 days of thawing as this potentially reduced mycoplasma load. The tubes were then incubated for a further 4 days or until confluent. The medium was then aspirated, the tubes washed with PBS and fixed for 5 min with absolute methanol, and then washed a further two times with PBS. Five μg/ml of Hoechst 22358 dissolved in PBS was added for 10 min, removed, and the tubes washed twice with PBS. The coverslip was removed and placed cell surface upwards on a glass microscope slide, a drop of PBS added and a further 22 x 50 mm glass coverslip was used to cover the original coverslip. The slide was then examined with a fluorescence microscope using

x 40 objective and UV illumination. Control cells showed intense blue-white staining of nuclei only, while cells growing mycoplasma were in addition covered in a fine 'lawn' of speckles. On one occasion three of the cell lines were positive and successfully treated with ciprofloxacin (20 μg/ml), Bayer, Germany.

2.5 Sulforhodamine B Assay

The growth characteristics for each cell line, including doubling times, required specific inoculation densities and cytotoxicity of chemotherapeutic drugs, were determined using the Sulforhodamine B (SRB) assay (Skehan et al, 1990). The SRB assay allows quantification of total cellular protein in each well of 96-well plates containing cells under investigation. To stain the plates, the supernatant medium was first flicked off. The cells were fixed with 100 μl of 30% (w/v) trichloroacetic acid for 20 min at 4°C, washed five times with tap water, then stained by adding 100 μl of 0.4% (w/v) SRB in 1% acetic acid and leaving for 20 min at room temperature. The plates were then washed five times with 1% acetic acid to remove any free stain, and left to dry. Once dry, protein bound dye was solubilised by adding 100 μl of 10 mM Tris buffer (pH 10.5) to each well and placing on a plate agitator for 20 min. Absorbance was determined by reading at 540 nm with a Titertek Multiskan MCC/340 colorimeter (Labsystems, Finland).

2.6 Flow cytometry (fluorescence-activated cell scanner [FACScan]) analysis

2.6.1 P-gp, MRP and LRP

P-gp, MRP1 and LRP protein expression was measured by labelling freshly trypsinised exponentially growing cells with the monoclonal antibodies MRK16 (TCS Biologicals Ltd, Botoloph Claydon, Buckingham, UK), MRPm6 and LRP56 (both Bradsure Biologicals Ltd, Loughborough, Leicestershire, UK), respectively, and anti-mouse IgG-FITC (DAKO, Dakopatts, Denmark) second antibody. Briefly, 1 x 10^6 cells were used for each antibody, the cells for MRP1 and LRP expression were permeabilised with permeabilisation reagents A (fixation medium) and B (permeabilisation medium) (An Der Grub, Kaumberg, Austria). Cells were resuspended in 0.5 ml 10 % albumin in PBS and incubated at 37°C for 10 min. The relevant antibodies were then added to each cell group (MRK16, MRPm6 and LRP56, and control mouse antibodies IgG2a, IgG2b and IgG1 for the control P-gp, MRP and LRP respectively) and incubated at 4°C for P-gp and 0°C for MRP1 and LRP. After washing twice with PBS, anti-mouse IgG-FITC was added to each tube and incubated for a further 45 min at the above temperatures. Ten thousand events were analysed on a FACScan flow cytometer. (Becton Dickson, Oxford, UK), equipped with a 15 mW argon laser. Fluorescence emission (488 nm excitation) was collected after passing through band pass filters (530 nm for FITC). Analyses were performed using Lysis II software (Becton Dickinson, Oxford). Values were expressed as median fluorescence index (MFI) relative to control i.e. the ratio of median antibody fluorescence/median control antibody fluorescence.

2.6.2 P-gp function

P-gp function was determined using 3,3'-diethyloxacarbocyanine iodide ($DiOC_2$), a fluorescent substrate for P-gp (Leith et al, 1995). Briefly, cells were incubated with DiOC2 with and without verapamil (vpm) (10 μM) or PSC833 (1 μM) for 30 min for substrate uptake. All tubes were washed with ice cold PBS and duplicate tubes incubated for a further 90 min. All tubes were further washed with ice cold PBS and 10,000 events were analysed on a FACScan flow cytometer. Values were expressed as Mean Fluorescence Index (MFI), ie ratio of median fluorescence in the presence of modulation to median fluorescence with absence of modulation.

2.7 Western blot analysis

The mouse monoclonal anti-P-gp antibody, C219 (Chemicon International Inc., Temecula CA) was used for Western Blot analysis. Cells (3×10^7) were mixed with 150 μl protein lysis solution (1 ml lysis buffer, 25 μl aprotinin, 1 μl β mercapto-ethanol, 30 μl VBF and 1 μl PMSF), incubated for 30 min at 0°C and centrifuged at 14000 rpm for a further 30 min. Protein concentration in the supernatant was measured using a standard absorbance assay (Bio-Rad Laboratories, Hemel Hempstead, UK). The supernatant was treated at 100°C for 5 min, and 20 μg of protein was electrophoresed on an 8-16% Tris-Glycine Gel in a minigel apparatus (Bio-Rad Laboratories, Hemel Hempstead, UK), transferred onto a 0.2 μm nitrocellulose membrane, and blocked with 5% nonfat dry milk in TBS at 4°C overnight. The monoclonal mouse anti-Pgp antibody, C-219, was hybridised to the membrane at 4°C for 1 h and washed x 3 in 1% nonfat dry milk-TBS-0.5% Tween. The secondary antibody, a goat antimouse IgG horseradish peroxidase conjugate was added at 1:2000 dilution in TBS for 30 min at room temperature, rinsed x 3 in TBS-

Tween, once with TBS and exposed to a chemiluminescent horseradish peroxidase substrate (ECL: Amersham Corp). Autoradiographs were digitally scanned, and the densities of specific bands were quantified using IP Lab Gel densitometry software (Molecular Dynamics, Amersham Biosciences UK Limited).

2.8 Intracellular glutathione (GSH) determination

All the following reagents were purchased from Sigma-Aldrich, UK and stored at 4°C: glutathione (reduced form) (GSSG), glutathione reductase (type IV from bakers yeast), 5,5'-dithiobis-(2-nitrobenzoic acid) (DTNB), DL-buthionine-(S,R)-sulfoxamine (BSO), 5-sulfosalicylic acid and β-NADPH (tetrasodium salt, type I). Three working solutions were made up in stock buffer (125 mM Na-phosphate, 6.3 mM EDTA (pH 7.5)). Reaction mixture I: 0.3 mM NADPH; reaction mixture II: 6.0 mM DTNB; reaction mixture III: 50 units glutathione reductase/ml. Cell lysis solution was made up with 0.6% 5-sulphosalicylic acid in distilled deionised water and 10 mM BSO made up in sterile PBS and added to cell culture medium to give a final concentration of 50 μM. All solutions were stored at 4°C and not kept for more than one week, apart from NADPH which was made up fresh immediately before each experiment. Standards were prepared by making up a 1 mM solution of GSSG in stock buffer and serially diluting to give a series of samples ranging from 6.25-150 μM. Two hundred μl aliquots of the solutions were assayed as described below. Cells were grown either in normal culture medium, or in medium containing 50 μM BSO for 24 h. Cell extracts were prepared by harvesting 1 x 10^6 cells and washing twice with cold PBS, then lysing with 1 ml 0.6% sulfosalicylic acid followed by a 10-minute incubation at 4°C. Two hundred μl of the supernatant was obtained for assay following centrifugation (270 G for 5-min at 4°C).

The total glutathione (GSH) content of the standards and the experimental cell lysates were determined by an enzymatic assay. Briefly, 700 µl of solution I, 100 µl of solution II and 200 µl of the GSH sample or experimental cell lysate were mixed in a cuvette (1 cm light path) and equilibrated to 30°C in an oven. Ten µl of solution III was added to the warm solution and the absorbance at 412 nm monitored continuously on a spectrophotometer until it exceeded 2.0. The DTNB is reduced to a yellow chromophore in the presence of GSH (Figure 2.1.A). For samples containing more than approximately 0.5 µl GSH, the rate of DTNB reduction was linear throughout. For samples containing less, the rate was taken from the linear portion of the data. The GSH content of the experimental cell lysates was determined by comparison of the rate observed to the standard curve generated with the known amounts of GSH (Figure 2.1.B). All experiments were performed in triplicate.

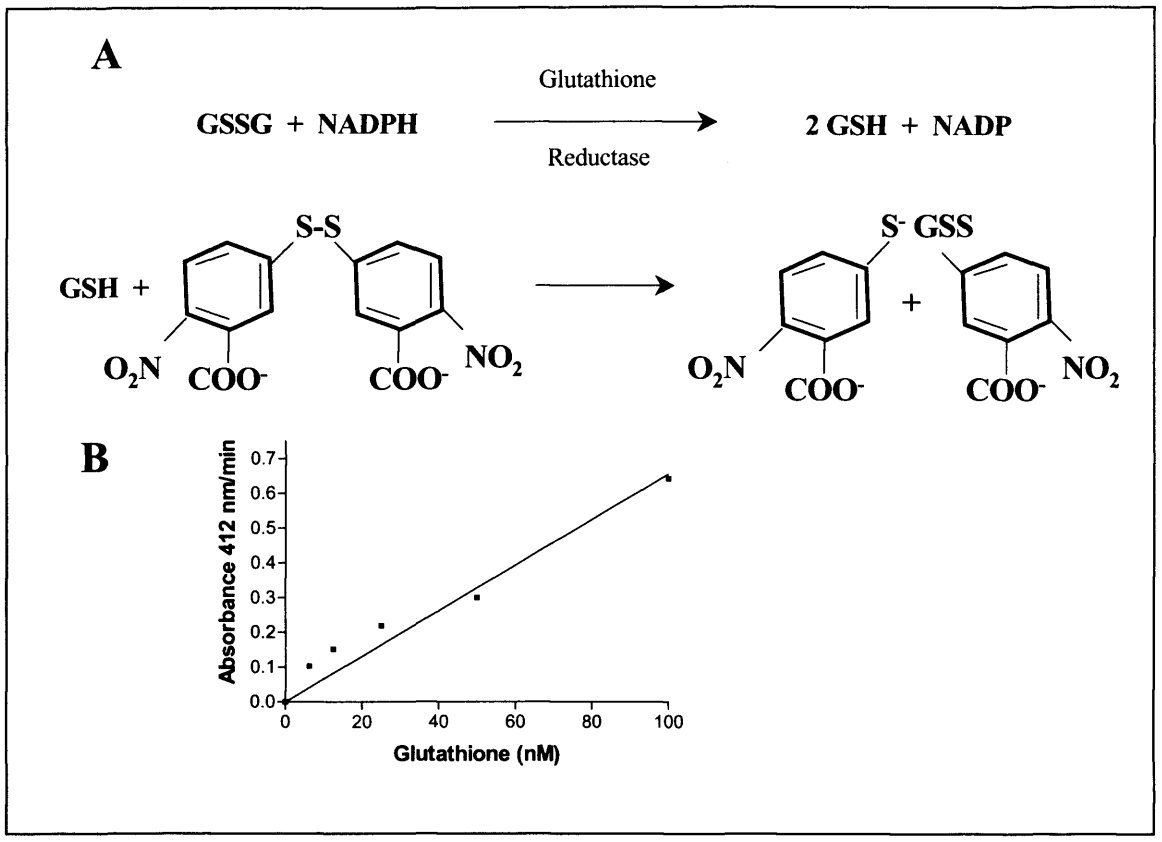

Figure 2.1.A. Enzymatic reaction in which the rate of reduction of DTNB to a yellow chromophore in the presence of GSH is dependent on the concentration of glutathione in the original reaction mixture. **B.** Standard curve derived from measurements of colour development following addition of GSH standards.

2.9 The comet assay

The single cell gel electrophoresis (comet) assay has been used to detect DNA damage in individual cells (Ostling and Johanson, 1984), particularly single strand breaks. The technique has been successfully applied to detect DNA repair deficiencies in human fibroblasts (Alapetite et al, 1996), and recently a modification has been described enabling interstrand DNA crosslinks to be measured in individual cells (Hartley et al, 1999; Spanswick et al, 1999). Cells are embedded in an agarose film on a glass slide, lysed, the DNA denatured and electrophoresed. Intact DNA remains in super-coiled bundles, which have virtually no electrophoretic mobility. Damage resulting in strand-breaks and fragmentation (such as the cytotoxic agent etoposide) allows the DNA to uncoil and stream away from the nucleus when subjected to electrophoresis, resulting in a 'comet' image as in Figure 2.2.

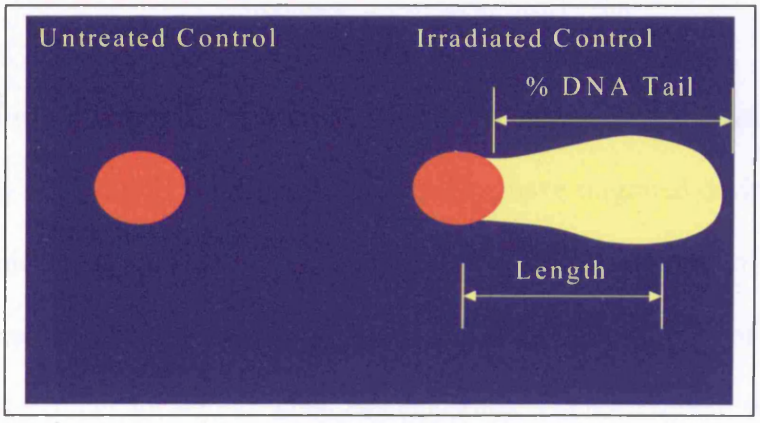

Figure 2.2. Representation of Comet Image.

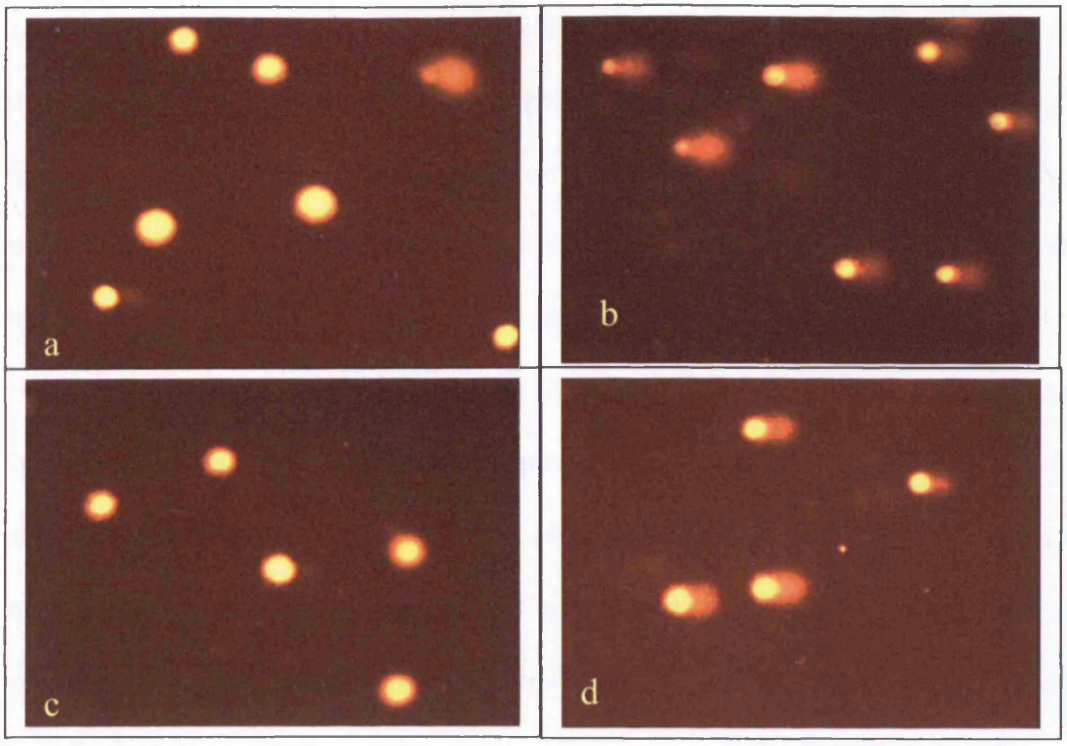

Figure 2.3. Samples Comet Assays Images. Samples (a) and (b) are untreated controls. Sample (a) is un-irradiated, whereas sample (b) has received 10 Gy in X-rays. Samples (c) and (d) are 24 h post cisplatin treatment (100 μM, 1 h). Sample (c) is un-irradiated, whereas (d) has received 10 Gy in X-rays.

The head of the comet represents the intact DNA, which has remained static, the tail consisting of the loops and small fragments that have migrated during electrophoresis. The modification of the assay introduces a standard dose of X-rays prior to electrophoresis, which induces a random but constant level of strand breakage, resulting in comet formation when electrophoresed. Pre-treament with a crosslinking agent causes the DNA fragments to be bound together, reducing their electrophoretic mobility and therefore the extent of the comet tail, as demonstrated in Figure 2.3. Untreated control cells are shown in (a). In (b) cells have received 10 Gy in X-rays, the DNA damage resulting in comet formation. Samples (c) and (d) are both drug

treated, (c) being un-irradiated, whereas (d) has received 10 Gy. The shorter the comet tail in (d) compared to (b) is due to the presence of interstrand crosslinks (ICL). The reduction in the extent of the comet tail, as compared to an untreated control, gives a measure of the quantity of ICLs present. Following these changes as time after drug exposure progresses enables repair of the ICLs to be measured, the comet tail increasing as the crosslinks are removed. A detailed description of the assay follows. Sufficient slides to perform the assay were prepared by pipetting onto the centre 1 ml of molten 1% Type-IA Agarose solution (40°C). A glass coverslip was placed on top, and then removed once the agarose had cooled and solidified. The slides were then left to dry overnight. The cell line to be investigated was harvested as previously described. After centrifugation, the cells were resuspended in MEM supplemented with 2 mM glutamine and 0.5% FCS (0.5% FCS MEM) in order to prevent cell division during the time course of the assay. After a cell count was performed, 6-well plates were seeded with 0.5-1 x 10^5 cells in 3 ml 0.5% FCS MEM per well, allowing sufficient wells for controls and treated samples. The plates were incubated under standard conditions over night to allow cell attachment to occur. After incubation, the plates were removed and all medium aspirated from the well to be treated. Drug solutions were prepared at the required concentrations by diluting the stock solution with serum-free MEM. These are added to the wells (recording the dose and time each well is exposed), and the plates incubated at 37°C for 1 h. Control wells received serum-free MEM alone. After the 1 h treatment, the drug solutions were aspirated and 3 ml of 0.5% FCS MEM replaced in each well. The plates were returned to incubate under standard conditions for the required post-treatment interval. All subsequent steps, until electrophoresis had been completed, were performed on ice and with the samples protected from light wherever possible, to minimise light-induced DNA

damage or cellular DNA repair. After the appropriate post-treatment interval, the treated cells were harvested as previously described. Alternatively cells obtained by fine needle aspiration (FNA) in the *in vitro* mice and isolated perfused rat and human liver experiments were simply defrosted. After centrifugation, the cell pellets were resuspended at 2.5 x 10^4 cells in 1 ml of serum-free MEM, in 1.75 ml Eppendorf™ tubes. Samples treated with cross-linking agents, plus one control, were subjected to 10 Gy X-irradiation. The second control remained un-irradiated. For samples treated with agents whose mode of cytotoxicity was the production of single strand breaks, irradiation was omitted. A 24-well plate was placed on ice. The 1 ml cell sample was placed in a well, to which 2 ml of a molten 1% Type-VII Agarose solution (no warmer than 40°C). After mixing, duplicate slides were prepared by pipetting 1 ml into the centres of two pre-coated slides. A coverslip was placed on top, and then removed once the gel had solidified. The slides were then covered with ice-cold lysis buffer [2.5 M NaCl, 100 mM EDTA, 100 mM Tris HCl (pH 10.5-11.5), 1% TritonX-100] for 1 h. After lysis, the slides were washed for 1 h using four changes of distilled water. Slides were arranged lengthwise in an electrophoresis tank (Flowgen Instruments, Lichfield, Staffs) and submerged in alkali buffer [50 mM NaOH, 1 mM EDTA (pH 12-12.5)] for 45 min. Slides were then electrophoresed for 25 min at 18 V (0.6 V/cm), 250 mA, then removed and washed with neutralisation buffer [0.5 M Tris HCl (pH 7.5)] for 10 min, followed by a PBS wash for a further 10 min. To stain the slides, after leaving to air-dry overnight, they were rehydrated with distilled water for 30 min, flooded with 2.5 μg/ml propidium iodide for 20-30 min and destained for a further 30 min in water. Slides were dried and stored until visualisation. Images were visualised using a NIKON inverted microscope DIAPHOT model TMD, with high pressure mercury light source and a 580 nm dichromic mirror, 510-560 nm excitation

filter, and 590 barrier filter at x 20 magnification. Images were captured using an on-line CCD camera and analysed using Komet assay software (Kinetic Imaging). The Komet Assay software captures individual comet images and measures the comet intensity, as demonstrated in Figure 2.4. By subtracting background levels from the portion of the captured image to be analysed (the 'cell'), the program determines the extent of the comet. The shape of the comets' head is assumed to be symmetrical, the extent of its' right border being determined by producing a mirror image of the left border about the peak value. Once the head is determined, all the residual DNA is allocated to the tail. Proportions of DNA in the comet head and tail, and the centres of mass of DNA in the head and tail, are then calculated from areas under each respective line.

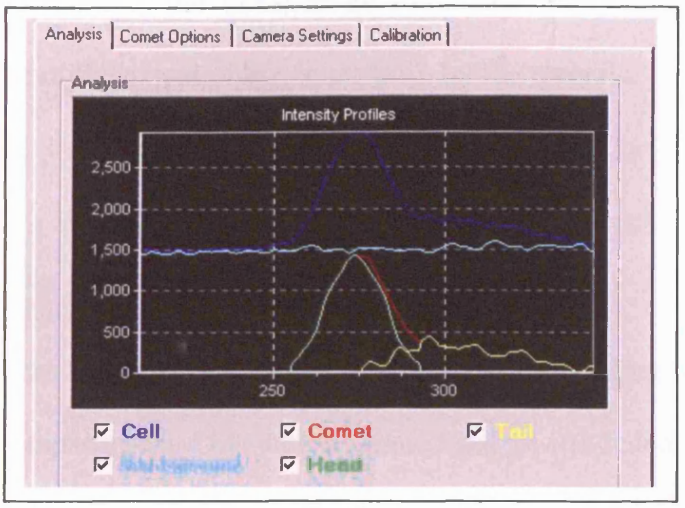

Figure 2.4. Screen Shot of Komet Assay software analysing a comet image.

Having determined the centres of mass of the comet head and tail, the distance between the centres of mass, '*d*', is measured (Figure 2.5).

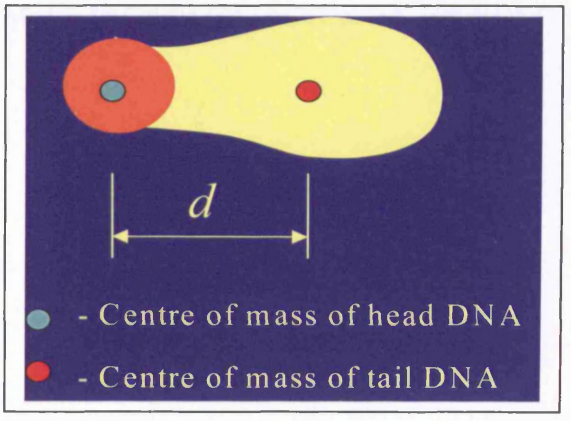

Figure 2.5. Centres of mass of comet head and tail DNA.

This enables the tail moment (TM) to be calculated, (which represents the most sensitive measure of the extent of the comet tail), by the formula:

$$\text{Tail Moment } (\mu m) = \% \text{ DNA in Tail x } d.$$

Calculation of the degree of crosslinking present in a drug-treated sample is determined by comparing the TMs with irradiated and un-irradiated untreated controls (Hartley et al, 1999). The reduction in the TM that occurs in relation to the TM of the irradiated, untreated control is proportional to the level of interstrand crosslinking present, and is calculated by the following formula:

$$\% \text{ decrease in TM} = 1 - \left[\left(\frac{TMdi - TMcu}{TMci - TMcu} \right) \right] \times 100$$

Where: TMdi = tail moment of drug-treated irradiated sample

TMcu = tail moment of untreated, un-irradiated control

TMci = tail moment of untreated, irradiated control

2.10. *In vivo* animal experiments

The animals used in the *in vivo* experiments were MFI nude mice, Sprague Dawley rats and Rowett nude rats supplied by the CBU unit, Royal Free Hospital (RFH). All procedures were carried out according to Home Office regulations and were covered by the Home Office Licence No. PPL 70/4517. These procedures were carried out at the CBU unit, Royal Free Hospital. Cell suspensions were prepared by trypsinisation of adherent cell lines from tissue culture flasks and washing with sterile PBS. Cells were counted and resuspended in the appropriate volume of cold-sterile PBS. The full details of the *in vivo* animal protocols are described in Chapters VII and VIII.

2.11 Immunohistochemistry

To study the effect of hypoxia, cell proliferation, P-gp expression and vascularity on the intratumoural topographic distribution of cisplatin-DNA adducts in intrahepatic xenografts of mice, immunohistochemistry was performed on parallel sections prepared from the same tumour in each relevant experiment. Point counting using two independent observers quantitated the staining reactions.

2.11.1 NCL-Ki67-MM1

Cell proliferation was visualised with the monoclonal antibody NCL-Ki67-MM1 (Novocastra Laboratories Ltd, Newcastle upon Tyne, UK), that recognises the Ki-67 antigen, which is expressed during G_1 phase, increases during the cell cycle and declines after mitosis. After the relevant experiment the tumours were rapidly removed and snap frozen in liquid nitrogen and stored at $-70^{\circ}C$ until they were sectioned. Frozen sections were cut at 4 μm thickness and stored at $-70^{\circ}C$ until required. All slides were stained in the same batch. Before staining, frozen sections

were air-dried and fixed with acetone at 4°C for 10 min. Endogenous peroxidase was blocked by incubating samples for 15 min at room temperature in PBS containing 0.03% hydrogen peroxide and sodium azide (15 mmol dm^{-3}). Non-specific staining was blocked by pre-incubating sections with PBS (0.5% Tween 20, 0.1% normal horse serum) for 1 h. Following this the fluid was drained off and a 0.1% monoclonal mouse anti-serum against the Ki-67 antigen (Novocastra Laboratories Ltd, Newcastle upon Tyne, UK) was applied and the sections incubated overnight. The fluid was then drained off and sections washed twice with PBS (0.5% Tween 20, 0.1% normal horse serum). Immunoperoxidase detection was achieved by using a standard Vector ABC kit with a peroxidase-conjugated second antibody to mouse IgG and a Vector DAB substrate kit (Vector Laboritories, California, USA) with Harris's haematoxylin counterstain (Raymond A Lamb Ltd, Eastbourne, UK).

2.11.2 7-(4'-(2-nitroimidazol-1-yl)-theophylline (NITP)

Tumour hypoxia has been shown to influence the efficacy of many chemotherapeutic agents. Numerous methods have been proposed for measuring tumour hypoxia in the hope that this would allow treatment to be optimised for individual patients on the basis of the oxygen status of their tumours. Hypoxia can be measured using bioreductive binding of the novel compound NITP, which consists of a 2-nitroimidazole with an immunologically recognisable theophylline sidechain. The 2-nitroimidazole component binds to cellular macromolecules under low-oxygen conditions, and the bound adducts of the probe, in hypoxic cells, can then be identified and quantified by antibodies raised against theophylline (Hodgkiss et al, 1991). NITP (0.5 μMg^{-1}) was administered by intra-peritoneal injection in peanut oil containing 10% DMSO to mice or added to perfusate during rat liver perfusion. After

the relevant experiment the tumours were rapidly removed and snap frozen in liquid nitrogen and stored at –70°C until they were sectioned. Frozen sections were cut at 4 μm thickness and stored at –70°C until required. All slides in each experiment were stained in the same batch, to avoid the methodologic error due to inter batch variation. Before staining, frozen sections were air-dried and fixed with acetone at 4°C for 10 min. Endogenous peroxidase was blocked by incubating samples for 15 min at room temperature in PBS containing 0.03% hydrogen peroxide and sodium azide (15 mmol dm^{-3}). Non-specific staining was blocked by pre-incubating sections with PBS (0.5% Tween 20, 0.1% normal goat serum) for 1 h. Following this the fluid was drained off and a 0.1% polyclonal rabbit anti-serum against theophylline (Biogenesis Ltd, Poole, UK) was applied and the sections incubated overnight. The fluid was then drained off and sections washed twice with PBS (0.5% Tween 20, 0.1% normal goat serum). Immunoperoxidase detection was achieved by using a standard Vector ABC kit with a peroxidase-conjugated second antibody to rabbit IgG and a Vector DAB substrate kit (Vector Laboritories, California, USA) with Harris's haematoxylin counterstain (Raymond A Lamb Ltd, Eastbourne, UK).

2.11.3 von Willebrand factor (factor VIII)

Blood vessels were identified by an immunohistochemical staining against the von Willebrand factor (factor VIII), which recognises endothelial cells. Before staining, The 4 μm frozen sections were air-dried and fixed with acetone at 4°C for 10 min. Endogenous peroxidase was blocked by incubating samples for 15 min at room temperature in PBS containing 0.03% hydrogen peroxide and sodium azide (15 mmol dm^{-3}). Non-specific staining was blocked by pre-incubating sections with PBS (0.5% Tween 20, 0.1% normal horse serum) for 1 h. Following this the fluid was drained off

and the slides were treated with MCA127 (mouse monoclonal anti-human von Willebrand factor) (Serotec Ltd, Oxford, UK) diluted 1:100 in PBS at 4°C overnight. The fluid was then drained off and sections washed twice with PBS (0.5% Tween 20, 0.1% normal horse serum) followed by treatment using a standard Vector ABC kit with a peroxidase-conjugated second antibody to mouse IgG and a Vector DAB substrate kit (Vector Laboritories, California, USA) with Harris's haematoxylin counterstain (Raymond A Lamb Ltd, Eastbourne, UK).

2.11.4 P-gp expression on tumour tissue sections

Frozen sections were cut using the same tumours used for NITP and NCL-Ki67-MM1 at 4 μm thickness and stored at –70°C until required. Before staining, frozen sections were air-dried and fixed with acetone at 4°C for 10 min. Endogenous peroxidase was blocked by incubating samples for 15 min at room temperature in PBS containing 0.03% hydrogen peroxide and sodium azide (15 mmol dm^{-3}). Non-specific staining was blocked by pre-incubating sections with PBS (0.5% Tween 20, 0.1% normal horse serum) for 1 h. Following this the fluid was drained off and treated with JSB-1 (mouse monoclonal anti-human P-gp antibody) (Chemicon International Inc., Temecula CA) diluted 1:20 overnight. The fluid was then drained off and sections washed twice with PBS (0.5% Tween 20, 0.1% normal horse serum). Immunoperoxidase detection was achieved by using a standard Vector ABC kit with a peroxidase-conjugated second antibody to mouse IgG and a Vector DAB substrate kit (Vector Laboritories, California, USA) with Harris's haematoxylin counterstain (Raymond A Lamb Ltd, Eastbourne, UK).

2.12 *Ex vivo* perfused human liver

Patients undergoing hepatic resection for either primary hepatocellular carcinoma or secondary colorectal metastases were selected. The Royal Free Hospital ethics committee approved the study and patients were consented for the use of resected specimens in research. The details of the ex *vivo* perfused human liver protocol are described in Chapter IX.

2.12.1 Laser Doppler Flowmetry

The hepatic microcirculation (HM) was assessed using a commercially available laser doppler flowmeter (LDF, DRT4, Moor Instruments Limited, Axminster, UK). It gives a continuous measure of red cell motion in the outermost layer of the tissue under study.

Principle

Laser Doppler is based on the principle of recording Doppler shifts in backscattered light caused by movements of red blood cells in the incident path of the monochromatic light of a laser beam. The device consists of a helium-neon laser and an optic fibre which transmits this light to the surface of the tissue to be studied. Light that is scattered by red blood cells undergoes a frequency shift and a portion of this spectrally broadened light is transmitted back by a fibre light-guide to two photodetectors. This signal is analyzed and the relative portion of light which has undergone a Doppler shift is proportional to the velocity of the blood flow. The microvascular bed consists of an intricate network of small blood vessels and hence the angle between the red cell velocity vectors and beam propagation vectors of the scattered light can be regarded as random.

Instrument

The operating principle of this instrument is a light guide which transmits a low-energy laser beam (2 mW He-Ne laser of 780 nm wavelength) to the tissue surface under examination via 8 emitting fibres and 8 collecting fibres. The bundle of collecting fibres returns light to the photodetectors where it is converted into an electrical signal. Further processing of this signal finally produces the actual Doppler signal that varies linearly with the product of the total number of moving red blood cells in the measured volume of few mm^3 multiplied by the mean velocity of these red blood cells (Seifalian et al, 1997). The numerical product is termed a perfusion unit or blood cell flux unit. The optical fibre probe was applied to the experimental tumour/s in the perfused hemiliver. HM expressed in units of flux was averaged over a period of 2 min. The light enters the tissue where it is repeatedly reflected, refracted, and absorbed increasingly. This produces a region of virtually isotropic illumination. All red blood cells passing through this region reflect some of the light and produce a shift in wavelength. Laser Doppler flowmetry (LDF) is a non-invasive technique that allows for continuous evaluation of microvascular perfusion (Seifalian et al, 1991). Its use for measurement of the hepatic microcirculation has been validated in animal models (Seifalian et al, 1991; Wheatley et al, 1993). Parenchymal perfusion measured by LDF correlates well with total liver blood flow and surface LDF measurements are representative of deep parenchymal perfusion (Kotzampassi et al, 1992). In human liver transplantation a significant correlation between the microcirculation of the liver graft at the time of transplantation using surface LDF and total liver blood flow measured by electromagnetic flowmeter (EMF) has been demonstrated. The perfusion measurements were reproducible with a coefficient of variation of 4% (Seifalian et al, 1997).

2.12.2 Transonic Flowmetry

The flow rate was measured with a dual Transonic Medical Flowmeter system (HT207, Transonic Medical System Inc, Ithaca NY, USA).

Principle

Transonic flowmetry uses an ultrasonic transit-time principle to sense liquid volume flow in vessels or tubing largely independent of flow velocity profile, turbulence and haematocrit. One ray of the ultrasonic beam undergoes a phase shift in transit time proportional to the average velocity of the liquid times the path length over which this velocity is encountered. With wide-beam ultrasonic illumination, the receiving transducer sums these velocities: averages the velocity times and the vessels cross sectional area. Since the transit time is sampled at all points across the vessel diameter, volume flow measurement is independent of the flow velocity profile. Ultrasonic beam rays which cross the acoustic window without intersecting the vessel do not contribute to the volume flow integral.

A Transonic flowprobe consists of a probe body which houses low ultrasonic transducers and a fixed acoustic reflector. The transducers are positioned on one side of the vessel and the reflector is positioned midway between the two transducers on the opposite site of the vessel. The flowmeter's electronic ultrasonic circuitry directs a flowprobe through the following cycles: an electrical excitation causes the downstream transducer to emit a plane wave of ultrasound. This ultrasonic wave intersects the vessel in the upstream direction, then bounces off the "acoustic reflector", again intersects the vessel and is received by the upstream transducer where it is converted into electrical signals. From these signals, the flowmeter then

derives an accurate measure of the "transit time" it took for the wave of ultrasound to travel from one transducer to the other. The same transit-receive sequence of the upstream cycle is repeated, but with the transmitting and receiving functions of the transducers reversed so that the liquid flow under study is bisected by an ultrasonic wave in the downstream direction.

The transit-time of ultrasound passing through a vessel is affected by the motion of liquid flowing through that vessel. During the upstream cycle, the sound wave travels against flow and total transit time is increased by a flow dependent amount. During the downstream cycle, the sound wave travels with flow and total transit time is decreased by a flow dependent amount. During the downstream cycle, the sound wave travels with flow and total transit time is decreased by the same flow-dependent amount. The Transonic flowmeter subtracts the downstream transit time from the upstream transit time utilizing wide-beam ultrasonic illumination.

Instrument

A dual Transonic Medical Flowmeter system (HT207, Transonic Medical System Inc, Ithaca NY, USA) consists of a bench-top electronic flow detection unit and volume flowsensing probes ranging from 1 to 8 mm in diameter.

CHAPTER III

GROWTH CHARACTERISTICS AND CYTOTOXICITY DETERMINATION OF HCC AND CRC CELL LINES

III. GROWTH CHARACTERISTICS AND CYTOTOXICITY DETERMINATION OF HCC AND CRC CELL LINES

3.1 Introduction

In vitro (cell culture) studies have been considered a valuable tool for assessing the toxicity of cytotoxic agents for decades, and have been useful in determining their *in vivo* application (Eagle and Foley, 1956). Although they fail to take into account the microenvironment of malignant cells, as they cannot mimic the complexities of drug delivery, metabolism and excretion found clinically, cell culture studies are straightforward to perform, inexpensive, use small amounts of reagents and can be performed relatively quickly. Prior to investigating the various mechanisms involved in drug resistance of the chosen panel of cell lines, their growth characteristics and relative drug sensitivities were determined.

3.2 Materials and Methods

3.2.1 Growth characteristics

The doubling time of each cell line was determined to act as an aid in cytotoxicity experiments, the SRB assay ideally requires 2-3 doubling times, and to examine the potential role of growth rate in drug resistance in subsequent selected sub-lines. A single experiment was performed utilising 4 replicates of each cell line. Cell growth was followed over 5 days by staining 24-well plates seeded with equal numbers of cells on successive days with SRB, allowing quantification of total cellular protein in each well. Plotting the increase in cell protein against time allowed growth of each cell line to be determined over the 5-day period. Briefly, a fixed number of cells of each cell line (5×10^4 in 2 ml of the appropriate culture medium) were plated into

four wells of 24-well plates. Each plate was incubated under standard conditions for a period of 1, 2, 3, 4 and 5 days. On each of these days a single plate was assayed by staining with SRB (1 ml rather than 100 µl used in 96-well plates, of 30% (w/v) trichloroacetic acid and 0.4% (w/v) SRB in 1% acetic acid). Once dry, the stained monolayer was re-suspended by adding 150 µl 10 mM Tris base and placing on a plate agitator for 20 min. Absorbance was determined by transferring 125 µl of each well's contents into the well of a 96-well plate and reading at 540 nm with a Titertek Multiskan MCC/340 colorimeter (Labsystems, Finland). The doubling times for each cell line were then calculated from the exponential portion of each line using GraphPad Prism 3 Software (GraphPad Software, San Diego, California, USA).

Before cytotoxicity determination of the cell lines, cell growth in the 96-well microculture plates was characterised at a variety of cell densities (5000, 10,000, 20,000, 40,000 and 50,000 cells per well) over a 5-day period of growth in order to select a suitable inoculation density. From these data, the specific inoculation density selected for each cell line was that which produced an optical density signal above the noise level of the assay and within the linear range of the SRB signal (ie, within the range of 0.2 - 2.0 OD units), for both the T_0 and control optical density measurements. The T_0 and control optical densities generated from SRB-stained cells are a function of cell mass and growth rate. Thus, cells with a small mass are inoculated at relatively high densities of 30 - 40,000 cells per well. Furthermore, cells that divide relatively slowly are inoculated at 20,000 per well, while more rapidly dividing cells are inoculated at 5000 per well.

3.2.2 Cytotoxicity determination

The cytotoxic agents cisplatin, etoposide, melphalan and 5FU were used in the initial screening of the cell lines, these were chosen for their different mechanisms of action (see Introduction). The cytotoxicity of drugs was assessed by the SRB colorimetric assay. The SRB assay measures the degree of growth inhibition of an established cell culture after drug treatment, by allowing quantification of total cellular protein. This assay measures cytotoxicity taking into account the negative metabolic effects and rate of cell death after drug exposure, in addition to impaired reproductive function of the cell. Exponentially growing cells were harvested as already described, inoculated into 96-well tissue culture plates in a volume of 100 μl at densities between 5000 and 20,000 cells per well and allowed to attach for 24 h at 37°C, 5% CO_2, in a humidified atmosphere. After overnight incubation, the plates were removed and all medium aspirated from the wells. For initial screening of drugs, each agent was routinely tested at five 10-fold dilutions, starting from a maximum concentration of 1×10^{-4} M (data not shown). The active concentration range for each drug on each cell line was thus determined and alternative concentrations chosen for re-testing. Drug solutions were prepared at the required concentrations (0.01-1000 μM) by diluting the stock solution with serum-free MEM, 100 μl was added to each well followed by a further 100 μl of the appropriate medium containing 10% FCS. Control wells received drug free medium alone. All wells were then cultured for a further 4-5 days, until the control wells were seen to have grown to an almost confluent state when examined by microscopy. At this stage the plates were stained and analysed. The cells were fixed, stained with SRB and read in a colorimeter. Full details of the protocol are given in Chapter II, Section 2.5. Mean absorbance values for control and drug treated wells

were determined, and values as a proportion of control calculated for each drug concentration using the following equation:

$$\text{Cell survival (\%)} = \frac{\text{OD (treated cells)}}{\text{OD (control cells)}} \times 100$$

A survival curve was subsequently constructed for each cell line. The IC_{50} value (concentration of drug required to inhibit growth by 50%) was determined from the survival curve, which is a measure of cytotoxicity of the drug in that cell line. All experiments were performed in triplicate.

3.3 Results

3.3.1 Growth characteristics

The means of the absorbance values obtained for each cell line over a 5 day period of growth are plotted in Figures 3.1 A and B (Appendix 3.1). The doubling times for each cell line, calculated from the exponential portion of each line are shown in Tables 3.1 A and B. The majority of the cell lines studied shared similar growth characteristics, each having doubling times within the range 47-58 hours. Three of the cell lines, HepG2, SW620 and CACO2, however, had substantially shorter doubling times (27, 33 and 39 h respectively), whilst PLC/PRF/5 had a much longer doubling time at 81 h.

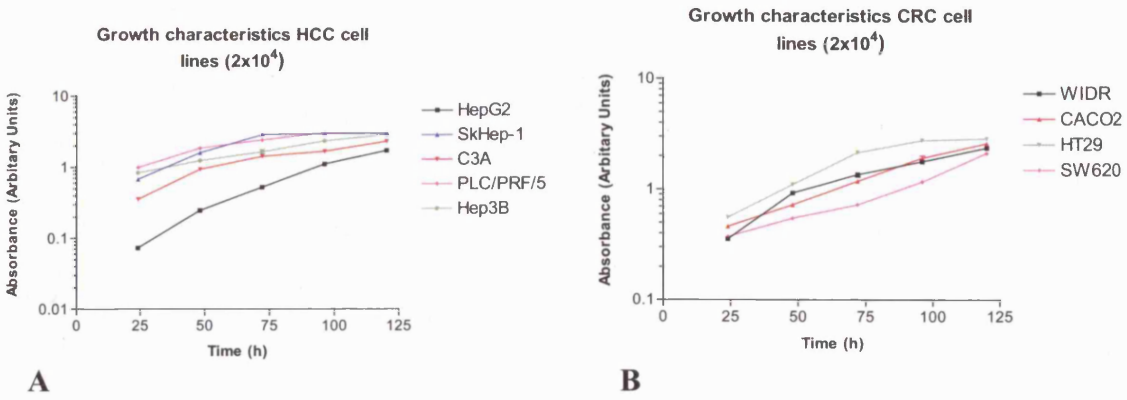

Figure 3.1. Growth characteristics of the HCC **A.** and CRC **B.** cell line panels.

Cell Line	Doubling Time/h	r^2
HepG2	27	0.99
SkHep-1	58	0.924
C3A	49	0.986
PLC/PRF/5	81	0.976
Hep3B	57	0.997

A

Cell Line	Doubling Time/h	r^2
WIDR	47	0.99
CACO2	39	0.993
HT29	49	0.953
SW620	33	0.995

B

Table 3.1. Doubling times for each HCC **A.** and CRC **B.** cell line.

The means of the absorbance values obtained for each cell line at different inoculation densities with time are plotted in Figures 3.2 and 3.3 (Appendix 3.2), whilst the chosen optimal inoculation densities are shown in Tables 3.2 and 3.3. Most of the cell lines were thus inoculated at 1 x 10^4. Although they had low growth rates, SkHep-1 and PLC/PRF/5 had a large cell mass requiring the lower inoculation density of 5 x 10^3. HepG2 and SW620 had a small cell mass so needed the higher inoculation density of 2 x 10^4.

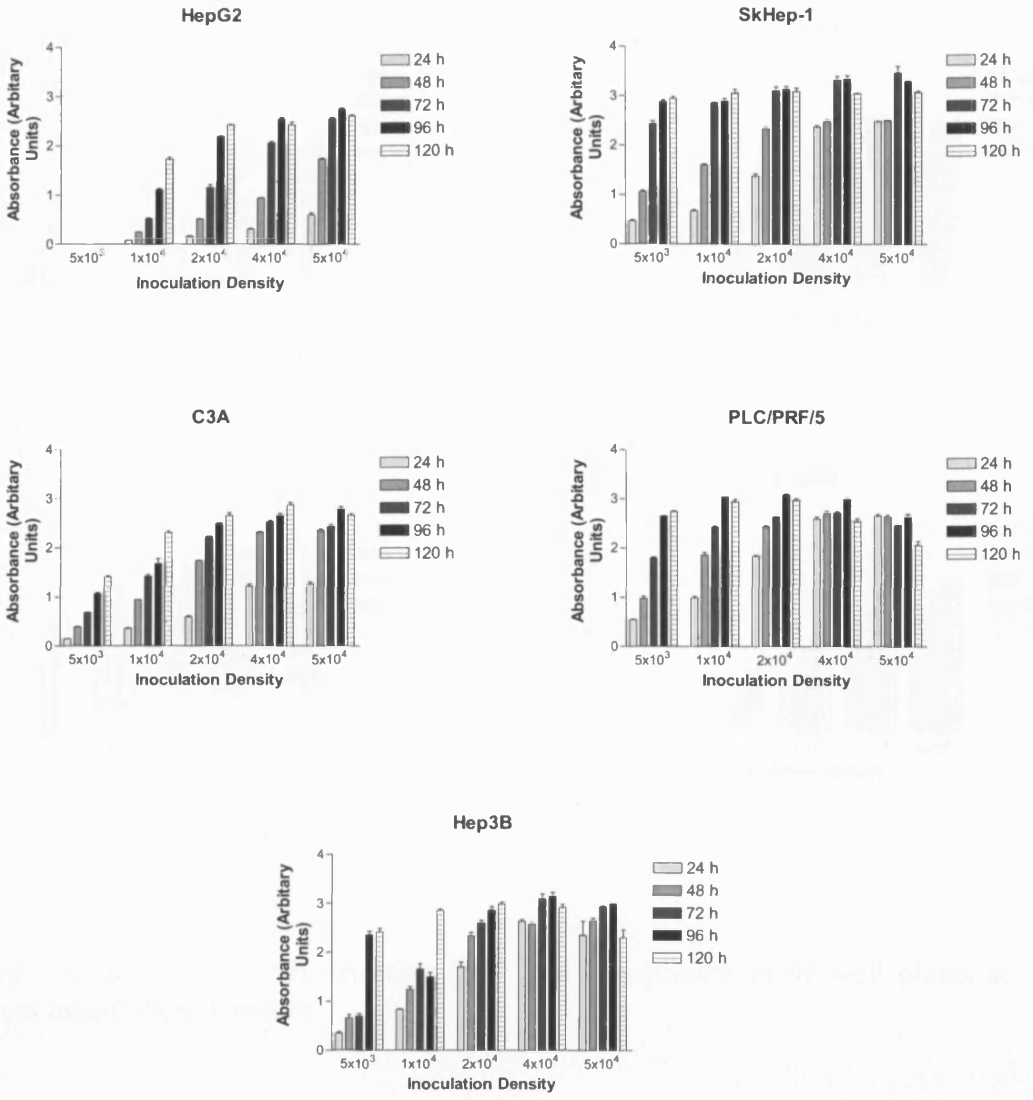

Figure 3.2. Bar graphs demonstrating HCC cell line growth in 96-well plates at different inoculation densities.

Cell Line	Inoculation Density
HepG2	2×10^4
SKHep-1	5×10^3
C3A	1×10^4
PLC/PRF/5	5×10^3
Hep3B	1×10^4

Table 3.2. Inoculation densities used in HCC cell lines.

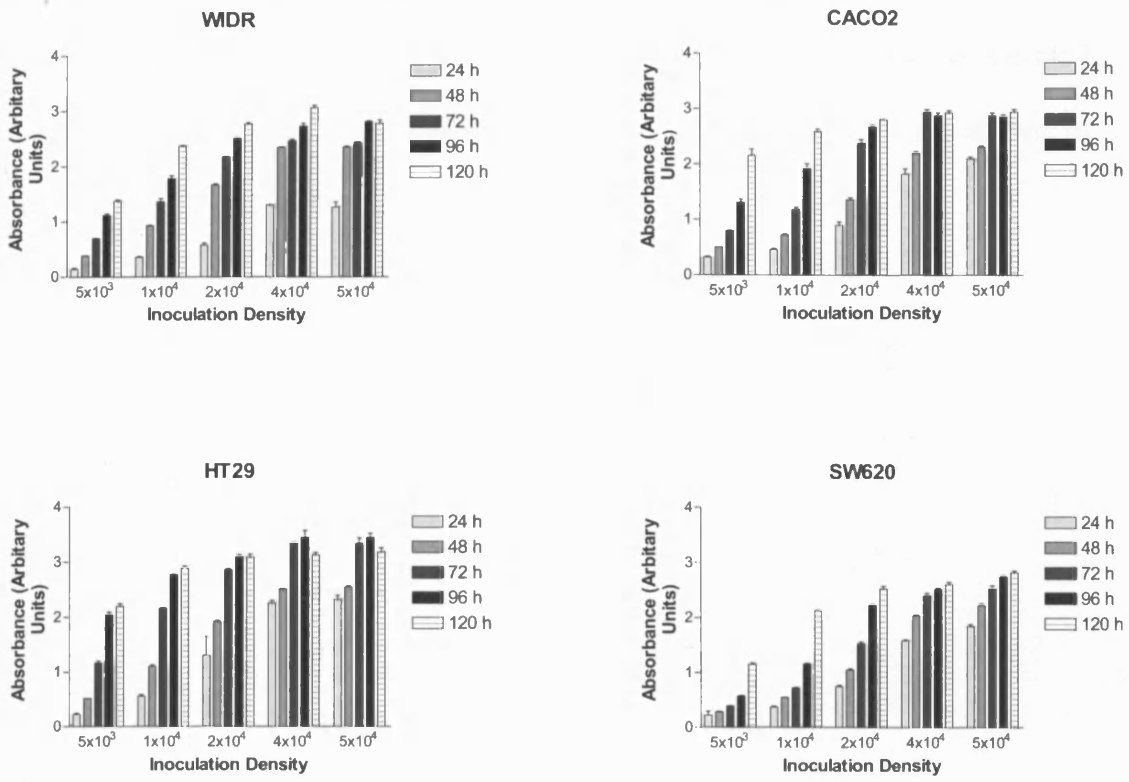

Figure 3.3. Bar graphs demonstrating CRC cell line growth in 96-well plates at different inoculation densities.

Cell Line	Inoculation Density
WIDR	1 x 10^4
CACO2	1 x 10^4
HT29	1 x 10^4
SW620	2 x 10^4

Table 3.3. Inoculation densities used in CRC cell lines.

3.3.2 Cytotoxicity determination

The dose response curves of both the HCC and CRC cell lines to the selected cytotoxic drugs are shown in Figures 3.4 and 3.5, whilst their IC_{50}s are shown in Tables 3.4 and 3.5 (Appendices 3.3 & 3.4).

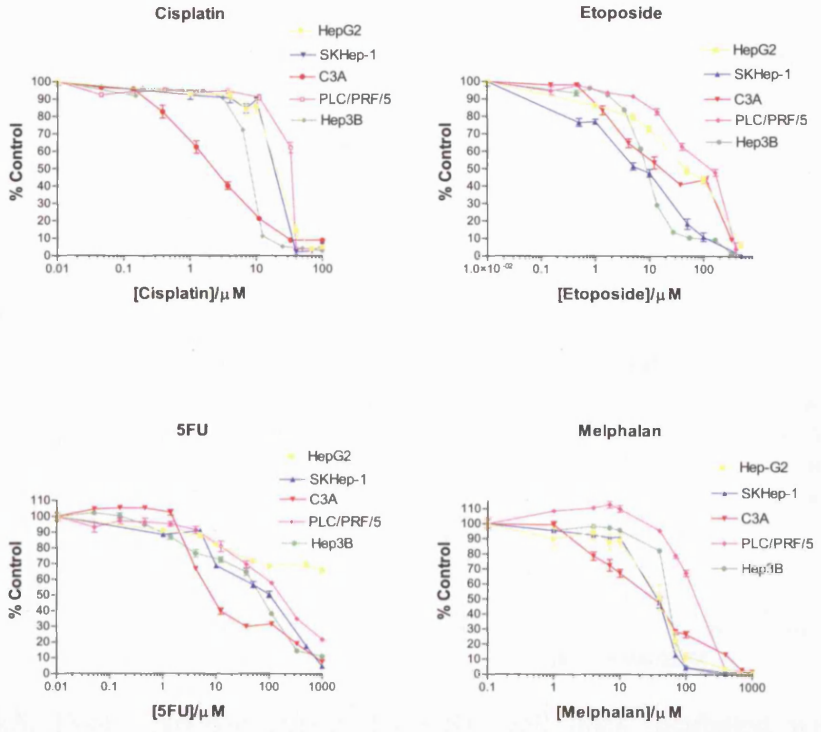

Figure 3.4. Dose response curves for HCC cell lines incubated with cisplatin, etoposide, 5-FU and melphalan for 120 h continuous exposure. Values represent the mean ± SEM of four independent experiments.

Drug	Cell Line				
	HepG2	**SkHep-1**	**C3A**	**PLC/PRF/5**	**Hep3B**
Cisplatin	25	20	2.5	34.3	9
Etoposide	45	9	18	100	10
5-FU	>1000	100	8	150	60
Melphalan	40	35	30	150	55

Table 3.4. Drug cross-resistance of HCC cell lines to multidrug resistant phenotype (MDR) and non-MDR drugs. Values given as IC_{50} (μM). The IC_{50} value was determined as the concentration of drug inhibiting cell growth to 50% of that in drug-free control.

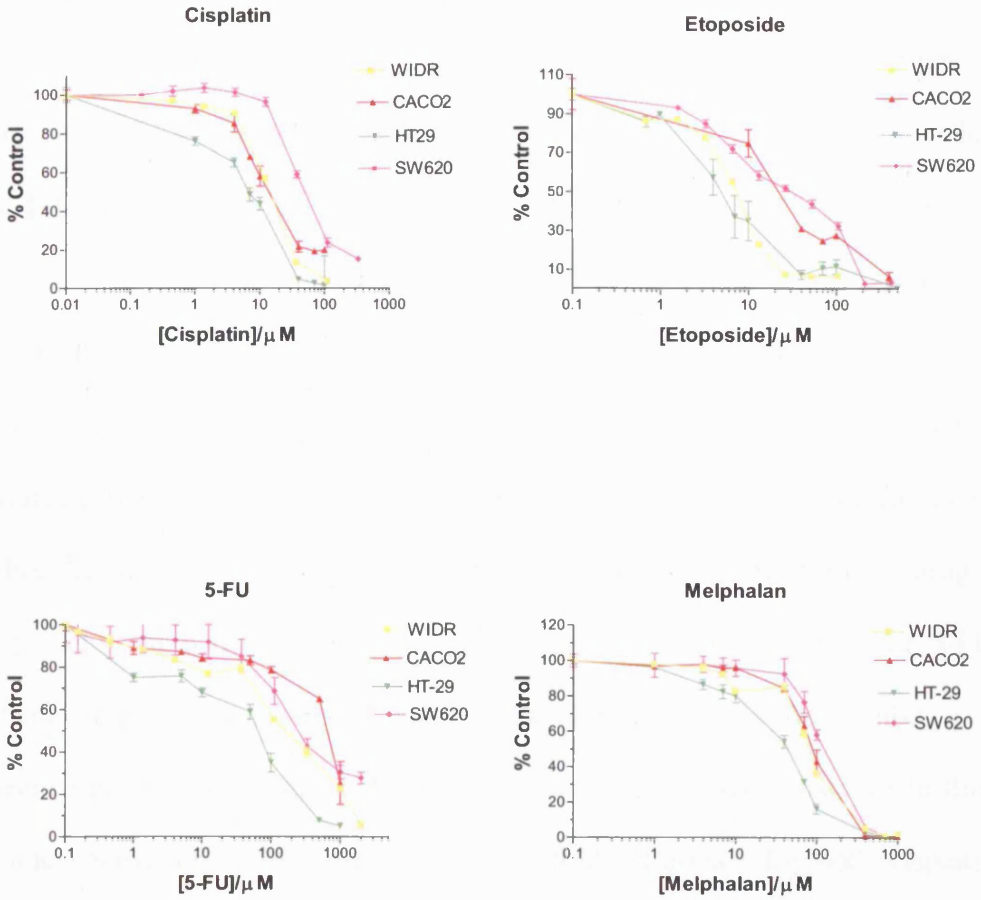

Figure 3.5. Dose response curves for CRC cell lines incubated with cisplatin, etoposide, 5-FU and melphalan for 120 h continuous exposure. Values represent the mean ± SEM of four independent experiments.

Drug	Cell Line			
	WIDR	CACO2	HT-29	SW620
Cisplatin	15	15	7	50
Etoposide	7	24	4.6	35
5-FU	159	650	65	240
Melphalan	87	90	44	122

Table 3.5. Drug cross-resistance of CRC cell lines to multidrug resistant phenotype (MDR) and non-MDR drugs. Values given as IC_{50} (μM). The IC_{50} value was determined as the concentration of drug inhibiting cell growth to 50% of that in drug-free control.

3.4 Discussion

The range of IC_{50} values observed in the panel of HCC and CRC cell lines appears quite broad. Of the HCC cell lines, C3A is extremely sensitive to all drugs except etoposide, whereas PLC/PRF/5 is strongly cross-resistant. Similarly, of the CRC cell lines, HT-29 is consistently sensitive to all drugs whilst SW620 is cross-resistant. Of note is PLC/PRF/5s prolonged doubling time, this cell cycle prolongation could theoretically allow increased time for repair of adduct-induced DNA damage, a theme which will be explored in Chapter VI. The range of relative resistance for the selected multidrug resistant phenotype (MDR) and non-MDR drugs is shown in Tables 3.6 and 3.7. For the HCC cell lines, the range of relative resistance varies for each drug with a > 125 and 13-fold difference in relative resistance levels observed for 5-FU and cisplatin, respectively, whereas both melphalan and etoposide exhibit a 5-fold difference in relative resistance levels. The range of relative resistance in the CRC cell lines, however, is less varied with a 7-fold difference for both cisplatin and etoposide, and 10- and 3-fold difference for 5-FU and melphalan respectively.

Cell Line[1]	Relative Resistance[2]			
	MDR	Non-MDR		
	Etoposide	Cisplatin	5-FU	Melphalan
SkHep-1	0.5	8	12.5	1.16
Hep3B	0.55	3.6	7.5	1.8
C3A	1	1	1	1
HepG2	2.5	10	>125	1.33
PLC/PRF/5	5.55	13.72	18.75	5

Table 3.6. Relative resistance of HCC cell lines to selected cytotoxic drugs. [1]Cell lines are listed in increasing rank order of resistance to etoposide (MDR associated drug). [2]Relative resistance (mean IC_{50} cell line/mean IC_{50} C3A).

MDR = multidrug resistant phenotype.

Cell Line[1]	Relative Resistance[2]			
	MDR	Non-MDR		
	Etoposide	Cisplatin	5-FU	Melphalan
HT-29	1	1	1	1
WIDR	1.52	2.14	2.44	1.97
CACO2	5.21	2.14	10	2.045
SW620	7.6	7.14	3.69	2.7

Table 3.7. Relative resistance of CRC cell lines to selected cytotoxic drugs. [1]Cell lines are listed in increasing rank order of resistance to etoposide (MDR associated drug). [2]Relative resistance (mean IC_{50} cell line/mean IC_{50} HT-29).

MDR = multidrug resistant phenotype.

CHAPTER IV

MULTIDRUG RESISTANCE TRANSPORT PROTEIN ANALYSIS IN HCC AND CRC CELL LINES

IV. MULTIDRUG RESISTANCE TRANSPORT PROTEIN ANALYSIS IN HCC AND CRC CELL LINES

4.1 Introduction

HCC and CRC are often regarded as intrinsically resistant to multiple chemotherapeutic agents(Lai et al, 1991; Mathurin et al, 1998; Simonetti et al, 1997). Although unresectable CRC liver metastases can be downstaged to resectable lesions (Bismuth et al, 1996; Giacchetti et al, 1999), frequently, when response to chemotherapy does occur, it is followed by acquired drug resistance and clinical relapse (Nerenstone et al, 1988). Tumour cells often show broad cross-resistance between unrelated classes of cytotoxic drugs, a phenomenon known as multidrug resistance (MDR). To date, at least two multidrug resistance mechanisms have been described, involving members of the ATP binding cassette transporter superfamily, namely P-gp and MRP1. P-gp and MRP1 function as transmembrane drug efflux pumps, decreasing intracellular accumulation, thereby confering resistance to various natural product drugs. LRP is another multidrug resistance related protein identified as the major vault protein (Scheffer et al, 1995). Although different from ATP binding cassette molecules, vaults have been implicated in transport of various substrates, including cytotoxic drugs (Chugani et al, 1993; Kickhoefer et al, 1998).

These MDR related proteins are broadly distributed in normal cells. P-gp is expressed on the bile canalicular surface of hepatocytes and the luminal surface of epithelial cells of biliary ductules in normal liver (Itsubo and Toda, 1996), and high levels of P-gp have also been localised to the apical surfaces of colonic epithelium (Meijer et al, 1999). MRP1 and LRP expression has also been found in normal liver and colon. An

increase in the expression of P-gp, MRP-1 and LRP has been observed in numerous clinical cancer specimens as well as cancer cell lines displaying the MDR phenotype *in vitro* (Izquierdo et al, 1996). Several reports suggest these MDR related proteins are clinically relevant in haematological malignancies (Guerci et al, 1995; Samdani et al, 1996; Senent et al, 1998; Wood et al, 1994), in particular elevated levels of LRP have been shown to be a strong and independent predictor of unfavourable outcome (Hart et al, 1997). Their contribution to clinical drug resistance in solid tumours, however, is less clear.

Expression of P-gp has previously been investigated in HCC, where levels in human HCC tissue has been shown to be inversely correlated with chemotherapeutic response (Chou et al, 1997; Ng et al, 2000), and in CRC where it has been linked to increased metastatic potential (Weinstein et al, 1991). Few studies, however, have assessed the expression of MRP1 and LRP in HCC and CRC. The MRP1 protein has been found to be highly expressed in HepG2 hepatoma cells (Roelofsen et al, 1997). Its gene expression was decreased by combined treatment with IFNα and cisplatin whilst the hepatoma cell lines HuH7 and SK-Hep-1 were not affected (Takeuchi et al, 1999). *MRP1* gene expression in ten childhood hepatoblastomas was higher than that observed in normal liver and nine HCCs from adult patients (Matsunaga et al, 1998). MRP1 has been found to be expressed in HT-29 colon adenocarcinoma cells, where the cytotoxic effect of camtothecin was increased by the specific modulators probenecid and MK571 (Chauvier et al, 2002). The expression of the *LRP* gene was not altered in three childhood hepatoblastoma xenografts incorporated into mice following treatment with adriamycin or cisplatin, indicating it is not involved in

resistance to these cytotoxic agents (Bader et al, 1998). LRP protein expression has not previously been investigated in CRC.

The aim of this section of the study was to analyse the expression of P-gp, MRP1 and LRP in the chosen panel of HCC and CRC cell lines, and to establish whether P-gp was functioning when present. The expression of MDR transport proteins was then related to the chemosensitivity of the cell lines. Correlations between MDR protein expression and the IC_{50} values of the HCC cells were determined by Spearman's rank correlation test, the correlation coefficients (r-values) and the P-values (two sided) were calculated. Only correlations with P-values of 0.05 or below were considered to be significant. The potentiating effect of inhibition of P-gp with vpm and PSC833 on chemosensitivity was also analysed to confirm the results of P-gp function on flow cytometry.

4.2 Materials and methods

4.2.1 Expression of MDR-related proteins

P-gp, MRP1 and LRP protein expression was determined by FACScan analysis using the monoclonal antibodies MRK16 MRPm6 and LRP56. Full details of the protocol are given in Chapter II, Section 2.6.1. Expression of P-gp was confirmed by Western blot analysis using the monoclonal antibody C219. Full details of the protocol are given in Chapter II, Section 2.7.

4.2.2 P-gp function

P-gp function was determined by FACScan analysis using $DiOC_2$, a fluorescent substrate for P-gp. Full details of the protocol are given in Chapter II, Section 2.6.2.

4.2.3 Expression of transport proteins related to cytotoxicity

To test the findings of the P-gp flow cytometry functional assay, and to determine whether P-gp contributed to resistance to etoposide and a further cytotoxic P-gp substrate vincristine, cytotoxic assays were carried out in the presence of PSC833 and vpm, both known modifiers of P-gp mediated MDR (Boesch et al, 1991). Exponentially growing cells were harvested as already described, inoculated into 96-well tissue culture plates in a volume of 100 µl at densities between 5000 and 20,000 cells per well and allowed to attach for 24 h at 37°C, 5% CO_2, in a humidified atmosphere. After overnight incubation, the plates were removed and all medium aspirated from the wells. The P-gp inhibitors were prepared at the required concentrations (1 or 6 µM) by diluting the stock solution with serum-free MEM, 50 µl was added to each well 30 min prior to each test drug. Drug solutions were then prepared at the required concentrations (0.01-500 µM) by diluting the stock solution with serum-free MEM, 50 µl was added to each well followed by a further 100 µl of the appropriate medium containing 10% FCS. Control wells received drug free medium alone. All wells were then cultured for a further 4-5 days, until the control wells were seen to have grown to an almost confluent state when examined by microscopy. At this stage the plates were stained and analysed using the SRB assay. Full details of the protocol are given in Chapter II, Section 2.5.

4.3 Results

4.3.1 Expression of MDR-related proteins

P-gp expression, determined by FACScan analysis using the anti-P-gp monoclonal antibody, MRK16, was demonstrated in 2 of the 5 HCC cell lines (HepG2 and C3A), with ratios of 4.07 and 3.92 respectively, relative to the control mouse antibody IgG2a (Figure 4.1A, Table 4.1A). Two of the 4 CRC cell lines (SW620 and CACO2) expressed P-gp with ratios of 4.88 and 1.55 respectively (Figure 4.1B, Table 4.1B). The P-gp positive control, CEM/$VLB_{100,}$ was strongly positive with a ratio of 19.12 (a ratio of > 1.5 was considered a positive result) (Figure 4.2, Tables 4.1A & B). MRP1, measured with MRPm6, was expressed in all HCC cell lines with ratios ranging from 1.9 (SKHep-1) to 7.5 (Hep3B) and two CRC cell lines (SW620 and WIDR) with ratios of 4.07 and 2.29 respectively (Figures 4.1A & B, Tables 4.1A & B). The immunofluorescence detection of LRP-56, a measure of the presence of LRP, was detected in all HCC cell lines except Hep3B cells, with ratios ranging from 2.64 (C3A) to 12.4 (SKHep-1), and all CRC cell lines except CACO2, with ratios ranging from 2.6 (SW620) to 11.13 (HT-29) (Figures 4.1A & B, Tables 4.1A & B).

The immunoblot data on P-gp expression were in agreement with FACScan analysis. HepG2, C3A, SW620 and CACO2 cell line protein lysates produced weak bands at molecular weight 170 KDa. Similar band signals were not visible with SK-Hep-1, PLC/PRF/5, Hep3B, WIDR and HT-29 cell lines (Figure 4.3).

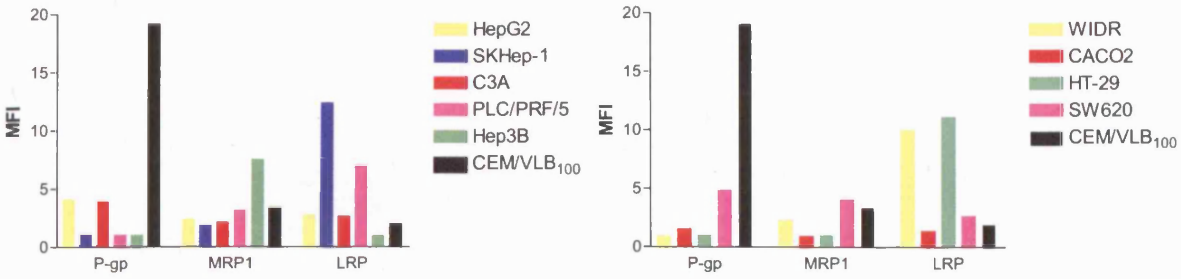

A B

Cell Line	HepG2	SKHep-1	C3A	PLC/PRF/5	Hep3B	CEM/VLB$_{100}$
P-gp	4.07	1.07	3.92	1.0	1.0	19.12
MRP1	2.37	1.9	2.13	3.16	7.5	3.4
LRP	2.74	12.4	2.64	6.98	1.0	1.98

A

Cell line	WIDR	CACO2	HT-29	SW620	CEM/VLB$_{100}$
P-gp	0.94	1.55	1.03	4.88	19.12
MRP1	2.29	0.93	1.04	4.07	3.4
LRP	10.01	1.38	11.13	2.64	1.98

B

Figure 4.1 & Table 4.1. Immunocytochemical MDR phenotype in **A.** human HCC and **B.** human CRC cell lines. P-gp, MRP and LRP expression was measured by FACScan, using the monoclonal antibodies MRK-16, MRPm6 and LRP56 respectively. Values were expressed as median fluorescence index (MFI).

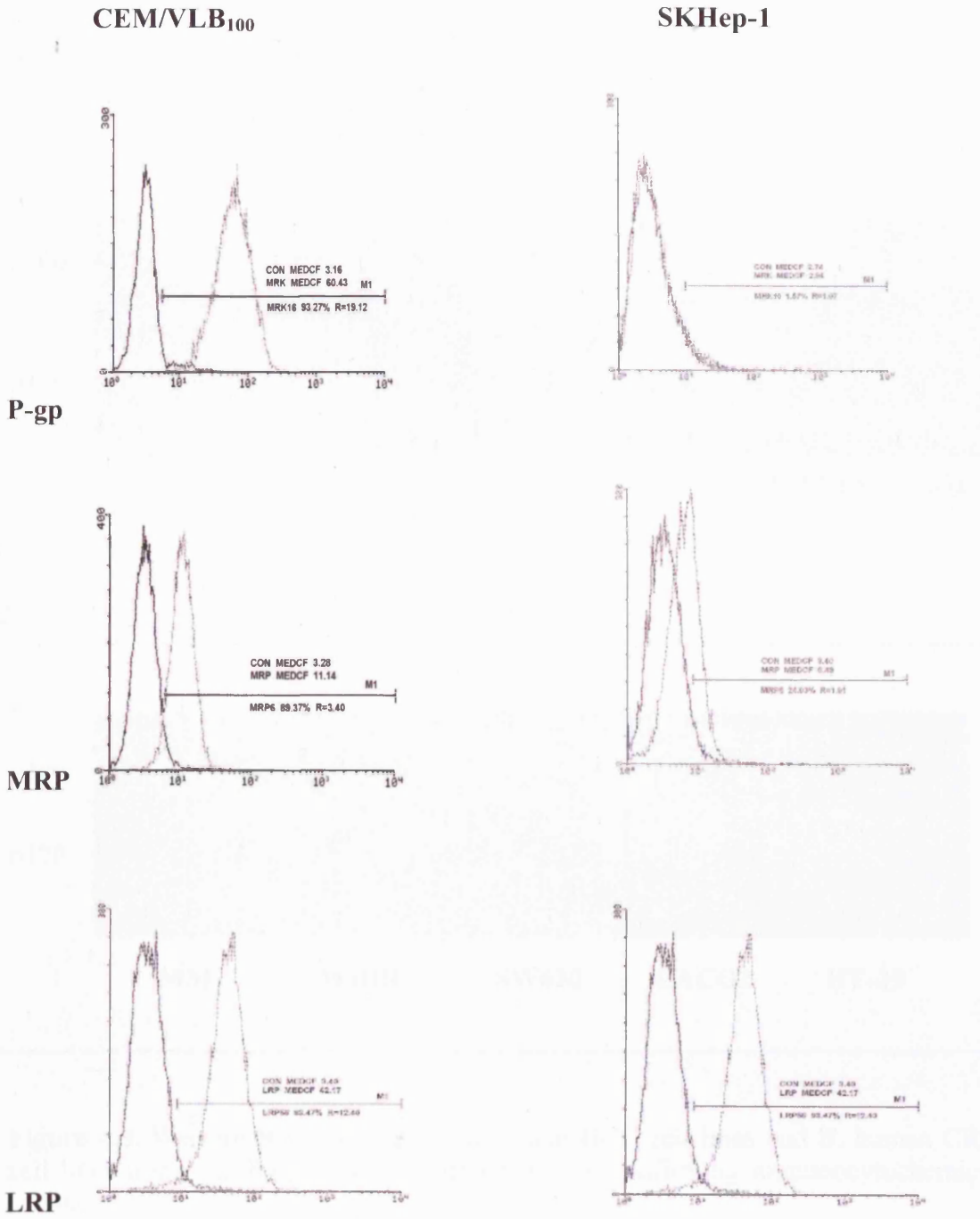

Figure 4.2. Immunocytochemical MDR phenotype of CEM/VLB$_{100}$ demonstrating strongly positive P-gp ratio of 19.12, and SKHep-1 which failed to demonstrate P-gp. **P-gp, MRP1** and **LRP** expression was measured by FACScan analysis using monoclonal antibodies MRK16, MRPm6 and LRP56 and compared with control mouse antibodies IgG2a, IgG2b and IgG1 respectively.

A

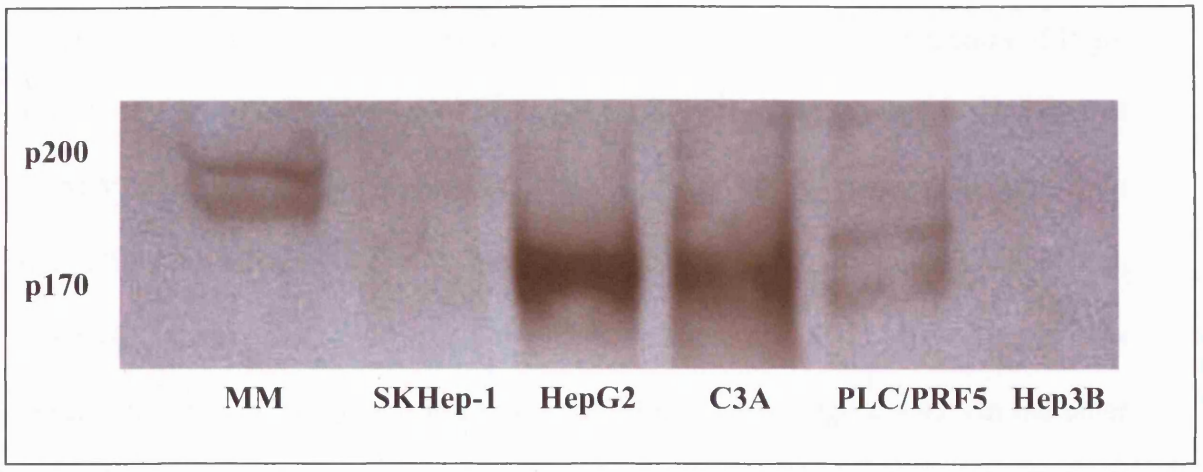

B

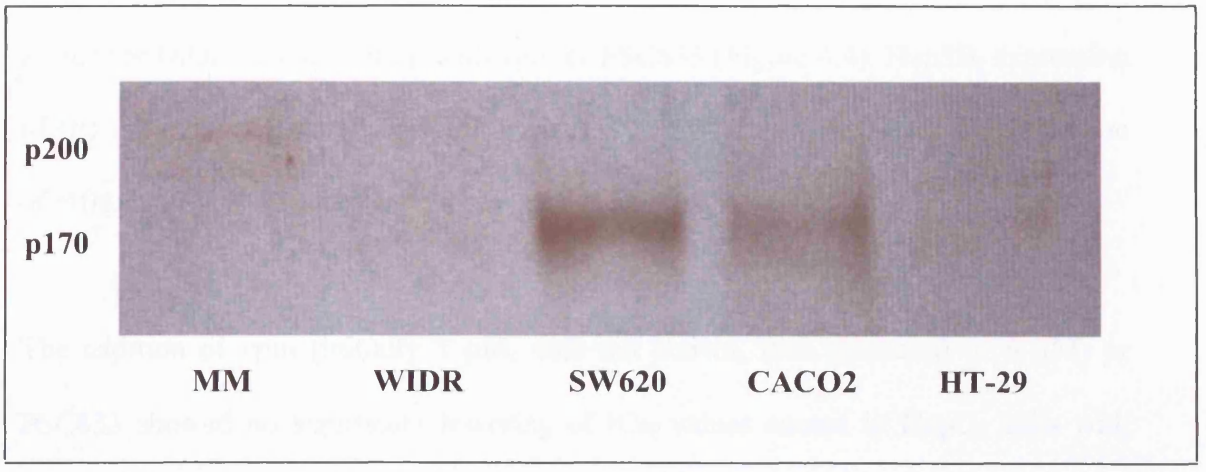

Figure 4.3. Western Blot analysis of **A.** human HCC cell lines and **B.** human CRC cell lines using the P-gp specific antibody C-219 confirming immunocytochemical results.

MM = Molecular Marker (MW 200 kDa)

4.3.2. P-gp function

The fluorescent dye $DiOC_2$ is a specific substrate for P-gp and provides a sensitive functional assay in addition to immunostaining approaches for the detection of P-gp. $DiOC_2$ uptake was significantly reduced in the strongly P-gp positive control CEM/VLB_{100} cells relative to the HCC cells. Conversely after treatment with the P-gp drug efflux inhibitors vpm (1 μM) and PSC833 (1 and 2 μM) for both 30 and 90 min, a strong enhancement of intracellular accumulation of $DiOC_2$ fluorescence was observed indicating functional P-gp in CEM/VLB_{100} cells (Figure 4.4). On the other hand the moderately P-gp positive HCC cell lines HepG2 and C3A, and CRC cell lines SW620 and CACO2, demonstrated no $DiOC_2$ efflux at 90 min and consequently no further $DiOC_2$ accumulation with vpm or PSC833 (Figure 4.4). Hep3B, expressing MRP1 only, demonstrated weak efflux of $DiOC_2$ at 90 min with associated inhibition of efflux with PSC833 but not vpm (Figure 4.5).

The addition of vpm (initially 1 μM, data not shown, then increased to 6 μM) or PSC833 showed no significant lowering of IC_{50} values except in $HepG_2$ cells with vincristine and vpm (Table 4.2 and Figure 4.6) (Appendix 4.1). The modulation ratios (MR), defined as the ratio of the IC_{50} value obtained with and without the addition of reversing agents, ranged between 0.92 and 8.6.

CEM/VLB$_{100}$ **C3A**

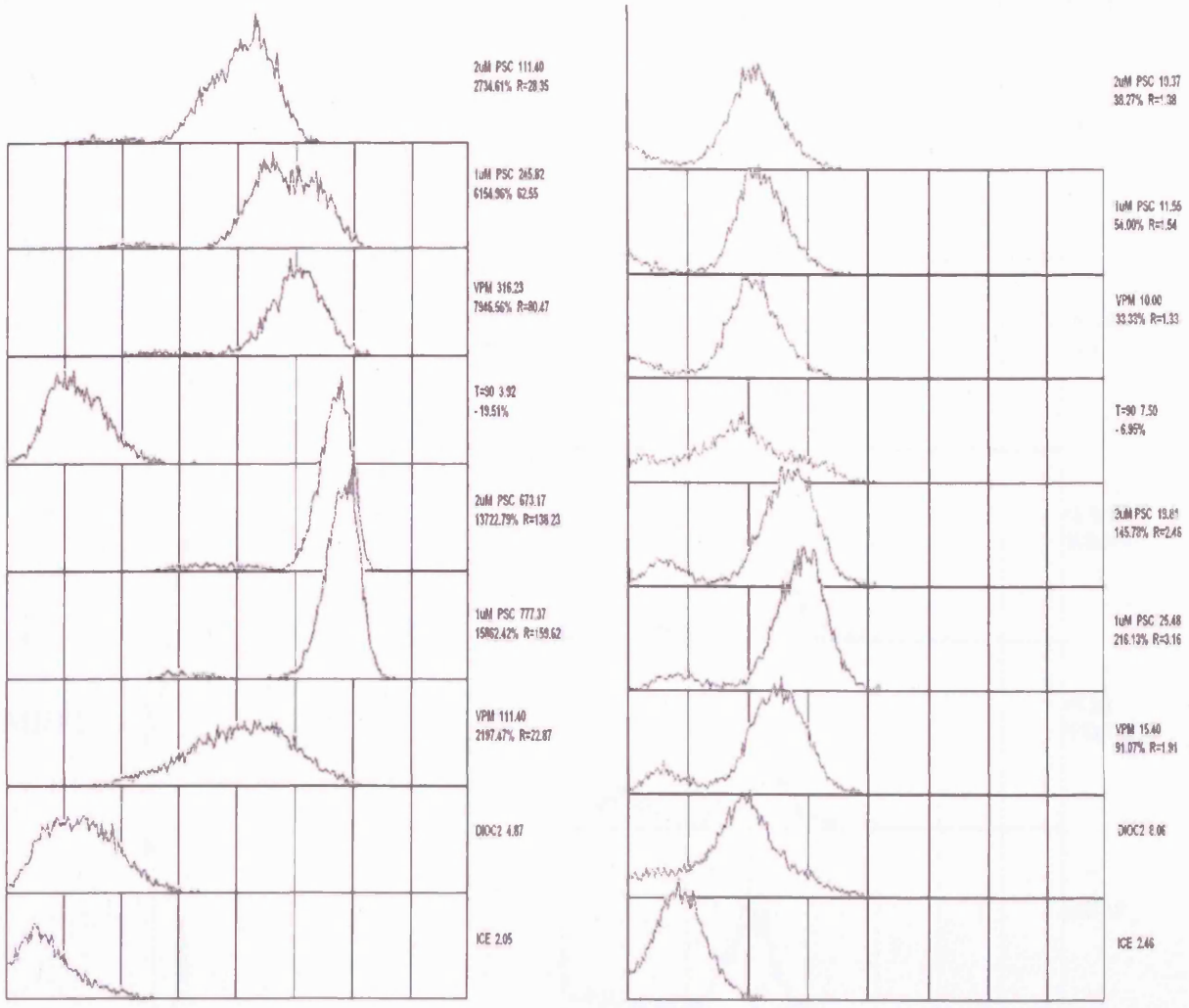

Figure 4.4. Flow cytometry using $DiOC_2$ on P-gp expressing cell lines CEM/VLB$_{100}$ and C3A. CEM/VLB$_{100}$ has functional P-gp as demonstrated by the effect of 1 μM vpm and 1 & 2 μM PSC833 on $DiOC_2$ uptake and retention. No function is shown with C3A as demonstrated by the lack of effect of 1 μM vpm and 1 & 2 μM PSC833 on $DiOC_2$ uptake and retention.

ICE = baseline; $DiOC_2$ = uptake of $DiOC_2$; VPM/1 μM and PSC 1 & 2 μM = effect on efflux.

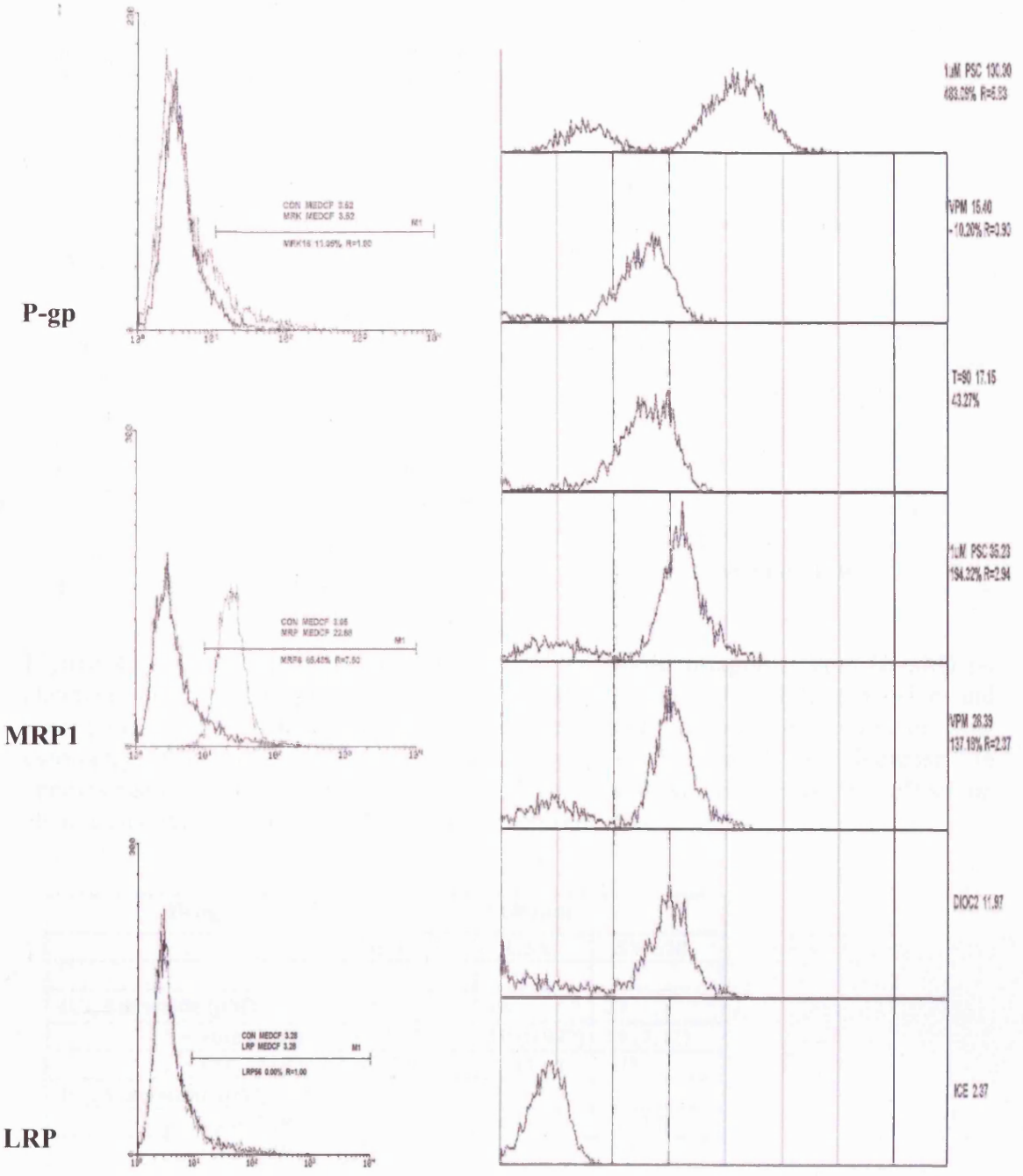

Figure 4.5. Flow cytometry using $DiOC_2$ on **MRP1** expressing cell line Hep3B, demonstrates weak efflux of $DiOC_2$ at 90 min with associated inhibition of efflux with PSC833 but not vpm.

ICE = baseline; $DiOC_2$ = uptake of $DiOC_2$; VPM/1 μM and PSC 1 & 2 μM = effect on efflux.

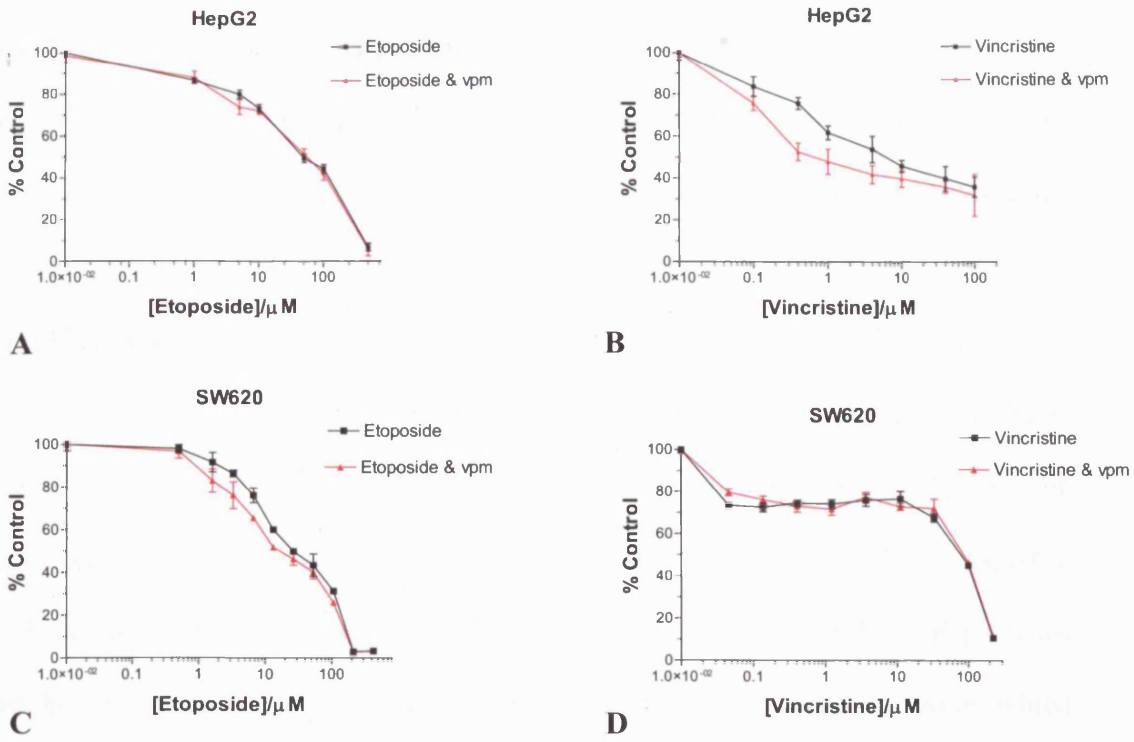

Figure 4.6. The effect of pre-treatment with the MDR antagonist vpm (6 μM) on chemosensitivity of P-gp positive cell lines HepG2 and SW620 to etoposide and vincristine (both substrates for P-gp) was determined to confirm results of flow cytometry functional assay of P-gp. Vpm demonstrated an increase in chemosensitivity only with the cell line HepG2 and vincristine **B.** No effect on chemosensitivity was observed in the other experiments.

Drug		Cell Line		
		Hep-G2	**C3A**	**SW620**
IC_{50} Etoposide (μM)		45	18	27
	+ vpm (MR)	42 (1.07)	19 (0.947)	19 (1.42)
	+ PSC (MR)	40 (1.125)	17 (1.05)	ND
IC_{50} Vincristine (μM)		6.5	1	85
	+ vpm (MR)	0.75 (8.6)	1 (1)	82 (1.03)
	+ PSC (MR)	7 (0.92)	1 (1)	ND

vpm = verapamil (6 μM); PSC = PSC833 (1 μM).
MR = modulation ratio. The ratio of the IC_{50} values without versus with addition of reversing reagent.
ND = not done.
Values are the mean of three experiments.

Table 4.2. Effect of reversing agents on the IC_{50} values of etoposide and vincristine for the two HCC and one CRC P-gp positive cell lines.

4.3.3 Expression of transport proteins related to cytotoxicity

The *in vitro* chemosensitivity of the HCC and CRC cell lines to four chemotherapeutic agents was determined in the previous chapter by the SRB assay (Chapter III, Figures 3.4 and 3.5). Etoposide is a drug known to be transported by the P-gp efflux pump. The two HCC P-gp positive cell lines, HepG2 and C3A, showed similar sensitivity to this drug in comparison to the P-gp negative cell lines. The most resistant HCC cell line to etoposide, PLC/PRF/5, expressed only MRP1 and LRP. The chemosensitivities of anticancer agents that are poor substrates for P-gp (cisplatin, melphalan and 5FU) were also examined. C_3A cells, expressing all 3 MDR proteins, were the most sensitive to all chemotherapeutic agents used, except etoposide, whilst PLC/PRF/5 cells, expressing MRP1 and LRP were the most resistant to all agents except 5FU (Table 4.3.A). Of the CRC cell lines, SW620, which expressed all three MDR proteins, was consistently resistant to all chemotherapeutic reagents, whilst HT-29, expressing LRP only, was consistently sensitive to all reagents (Table 4.4.A).

The expression of P-gp, MRP1 and LRP proteins and their relationship to chemosensitivity was also investigated using Spearman's rank correlation test, no statistically significant correlation was observed (Tables 4.3.B & 4.4.B).

Cell Lines	IC_{50} Etoposide (μM)	IC_{50} Cisplatin (μM)	IC_{50} 5-FU (μM)	IC_{50} Melphalan (μM)	P-gp	MRP1	LRP
HepG2	45	25	1000	40	4.07	2.37	2.74
SK-Hep-1	9	20	100	35	1.07	1.9	12.4
C3A	18	2.5	8	30	3.92	2.13	2.64
PLC/PRF/5	100	50	150	150	1	3.16	6.98
Hep3B	10	9	60	55	1	7.5	1

Table 4.3.A. IC_{50} values and expression of MDR related proteins of HCC cell lines.

Transport protein	Cisplatin		Etoposide		5-FU		Melphalan	
	r-value	P - value	r-value	P - value	r-value	P - value	r-value	P - value
P-gp	-0.154	0.783	0.0513	0.95	0.2	0.783	0.667	0.233
MRP	0.2	0.783	0.4	0.517	0.1	0.95	0.8	0.133
LRP	0.6	0.35	0.000	1.05	0.5	0.45	0.00	1.05

Table 4.3.B. Correlation between IC_{50} values of HCC cell lines and the expression of MDR related proteins. The Spearman rank correlation coefficient (r - values) and significancies (P - values) are given. Only correlations with P-values of 0.05 or below were considered significant.

Cell Lines	IC_{50} Etoposide (μM)	IC_{50} Cisplatin (μM)	IC_{50} 5-FU (μM)	IC_{50} Melphalan (μM)	P-gp	MRP1	LRP
WIDR	7	15	159	87	0.94	2.29	10.01
CACO2	24	15	650	90	1.55	0.93	1.38
HT-29	4.6	7	65	44	1.03	1.04	11.13
SW620	35	50	240	122	4.88	4.07	2.64

Table 4.4.A. IC_{50} values and expression of MDR related proteins of CRC cell lines.

Transport protein	Cisplatin		Etoposide		5-FU		Melphalan	
	r-value	P - value	r-value	P - value	r-value	P - value	r-value	P - value
P-gp	0.63	0.417	0.8	0.33	0.6	0.416	0.8	0.33
MRP	0.632	0.417	0.4	0.75	-0.2	0.916	0.4	0.75
LRP	-0.63	0.417	-0.8	0.33	No correlation		-0.8	0.33

Table 4.4.B. Correlation between IC_{50} values of CRC cell lines and the expression of MDR related proteins. The Spearman rank correlation coefficient (r - values) and significancies (P - values) are given. Only correlations with P-values of 0.05 or below were considered significant.

4.4 Discussion

Despite advances in diagnostic imaging techniques leading to the earlier detection of smaller HCCs, only 5-15% of HCC patients are suitable for surgical resection (Bismuth et al, 1999), whilst only 20-25% of CRC liver metastases are candidates for surgery. Chemotherapy is therefore an important treatment modality for HCC and CRC. They are, however, only moderately sensitive to systemically administered chemotherapeutic agents. To investigate the poor response rates of HCC and CRC to chemotherapy the intrinsic expression of MDR-related proteins, a factor known to be associated with drug resistance, has been evaluated in the chosen panel of HCC and CRC cell lines.

P-gp was found in low levels or was absent in the HCC and CRC cell lines studied. For the HCC cell lines, this is in agreement with most other studies (Isshiki et al, 1993; Lin et al, 1999; Prokipcak et al, 1999). Koike et al, however, failed to demonstrate any P-gp expression in HepG2 cells when transfecting them with cMOAT antisense cDNA (Koike et al, 1996) and low levels of P-gp have been demonstrated in Hep3B (Park et al, 1994 ; Tong et al, 1996), PLC/PRF/5 (Leveille-Webster and Arias, 1996; Marucci et al, 1997; Tong et al, 1996) and SKHep-1 cells (Ihnat et al, 1997). For the CRC cell lines similar observations to the current results have been found in the majority of previous studies (Barnes et al, 1996; Bates et al, 1992; Beaumont et al, 1998; Chauvier et al, 2002a; Kramer et al, 1993; Kunzelmann et al, 1994; Lai et al, 1991; Lalloo et al, 2004; Laska et al, 2002; Luo et al, 2002; Peters and Roelofs, 1992; Vredenburg et al, 2001). Beaumont et al, however, failed to demonstrate P-gp expression in CACO2 cells as did Kramer et al with SW620 cells (Beaumont et al, 1998; Kramer et al, 1993).

An important issue is whether P-gp, once detected in a tumour cell, is also functionally active. P-gp function in HCC cell lines has previously been studied with HepG2 and Hep3B cells using the fluorescent P-gp substrate Rhodamine 123 (Rh 123), with minimal function being demonstrated in HepG2 cells (Lin et al, 1999). In CRC cell lines only CACO2 and SW620 have been examined, neither of which demonstrated any function (Kramer et al, 1993). The current experiments fail to demonstrate any P-gp function using either $DiOC_2$ or Rh 123 (data not shown) in the 4 P-gp positive cell lines. In several studies, the expression of P-gp does not correlate with its drug efflux function (Bailly et al, 1995) and therefore determining the functional role appears to be more informative than quantification of the MDR protein. Kramer et al, investigated P-gp biosynthesis in 19 wild type human CRC cell lines and concluded that only the mature 170 kDa P-gp molecule, but not the 140 kDa precursor, can be phosphoralated and located at the cell surface. Furthermore, they observed a correlation between the phosphorylation status and membrane association of P-gp with the MDR phenotype, emphasising that both of these factors are important in establishing cellular drug resistance (Kramer et al, 1993). The increase in cell associated $DiOC_2$ accumulation produced by vpm and PSC833 treatment in CEM/VLB_{100}, a cell that has been shown to express high levels of P-gp, demonstrates that the $DiOC_2$ uptake assay employed is appropriate for examining P-gp functional activity. The accumulation of $DiOC_2$ was similar in both control and vpm/PSC833 treated HCC and CRC cells. The absence of an effect on $DiOC_2$ uptake with the P-gp modifying agent's vpm and PSC833, suggests that either there is no functional P-gp present in these cells or the activity is too low to be measured. A controversial point is how specific an accumulation defect of $DiOC_2$ is for the action of the pump. The dye has been used in flow cytometry as a mitochondrial dye, thus potentially fluorescence

intensity per cell may vary, not only by virtue of a dye efflux pump, but also with proliferative and/or metabolic activity.

Resistance in P-gp over-expressing cell lines can be reversed by a wide variety of compounds, although the mechanisms underlying chemosensitisation are poorly understood. The most extensively studied reversing agents are the calcium channel blocker vpm and the immunosuppressive compound cyclosporin A. It has been suggested that these compounds reverse resistance by directly binding to P-gp and inhibiting its drug efflux activity. In this study, vpm and PSC833 produced no reversal of resistance except when vpm was used with vincristine on the P-gp positive but drug efflux negative HepG2 cells. The reason for this result is unclear, though an explanation could be the presence of an undescribed non-P-gp, non-MRP1, non-LRP transporter. A recent study on cells from acute myeloid leukaemia (AML) patients reported a cyclosporine-resistant efflux not associated with P-gp, MRP1, or LRP expression in 18% of cases, implying the presence of as yet undefined efflux mechanisms (Leith et al, 1999). The ABC transporter termed breast cancer resistance protein (BCRP) has subsequently been identified in human breast carcinoma cells selected for resistance to doxorubicin in the presence of vpm (Chen et al, 1990; Doyle et al, 1998).

In the current study, MRP1 was demonstrated in all HCC cell lines and the CRC cell lines SW620 and WIDR. This is in agreement with previous studies on HepG2 cells (Roelofsen et al, 1997; Takeuchi et al, 1999) but not with SKHep-1 cells (Takeuchi et al, 1999) or with HT-29 cells (Chauvier et al, 2002a; Chauvier et al, 2002b). No correlation was found between MRP1 expression and the IC_{50} values of the

chemotherapeutic drugs studied, therefore, MRP1 is probably not important in the chemosensitivity of these cell lines. Overexpression of MRP1, which confers resistance to danorubicin, vincristine and other drugs, has been demonstrated to reduce ATP-dependent accumulation of drugs and to enhance drug efflux (Cole et al, 1994). MRP-1 transport has been shown to be dependent on the presence of GSH (Lautier et al, 1996), this is examined in greater detail in Chapter V.

High expression of the LRP protein in AML and ovarian carcinomas has been associated with a poor response to chemotherapy, in particular cisplatin treatment (Izquierdo et al, 1995). In the HCC cell lines, LRP was detectable in all except the Hep3B cells, and present in all the CRC cell lines. No correlation was found between LRP expression and the IC_{50} values of the chemotherapeutic drugs studied. Although their study did not include HCC or CRC cell lines, Izquierdo et al demonstrated a predictive value of LRP expression for *in vitro* sensitivity to several types of drugs, including cisplatin, in a number of different types of cancer cells (such as ovarian and small cell lung cancers) (Izquierdo et al, 1996). The results in these cell lines in the current study indicate that mechanisms other than LRP may control their response to cisplatin. These may include DNA damage recognition proteins in DNA repair and the nucleotide excision repair system in repairing cisplatin DNA damage (Barret and Hill, 1998).

The lack of either functional or significant biochemical evidence for the expression of P-gp in the cell lines examined in this present study would suggest that P-gp has little role in the intrinsic resistance found in HCC and CRC. Similarly, the lack of correlation of MRP1 and LRP with chemosensitivity also suggests that this has a

limited role in MDR resistance in the HCC and CRC cell lines. It is likely that additional drug resistance mechanisms contribute to the overall level of intrinsic tumour drug resistance.

CHAPTER V

INTRACELLULAR GSH LEVELS IN HCC AND CRC CELL LINES

V. INTRACELLULAR GSH LEVELS IN HCC AND CRC CELL LINES

5.1 Introduction

A form of drug resistance that can affect several classes of drugs is associated with increased cellular levels of glutathione (GSH) and/or glutathione S-transferase (GST). GSH has been firmly established in resistance to cisplatin where conjugation of cisplatin and GSH can occur either nonenzymatically under physiological conditions, or be catalysed by GST. The conjugate is then eliminated from the cell by an ATP-dependent glutathione S-conjugate export pump (Goto et al, 1995; Ishikawa and Ali-Osman, 1993). Although cisplatin is not known to induce MDR itself, MDR induced cells can become cross-resistant to cisplatin (Loe et al, 1996a). The possible involvement of MDR in the response to platinum based treatments has also been reported in a panel of 61 human cell lines of eight different tumour types (Izquierdo et al, 1996).

MRP1 confers resistance to heavy metals that interact with GSH (Cole et al, 1994) and to anthracyclines, epipodophyllotoxins, and vinca alkaloids (Grant et al, 1994). Buthionine sulfoxamine (BSO) is a potent irreversible inhibitor of γ-glutamylcysteine synthesis, the enzyme that catalyses the first, rate-limiting step in the synthesis of GSH (Chapter I, Figure 1.9). Treatment of cells with BSO results in the reduction of intracellular GSH levels by up to 90% within 24 h, depending on the cell line examined. A number of studies have shown that BSO-treatment is capable of enhancing drug accumulation and toxicity in MRP1-overexpressing cell lines (Lautier et al, 1996). The mechanism by which BSO inhibits drug transport by MRP1 is believed to be as a direct result of depletion of GSH, and not an interaction between

BSO and MRP1. Evidence supporting this includes the finding that acute exposure to BSO had no effect on drug accumulation (Schneider et al, 1995), and treatment with GSH ethyl ester increased cytoplasmic GSH and decreased daunorubicin accumulation in two BSO-treated MRP1-overexpressing cell lines (Versantvoort et al. 1995).

In this section of the study the total GSH content was determined in the chosen panel of HCC and CRC cell lines, the cell lines were then treated with BSO for 24 h to establish the extent of reduction of intracellular GSH levels and its effect on chemosensitivity to cisplatin. This was then related to each cell lines expression of MRP1 to determine whether it contributed to its intrinsic resistance. Cisplatin was chosen to investigate the effect of GSH on resistance because it is known to conjugate with GSH and the resulting cisplatin-GSH complex has been proposed to be ejected from the cell in an ATP-dependent fashion by the MRP/GS-X pump (Ishikawa, 1992). Cisplatin is also the main drug used in the experiments in the following Chapters.

5.2 Materials and methods

5.2.1 Determination of GSH levels

Intracellular total GSH was determined in 1 x 10^6 cells, both untreated and after exposure to 50 μM BSO for 24 h, by an enzymatic recycling assay based on the glutathione reductase method. Full details of the protocol are given in Chapter II, Section 2.8.

5.2.2 Reversal of drug resistance with BSO

The chemosensitivity of the HCC and CRC cell lines to cisplatin was repeated with and without prior exposure to BSO for 24 h. Briefly, exponentially growing cells were

harvested as already described, inoculated into 96-well tissue culture plates in a volume of 100 µl at densities between 5,000 and 20,000 cells per well and allowed to attach for 24 h at 37°C, 5% CO_2, in a humidified atmosphere. After overnight incubation, the plates were removed and all medium aspirated from the wells. Fifty µM of BSO was prepared by diluting the stock solution with serum-free MEM, 100 µl was then added to each well and the cells incubated for a further 24 h. After overnight incubation, the plates were removed and all medium aspirated from the wells. Cisplatin solutions were then prepared at the required concentrations (0.01-200 µM) by diluting the stock solution with serum-free MEM, 100 µl was added to each well followed by a further 100 µl of the appropriate medium containing 10% FCS. Control wells received drug free medium alone. All wells were then cultured for a further 4-5 days, until the control wells were seen to have grown to an almost confluent state when examined by microscopy. At this stage the plates were stained and analysed using the SRB assay. Full details of the protocol are given in Chapter II, Section 2.5.

5.3 Results

5.3.1 Determination of GSH levels

The total levels of GSH in the HCC cell lines ranged between 3.53 and 7.13 nM/10^6 cells (Figure 5.1.A and Table 5.1). The highest levels were seen in the relatively cisplatin resistant cell lines HepG2 (IC_{50} 24.67 µM) and SkHep1 (IC_{50} 23.39 µM) (7.13 and 6.11 nM/10^6 cells respectively). PLC/PRF/5 (IC_{50} 35.35 µM), the cell line most resistant to cisplatin, however, had the lowest level of GSH (3.53 nM/10^6 cells). The addition of BSO led to a decrease in GSH in the range of 1.52 to 3.34 fold, the highest fold difference being seen in HepG2 (3.34 fold) and SkHep1 and Hep3B (both 2.17 fold). The total levels of GSH in the CRC cell lines ranged between 4.67 and

6.52 nM/10^6 cells. The addition of BSO lead to a decrease in GSH in the range of 1.67 to 2.31 fold (Figure 5.1.B and Table 5.2).

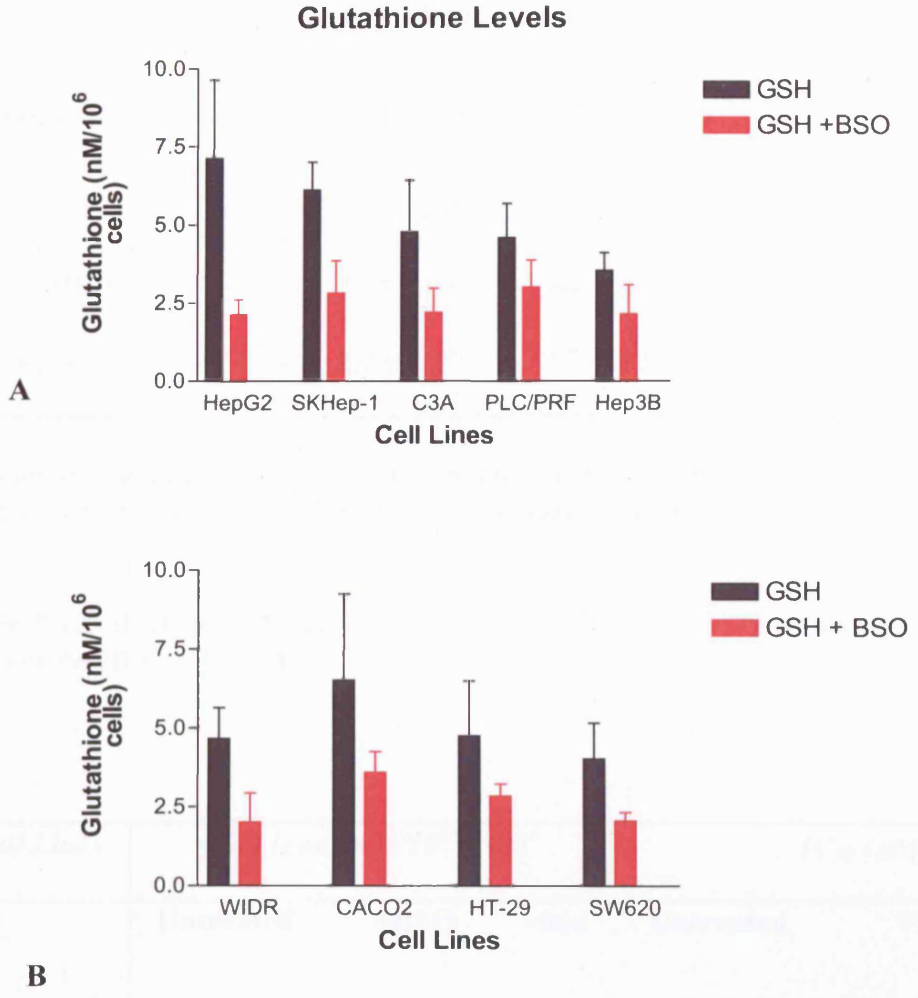

Figure 5.1. Intracellular GSH content measured in untreated **A.** HCC and **B.** CRC cells, and cells exposed to BSO. Cells (1 x 10^6), after a 24 h attachment period, had their medium replaced with either normal culture medium or medium containing 50 μM BSO for 24 h prior to harvesting and measurement of their total GSH content by an enzymatic recycling procedure. Values represent the mean ±SEM of three independent experiments.

Cell Lines	*GSH level (nM/10^6 cells)*[a]			*IC_{50} (μM)*[b]		
	Untreated	**+BSO**	**-fold**	**Untreated**	**+BSO**	**-fold**
HepG2	7.13 ±2.51	2.13 ±0.48	3.34	24.67 ± 0.67	15.86 ± 1.33	1.55
SkHep-1	6.11 ±0.89	2.81 ± 1.04	2.17	23.39 ± 1.87	17.02 ± 1.8	1.37
C3A	4.58 ± 1.1	3.0 ± 0.87	1.52	7.16 ±0.93	7.15 ± 0.4	1.0
PLC/PRF/5	3.53 ± 0.57	2.15 ± 0.92	1.64	35.35 ± 1.57	22.27 ± 1.35	1.58
Hep3B	4.78 ± 1.64	2.2 ± 0.77	2.17	17.34 ± 0.71	8.31 ±0.933	2.08

[a] Values are the means ±SEM of three independent experiments.
[b] Values are the means ±SEM of four independent experiments.

Table 5.1. Effect of 24 h incubation of 50 μM BSO on GSH levels and IC_{50}s with cisplatin on HCC cell lines.

Cell Lines	*GSH level (nM/10^6 cells)*[a]			*IC_{50} (μM)*[b]		
	Untreated	**+BSO**	**-fold**	**Untreated**	**+BSO**	**-fold**
WIDR	4.67 ± 0.98	2.02 ± 0.92	2.31	14.52 ± 2.98	9.68 ± 1.77	1.5
CACO2	6.52 ± 2.73	3.6 ± 0.66	1.81	11.95 ± 2.34	10.87 ± 0.99	1.09
HT-29	4.75 ± 1.75	2.85 ± 0.38	1.67	9.21 ± 0.95	8.73 ± 2.3	1.05
SW620	4.03 ± 1.26	2.07 ± 0.26	1.94	48.25 ± 1.52	25.5 ± 1.64	1.89

[a] Values are the means ±SEM of three independent experiments.
[b] Values are the means ±SEM of four independent experiments.

Table 5.2. Effect of 24 h incubation of 50 μM BSO on GSH levels and IC_{50}s with cisplatin on CRC cell lines.

5.3.2 Reversal of drug resistance with BSO

The effect on IC_{50}s in the HCC cell lines ranged between 1 and 2.08 fold, the highest fold difference being seen in Hep3B (2.08 fold) (Figure 5.2 and Table 5.1). The effect on IC_{50}s in the CRC cell lines ranged between 1.05 and 1.89 fold, the highest fold difference being seen in SW620 (1.89 fold) (Figure 5.3 and Table 5.2).

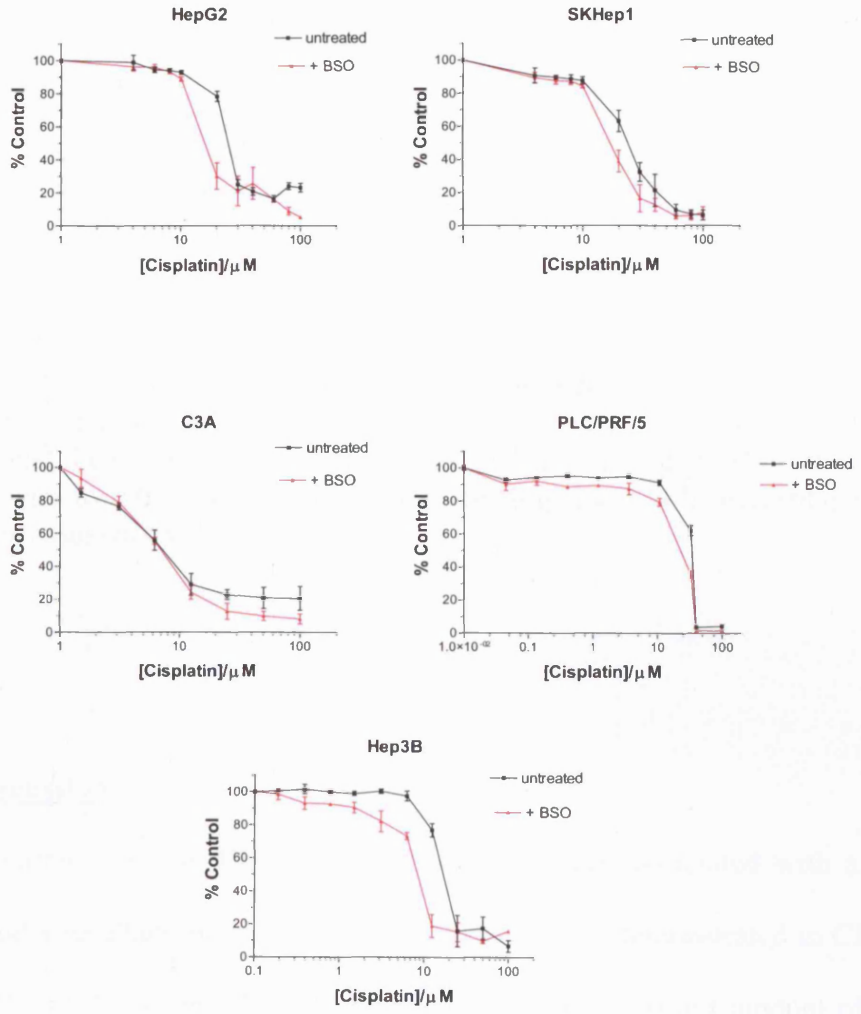

Figure 5.2. The effect of reduction of GSH using BSO on inhibition of cell growth by cisplatin in human HCC cell lines. Cells (5 x 10^3 - 2 x 10^4), after a 24 h attachment period, had their medium replaced with medium containing 50 μM BSO for 24 h prior to exposure to 0.01-100 μM cisplatin or no drug for 120 h. Percentage cell growth was then assessed by the SRB assay.

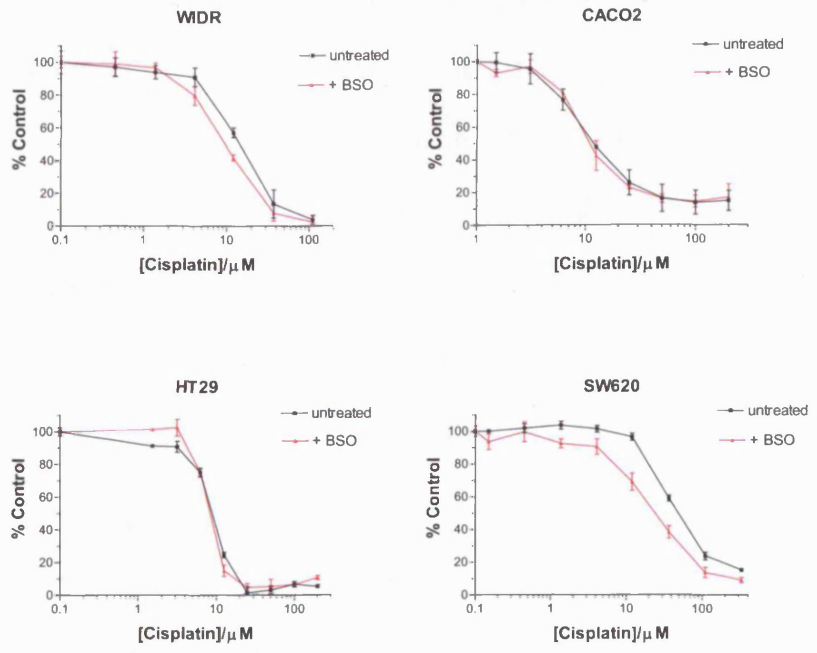

Figure 5.3. The effect of reduction of GSH using BSO on inhibition of cell growth by cisplatin in human CRC cell lines. Cells ($1x10^4$ - 2×10^4), after a 24 h attachment period, had their medium replaced with medium containing 50 μM BSO for 24 h prior to exposure to 0.01-100 μM cisplatin or no drug for 120 h. Percentage cell growth was then assessed by the SRB assay.

5.4 Discussion

In the current section, BSO treatment was generally associated with a decrease in GSH and a resultant increase in chemosensitivity. As demonstrated in Chapter IV, of the HCC cell lines, only Hep3B cells expressed a significant amount of MRP1 (7.5 MFI) (Chapter IV, Figure 4.1A, Table 4.1A). This has now shown to be associated with modest levels of intracellular GSH (4.78 nM/10^6cells), but a 2.17 fold reduction with BSO and an associated 2.08 fold increase in sensitivity to cisplatin. Of the CRC cell lines, SW620 cells expressed the largest amount of MRP1 (4.07 MFI) (Chapter

IV, Figure 4.1B, Table 4.1B), this was again associated with modest levels of intracellular GSH (4.03 nM/10^6cells), but a 1.94 fold reduction with BSO and an associated 1.89 fold increase in sensitivity to cisplatin. This suggests that the combination of MRP1 and GSH contributes to cisplatin resistance in these cell lines. Of the other MRP1 expressing cell lines (HepG2, SkHep1, C3A, PLC/PRF/5 and WIDR), even though they demonstrated similar or higher levels of GSH, and had significant reduction of GSH levels this led to minimal fold differences in chemosensitivity.

Of the numerous mechanisms involved in drug resistance, a decrease in drug accumulation is believed to play a major role in resistance to cisplatin (Tew, 1994). Cisplatin rapidly interacts with GSH thus MRP1 may be a GSX pump that promotes the ATP dependent efflux of GSH conjugated cisplatin (Ishikawa et al, 1996). However, cells transfected with the sense MRP1 cDNA and drug selected MRP1 overproducing cells did not show any altered sensitivity to cisplatin (Cole et al, 1994; Koike et al, 1996).

Observations that the GSH-conjugated chemotherapeutic drugs doxorubicin and daunorubicin, but not the unconjugated drugs were capable of competitively inhibiting the MRP-mediated transport of leukotriene C_4 (LTC_4) *in vitro* (Priebe et al, 1998) have led to speculation that MRP-mediated drug resistance occurs by the transport of drug conjugates from cells. As mentioned above MRPs have previously been called MRP/GS-X pumps (Ishikawa, 1992). This, however, has turned out to be inappropriate as MRP1 and MRP2 have been shown to be capable of transporting compounds not conjugated to GSH such as bilirubin mono- and diglucuronides.

Although many substrates for MRPs are conjugated compounds, the conjugation is thought not to be critical for transport. There has been some evidence that reduced GSH can also act as either a co-substrate or possess the ability to activate MRPs. Evidence for this comes from the observation that unconjugated chemotherapeutic agents, such as doxorubicin and daunorubicin, fail to inhibit LTC_4 transport in isolated vesicles even at very high doses (Loe et al, 1996b). The addition of reduced GSH, however, increases the inhibitory effect of some of these drugs. Vincristine uptake into membrane vesicles from MRP1-transfected HeLa cells has been shown to be both ATP and GSH dependent and can be inhibited by the MRP1-specific mouse antibody QCRL-3 (Loe et al, 1998). In this study, vincristine transport in the absence of GSH was extremely low and showed no ATP dependence, whereas active vincristine transport increased with increasing concentrations of GSH. As GSH appears not to be a substrate for MRP-1, there is evidence for the co-substrate theory provided by a study showing that the ATP-dependent uptake of [^{3}H]GSH into membrane vesicles from MRP1-transfected cells could be stimulated by vincristine in a dose-dependent manner (Loe et al, 1996b).

In summary, the evidence so far collected on the transport of compounds by MRP1 suggests that GSH is required and may act as a co-substrate during transport of compounds. The mechanism by which this occurs is not clear, but GSH may act as a co-substrate with unconjugated compounds, or if the compound is already conjugated, the conjugate attached to the compound acts as a co-substrate.

CHAPTER VI

CISPLATIN SENSITIVITY AND DNA REPAIR OF CROSSLINKS IN HCC AND CRC CELL LINES

VI. CISPLATIN SENSITIVITY AND DNA REPAIR OF CROSSLINKS IN HCC AND CRC CELL LINES

6.1 Introduction

Cisplatin is one of the most important anticancer drugs in the treatment of a wide variety of solid tumours including ovarian, testicular, bladder and small-cell lung carcinomas. Its success in the treatment of HCC and CRC, however, has been limited. In HCC, cisplatin has been administered systemically as both a single agent with response rates (RR) of 17% and median survival (MS) of 3.5 months (Falkson et al, 1987), and in combination with doxorubicin, 5-fluorouracil (5-FU) and interferon α (IFNα) (RR 26%, MS 8.9 months) (Leung et al, 1999); via hepatic arterial infusion combined with 5-FU (RR 71%, 5-year survival 45.7%) (Okuda et al, 1999), and using transcatheter arterial chemoembolisation (TACE) combined with doxorubicin and mitomycin C (RR 23%, MS 6.8 months) (Ueno et al, 2000). It has also been combined with radiotherapy giving an overall RR of 43% (Abrams et al, 1997). In metastatic CRC, a randomized phase II clinical trial demonstrated a RR of 29% to cisplatin in patients pre-treated with 5-FU, and 56% in chemotherapy naive patients with cisplatin administered as a single agent, MS was 12 and 16 months respectively (Falcone et al, 2001). Combining continuous 5-FU and bolus doses of cisplatin have achieved RRs of 40% and 1 and 2 year survivals of 56 and 29% respectively (Tsuji et al, 2000). Cisplatin is thus potentially effective in the treatment of HCC and CRC. A major limitation of cisplatin therapy, however, is that many tumours are intrinsically resistant or develop resistance over the course of treatment.

It is generally accepted that the cytotoxic activity of cisplatin results from its interactions with DNA (Chapter I, Figure 1.2). Platinum-DNA (pt) covalent adducts inhibit fundamental cellular processes, including replication, transcription, translation and DNA repair (Suo et al, 1999). As previously discussed interstrand crosslinks (ICL) represent a small amount of the total cisplatin lesions but several studies have suggested that they could also be responsible for the cytotoxicity of the drug. The distortions induced by these crosslinks exhibit specific features such as location of the platinum residue in the minor groove, extrusion of the cytosines of the crosslinked d(GpC) d(GpC) site, bending of the helix axis towards the minor groove and large DNA unwinding (Malinge et al, 1999).

HCC and CRC often show intrinsic resistance to cisplatin or develop resistance after initially responding to treatment (Falkson et al, 1987). The problem is complicated by the multitude of molecular mechanisms that have been associated with cisplatin resistance. These mechanisms include 1) reduced intracellular accumulation of the drug (Kuppen et al, 1988). When decreases in cisplatin accumulation are observed they are usually modest, and often do not correlate with the level of resistance. To date, the search for a specific cisplatin membrane transport system has been inconclusive (Andrews and Howell, 1990). 2) Increased pt-DNA damage tolerance as manifested by defects in mismatch repair and enhanced replicative bypass (Vaisman et al, 1998). 3) Increased drug inactivation by intracellular thiols. The role of glutathione (GSH) in cisplatin resistance seems to be important as cells with *in vitro* acquired resistance often show elevated levels of GSH compared with parental cells (Meijer et al, 1992). Glutathione S-transferase (GST) catalyses the conjugation of cisplatin to GSH, the cisplatin-GSH complex has been proposed to be ejected from

the cell in an ATP-dependent fashion by the glutathione S-conjugate export pump (Goto et al, 1995). 4) Enhanced pt-DNA repair. Prior studies have demonstrated increased sensitivity of cells deficient in excision repair of cisplatin (Fraval et al, 1978). Many pt-resistant cell lines appear to have enhanced repair activity based on the rate of disappearance of intrastrand adducts from unreplicated DNA (Lai et al, 1988; Parker et al, 1991), and the rate of disappearance of ICLs (Johnson et al, 1994a; Johnson et al, 1994b).

Previous studies on the rate of repair of ICLs have been predominately on cisplatin-resistant human ovarian cancer cell lines in view of its effectiveness clinically (Johnson et al, 1994a; Johnson et al, 1994b; Lai et al, 1988; Parker et al, 1991; Zhen et al, 1992). Further studies have also been performed using murine leukaemia L1210 cells (Eastman and Schulte, 1988) and human BE colon carcinoma cells (Fram et al, 1990). In most, enhanced cisplatin ICL repair has been observed in cisplatin-resistant cells, however some have demonstrated no differences in the kinetics of excision (Fram et al, 1990). The contribution of DNA repair to resistance to cisplatin in HCC has not been previously investigated. Genomic ICL formation and repair in cells has been measured most frequently using the alkaline elution technique (Fram et al, 1990; Zhen et al, 1992). An equally sensitive, but simpler and quicker method is the single cell gel electrophoresis (comet) assay. Although established for measuring DNA strand breaks, the technique can be easily modified to allow the sensitive detection and quantification of DNA ICLs at the single cell level (Blasiak et al, 2000).

In this section of the study, the induction and excision of cisplatin DNA ICLs in human HCC and CRC cell lines were determined at the level of the overall genome by the comet assay, and related to pt chemosensitivity. The objective was to evaluate the

extent of initial ICL formation and the contribution of DNA repair to pt resistance with HCC and CRC cell lines.

6.2 Materials and methods

6.2.1 One hour cytotoxicity determination

When cisplatin is given intravenously (i.v.) in a clinical situation it is rapidly sequestered by protein binding, such that 1 h after administration no free drug remains in the plasma. The IC_{50}s of HCC and CRC cell lines to cisplatin exposure for 1 or 120 h were therefore determined by the SRB assay to assess cisplatin cytotoxicity and allow comparison with ICL formation and repair rates. Full details of cytotoxicity determination are given in Chapter III, Section 3.2.2, and the protocol for the SRB assay is given in Chapter II, Section 2.5.

6.2.2 Interstrand cross-linking and repair

6.2.2.1 Extent of ICL formation

Since DNA ICLs are critical lesions for cisplatin cytotoxicity, the comet assay was used to quantify these lesions in the overall genome. Cells were initially treated with 10-100 μM cisplatin for 1 h, washed, and incubated in drug free medium for 12 h. The treated samples, plus one control, were subjected to 10 Gy X-irradiation. The second control remained un-irradiated, the comet assay was then performed as described in Chapter II, Section 2.9. A 12 h incubation was chosen since peak levels of ICLs have been shown to be formed during this time interval over a wide range of doses (Zwelling et al. 1978).

6.2.2.2 Rates of formation and repair of ICLs

The relative rates of formation and removal of DNA ICLs were determined at equimolar concentrations of cisplatin. Cells were exposed to 10-100 μM of cisplatin for 1 h, washed, and ICLs measured over the course of 72 h using the comet assay.

6.3 Results

6.3.1 One hour cytotoxicity determination

The HCC cell lines 1 h IC_{50}s were 1.6-4.5-fold higher relative to the 120 h values, the relative resistance, however, remained similar regardless of the duration of drug exposure (Table 6.1A and Figure 6.1). Three of the cell lines tested (HepG2, SKHep-1 and PLC/PRF/5) were resistant to cisplatin with IC_{50}s of 20.66, 21.84 and 36.7 μM at 120 h and 91.18, 93.32 and 88.44 μM at 1 h respectively. The other cell lines (C3A and Hep3B) were sensitive with IC_{50}s of 5.2 and 14.63 μM at 120 h, and 10.96 and 24.54 μM at 1 h. One resistant (SW620) and 1 sensitive (HT-29) CRC cell line was examined, the 1 h IC_{50}s were 3.55 and 6-fold higher relative to the 120 h values respectively, again the relative resistance remained similar (Table 6.1B and Figure 6.2).

A

HCC Cell lines	*IC_{50} (1 h) μM*	*IC_{50} (120 h) μM*
HepG2	91.18 ± 6.8	20.66 ± 1.88[a]
SKHep-1	93.32 ± 4.4	21.84 ± 1.66[a]
C3A	10.96 ± 7.5	5.2 ± 1.82[a]
PLC/PRF/5	88.44 ± 5.4	36.7 ± 2.8
Hep3B	24.54 ± 5	14.63 ± 3.28

B

CRC Cell lines	*IC_{50} (1 h) μM*	*IC_{50} (120 h) μM*
HT-29	40.2 ± 3.21	6.5 ± 3.4
SW620	160.46 ± 4.7	45 ± 2.93 [a]

Values are the means ± SEM of three independent experiments.
[a]Values are the means ± SEM of four independent experiments.

Table 6.1. Sensitivity of **A.** HCC and **B.** CRC cell lines to cisplatin at 1 h and 120 h drug exposure times.

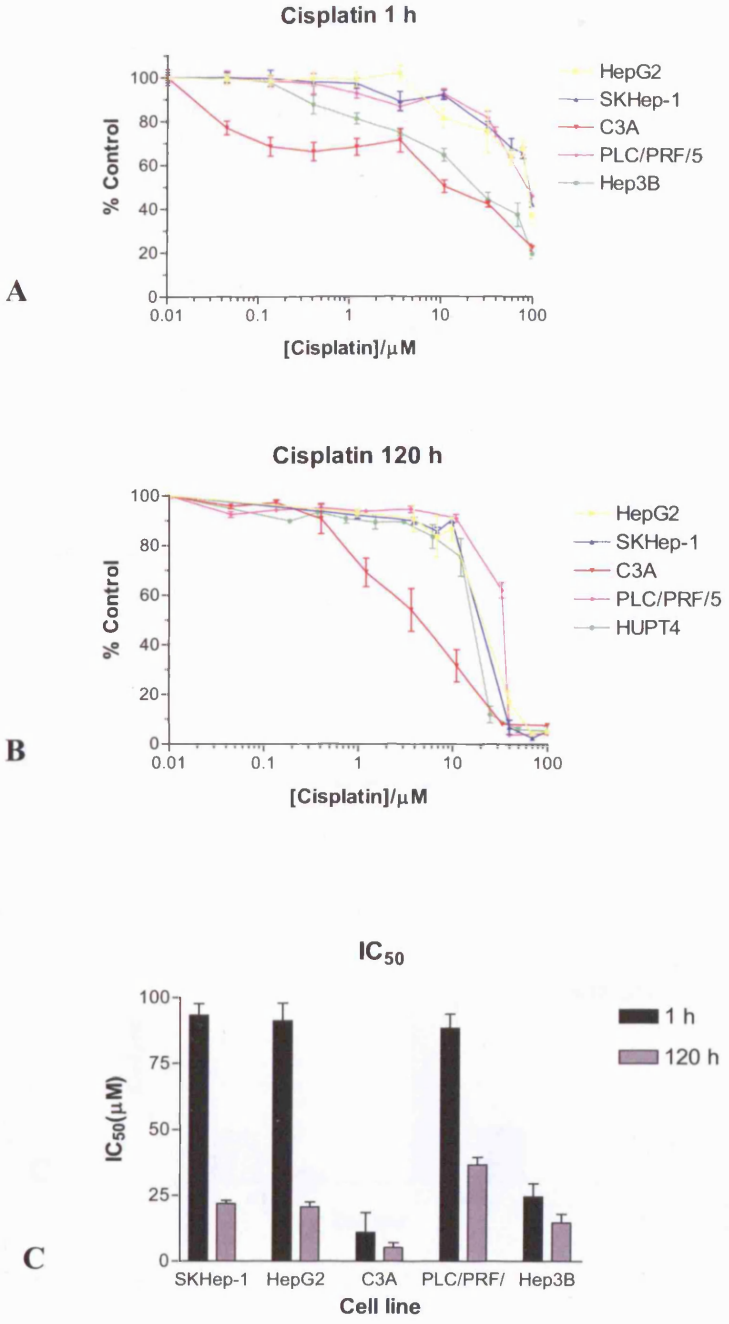

Figure 6.1. Inhibition of cell growth by cisplatin in human HCC cell lines. Cells (1 x 10^4) were exposed to 0.01-100 μM cisplatin or no drug for either **A.** 1 h or **B.** 120 h. Percentage cell growth was then assessed. **C.** Comparisons of the drug concentration that causes a 50% inhibition of control cell growth (IC_{50}) after 1 and 120 h exposure. Values represent the mean ± SEM of three (1 h) and four (120 h) independent experiments.

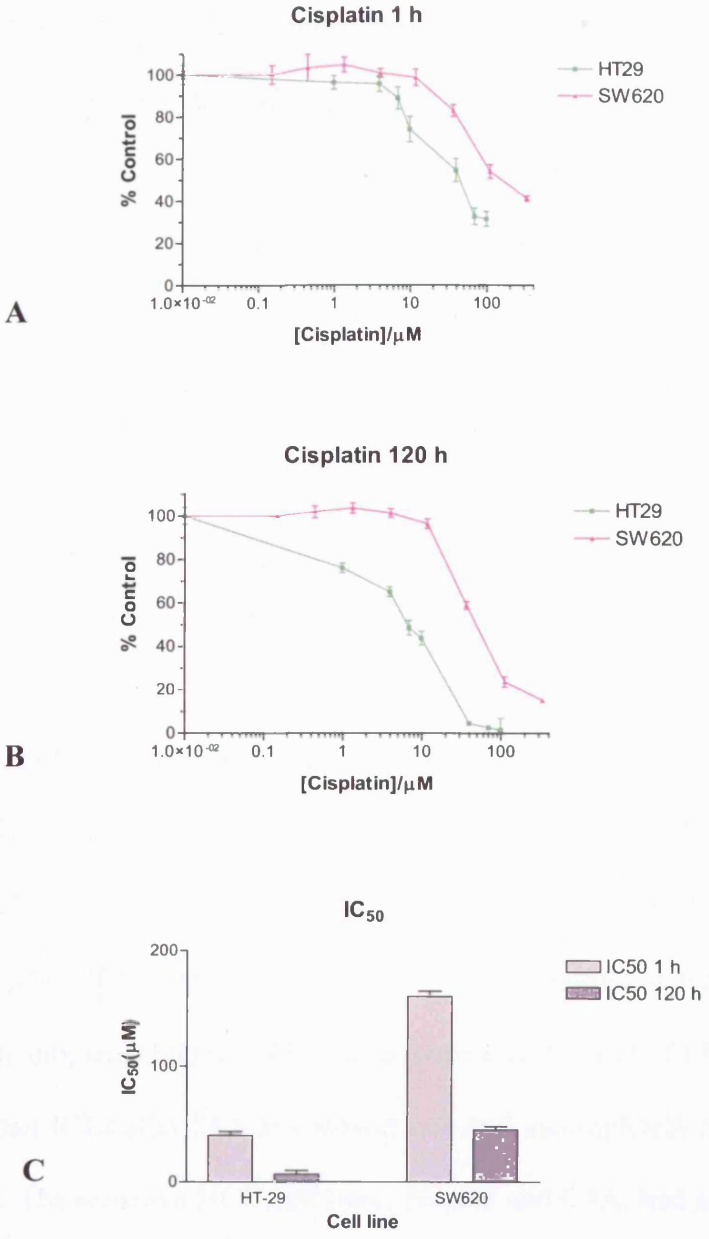

Figure 6.2. Inhibition of cell growth by cisplatin in human CRC cell lines. Cells (1 x 10^4) were exposed to 0.01-100 μM cisplatin or no drug for either **A.** 1 h or **B.** 120 h. Percentage cell growth was then assessed. (C) Comparisons of the drug concentration that causes a 50% inhibition of control cell growth (IC_{50}) after 1 and 120 h exposure. Values represent the mean ± SEM of three (1 h) and four (120 h) independent experiments.

6.3.2 Interstrand cross-linking and repair

6.3.2.1 Extent of ICL formation

As shown in Figure 6.3A, at 12 h ICL formation increased with cisplatin concentration in all cell lines studied. The resistant HCC cell line PLC/PRF/5 had between 1.5 and 3-fold lower levels of ICLs in total cellular DNA compared to the sensitive cell line C3A over the range of drug concentrations measured. This trend was also observed in the resistant and sensitive CRC cell lines, although the magnitude of difference was less marked (1.3 to 2.5-fold), at 100 μM cisplatin SW620 and HT-29 had equivalent ICLs (Figure 6.3B).

6.3.2.2 Rates of formation and repair of ICLs

Two of the HCC cell lines resistant to cisplatin (HepG2 and SKHep-1) began to repair ICLs with all cisplatin concentrations at 18-24 h. At lower concentrations of cisplatin (10 and 25 μM), ICLs were fully repaired at 72 h, whilst at higher concentrations repair was incomplete (Figure 6.4). The resistant cell line PLC/PRF/5 in contrast, only began to repair ICLs after 24 h at a slower rate and incompletely at all concentrations (Figure 6.4). The sensitive HCC cell lines, Hep3B and C3A, had a similar initial rates of removal of ICLs with 10-45 μM at 18-24 h as HepG2 and SKHep-1, the repair rate then decreased with failure to fully repair at any concentration. Essentially no repair was noted at 100 μM (Figure 6.5). The CRC cell lines demonstrated similar initial rates of repair with 10-45 μM at 18-24 h, neither was effective at removing ICLs with 100 μM, SW620 cells completely repaired with 10 μM at 72 h (Figure 6.6).

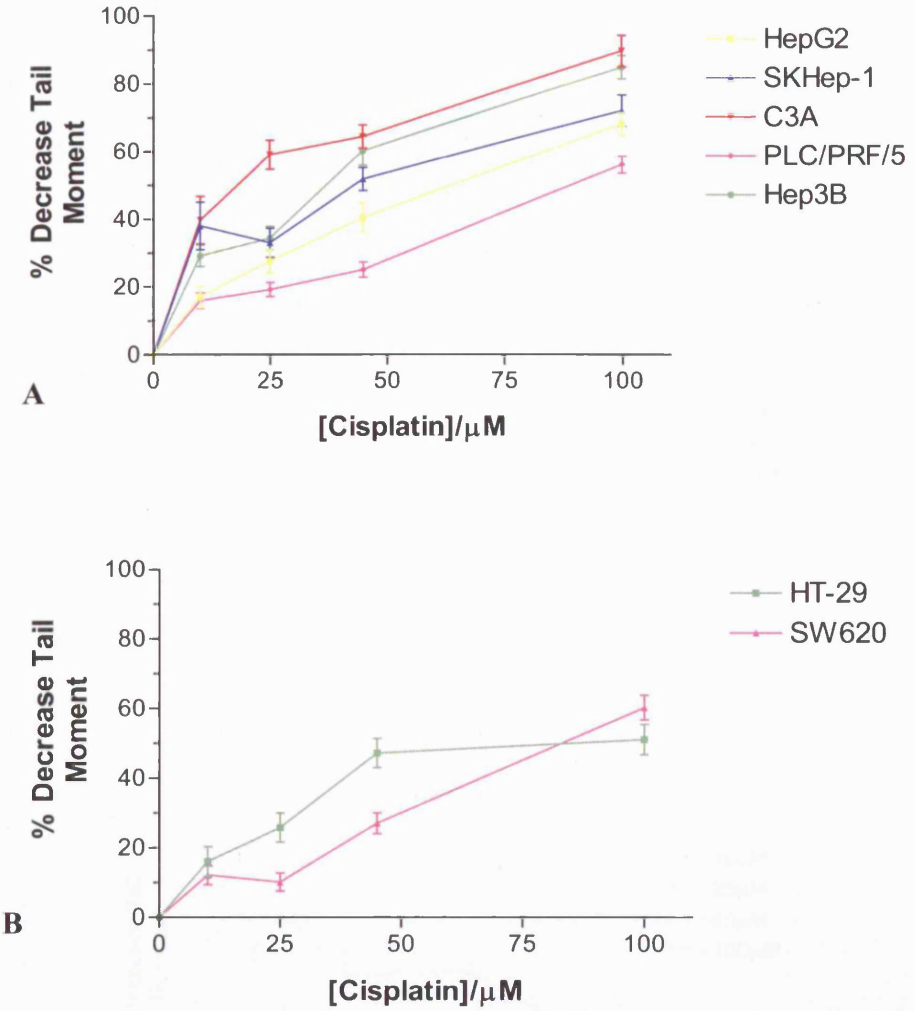

Figure 6.3. Dose response for cisplatin ICL formation in the overall genome in human A. HCC and B. CRC cell lines. Cells were exposed to 10-100 μM cisplatin for 1 h, washed and then incubated for 12 h at 37°C, 5% CO2. Cells were trypsinised and the comet assay performed.

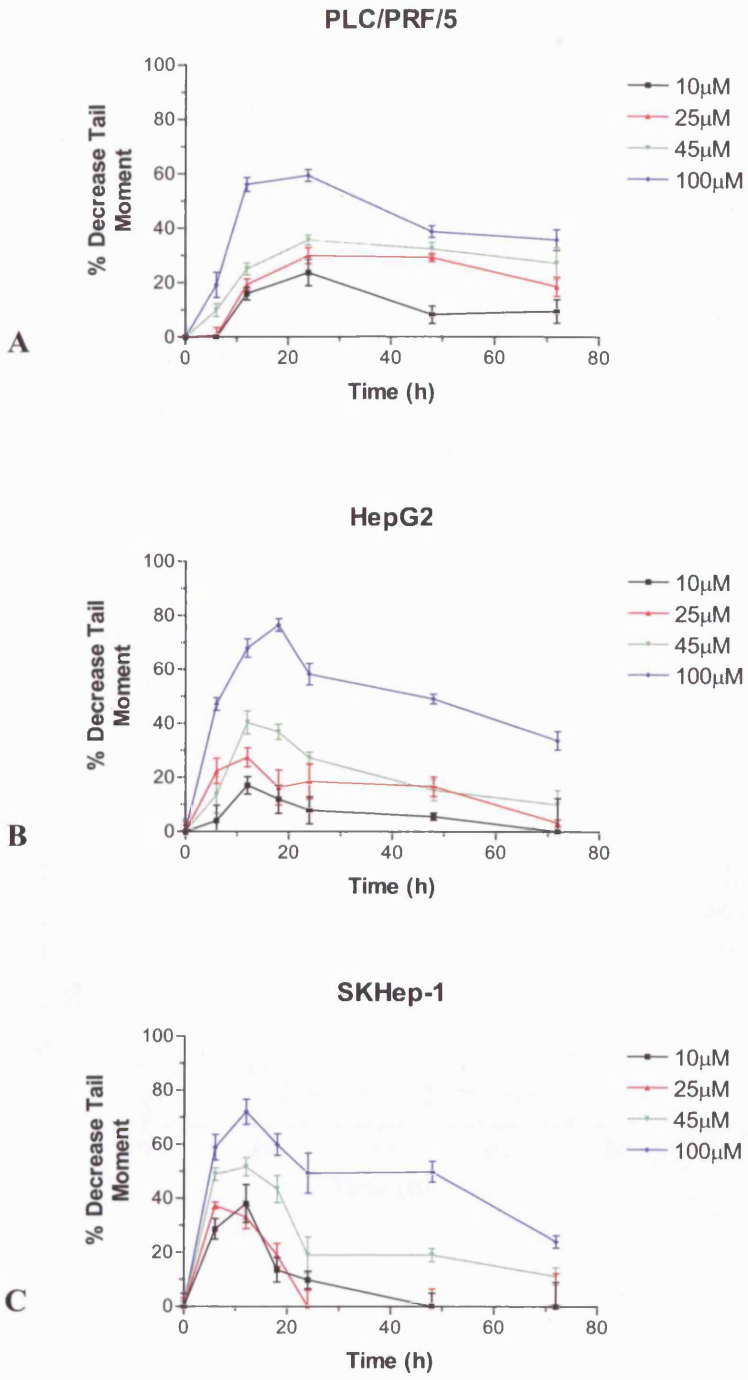

Figure 6.4. Rate of formation and excision of cisplatin ICL in the overall genome of relatively resistant HCC cell lines. Cells were incubated with 10, 25, 45 and 100 μM cisplatin for 1 h at 37°C and then allowed to repair in fresh medium. ICLs were quantified by the comet assay at 6-72 h after cisplatin treatment.

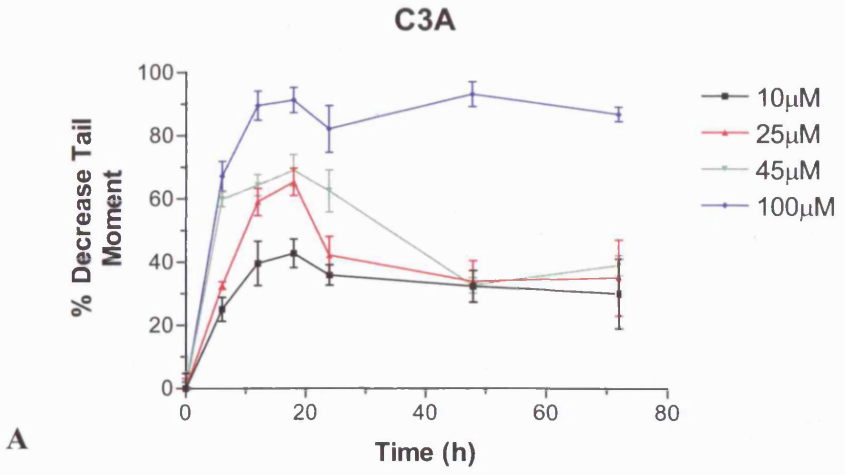

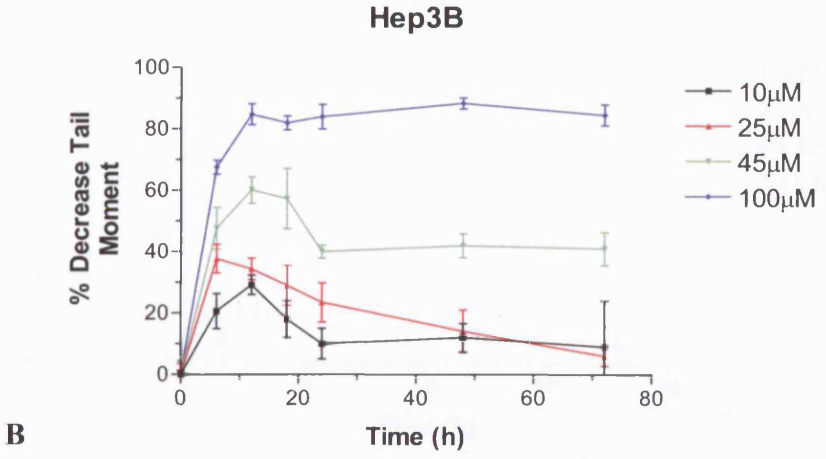

Figure 6.5. Rate of formation and excision of cisplatin ICL in the overall genome of relatively sensitive HCC cell lines. Cells were incubated with 10, 25, 45 and 100 μM cisplatin for 1 h at 37°C and then allowed to repair in fresh medium. ICLs were quantified by the comet assay at 6-72 h after cisplatin treatment.

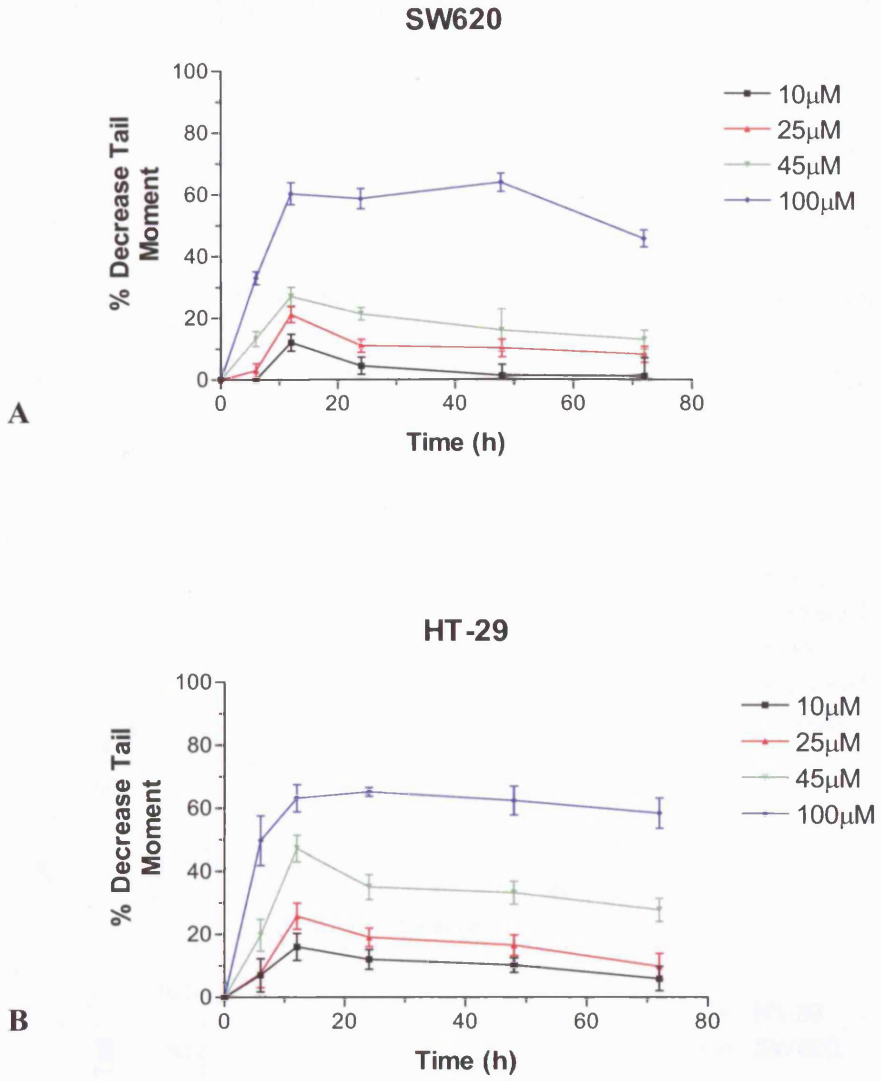

Figure 6.6. Rate of formation and excision of cisplatin ICL in the overall genome of relatively **A.** resistant and **B.** sensitive CRC cell lines. Cells were incubated with 10, 25, 45 and 100 μM cisplatin for 1 h at 37°C and then allowed to repair in fresh medium. ICLs were quantified by the comet assay at 6-72 h after cisplatin treatment.

The role of formation and excision of DNA ICLs in mediating resistance to cisplatin is further emphasised by comparing these lesions at the same high concentration of cisplatin. When resistant and sensitive HCC cell lines are both exposed to 100 μM cisplatin for 1 h and ICL formation measured 12 h after drug removal, a 1.5-fold difference is noted. Seventy-two h after drug removal, however, more than a 3-fold difference in ICL formation is present suggesting these resistant HCC cell lines have enhanced DNA repair (Figure 6.7). The CRC cell lines failed to show any significant difference in repair rates at this concentration.

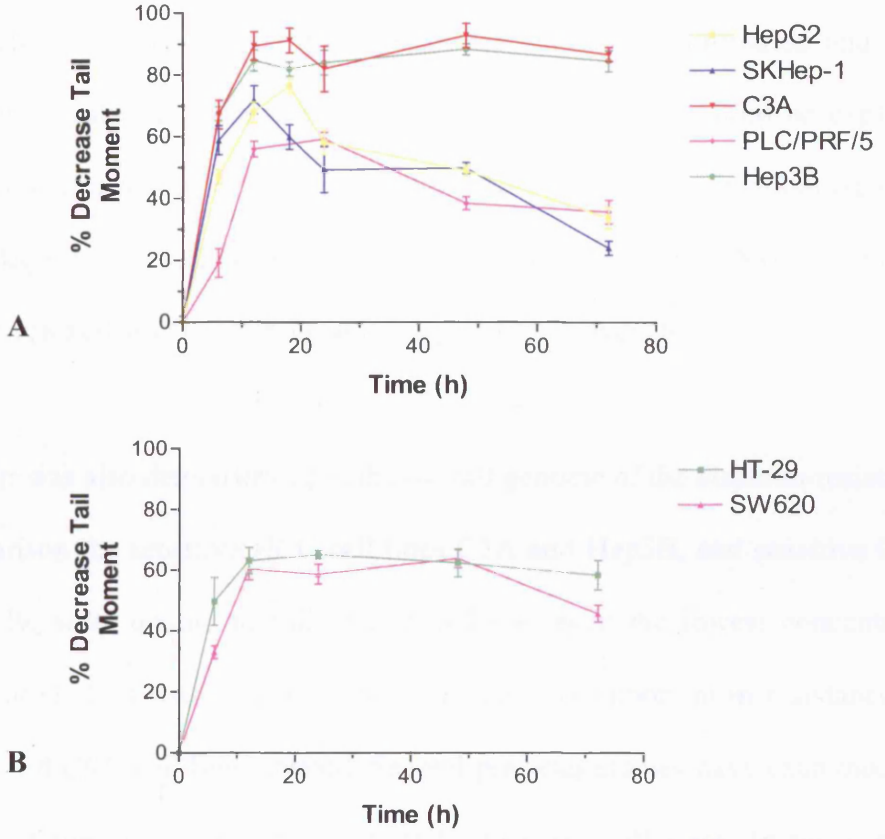

Figure 6.7. Comparison of the formation and excision of DNA ICLs in **A.** HCC and **B.** CRC cell lines treated with 100 μM cisplatin. Cells were incubated with 100 μM cisplatin for 1 h at 37°C and allowed to repair in fresh medium. ICLs were quantified by the comet assay at 6-72 h after cisplatin treatment.

6.4 Discussion

The objective of this section of study was to examine mechanistically important features underlying resistance to cisplatin in the chosen panel of human HCC cell lines and two CRC cell lines. The results would support previous studies highlighting the importance of ICL formation to cisplatin resistance. At the level of the overall genome, between 1.5 and 3-fold fewer ICLs were formed in the most resistant HCC cell line compared to the most sensitive cell line over the range of drug concentrations measured. These results are consistent with previously published data for resistant human ovarian (Behrens et al, 1987; Zhen et al, 1992) and colon (Fram et al, 1990) cancer cells. There have been no previous reports on ICL formation and repair in human HCC cell lines. The quantitative decrease in ICLing could be explained by mechanisms of cisplatin resistance which prevent active drug from damaging DNA, such as decreased cellular drug accumulation (Andrews et al, 1988) and inactivation via protein (Kasahara et al, 1991) and non-protein sulfhydryls.

ICL repair was also demonstrated in the overall genome of the cisplatin-resistant cells. In comparison the sensitive HCC cell lines C3A and Hep3B, and sensitive CRC cell line HT-29, were unable to fully repair ICLs at even the lowest concentration of cisplatin used. This would suggest that ICL repair is important in resistance in both the HCC and CRC cell lines studied. Several previous studies have examined the rate of repair of the overall genome in cisplatin-resistant cell lines. In most, enhanced cisplatin ICL repair has been observed (Johnson et al, 1994b; Masuda et al, 1988; Parker et al, 1991), however some have demonstrated no differences in the rate of repair (Fram et al, 1990).

There is good evidence that actively transcribed genes are repaired at a faster rate than background genomic DNA lesions (Sancar, 1996). It is conceivable that the survival of cisplatin-resistant cells may depend more on the speed or efficiency of repair in essential regions of their genomes than in bulk DNA. If this is the case, differences in gene-specific repair may be more dramatic and correlate more closely to relative cisplatin resistance than does repair in the overall genome. It has been reported that the gene-specific repair of cisplatin ICLs may be associated with cellular resistance to cisplatin in human ovarian cancer cell lines (Zhen et al, 1992). Studying repair at the gene-specific level in this cell panel would help clarify the role of the cisplatin ICLs in cytotoxicity, and the mechanism of repair.

The mechanism used by cells to repair ICLs is not clearly understood. However, several studies have suggested that excision repair cross-complementing group 1 (ERCC1) and XPF, probably formed by a complex containing ERCC4 and ERCC11, may be involved in this mechanism (Larminat and Bohr, 1994). As shown for classical nucleotide excision repair (NER), the ERCC1/XPF complex might also interact with XPA to facilitate the repair of ICLs. The mechanism might involve co-operation between NER and recombination, certainly outside the normal context of NER (Sijbers et al, 1996). An increased expression of the human NER repair genes *XPA* and *ERCC1* has been reported in tumour tissue of patients with ovarian cancer who did not respond to pt-based chemotherapy (Li et al, 2000). It has also been shown that *ERCC1* mRNA levels correlate with clinical resistance to cisplatin-based chemotherapy in human gastric cancer (Metzger et al, 1998). While transfection of an XPA-expressing vector into XPA-deficient cell lines can restore NER activity, overexpression of the same plasmid in repair-proficient cell lines do not appear to

have any effect on the activity levels (Cleaver et al, 1995). To date there is no clear evidence of overexpression of NER genes in resistant cell lines or in resistant tumours.

The 1h IC_{50} for the resistant cell lines in this study was approximately 100 μM. It has been demonstrated that at this concentration the cytotoxicity is related to their inability to fully repair the ICL formed. However, the cell lines were also unable to fully repair the ICLs formed at 45 μM. These findings suggest that DNA damage tolerance pathways are also present in the resistant cells, in particular PLC/PRF/5, which demonstrated high resistance but low repair rates. One mechanism by which a cell can exhibit damage tolerance is through increased replicative bypass of pt-DNA adducts and defects in mismatch repair. This has been reported to occur in human ovarian carcinoma cells (Vaisman et al, 1998) in which mismatch repair defects resulted in 1.5-4.8 fold increased cisplatin resistance and 2.5-6 fold increased replicative bypass of cisplatin adducts.

If enhanced repair activity does contribute to resistance, it is theoretically possible to enhance the efficacy of alkylating chemotherapeutic agents by altering the repair of the adducts they form. There are, however, a number of barriers to adopting this strategy. The most important being the multifactorial nature of resistance. Decreased accumulation, efflux increased by GSH and GST or by metallothionene, altered metabolism and increased tolerance of unrepaired damage all contribute to resistance to chemotherapeutic drugs (Kuppen et al, 1988; Meijer et al, 1992). Repair activity is usually only enhanced 1.5 to 2.0-fold, even in cell lines that are 20 to100-fold resistant to chemotherapeutic drugs. However, even a 1.5-fold to 2.0-fold decrease in

repair activity may be enough to elicit a response in some resistant tumours especially if inhibitors of repair could be combined with agents that block mechanisms of resistance.

CHAPTER VII

ORTHOTOPIC MODEL OF LIVER CANCER IN NUDE MICE IN WHICH TO EVALUATE CISPLATIN CYTOTOXICITY BY THE COMET ASSAY

VII. ORTHOTOPIC MODEL OF LIVER CANCER IN NUDE MICE IN WHICH TO EVALUATE CISPLATIN CYTOTOXICITY BY THE COMET ASSAY

7.1 Introduction

The translation of molecular mechanisms of action of cytotoxic agents from *in vitro* tissue culture models to tumours *in vivo* remains challenging. *In vitro* tissue culture models are extremely useful for examining the response of cancer cells to cisplatin and play a role in dissecting molecular events following exposure. Comparison of ovarian tumours treated *in vivo* and *in vitro* with cisplatin have demonstrated that their relative sensitivity observed *in vitro* is preserved *in vivo* (Kelland et al, 1992b). However, use of tumour cells that have been adapted to growth in culture may have limitations as it is frequently necessary to employ concentrations higher than those achieved in patients to detect measurable effects *in vitro* (Potapova et al, 1997). Moreover, *in vitro* cancer cells often generate degrees of resistance to cytotoxic agents that are higher than those observed in patients (Teicher et al, 1991). Several studies have also noted that cisplatin-resistant tumours established by *in vivo* treatment with cisplatin show acquired resistance in three-dimensional spheroid *in vitro* cultures, but not when cultured as monolayers *in vitro* (Kobayashi et al, 1993).

Many methods have been developed and applied to measure DNA damage produced by a wide variety of cytotoxic agents (Iliakis, 1991). With few exceptions, these are population-based assays and it must be assumed that all cells within a population will respond identically to a DNA-damaging agent. While, generally, a reasonable assumption for cells in tissue culture incubated with an agent in a well-controlled

environment, a global measure of DNA damage is unlikely to be adequate to describe damage produced in cells exposed in solid tumours. Drug uptake and accumulation is an important determinant for tumour cell sensitivity and subsequent response to cisplatin therapy *in vivo*. Little is known about the distribution patterns of cisplatin within tumours *in vivo*. A number of physiological barriers can lead to heterogeneous accumulation of therapeutic agents in solid tumours including variations in angiogenesis and blood flow, heterogeneous permeability of tumour vessels, the physico-chemical properties of the interstitium, and interstitial hypertension (Jain, 1998). At a cellular level many cells have intrinsic resistance due to the presence of energy dependent efflux pumps (eg. P-gp and MRP1) which can decrease the net intracellular accumulation of cytotoxic agents. The chemotherapeutic agent must also be effective in the *in vivo* microenvironment. The diverse microenvironments within solid tumours often include areas of low pH, hypoxia, and are deficient in nutrients and growth factors. Hypoxia is known to aid cytotoxicity of alkylating agents (Skarsgard et al, 1995), and inhibit effectiveness of bleomycin (Teicher et al, 1981). The level of cell proliferation may also play a role in tumour sensitivity. Proliferating cells are more susceptible to damage by cisplatin (Shalinsky et al, 1996), but whether the drug accumulation is higher in proliferating cells is unknown.

Present murine models involve growth of human tumour xenografts at ectopic sites where the local environment would be different from their natural (orthotopic) sites, thus limiting extrapolation of results to solid tumours. Intraperitoneal (i.p.) ascitic tumour models, which are often treated by i.p. drug injections, fail to consider the efficiency of vascular drug delivery to the tumour site and the need for drug penetration through multiple cell layers, which are critical determinants of successful

clinical therapy of solid tumours. In mice bearing subcutaneous (s.c.) tumour xenografts, tumour size can be directly measured using calipers and response to therapeutic intervention monitored quantitatively. However, when some cell lines are injected subcutaneously, resultant tumours grow as well-encapsulated, poorly vascularised masses so that early tissue necrosis and haemorrhage may complicate evaluation of tumour volume. Both ascitic and s.c. models fail to consider the concept that the microenvironment in which the tumour cells grow can profoundly influence their response to cytotoxic therapy (Dong et al, 1994). It is generally accepted that the host microenvironment influences tumour biology. There are discrepancies in growth rate, angiogenesis, metastatic potential and related gene expression (Takahashi et al, 1996), and the efficacy of systemic treatments between ectopic and orthotopic tumours (Fidler, 1995). The liver is the most common and critical site of distant metastasis of CRC. Tumourigenicity and efficacy of chemotherapeutic agents in CRC tumours are different in liver and subcutaneous sites (Fidler et al, 1994). Such limitations may explain, in part, the discrepancy between successes reported with *in vivo* chemosensitisation protocols in murine models and failure of these protocols in clinical trials with solid tumours.

The purpose of this section of the study is to describe the intratumoural topographic distribution of cisplatin induced DNA damage in intrahepatic xenografts of human HCC and CRC in nude mice in terms of cisplatin-DNA adducts assessed by the comet assay. As only a few thousand cells are required for this assay, samples can be taken by fine needle aspirate (FNA) biopsies from a variety of sites within each tumour. This allows the residual tumour to be utilised for immunohistochemical staining of

parallel tissue sections to investigate the potential influence of cell proliferation, hypoxia, vascularity and P-gp expression on intratumoral adduct distribution.

7.2 Materials and Methods

7.2.1 Orthotopic model of liver cancer in nude mice in which to evaluate cisplatin cytotoxicity by the comet assay

To study the effect of cell proliferation, hypoxia, vascularity and P-gp expression on the intratumoural topographic distribution of cisplatin-DNA adducts in intrahepatic xenografts, a cisplatin sensitive and resistant HCC and CRC cell line was initially selected from *in vitro* data (Table 7.1). The animals were supplied by, and the *in vivo* experiments were carried out at the Comparative Biology Unit (CBU), Royal Free Hospital (RFH). All procedures were within national ethical guidelines, were in compliance with the United Kingdom Coordinating Committee on Cancer Research Guidelines for the welfare of Animals in Experimental Neoplasia, and covered by the Home Office Licence No. PPL 70/4517. Tumour volume was determined by external measurement in two dimensions according to the published method using the equation $V = (L \times W^2)/2$, where V = volume, L = length, and W = width (Johnsson and Cavallin-Stahl, 1996).

A

HCC Cell lines	*IC_{50} (1 h) μM*	*IC_{50} (120 h) μM*
C3A	10.96 ± 7.5	5.2 ± 1.82[a]
PLC/PRF/5	88.44 ± 5.4	36.7 ± 2.8

B

CRC Cell lines	*IC_{50} (1 h) μM*	*IC_{50} (120 h) μM*
HT-29	40.2 ± 3.21	6.5 ± 3.4
SW620	160.46 ± 4.7	45 ± 2.93[a]

Values are the means ±SEM of three independent experiments.
[a]Values are the means ±SEM of four independent experiments.

Table 7.1. *In vitro* data on chemosensitivity of **A.** HCC and **B.** CRC cell lines to cisplatin at 1 h and 120 h drug exposure times.

Experiment series I: Direct injection of tumour cell suspension (in PBS) into mouse liver parenchyma

MFI nude mice (3-4 weeks old) weighing between 20-25 g were housed in cages and fed a standard laboratory diet and tap water. The strict use of surgical asepsis was performed in order to prevent infective complications. A million C3A or PLC/PRF/5 HCC, or HT-29 or SW620 CRC cells were prepared by trypsinisation of adherent cells from tissue culture flasks. Cells were washed once with sterile PBS, counted and resuspended in 100 µl cold-sterile PBS. Anaesthesia was induced and maintained with halothane and a 2:1 mixture of nitrous oxide:oxygen. The skin was cleansed with antiseptic solution, laparotomies were performed through a midline abdominal incision and the bowel retracted to the left to reveal the liver. Cells were injected subcapsularly into the right lobe of the liver. After applying pressure for a few minutes to stop bleeding at the injected site, the abdominal wall was closed using 4/0 vicryl. Mice recovered within minutes of discontinuing the halothane. Analgesia (Temgesic) was provided for the first 24 h. The animals were inspected on a daily basis for any adverse effects. Animals were killed at 45 days by a schedule 1 method. The liver, lung and peritoneal cavity were examined for evidence of tumour.

Results

A total of 12 mice (3 mice with each cell line) were implanted with cells. After 45 days, all the animals were sacrificed. No evidence of macroscopic tumour was found in liver, lung or peritoneal cavity.

Experiment series II: Direct injection of tumour cell suspension (in Matrigel) into mouse liver parenchyma

All procedures were performed as described in experimental series I except the cells were suspended in Matrigel (Collaborative Biochemical Products, Becton Dickson, Bedford (MA), USA). Matrigel is stored at –20°C and thawed at 4°C at the time of use. A dilution of 1:2 of Matrigel in serum-free RPMI-1640 was prepared. One hundred microlitres of cell suspension containing 1 x 10^6 cells in a 1-ml syringe was carried in ice and warmed in a 37°C incubator before injection. Mice were divided into groups as in experimental series I. Animals were killed at 45 days by a schedule 1 method.

Results

Cell suspensions in Matrigel were viscous but not difficult to inject into the liver paranchyma. The cell suspension was also separately grown in a 25-cm^2 culture flask to test the viability of cells. The results showed that cells resuspended in Matrigel survived and grew normally *in vitro*. A total of 12 mice (3 mice with each cell line) were implanted with cells. During inoculation of the cell suspension, 2 mice suddenly arrested intraoperatively. The complication was not related to cell type. The other 10 mice survived without complication until terminated at 45 days. Again, no evidence of macroscopic tumour was found in liver, lung or peritoneal cavity.

Experiment series III: Injection of tumour cell suspension (in PBS or Matrigel) into subcutaneous tissues of nude mice

Nude mice were injected subcutaneously into their flanks using 25-gauge needles. Three million cells were prepared from tissue culture flasks and resuspended in 500 µl of either cold-sterile PBS or Matrigel. Mice were divided into the same groups as in experiment series I. A successful s.c. injection resulted in the formation of a bleb during discharge of the cell suspension. Mice were then left to recover and were intermittently assessed for weight loss and other signs of discomfort. The size of tumour was recorded and animals anaesthetised at 30 days to perform experiment series IV.

Results

Eight mice (2 mice with each cell line) were implanted with cells resuspended in cold-sterile PBS and 8 mice (2 mice with each cell line) were implanted with cells resuspended in Matrigel. After 30 days, none of the cells resuspended in cold-sterile PBS resulted in subcutaneous tumour nodules, the mean tumour volumes of C3A, PLC/PRF/5, HT-29 and SW620 cells resuspended in Matrigel were 489, 344, 264 and 566 mm^3, respectively (Figure 7.1). The presence of tumours was confirmed histologically.

A

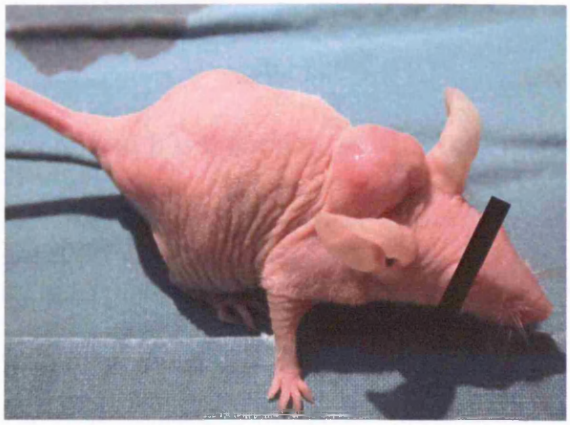

B

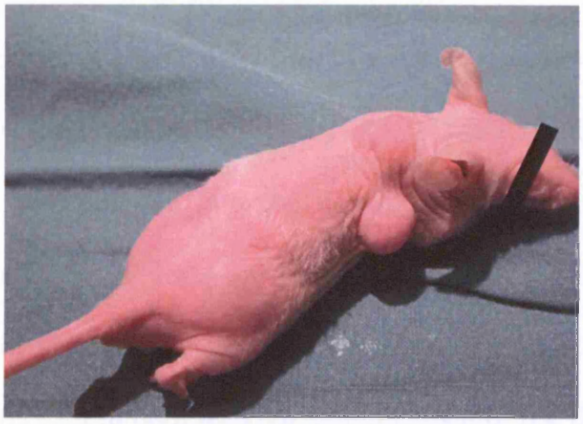

Figure 7.1. Examples of tumour nodules generated in subcutaneous tissues of nude mice. **A.** SW620 and **B.** C3A xenografts.

Experiment series IV: Implantation of the tumour tissue generated in subcutaneous tissues of nude mice into mouse liver parenchyma

The same mice and groups with s.c. tumours generated with Matrigel were used as in experiment series III. General experimental procedures were similar to those described in experiment series I. On the 30^{th} day the nude mice were anaesthetised, subcutaneous tumours were measured, excised, and cut into small cubes of approximately 2 mm^3. After disinfection, the mice underwent a midline abdominal incision. The bowel was retracted to the left to expose the liver. A small superficial incision on the liver was made using the tip of a No.11 surgical blade with the knife at a 15° angle to the liver surface. A small piece of Gelfoam (Pharmacia & Upjohn, London, England) was inserted into the incision for approximately 1 min and the incision compressed with a piece of gauze. When the bleeding had stopped, the Gelfoam was removed and a tumour fragment gently placed into the incision. The procedure was performed in both the right and left lobe of the liver. After the bleeding had ceased, 2 ml of balanced salt solution was placed into the peritoneal cavity and the abdominal incision closed as previously described. Animals were killed at 45 days by a schedule 1 method.

Results

The same 8 mice (2 mice with each cell line) with s.c. tumours generated with Matrigel from experiment series III were studied. The procedure was uncomplicated. The bleeding from the incision in the liver parenchyma was easily controlled by Gelfoam and packing for a few minutes. There was no intraoperative or postoperative mortality. All implantation's resulted in intrahepatic tumours. The mean tumour

volumes of C3A, PLC/PRF/5, HT-29 and SW620 cells were 750, 421.8, 351.6, and 1171.9 mm^3, respectively (Figure 7.2). The presence of tumours was confirmed histologically.

A

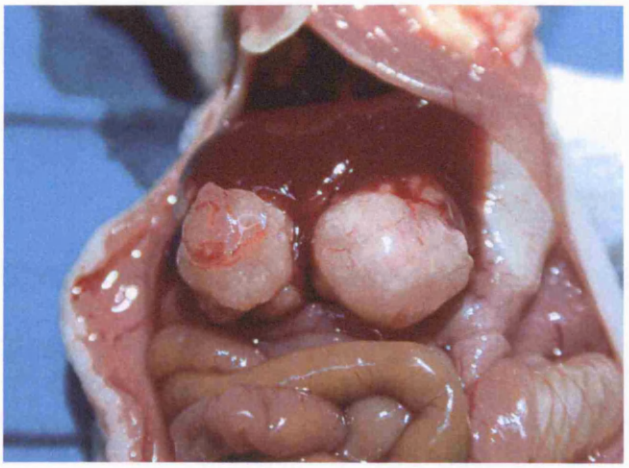

B

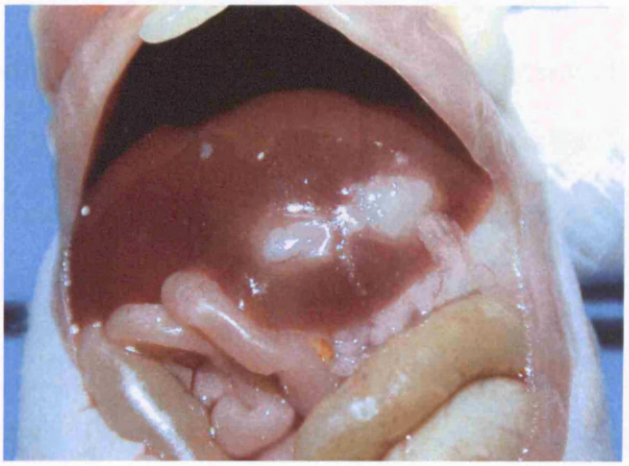

Figure 7.2. Subcutaneous tumour nodules from nude mice implanted into liver parenchyma of nude mice, **A.** SW620 and **B.** PLC/PRF/5 xenografts.

7.2.2 Analysis of spatial and temporal tumour cisplatin induced DNA damage

The human HCC cell line C3A and CRC cell line SW620 were chosen for this part of the study. This was based on both *in vitro* data of cisplatin chemosensitivity demonstrating them to be sensitive and resistant respectively with different rates of formation and removal of DNA interstrand crosslinks (ICLs), and *in vivo* data confirming adequate intrahepatic solid tumour growth. Subcutaneous xenografts were established in the flanks of a total of 6 nude mice (3 mice for each cell line) as detailed in experiment series III. Animals were killed at 30 days by a schedule 1 method. Subcutaneous tumours were measured, excised, and cut into small cubes of approximately 2 mm^3 then transplanted under anaesthesia into both the right and left lobe of the liver parenchyma of other mice (18 mice for each cell line) as detailed in experiment series IV. Drug treatment did not start until day 45, whereupon mice were randomised into groups. There were 3 animals in each control or treatment group. The mice in the treatment groups were treated intravenously (i.v.) (via the tail vein) with a single dose of 4 mg/kg cisplatin in 0.9% NaCl (time = 0). The route and dose was selected on the basis of maximum-tolerated dose determination experiments in non-tumour-bearing mice before drug testing in tumour-bearing mice. Tumours were sampled before dosing (control group) and in groups of animals at 6, 12, 24, 48 and 72 h post treatment. The mice in each control and treatment group were killed by a schedule 1 method. Fine needle aspiration (FNA) biopsies were taken from two sites (A & B) and depths (0.25 & 0.5 cm) in each tumour and frozen immediately in 1 ml RPMI, 10% foetal calf serum and 10% DMSO at −70°C until analysed by the comet assay as described in Chapter II, Section 2.9. As cisplatin is an alkylating agent cells were irradiated immediately prior to analysis to deliver a fixed level of random strand

breakage and crosslinks were quantitated as the decrease in the comet tail moment (TM) compared to unirradiated controls.

Statistical Analysis

Values are expressed as mean ± SEM. For comparison between depths and sites, the two-tailed unpaired t-test was used. One-way ANOVA followed by the Bonferroni multiple t-test was used to compare DNA-adduct formation between tumours. $P < 0.05$ was considered statistically significant.

Results

Assays performed on FNAs of tumours from untreated animals showed no evidence of ICLs. Peak levels of ICLs were observed at 12 h in both xenografts (Figure 7.3). The resistant cell line SW620 had 1.5-fold fewer ICLs compared to the sensitive cell line C3A at both superficial and deep levels (at 0.25 cm and 12 h, 42 *vs* 63 % decrease in TM [$P < 0.001$]) (Table 7.2). Both cell lines demonstrated fewer ICLs when grown as xenografted tumours when compared with *in vitro* data with 100 μM of cisplatin (Table 7.2).

	% Decrease in Tail Moment		
Cell line	***In vivo***		***In vitro***
	0.25 cm	**0.5 cm**	**100 μM**
SW620	42	30.3	60
C3A	63	50.9	89

Table 7.2. Percentage decrease in Tail Moment of SW620 and C3A at 12 hours *in vivo* and *in vitro*.

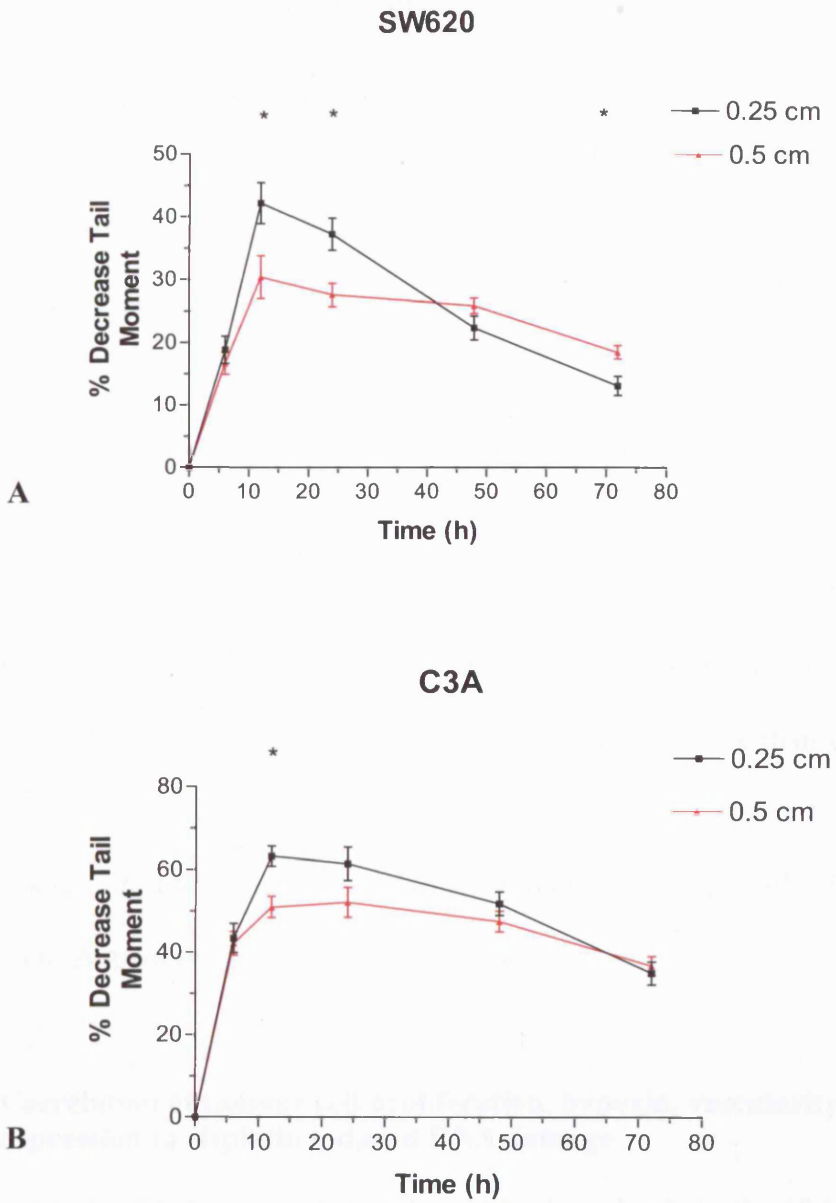

Figure 7.3. Rate of formation and excision of cisplatin ICLs in the overall genome of *in-vivo* **A.** SW620 and **B.** C3A intrahepatic xenografts of nude mice. Mice were treated i.v. via the tail vein with a single dose of 4 mg/kg cisplatin in 0.9% NaCl at time = 0. Values are the mean ±SEM of three mice (each with 2 tumours and 2 sample sites), * indicates $P < 0.05$ with two-tailed unpaired t-test.

Rates of repair of ICLs were both quantitatively and qualitatively different from *in vitro* data with growth of cells in xenografts. *In vitro* there was little repair in either cell line with 100 μM of cisplatin, *in vivo,* however, percentage decrease in TM was reduced to approximately 13 and 35% in SW620 and C3A xenografts at 72 h respectively (Figure 7.3).

Differences in ICLs were noted at different depths in xenografts, with superficial cells having higher levels of ICLs. With SW620 these were statistically significant at 12, 24 and 72 h, with C3A statistical significance was only noted at 12 h (Figure 7.3) (Appendix 7.1). Superficial cells were more efficient at repair of ICLs, by 72 h superficial SW620 cells had statistically significant less ICLs than deep cells ($P = 0.0086$) (Figure 7.3) (Appendix 7.1). Differences between sites in the same tumour, and tumours in the same mouse were minimal and generally not statistically significant (Appendix 7.2).

7.2.3 Correlation of tumour cell proliferation, hypoxia, vascularity and P-gp expression to cisplatin induced DNA damage

As peak levels of ICLs were observed at 12 h, the animals in the 12 h post-treatment group were used to study the effect of cell proliferation, hypoxia, vascularity and P-gp expression and on the intratumoural topographic distribution of cisplatin-DNA adducts in intrahepatic xenografts (3 mice with six tumours). Eleven hours after i.v. cisplatin administration, 7-(4'-(2-nitroimidazol-1-yl)-theophylline (NITP) was injected i.p into each mouse: 70 mg NITP in 0.5 ml 10% DMSO with 4.5 ml peanut oil, 0.3 ml per animal (155 mg/kg) (For full details see Chapter II, Section 2.11.2.). One hour after the administration of NITP the animals were killed by a schedule 1 method. Fine needle aspiration biopsies were taken for analysis by the comet assay.

The tumours were measured to calculate their volumes and then frozen immediately in liquid nitrogen and stored at –70°C until they were sectioned. From each of the 12 tumours four parallel 4 μm cryostat sections were prepared on poly-L-lysine coated slides from both the superficial and deep parts (0.25 & 0.5 cm respectively) for immunohistochemical analysis of MIB-1, NITP, Factor VIII and P-gp. Details of the immunohistochemical staining techniques of each are given in Chapter II, Sections 2.11.1-4. All slides in each immunohistochemical experiment were stained in the same batch, to avoid the methodological error due to inter-batch variation.

Quantitative and statistical analysis

Point counting using two independent observers quantitated the staining reactions. Cell proliferation, hypoxia and P-gp expression were assessed using 10 high power fields (x 40 objective lens, field size 150 x 80 μm) in each section. Each high powered field consisted of 50-100 cells, and the average labelling index (LI) was calculated as the total number of labelled cells *vs* the total tumour cells counted and expressed as a percentage. As a measure of vascularity, the numbers of vascular structures per mm2 (vascular density, VD) were calculated from 10 low powered fields (x 10 objective lens, field size 1.22 mm^2) in each section. The heterogeneity between measured fields was calculated as standard deviations (SD) and relative standard deviations (coefficients of variation, CV). Only areas with morphologically intact tumour cells were analysed. Stromal cells and necrotic cells were not measured. Comparisons of parameters between depths and tumours were made using the two-tailed unpaired t-test. Correlations were calculated as Pearson's correlation coefficients (*r*).

Results

I. Proliferation

The MIB-1 staining was strong in all tumours (Figure 7.4, A & B). On each slide 10 fields representing 500-1000 cells per section were analysed. The staining was distributed fairly evenly on each section, with CV values for both xenographs ranging from 8 to 34% at 0.25 cm and 20 to 40% at 0.5 cm (Table 7.3). Proliferation was generally higher in superficial cells with statistically significant intra-tumour differences between peripheral and central cells noted in 3 SW620 and 2 C3A xenografts (Appendix 7.7). Strong statistical differences in proliferation between depths were observed for both xenografts, however, when all results were pooled (SW620, 12.37 *vs* 9.48% [$P < 0.0001$] and C3A, 16.25 *vs* 13.41% [$P < 0.0001$] at 0.25 and 0.5 cm respectively) (Table 7.3, Figure 7.5, A & B). C3A xenografts demonstrated higher proliferation levels at both depths when compared with SW620 xenografts (Figure 7.5 C).

II. Hypoxia

Bound metabolites of NITP occurred mainly at the edges of tumour cords. Little staining was found within the tumour cords or in the surrounding necrotic material. A wide intra- and inter-tumour variation of hypoxia was noted as reflected by high CV values (33 to 70% at 0.25 cm and 25 to 50% at 0.5 cm) (Table 7.3). Overall hypoxic staining was higher in deep cells. Although statistically significant intra-tumour differences between superficial and deep cells were noted in only 2 of each cell line xenografts (Appendix 7.8), strong statistical differences for both were observed when all results were pooled (SW620, 7.5 *vs* 10.29% [$P = 0.0007$] and C3A, 7.71 *vs* 13.16% [$P < 0.0001$] at 0.25 and 0.5 cm respectively) (Table 7.3, Figure 7.5 D & E). C3A

xenografts demonstrated higher levels of hypoxia at 0.5 cm only when compared with SW620 xenografts (Figure 7.5 F).

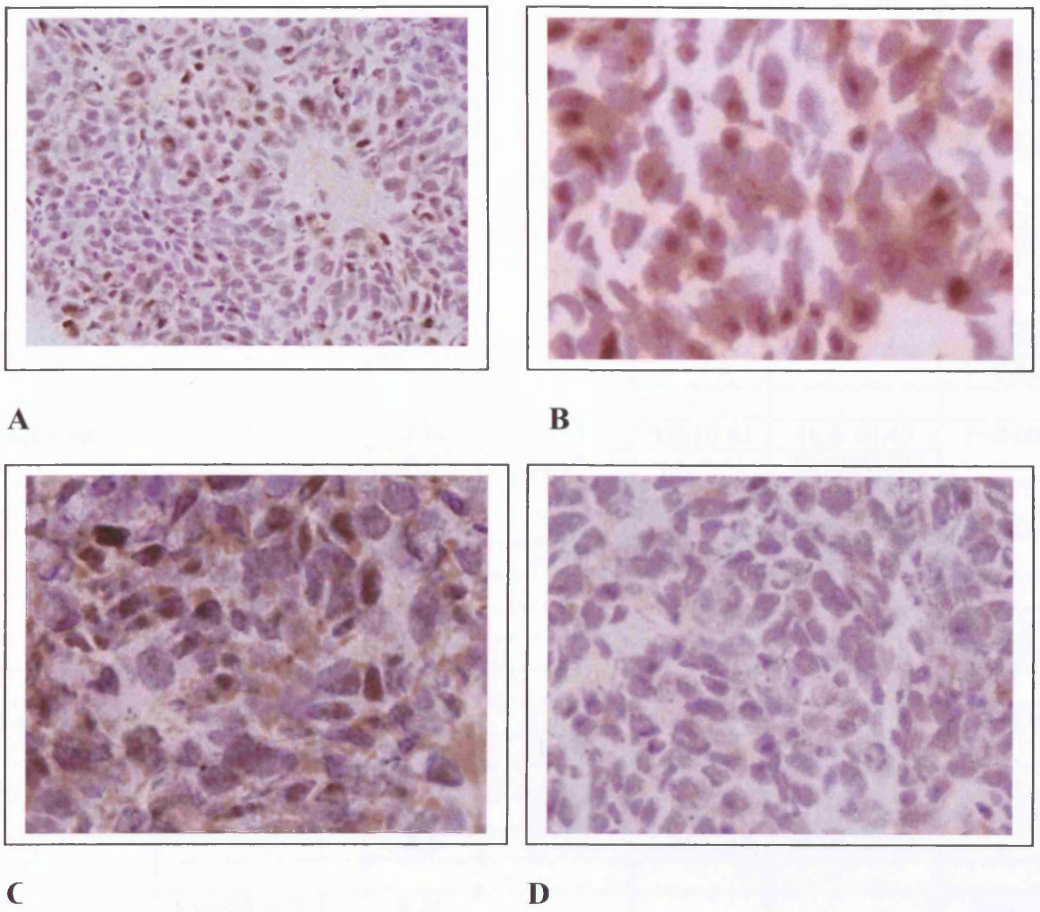

Figure 7.4. Microscopic images (40 x magnification) of sections from xenografted tumours from nude mice at 12 h after injection of 4 mg cisplatin/kg i.v. MIB-1 staining in **A.** SW620 xenograft and **B.** C3A xenograft indicating cell proliferation. **C.** NITP staining in SW620 xenograft indicating hypoxia. **D.** P-gp staining in SW620 xenograft.

Parameter	Cell Line	Depth (cm)	Mean (%) (n=60)	SD range	CV (%) range	t-test (Total)
Proliferation	**SW620**	**0.25**	12.37	2.11-3.55	18.09-25.78	P<0.0001
		0.5	9.48	1.85-3.19	20.06-33.57	
	C3A	**0.25**	16.25	1.38-5.87	8.35-34.5	P<0.0001
		0.5	13.41	2.8-5.48	22-39.67	
	SW620 vs C3A	**0.25**				P<0.0001
		0.5				P<0.0001
Hypoxia	**SW620**	**0.25**	7.5	2.81-7.44	42.33-70.2	P=0.0007
		0.5	10.29	2.18-5.47	25.89-46.79	
	C3A	**0.25**	7.71	2.35-4.56	33.11-54.64	P<0.0001
		0.5	13.16	4.42-6.15	38.22-50.37	
	SW620 vs C3A	**0.25**				P=0.7677
		0.5				P=0.0152
Vascularity	**SW620**	**0.25**	26.33	4.9-10.81	16.8-44.49	P=0.0004
		0.5	21.57	4.6-7.51	20.52-37.93	
	C3A	**0.25**	28.2	4.8-8.2	15.88-29.95	P<0.0001
		0.5	20.87	5.1-6.88	24.77-33.01	
	SW620 vs C3A	**0.25**				P=0.1645
		0.5				P=0.5269
P-gp expression	**SW620**	**0.25**	17.25	6.48-8.66	40.67-48.57	P=0.01
		0.5	14.13	4.24-6.5	27.21-51.1	
	C3A	**0.25**	13.73	3.57-6.46	31.51-48.09	P=0.33
		0.5	12.88	2.05-5.33	20.93-38.25	
	SW620 vs C3A	**0.25**				P=0.003
		0.5				P=0.157

Table 7.3. Summary of immunohistochemical results of *in vivo* tumour cell proliferation, hypoxia, vascularity and P-gp expression (total of 6 tumours in 3 mice).

SD, standard deviation; CV, coefficient of variation.

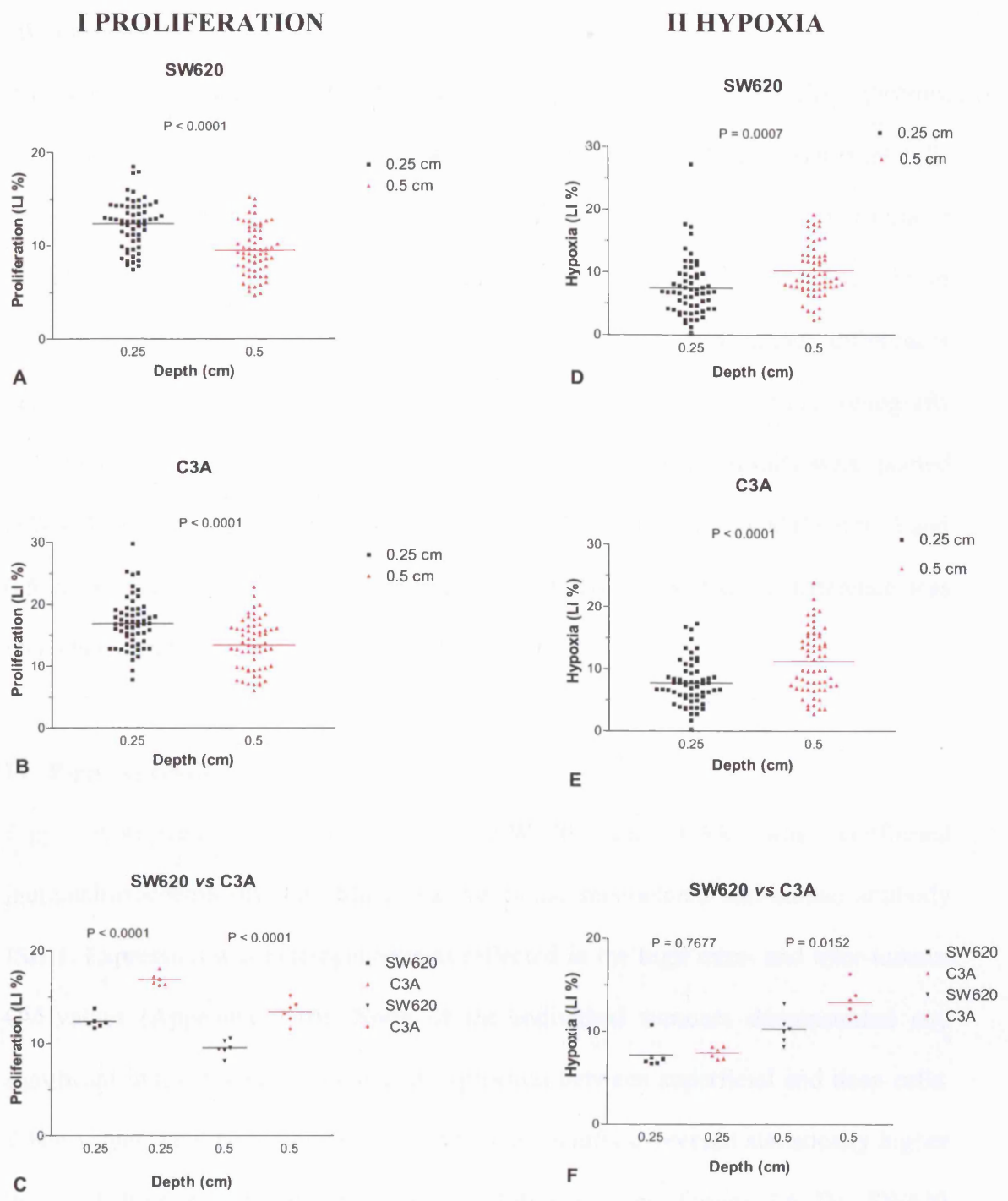

Figure 7.5. Parallel tissue sections of nude mice intrahepatic SW620 and C3A xenografts were stained with MIB-1 to analyse cell proliferation **A-C.** and anti-theophylline antibody to detect hypoxia **D-F.** at 0.25 & 0.5 cm. Three mice with a total of 6 tumours were studied, on each section 10 fields were analysed. Each bar indicates the mean LI of 60 or 6 values. Comparisons between depths were made using the two-tailed t-test.

III. Vascularity

All tumours were well vascularised. Factor VIII-positive endothelial cells indicating capillaries, were seen mainly in stromal parts of tumours. Scattered endothelial cells were also seen within tumour nodules. There was little intra- and inter-tumour variation (CV values 16 to 44% at 0.25 cm and 20 to 37% at 0.5 cm) (Table 7.3). In general vascularity was greater superficially. Significant intra-tumour differences between superficial and deep areas were noted in only 2 of each cell line xenografts (Appendix 7.9), statistical differences were apparent when all results were pooled (SW620, 26.33 vs 21.57 [$P = 0.0004$] and C3A 28.2 vs 20.87 [$P < 0.0001$] at 0.25 and 0.5 cm respectively) (Table 7.3, Figure 7.6 A & B). No statistical difference was noted between tumours at either depth (Figure 7.6 C).

IV. P-gp expression

P-gp expression in xenografts of SW620 and C3A was confirmed immunohistochemically with M*drI*-reactive mouse monoclonal anti-human antibody JSB-1. Expression was heterogeneous as reflected in the high intra- and inter-tumour CV values (Appendix 7.10). None of the individual tumours demonstrated any significant intratumoural difference in expression between superficial and deep cells. When values were pooled, however, SW620 xenografts expressed statistically higher levels of P-gp superficially ($P = 0.01$) (Table 7.3 and Figure 7.6 D). SW620 xenografts also demonstrated higher levels of P-gp expression when compared with C3A xenografts at 0.25 cm (Table 7.3, Figure 7.6 F).

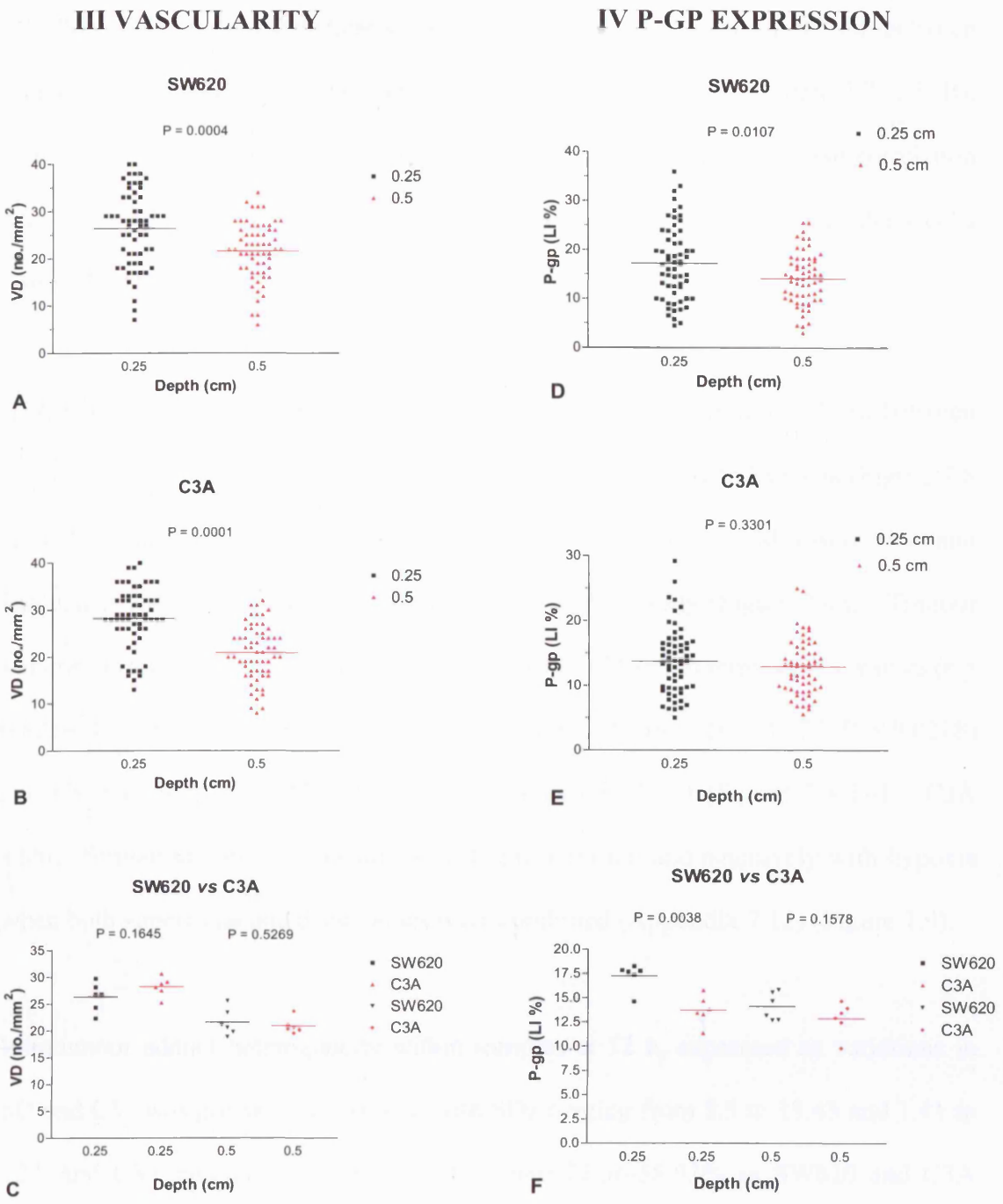

Figure 7.6. Parallel tissue sections of nude mice intrahepatic SW620 and C3A xenografts were stained with Factor VIII to detect vessels **A-C.** and JSB-1 to detect P-gp **D-F.** at 0.25 & 0.5 cm. Three mice with a total of 6 tumours were studied, on each section 10 fields were analysed. Each bar indicates the mean LI of 60 or 6 values. Comparisons between depths were made using the two-tailed t-test.

SW620 xenografts had statistically significant inverse correlations at 0.5 cm between tumour volume and proliferation, and vascularity (Appendix 7.11, Figure 7.7 A & B), and a positive correlation with hypoxia (Figure 7.7 C). A similar inverse correlation was observed between vascularity and hypoxia in both superficial and deep cells Figure 7.7 D & E).

C3A xenografts had a statistically significant inverse correlation at 0.5 cm between tumour volume and proliferation, and a positive correlation with hypoxia (Figure 7.8 A & B). There was no correlation between tumour volume and vascularity, and vascularity inversely correlated with hypoxia at 0.25 cm only (Figure 7.8 C). Tumour volume correlated with heterogeneity of adducts at 0.25 cm in terms of CV values (r = 0.8254, P =0.043), and at 0.5 cm in terms of both SD values (r = 0.877, P = 0.0218) and CV values (r = 0.8832, P = 0.0197) (Appendix 7.11) (Figure 7.8 D-F). C3A adduct formation correlated positively with proliferation and negatively with hypoxia when both superficial and deep values were combined (Appendix 7.12) (Figure 7.9).

Intratumour adduct heterogeneity within samples at 12 h, expressed as variations in SD and CV, was greater in deep cells with SDs ranging from 3.5 to 13.43 and 1.41 to 12.7 and CVs ranging from 29.11-67.14% and 22.36-58.93% in SW620 and C3A xenografts respectively (Appendix 7.11).

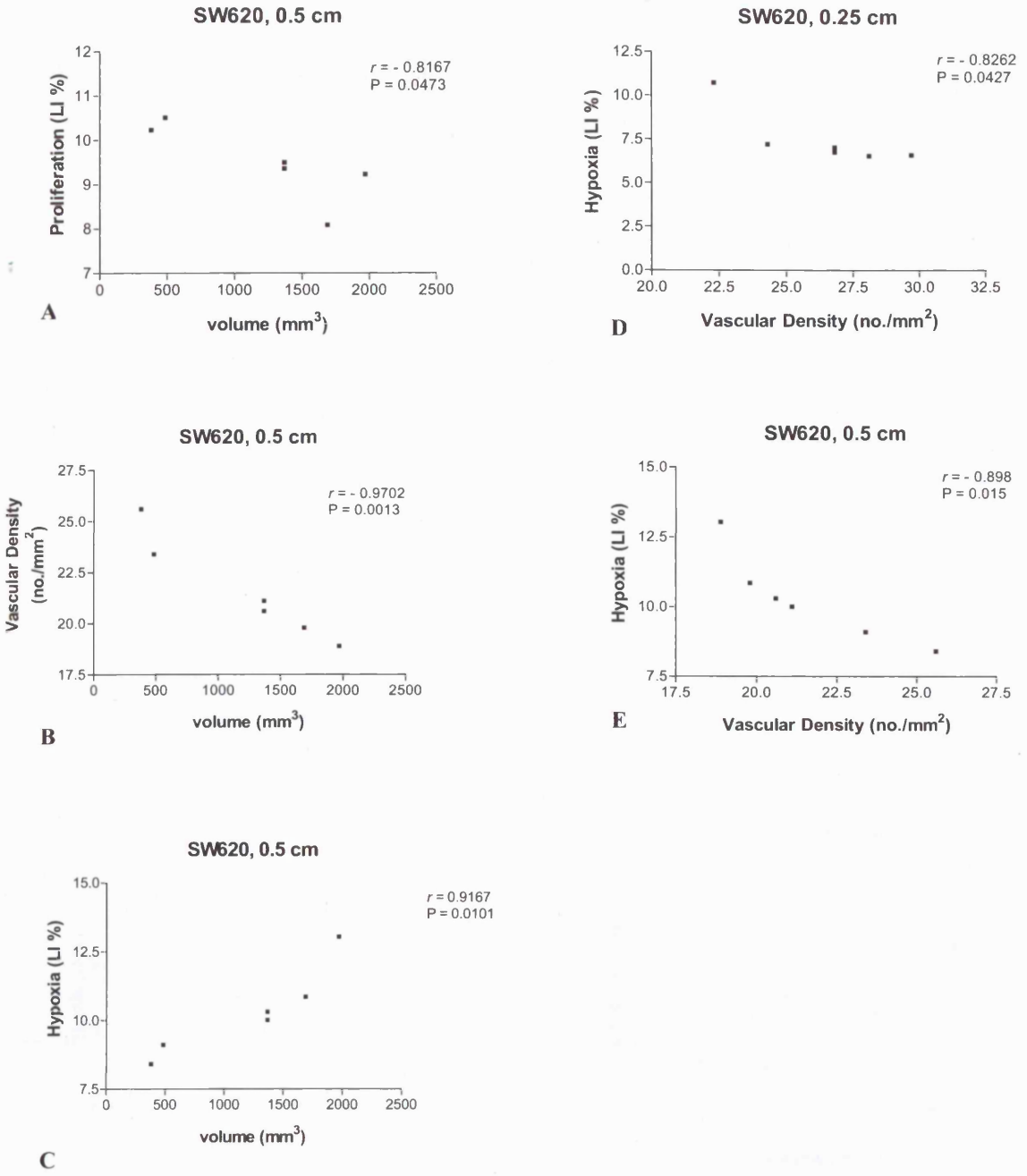

Figure 7.7. Correlation between tumour volume and **A.** proliferation, **B.** vascular density and **C.** hypoxia at 0.5 cm. Correlation between vascular density and hypoxia at **D.** 0.25 and **E.** 0.5 cm. Ten sections were analysed in 6 intrahepatic xenografted SW620 tumours at 12 h after injection of 4 mg/kg cisplatin i.v.

Correlations are calculated as Pearson's correlation coefficients (*r*).

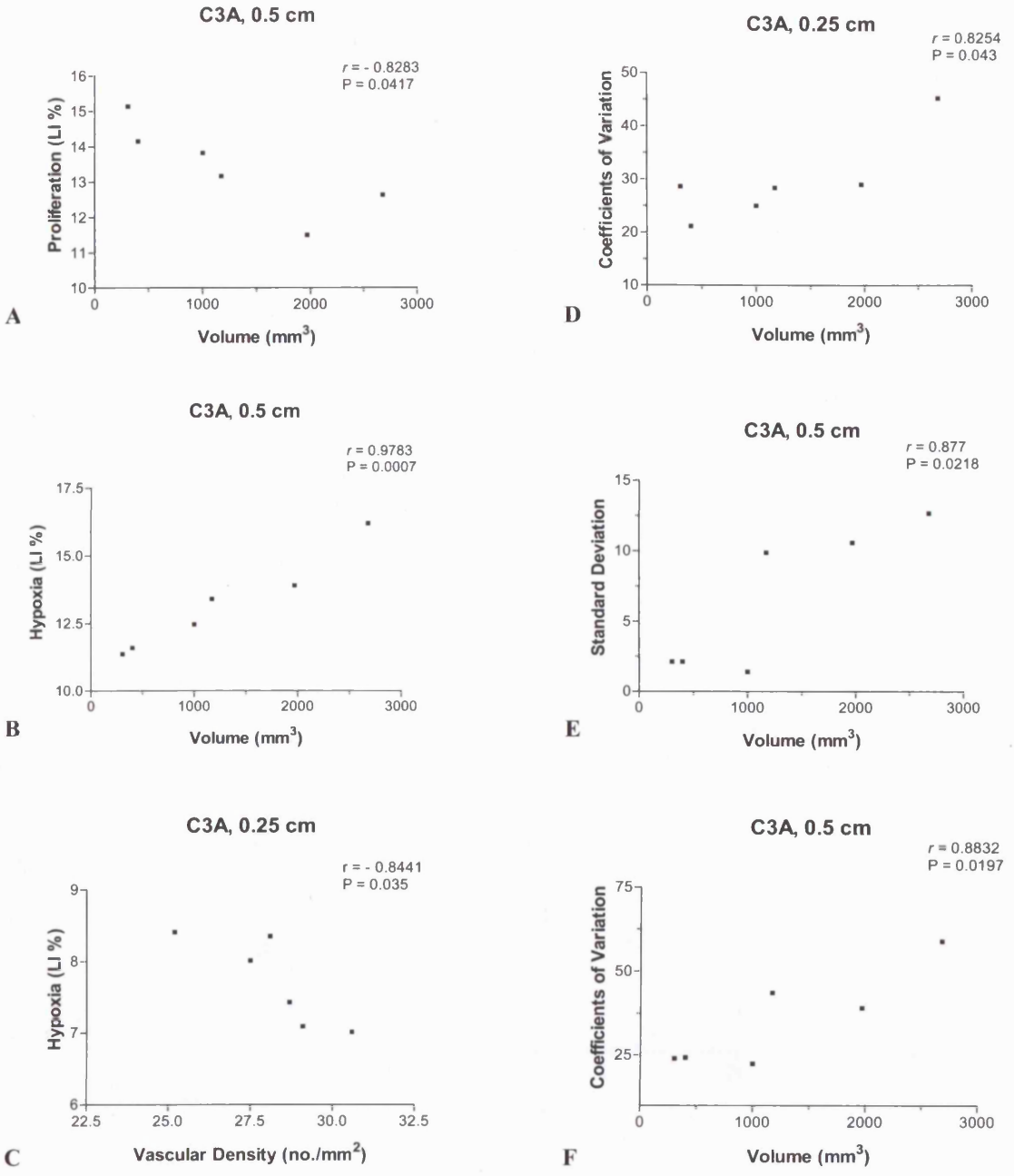

Figure 7.8. Correlation between tumour volume and **A.** proliferation and **B.** hypoxia at 0.5 cm. **C.** Correlation between vascular density and hypoxia at 0.25 cm. **D-F.** Correlations between tumour volume and heterogeneity. Ten sections were analysed in 6 intrahepatic xenografted C3A tumours at 12 h after injection of 4 mg/kg. cisplatin i.v.

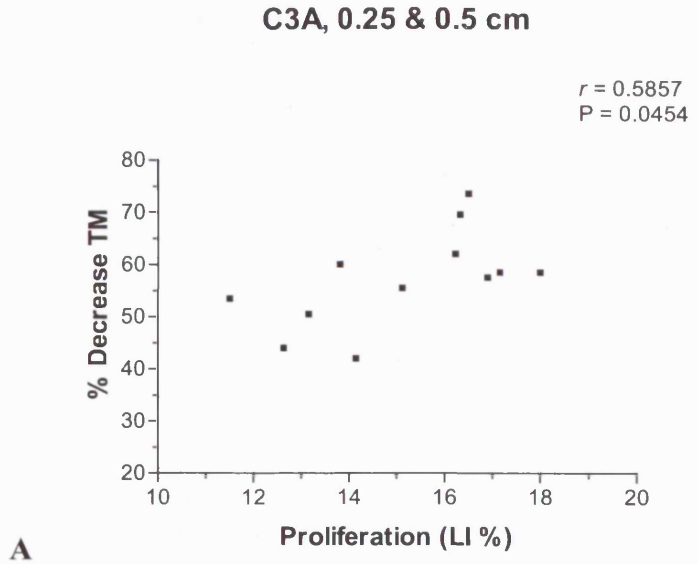

A

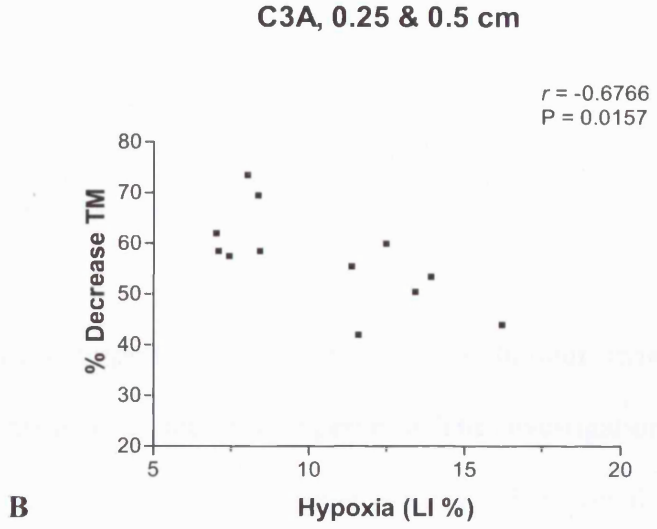

B

Figure 7.9. Correlation between cisplatin DNA-adducts and **A.** cell proliferation, and **B.** hypoxia, at 0.25 & 0.5 cm in 6 C3A xenografted tumours from nude mice at 12 h after injection of 4 mg cisplatin/kg i.v.

Correlations are calculated as Pearson's correlation coefficients (*r*).

7.3 Discussion

This section of the study describes the topographic distribution of cisplatin DNA-adducts within tumours, using an *in vivo* model with intrahepatic xenografted HCC and CRC in nude mice. Potential mechanisms for drug heterogeneities have also been explored by using different immunohistochemical stainings on parallel tissue sections. Factors influencing the cytotoxicity of cisplatin at a cellular level have been examined *in vitro* in previous chapters, including reduced uptake or increased drug efflux, inactivation by glutathione, DNA repair, and tolerance of DNA damage. Thus, although drug uptake into the tumour cell is not the only determinant for cytotoxicity of cisplatin, it is certainly a prerequisite for antitumour activity. *In vitro* studies often show correlations between cisplatin sensitivity and accumulation (Andrews and Howell, 1990). One potential reason for treatment failure with cisplatin is heterogeneities in drug distribution within the tumour, with some cells receiving sublethal intracellular concentrations.

It is increasingly important to directly analyse tumour material to determine if proposed mechanisms of action are operative. The investigation of material obtained following treatment with DNA-damaging agents has been revolutionised by the use of the comet assay. This allows quantitative estimation of DNA damage and repair in individual cells following drug exposure, thus heterogeneity in response can be evaluated, and has recently been applied to monitor ICLs in the clinical setting (Hartley et al, 1999; Webley et al, 2001).

In the present section, DNA ICLs were detected in samples taken by FNAs from human HCC and CRC intrahepatic xenografts after administration of a therapeutic

dose of cisplatin. After a single administration ICLs were detected at 6 h, with peak levels being observed at 12 h which correlates well with previous reports on the time of DNA damage with cisplatin administration. The resistant xenografts had 1.5-fold fewer ICLs at the level of the overall genome compared to the sensitive xenografts in both superficial and deep cells, reflecting *in vitro* observations. Quantitatively fewer ICLs were noted, however, in cells grown as xenografted tumours when compared with *in vitro* cells. The dose of cisplatin used in these experiments was 4mg/kg i.v. Assuming a mouse has a blood volume of 72 ml/kg this is equivalent to 185 μM or 12 mg/m^2 (where dose in mg/m^2 = km x dose in mg/kg [km = 3 for nude mice with a body weight of 20 g]) (Freireich et al, 1966). This is higher than the highest *in vitro* dose used in previous chapters (100 μM) and slightly lower than human clinical doses (15-20 mg/m^2). When cisplatin is given i.v. to nude mice it is rapidly sequestered by protein binding, such that 1 h after administration no free drug remains in the plasma (Siddik et al, 1987). Therefore, with a single i.v. dose of 4mg/kg we are measuring the response to a brief genotoxic insult induced by cisplatin treatment at a dose close to that used *in vitro* and clinically. In addition, once the cisplatin molecule is injected into the blood stream, it encounters the following "resistances" before reaching the intracellular space: (i) distribution through the vascular space; (ii) transport across the microvascular wall; (iii) transport through the interstitial space; and (iv) transport across the cell membrane. The combination of these factors would explain the quantitative differences between *in vivo* and *in vitro* findings.

Interstrand crosslinks were noted to be quantitively higher in superficial cells of xenografts, and these cells were more efficient at repair than central cells. Rates of repair of ICLs in superficial cells were generally greater than those observed in *in*

vitro cells. Intratumour adduct heterogeneity within samples at 12 h, expressed as variations in CV, was greater in deep cells with CVs ranging from 29.11-67.14% and 22.36-58.93% in SW620 and C3A xenografts respectively. Although a number of studies have examined the distribution of platinum within tumours (Deurloo et al, 1991; Richmond et al, 1992), few have examined the topographic distribution of cisplatin-DNA adducts and none have used the comet assay. Johnsson et al studied the intratumoural distribution of cisplatin-DNA adducts in squamous cell carcinoma xenografted tumours in nude mice immunohistochemically using NKI-A59 antiserum elicited against cisplatin-DNA interaction products and reported CV values between 75 and 115% (Johnsson and Cavallin-Stahl, 1996). A three-dimensional image of adduct distribution was produced which showed a 2-fold difference between high and low adduct levels. No specific mention was made on differences between superficial and deep areas.

Potential reasons for heterogeneity in cisplatin-DNA adduct distribution were also investigated in this study. Larger tumours were found to have greater intratumoural variation in adducts in C3A xenografts. Although Johnsson et al demonstrated positive correlation coefficients between tumour size and heterogeneity of cisplatin-DNA adducts, these were not statistically significant (Johnsson and Cavallin-Stahl, 1996).

An adequate vascular system is required for sufficient drug delivery to tumour cells. The three-dimensional growth of solid tumours requires a vascular network of new capillaries. These new capillaries lack a supporting architecture and are thin-walled and leaky. The lack of a smooth muscle wall also renders them less responsive to

vasoactive stimuli and more prone to compression, especially in larger tumours in which the interstitial pressure is raised. Thus, a tumour often has oxygen diffusion gradients and a relatively poor nutrient supply, which may result in necrosis (Trotter et al, 1989). Immunohistochemical staining for Factor VIII related antigen (von Willebrand factor) is considered a valuable method of demonstrating endothelial cells giving a distinct picture of the vascular pattern in normal and malignant tissue (Sehested and Hou-Jensen, 1981). The tumours used in this section were well vascularised and in general vascularity was greater superficially. Theoretically cisplatin-DNA adduct levels should be higher in areas that are well vascularised reflecting better drug delivery, and higher in tumour cells close to capillaries. Johnsson et al, however, analysed cisplatin-DNA adduct levels at different distances from large capillaries, and found there was a tendency for lower adduct levels close to capillaries (Johnsson and Cavallin-Stahl, 1996). It was suggested that cisplatin, being a small molecule, diffuses so easily into surrounding tissue that distance from the delivering capillary is of minor importance. Alternatively the lack of correlation could have been due to the fact that the tumours studied were extremely well vascularised.

Cell proliferation is an important determinant for cytotoxicity of cisplatin and most other cytotoxic agents. Cells in active cell cycle are more susceptible to damage by cisplatin than quiescent cells in G_0 phase (Shalinsky et al, 1996). Whether proliferating cells also accumulate more drug and form more adducts is as yet unknown. The MIB-1 staining was strong in all tumours indicating a high proliferating activity. Labeling index values were within the same range noted in other human CRC mouse xenografts (Sharma et al, 1997). Proliferation was generally higher in superficial cells in both xenografts, and significantly higher values were

noted in superficial C3A cells in comparison with SW620 xenografts. Tumour volume was inversely correlated with proliferation in cells aspirated from deep areas of both xenografts. There was a positive correlation between proliferation and adduct formation in C3A xenografts. This suggests that the higher uptake and adduct formation noted in C3A xenografts is a result of their higher proliferating activity and could in part account for adduct heterogeneity. A weak correlation between proliferation and adducts in human squamous cell carcinoma xenografted tumours in nude mice has previously been noted, but was not statistically significant (Johnsson and Cavallin-Stahl, 1996).

Central necrosis is a common feature of larger tumours. Cells close to the areas of necrosis may sustain hypoxia due to oxygen diffusion limitations. Transient, acute hypoxia has also been demonstrated in tumours (Trotter et al, 1989). This is a perfusion-limited hypoxia that is caused by a temporary interruption of blood flow within the vasculature as the vessels undergo spontaneous opening and closing. Both chronic and acute mechanisms are responsible for the presence of hypoxic cells in tumours (Chaplin et al, 1987). The LI for NITP ranged from 6.58 to 13.04%, there was a wide inter- and intratumour variation. This large variation was also observed in immunohistochemical studies with NITP staining in human squamous cell carcinoma xenografts in nude mice (Bussink et al, 1999). An inverse correlation between hypoxia and adduct formation was seen in the C3A xenografts, suggesting aerobic conditions favour cisplatin-DNA adducts. There is conflicting evidence regarding the effect of hypoxia on the cytotoxicity of cisplatin. Several studies have indicated that hypoxia enhances the cytotoxicity of cisplatin (Douple and Richmond, 1979; Skov et al, 1998; Stratford et al, 1980), while others have found that cisplatin is more

cytotoxic under aerobic conditions (Donnelly et al, 2004; Grau and Overgaard, 1988; Melvik and Pettersen, 1988). It has also been reported that the cytotoxicity of cisplatin is not influenced by the cellular oxygenation state (Korbelik and Skov, 1989; Teicher et al, 1981). The majority of these studies have been *in vitro* studies culturing mammalian cells with cisplatin under aerobic and hypoxic conditions (Korbelik and Skov, 1989; Melvik and Pettersen, 1988; Skov et al, 1998; Stratford et al, 1980; Teicher et al, 1981), whilst two studies have used *in vivo* s.c. murine tumour models (Donnelly et al, 2004; Grau and Overgaard, 1988), all have used clonogenic assays to determine cytotoxicity. Although two studies have specifically examined cisplatin-DNA crosslinking using alkaline elution (Skov et al, 1998; Teicher et al, 1981), and another has indirectly determined the hypoxic fraction within solid tumours (Grau and Overgaard, 1988), no previous study, however, has correlated the extent of cisplatin-DNA crosslinking directly with local hypoxia.

In summary, this section confirms the use of FNAs to obtain individual cells from human HCC and CRC xenografts in nude mice in their orthotopic sites for analysis by the comet assay. It has demonstrated the feasibility of characterising and quantitating DNA damage and repair in an animal model that could be transferred to a clinical setting. Differences have been demonstrated in both the topographic distribution of cisplatin-DNA adducts, and in the quantitative and qualitative rates of repair of ICLs in comparison to *in vitro* data. The findings from this series of experiments are consistent with those of previous studies suggesting a correlation between proliferation and adduct formation (Johnsson and Cavallin-Stahl, 1996), and also provide support to the observation that cisplatin is more cytotoxic to well-oxygenated tumour cells than to hypoxic tumour cells (Donnelly et al, 2004).

CHAPTER VIII

ORTHOTOPIC MODEL OF CRC LIVER METASTASES IN NUDE RATS IN WHICH TO EVALUATE DRUG CYTOTOXICITY BY THE COMET ASSAY USING THE ISOLATED DUAL - PERFUSED RAT LIVER

VIII. ORTHOTOPIC MODEL OF CRC LIVER METASTASES IN NUDE RATS IN WHICH TO EVALUATE DRUG CYTOTOXICITY BY THE COMET ASSAY USING THE ISOLATED DUAL-PERFUSED RAT LIVER

8.1 Introduction

For any therapeutic agent to be effective, it must accumulate in target cells in optimal concentrations for a required duration of time. Unfortunately, physico-chemical and physiological barriers can lead to heterogeneous accumulation of therapeutic molecules, particles and cells in solid tumours (Jain, 1998). In cancer, failure to treat a small fraction of cells can result in tumour regrowth. Thus, it is crucial to know which cells have been successfully treated and which have not. To determine this, simultaneous and continuous high-resolution imaging of drug distribution and its physiological determinants is required. Only with this knowledge can drug delivery be improved to all regions of a tumour. Invasive methods such as immunohistochemistry used in Chapter VII can provide the desired spatial resolution, but require tumour removal, so the temporal dynamics are missed.

Not only is the comet assay sensitive to low levels of DNA damage, but more important it provides sufficient resolution to detect subpopulations of cells that differ in damage by as little as a factor of 2 (Olive et al, 1993). The fact that the method can be applied to tumour samples obtained by FNA biopsy means there is the potential to examine both spatial resolution, by taking samples from different sites of a tumour, and temporal dynamics, by taking samples at different times from the same tumour.

The ability to perform sequential or multiple samples has the additional advantage of using the given tumour as its own control.

Although it has been over 100 years since the first reported use of the isolated perfused rat liver (IPRL) (Miller, 1972), this model is still a valuable and commonly used tool for exploring the physiology and pathophysiology of the liver, and pharmacological investigations. The IPRL remains an important experimental model despite the availability of newer techniques (such as liver slices, isolated and cultured cells, and isolated organelles) for evaluating hepatic function. This popularity is due to the fact that, in contrast to *in vivo* models, the IPRL allows repeated sampling of the perfusate and liver, permits easy exposure of the liver to different concentrations of test substances and is amenable to alterations in temperature that would not be tolerated *in vivo*. Furthermore, experiments can be done independent of the influence of other organ systems, plasma constituents and neural-hormonal effects. In contrast to the other *in vitro* models, such as isolated and cultured hepatocytes and isolated organelles, hepatic architecture, cell polarity and bile flow are preserved in the IPRL.

Typical experiments with the IPRL are performed under conditions that differ markedly from the *in vivo* situation such as lack of perfusion via the hepatic artery (HA) and the composition of the perfusate. Although perfusion solely through the portal vein (PV) with an oxygen-rich medium is sufficient to maintain the viability of the liver (Meijer et al, 1981; Ross, 1972) , this model is still clearly unphysiological as it excludes the possible contribution that arises from input via the HA. Furthermore, anatomical studies show that metastasising tumour cells entering the liver via the portal vein develop into liver tumours, which are mainly vascularised by the HA

(Sigurdson et al, 1987). Studies of the blood supply of liver tumours show that the HA provides up to 95% of their total blood flow (Wang et al, 1994). In contrast to normal liver tissue the PV plays a minor role in the blood supply of liver tumours (Taylor et al, 1978).

The ideal perfusate for continuous perfusion of the IPRL has not yet been defined. However, the perfusate should deliver oxygen to the liver by using an oxygen carrier for the full benefit of perfusion to be realised (Kamada et al, 1980), (Gores et al, 1986). Simple oxygenated buffer solutions require higher flows for adequate oxygen delivery and create degenerative changes in the perfused tissues that are not seen when red blood cells are used as the oxygen carrier (Riedel et al, 1983; Starnes et al, 1991). In addition to tissue damage, high flows can decrease first-pass hepatic clearance (Pries et al, 1981). Similarly, high pressures cause hepatic barotrauma and enlarge sinusoidal fenestrations (Fraser et al, 1980). A Haematocrit of 20% has been suggested to provide the optimum combination of haemodynamics and oxygen-carrying capacity (Pegg et al, 1984). Also, red cells can attenuate sinusoidal damage by scavenging xanthine-oxidase-dependent radicals (which cause respiratory burst leading to lipid peroxidation and cellular destruction) in IPRLs.

The prime aim of this section of the study was to establish an intrahepatic xenograft of human CRC in rats, and to use the isolated dual-perfused rat liver (IDPRL) thus mimicking physiological delivery of chemotherapeutic agents, to assess the spatial and temporal pattern of chemotherapy related cancer DNA damage using the comet assay.

8.2 Materials and methods

8.2.1 Orthotopic model of liver cancer in nude rats in which to evaluate drug cytotoxicity by the comet assay

To study the spatial and temporal pattern of drug induced DNA damage in rat intrahepatic xenografts using IDPRLs, the HCC cell line C3A and CRC cell line SW620 used in the study of intrahepatic xenografts in nude mice (Chapter VII) were initially selected. All animals were supplied by, and the *in vivo* experiments were carried out at the Comparative Biology Unit (CBU), Royal Free Hospital. All procedures were within national ethical guidelines, were in compliance with the United Kingdom Coordinating Committee on Cancer Research Guidelines for the welfare of Animals in Experimental Neoplasia, and covered by the Home Office Licence No. PPL 70/4517. Tumour volume was determined by external measurement in two dimensions according to the published method using the equation $V = (L \times W^2)/2$, where V = volume, L = length, and W = width (Johnsson and Cavallin-Stahl, 1996).

Experiment series I: Implantation of tumour tissue generated in subcutaneous tissues of nude mice into rat liver parenchyma

Three million cells were prepared from tissue culture flasks and resuspended in 500 µl of Matrigel. Mice were divided into two groups (2 mice for each cell line) and the cells injected subcutaneously into their flanks using 25-gauge needles. Mice were then recovered and were intermittently assessed for weight loss and other signs of discomfort. The mice were killed at 30 days by a schedule 1 method, the size of subcutaneous (s.c.) tumours were recorded, excised, and cut into small cubes of approximately 2 mm^3. Sprague-Dawley rats weighing 200-250 g were anaesthetised with halothane and a 2:1 mixture of nitrous oxide:oxygen. Removal of hair was carried out with electrical clippers and the skin cleansed with antiseptic solution. Laparotomies were performed through a midline abdominal incision and the bowel retracted to the left to expose the liver. A small superficial incision on the liver was made using the tip of a No.11 surgical blade with the knife at a 15° angle to the liver surface. A small piece of Gelfoam was inserted into the incision for approximately 1 minute and the incision compressed with a piece of gauze. When the bleeding had stopped, the Gelfoam was removed and a tumour fragment gently placed into the incision. The procedure was performed in both the right and left lobe of the liver. After the bleeding had ceased, 20 ml of balanced salt solution was placed into the peritoneal cavity and the abdominal incision closed using 4/0 vicryl. Rats recovered within minutes of discontinuing the halothane. Analgesia (Temgesic) was provided postoperatively for the first 24 h. The animals were inspected on a daily basis for any adverse effects. Animals were killed at 45 days by a schedule 1 method. The liver, lung and peritoneal cavity were examined for evidence of tumour.

Results

A total of 12 rats (6 rats in each group) were implanted with the human HCC cell line C3A and human CRC cell line SW620. After 45 days, all animals were sacrificed. No evidence of tumour was found in liver, lung or peritoneal cavity. In four of the animals evidence was found of intrahepatic abscesses at the site of solid tumour insertion (Figure 8.1.B).

Experiment series II: Implantation of tumour tissue generated in subcutaneous tissues of nude mice into nude rat liver parenchyma

All procedures were performed as described in experiment series I except Rowett (*rnu/rnu*) nude rats were used as the experimental animals. These rats have a congenital absence of the thymus resulting in a severely deficient cell-mediated branch of the immune system. When maintained under specific pathogen-free (SPF) conditions, wasting and infections do not occur as frequently as in the nude mouse counterpart. The lack of T lymphocyte cells, combined with the size and robustness of the *rnu/rnu* rat and the absence of major endocrinological abnormalities observed in some strains, make it an attractive experimental model for biomedical research. In particular, the nude rat allows human tumour cells to grow without a mechanism for immunological rejection allowing potential use of the animal in xenografting human tumours (Fossum et al, 1980; Vos et al, 1980). Subcutaneous tumours were generated in nude mice and implanted intrahepatically into nude rats as described in experiment series I. Animals were killed at 45 days by a schedule 1 method. The liver, lung and peritoneal cavity were examined for evidence of tumour.

Results

A total of 4 Rowett nude rats (2 rats in each group) were implanted with the human HCC cell line C3A and human CRC cell line SW620. After 45 days, all animals were sacrificed. All implantation's resulted in intrahepatic tumours (Figure 8.1.C). The mean tumour volumes of C3A and SW620 cells were 265 and 452 mm^3, respectively. In view of the larger size of SW620 intrahepatic xenografts, this cell line was selected for further experiments.

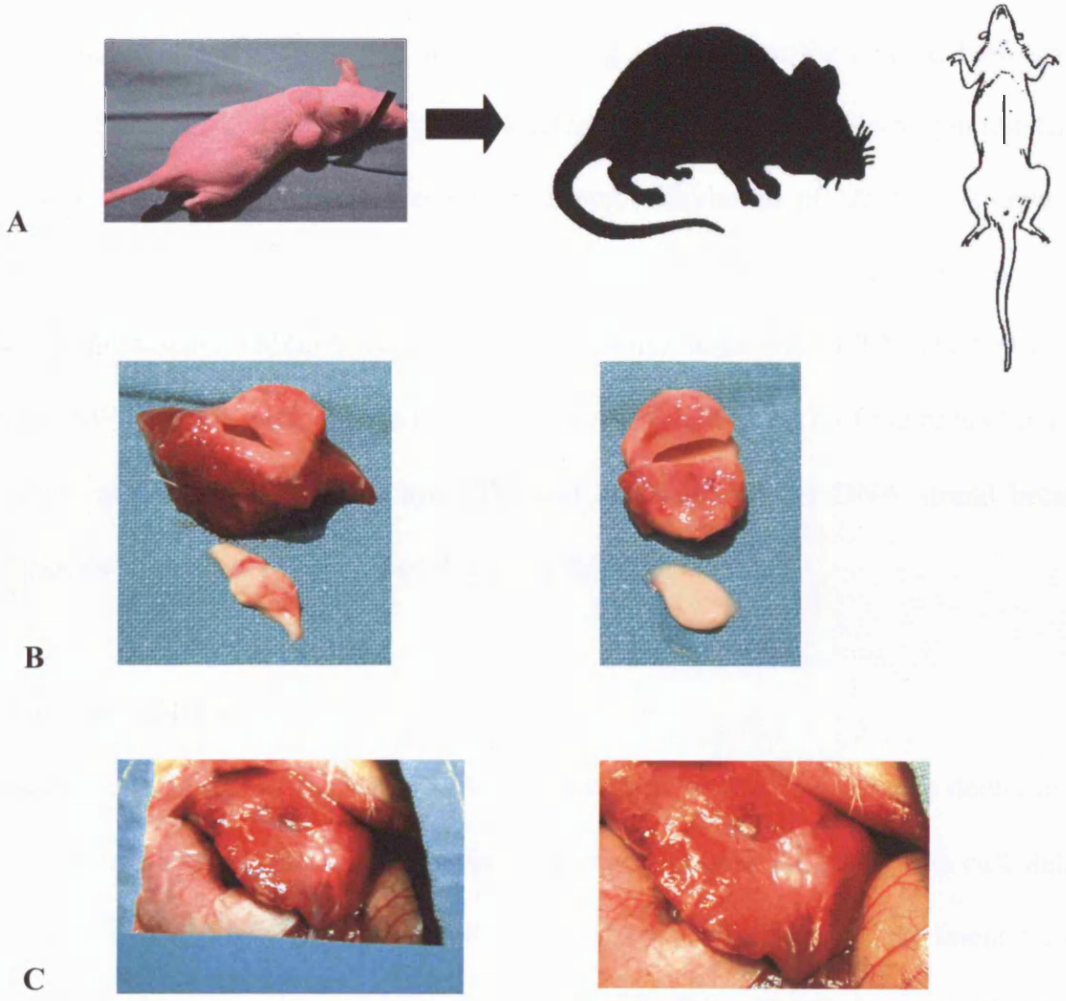

Figure 8.1. A. Subcutaneous SW620 tumour nodules from nude mice implanted into rat liver parenchyma, **B.** examples of intrahepatic abscesses observed implantation into in Sprague Dawley rats, **C.** examples of intrahepatic xenografts of in Rowett nude rats.

8.2.2 *In vitro* studies to determine drugs producing rapid DNA damage

As the life-span of the IPRL is generally considered to be approximately 3 to 4 hours under usual conditions (Gores et al, 1986), it was important to ensure that the cytotoxic drugs used in the perfusion experiments produced significant DNA damage within this time-span. Four drugs were initially chosen to examine the speed of onset of DNA damage on SW620 cells *in vitro*. First, cisplatin, which is known to cause peak interstrand crosslinks (ICLs) between 6 and 12 h over a wide range of doses (Chapter VI and [Zwelling et al, 1978]). Second, etoposide, which acts as an efficient DNA double strand (ds) breaker in proliferating cells with effects noted between 1 and 2 h (Huang et al, 1998). Third, mechlorethamine hydrochloride (nitrogen mustard, HN_2), whose primary mode of action is through alkylation of DNA, is known to exhibit increased ICLs for 1 to 2 h following which they are repaired (Ross et al, 1978), and finally chlorambucil, which demonstrates ICLs within 3 h (Hartley et al, 1999). SW620 cells were exposed to either 50 or 100 μM of each of the drugs for 1 h, washed, and either ICLs (cisplatin, HN_2 and chlorambucil) or DNA strand breaks (etoposide) measured at 1, 2, 3 and 4 h using the comet assay.

Statistical analysis

Results were expressed as mean ±SEM. Comparison between percentage decrease in tail moment (TM) or TM with time for each chemotherapeutic agent was calculated by one-way analysis of variance (ANOVA) followed by a post test for linear trend, differences between doses were examined with the one-tailed unpaired t-test. Statistical significance was defined at $P < 0.05$.

Results

Differences were observed in the timing of maximal DNA damage between drugs. Cisplatin and chlorambucil demonstrated a gradual increase in ICLs over 4 h, with a maximum percentage decrease in TM of over 30 and 50 % with 100 μM at 4 h respectively (Figure 8.2 A & D, Appendix 8.1). Both HN_2 and etoposide demonstrated maximal DNA damage after 1 h (Figure 8.2 B & C, Appendix 8.1). DNA damage increased linearly with time with 100 μM cisplatin and with both concentrations of HN_2 and chlorambucil (Figure 8.2 A, C & D, Appendix 8.2). After 1 h, DNA damage decreased linearly with time with 100 μM etoposide indicating repair (Figure 8.2 B, Appendix 8.2). Greater DNA damage was noted as the chemotherapeutic dose increased. This was statistically significant between 50 and 100 μM at all time points with cisplatin and HN_2, and at only 1 and 4 h with etoposide. There was no statistically significant difference in DNA damage between doses with chlorambucil (Figure 8.2, Appendix 8.3).

Nitrogen mustard and etoposide were selected for the following perfusion experiments because of their speed of action. Although chlorambucil caused more ICLs within 4 h than cisplatin, it did not demonstrate statistically significant differences in DNA damage between doses. Thus cisplatin was chosen in preference, cisplatin also provided continuity with the *in vitro* and *in vivo* work performed in Chapters VI and VII.

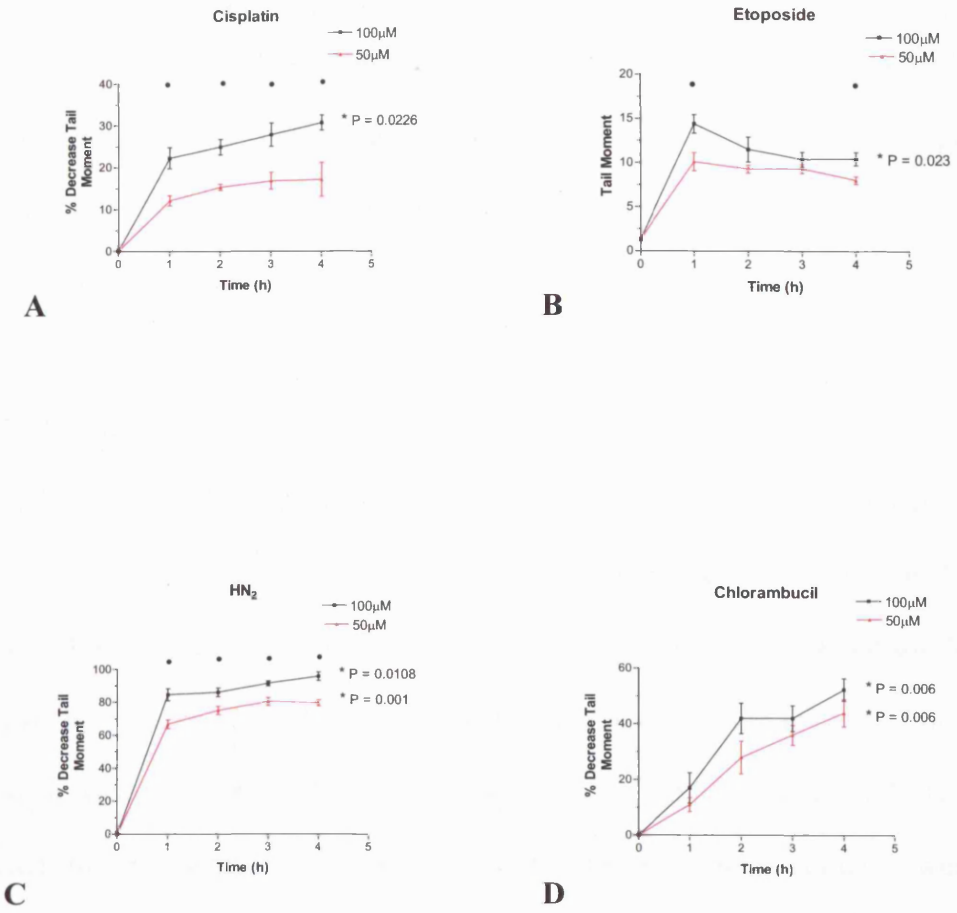

Figure 8.2. Rate of formation of ICLs *in vitro* in SW620 cells with **A.** cisplatin, **C.** HN_2 and **D.** chlorambucil, and **B.** rate of formation of ds DNA breaks with etoposide. Cells were incubated with 50 and 100 μM of each cytotoxic agent for 1 h at 37°C, the cytotoxic agents were then removed and replaced by fresh medium. The comet assay was then used to quantify DNA damage at 1, 2, 3 and 4 h. Cells treated with alkylating agents (**A.**, **C.** and **D.**) were irradiated immediately prior to analysis to deliver a fixed level of random strand breakage.

Values are the mean of three individual experiments ±SEM.

* one-way ANOVA with post test for linear trend.

• $P < 0.05$ between 50 & 100 μM (one-tailed unpaired t-test).

HN_2, nitrogen mustard; ds, double strand breaks

8.2.3 Isolated dual-perfused rat liver – perfusion via portal vein and hepatic artery

SW620 tumours generated subcutaneously in nude mice, were implanted into the right and left lobes of livers of 10 Rowett (*rnu/rnu*) nude rats as described in experiment series I and II. On day 45 anaesthesia was induced with halothane and a 2:1 mixture of nitrous oxide:oxygen.

Surgical procedure

The abdomen was opened through a midline incision and the abdominal contents displaced to the left to expose the liver and common bile duct. The bile duct was cannulated with tubing obtained from a 22 GA catheter (Beckton Dickinson Infusion Therapy, Helsingborg, Sweden, 0.8 mm) and then tied securely in place. For smaller animals it was necessary to draw out the tubing to approximately one-half its starting diameter to successfully cannulate the duct. The abdominal contents were then displaced to the animal's right and the thin strands of connective tissue between the left liver lobes and the stomach were cut. The lower oesophagus was cut between ligatures and then gently displaced inferiorly to expose the aorta and coeliac artery. The superior mesenteric artery, left and right renal arteries, and ileolumbar arteries were ligated. The left gastric and splenic arteries, branches of the coeliac artery and gastroduodenal artery were also ligated. Two loose ligatures were placed around the aorta, one above the coeliac artery and the other at the level of the left renal artery. Following these procedures, only the hepatic artery was left patent.

The abdominal contents were again displaced to the animals left, the strands of connective tissue between the right lobe of the liver and vena cava above the right kidney were cut, and a loose ligature passed around the abdominal vena cava. After

heparinisation (0.2 IU/g/iv), the PV was cannulated using an 18 GA catheter (Beckton Dickinson Infusion Therapy, Helsingborg, Sweden, 1.2 mm) and flushed with 20 ml oxygenated perfusate. The inferior vena cava above the kidneys was tied to ensure unidirectional flow, whereas the lower abdominal vena cava was severed to allow immediate drainage. The diaphragm was then opened and the suprahepatic inferior vena cava cannulated with an 18 GA catheter (Beckton Dickinson Infusion Therapy, Helsingborg, Sweden, 1.2 mm) to collect outflow from the hepatic veins.

The aorta was tied below the level of the left renal artery and above the coeliac artery, then cannulated with an 18 GA catheter (Beckton Dickinson Infusion Therapy, Helsingborg, Sweden, 1.2 mm) and flushed with 2 ml heparinised saline. Finally, all loose ligatures were secured, the livers were excised, weighed, and placed on the perfusion circuit. All operative procedures were completed within 40-50 min.

Liver perfusion

The liver was placed on a removable petri dish and connected to the liver perfusion circuit in a closed recirculating system. The perfusion circuit consisted of two independent low-flow roller pumps (Watson-Marlow Limited, Falmouth, Cornwall, England, UK), and used polyvinylchloride tubing (Medtronic, Watford, UK) with an internal diameter of 3/16 inches. Grooves at the edge of the dishes stabilised the cannulae. The HA and PV cannulae were perfused at constant flow rates of 0.3 and 1.5 ml/min/g liver, respectively. The instantaneous flow rate was measured by a 6 mm tubular flow probe connected to a Transonic Medical Flowmeter system (HT207, Transonic Medical System, NY, USA). Serial intraluminal pressure measurements were made by a Millar Mikro-tip catheter transducer (Millar Instruments, Houston,

TX, USA) introduced via a Y-connection port. All outputs were fed into a commercial analogue-to-digital data acquisition recording system (ADC/MacLab, AD Instrument, Hastings, UK). The perfusate was collected from the suprahepatic inferior vena cava and returned to a shared reservoir by gravity. Circulating perfusate was oxygenated through a Maxima hollow-fibre oxygenator (Johnson & Johnson Cardiovascular, Division of McNeilab, Anaheim, CA, USA) with a mixture of 95% oxygen and 5% carbon dioxide. The pH, pO_2 and pCO_2 of the circulating perfusate were monitored at regular time intervals with an automatic blood gas, electrolyte and haematocrit analyser (BG Electrolytes System, Instrumentation Laboratory, Lexington, MA, USA), and corrections made accordingly to ensure constant physiological values. The temperature was kept constant at 37°C by keeping the reservoir within a heated water bath (Figure 8.3).

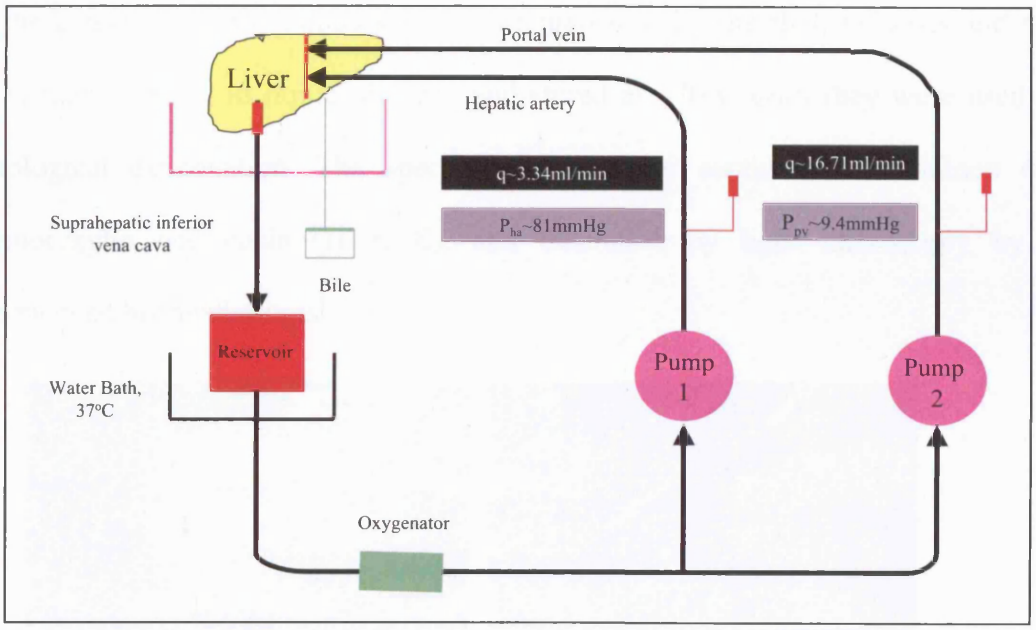

Figure 8.3. Rat liver perfusion circuit.

P, pressure; q, flow,

The perfusate consisted of a modified Krebs' solution (NaCl 150 mM, Hepes 10 mM, $NaHCO_3$ 10 mM, Glucose 5 mM, $MgCl_2$ 1.18 mM, KH_2PO_4 5 mM in 100 ml Gelofusine [Vifor Medical, Sempach, Switzerland], a colloid solution of 4% succinylated gelatin in 0.9% NaCl, and 100 ml H_2O) containing 20% (vol./vol.) of outdated human Type O RBC's (obtained from Blood Transfusion Services) and 1 IU heparin/ml (Ellis et al, 1996; Rothbarth et al, 2002).

Liver viability was assessed by gross liver appearance, stable HA and PV pressures, alanine aminotransferase (ALT) levels of the perfusate (measured using a standard clinical biochemistry autoanalyser [Hitachi 747 Autoanalyser, Boehringer Mannheim, Germany]), and bile production (measured directly with a calibrated collection vessel). At the end of each experiment, after FNA biopsies had been taken for analysis by the comet assay, the tumours were measured to calculate their volumes and then immediately frozen in liquid nitrogen and stored at –70°C until they were used for histological examination. The specimens were later sectioned and stained with haemotoxylin and eosin (H & E), and examined by light microscopy by an experienced histopathologist.

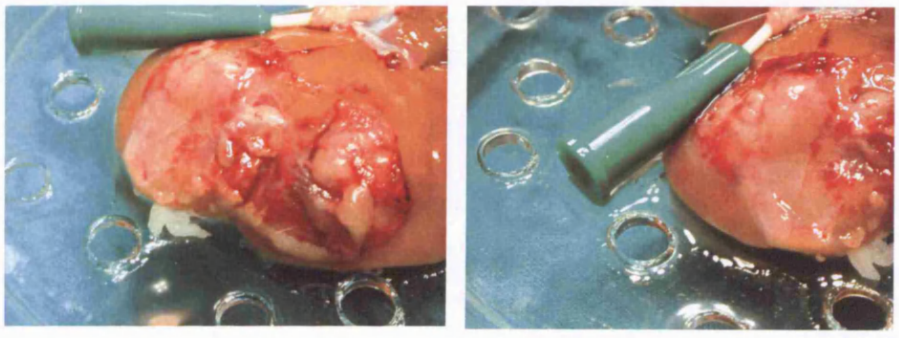

Figure 8.4. Examples of SW620 intrahepatic rat xenografts post perfusion.

8.2.4 Analysis of spatial and temporal tumour drug induced DNA damage

One of the Rowett (*rnu/rnu*) nude rat livers was perfused with drug free perfusate as a control. As well as observing gross liver appearance, post perfusion histology, HA and PV pressures, ALT levels of the perfusate and bile production; FNA biopsies of tumour and wedge biopsies of normal liver were taken hourly to examine DNA integrity, and oxygen consumption (μM/min/g of liver) was calculated by (Mischinger et al, 1992):

$$\frac{PV\ O_2\ content - IVC\ O_2\ content}{100 \times W\ (liver)} \times flow\ (ml/min) \times 44.6$$

The normal liver wedge biopsies were reduced to a single cell suspension by finely mincing and filtering through a 30 μm nylon mesh, and then along with the procured FNA's frozen immediately in 1 ml RPMI, 10% foetal calf serum and 10% DMSO at –80°C.

The other livers were initially perfused with drug free perfusate for 20 min to allow stabilisation. Prior to initiation of cytotoxic perfusion (i.e. Time = 0 h), tumour FNA biopsies were obtained. The cytotoxic agent was then added to the recirculating perfusate. Three cytotoxics were used in total; cisplatin, etoposide, and HN_2 (see Section 8.2.2), a single agent was used in each experiment. Tumour FNA biopsies were taken at 60 min intervals at accessible sites and depths depending on the size of the tumour studied. FNA biopsies were frozen immediately in 1 ml RPMI, 10% foetal calf serum and 10% DMSO at –80°C. All samples were analysed using the comet assay (for details see Chapter II, Section 2.9). For the samples treated with alkylating agents one group was irradiated with 10 Gy using an X-ray source (dose rate 2.35

Gy/min) and the other group remained unirradiated. For the samples treated with etoposide this step was omitted and thus only one group analysed.

Statistical analysis

Results were expressed as mean ±SEM. Statistical analysis of differences in perfusion characteristics with time were calculated using the two-tailed paired t-test. Comparison between percentage decrease in TM or TM with time and dose of each chemotherapeutic agent was calculated by one-way ANOVA followed by a post test for linear trend or the one-tailed unpaired t-test. Intra- and intertumour variability in percentage decrease in TM or TM with depth and site was calculated with either the two-tailed unpaired t-test or one-way ANOVA followed by the Bonferroni multiple t-test when three or more groups were compared. Statistical significance was defined at $P < 0.05$.

Results

A total of 10 Rowett (*rnu/rnu*) nude rats were implanted with SW620 tumours. One of the rats died 7 days post-implantation, the cause was unknown as it was ingested by the other animals within the cage. Table 8.1 summarises the pathological characteristics of the remaining 9 rats. Two rats generated only 1 intrahepatic xenograft, all the others produced a tumour in each lobe of the liver, giving a total of 16 tumours with a median volume of 269.5 (range 22.5-1152) mm^3.

Table 8.2 summarises the perfusion characteristics. All livers were perfused for 4 h, and median total perfusion flow was 20 (range 15-23) ml/min, the HA contributing 17% (3.3 [range 2.5- 3.83] ml/min) and PV 83% (16 [range 13-19] ml/min).

Experiment	Tumour implant	No.tumours	Tumour No.	Size (mm)	Tumour volume (mm^3)	Cytotoxic perfused
1	SW620	1x	1	5 x 3	22.5	Cisplatin 50μM
2	SW620	2x	2	10 x 5	125	Cisplatin 100μM
			3	5 x 4	40	
3	SW620	2x	4	15 x 5	187.5	Cisplatin 100μM
			5	10 x 5	125	
4	SW620	2x	6	16 x 9	648	Etoposide 50μM
			7	18 x 8	1152	
5	SW620	2x	8	12 x 8	768	Etoposide 100μM
			9	15 x 7	735	
6	SW620	2x	10	16 x 7.5	450	HN_2 50μM
			11	7 x 4	56	
7	SW620	2x	12	16 x 8	512	HN_2 100μM
			13	11 x 7	269.5	
8	SW620	2x	14	14 x 7	343	HN_2 100μM
			15	4 x 4	32	
9	SW620	1x	16	7 x 6	126	Control

Tumour volume = (length x $width^2$)/2 mm^3

Table 8.1. Isolated Perfused Rat Liver characteristics.

Characteristics	Median	Range
Liver weight (g)	11.08	7.14 - 11.84
Hepatic artery flow (ml/min)	3.34	2.5-3.84
Portal vein flow (ml/min)	16.71	12.93-19.24
Hepatic artery pressure (mm Hg)	81.75	67-89
Portal vein pressure (mm Hg)	8.73	6.2-13.3
Bile flow (ml/hr)	0.24	0.15-0.43
ALT (IU/L)	21.5	17 - 33

ALT, alanine aminotransferase

Table 8.2. Isolated Perfused Rat Livers: Perfusion Characteristics at 1 h (n=9)

Figure 8.5 summarises the viability parameters of the nude rat liver perfused with drug free perfusate as a control. It maintained a normal gross appearance, remaining homogenous in colour without the evidence of white spots caused by air emboli or red spots due to nonhomogenous perfusion. Although swelling of hepatocytes was noted on histological examination there was no necrosis and tissue structures of both tumour and normal liver were preserved. Hepatic arterial pressure, bile production and oxygen consumption values tended to decrease, whilst PV pressure and ALT levels of the perfusate tended to increase with time. All values were solitary during a single experiment, thus statistical significance could not be calculated. The TMs of the control tumour and wedge biopsies of normal liver remained stable within the experiment with no statistically significant differences in values between 1 and 4 h ($P = 0.8101$ and 0.7879 respectively).

Liver viability whilst on the perfusion circuit of the IDPRLs treated with cytotoxics was confirmed by gross appearance, histological examination, stable HA and PV pressures, and bile production (Figure 8.6 A-C). Although the overall trend for the pressures was to increase and bile production to decrease, they were not statistically significant between 1 and 4 h. The increase in mean levels of ALT during perfusion, however, were statistically significant between 1 and 4 h (Figure 8.6 D).

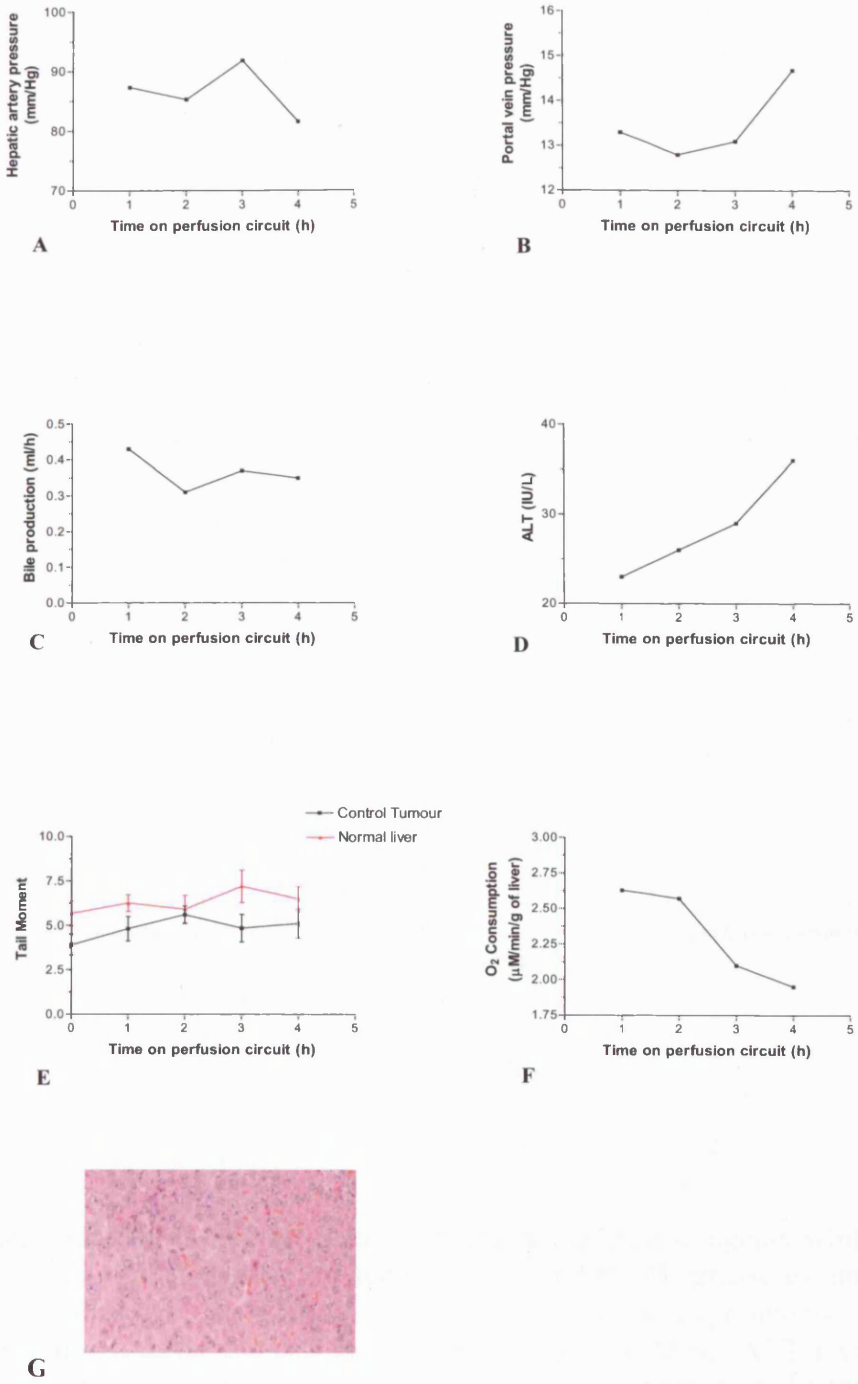

Figure 8.5. Viability parameters of the control liver and tumour whilst on the perfusion circuit. **A.** HA pressure, **B.** PV pressure, **C.** bile production, **D.** ALT levels of the perfusate, **E.** TM as assessed by the comet assay of the control tumour and normal liver, and **F.** O_2 consumption (values are a single measurement except **E.** where values are the mean ±SEM of 25 measurements and $P > 0.05$ between 1 and 4 h using the two-tailed t-test). **G.** Histology of control liver post perfusion demonstrating swelling of hepatocytes (high power view, x 10 objective lens).

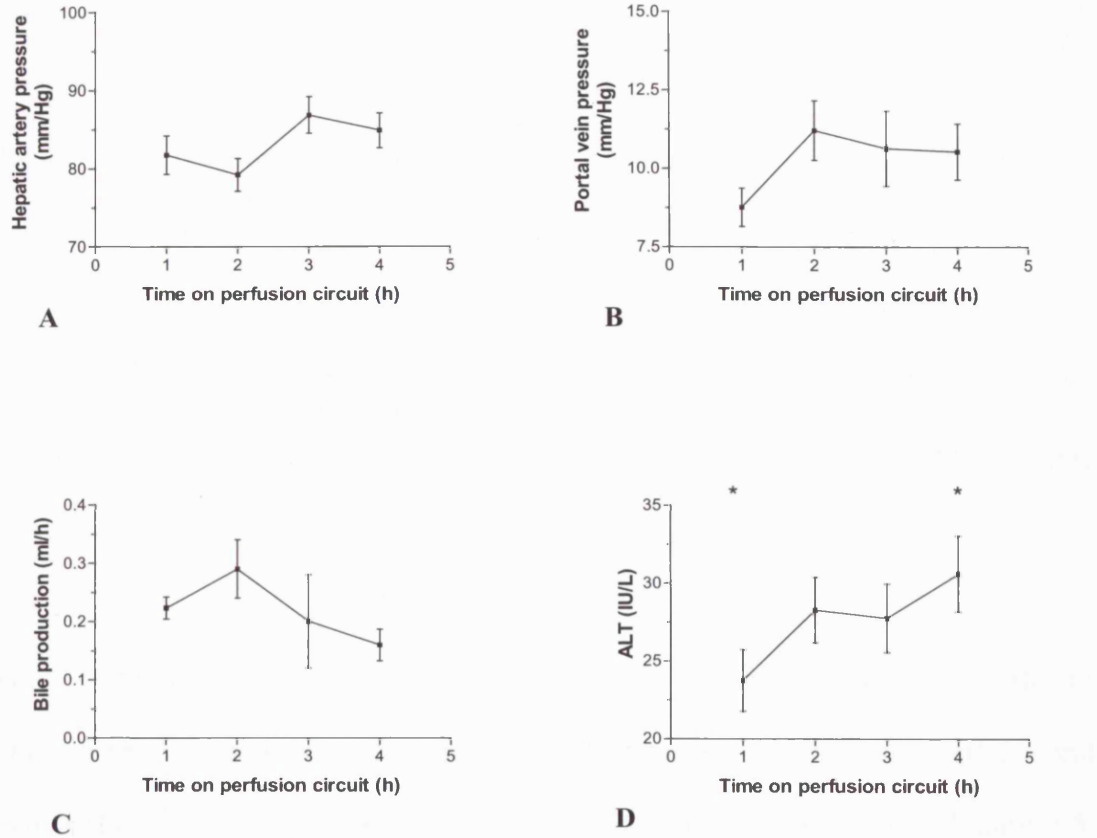

Figure 8.6. Viability of livers treated with chemotherapeutic agents whilst on the perfusion circuit was confirmed by stable **A.** HA and **B.** PV pressures, and **C.** bile production (values are the mean [±SEM] of 8 individual experiments, $P > 0.05$ between 1 and 4 h using the two-tailed paired t-test). **D.** Mean ALT levels of the perfusate increased significantly between 1 and 4 h using the paired t-test (*, $P = 0.0423$).

Greater DNA damage was noted as the chemotherapeutic dose increased. This was statistically significant between 50 and 100 μM at all time points with etoposide and HN_2, and from 2 h onwards with cisplatin (Figure 8.7, Appendices 8.4 & 8.5). Differences were observed in the timing of maximal DNA damage between drugs during perfusion. Both etoposide and HN_2 had maximal effects after 1 h, whilst cisplatin demonstrated a gradual increase in ICLs over the 4 h experiment (Figure 8.7). DNA damage increased linearly with time at both cisplatin concentrations, and decreased linearly with time after 1 h with 100 μM etoposide. There was no statistically significant linear relationship with either dose of HN_2 or 50 μM etoposide (Figure 8.7, Appendix 8.6).

Only 7 of the intrahepatic xenografts were large enough to take samples at different depths. There was no statistically significant difference in TM between superficial and deep portions of the tumours prior to perfusion with cytotoxic drugs (Figure 8.8, Appendix 8.7). Once perfusion with cytotoxics commenced, however, superficial cells generally had higher levels of DNA damage in comparison to deep cells, these were statistically significant in at least 3 time-points in 4 of the 7 perfused tumours large enough to take samples at different depths (Figure 8.9, Appendix 8.8).

When comparing cytotoxic induced DNA damage at different sites at the same depth in the same tumour, statistically significant differences were observed in only one tumour (Appendix 8.9). No significant differences were observed between different tumours in the same liver at the same depth (Appendix 8.10).

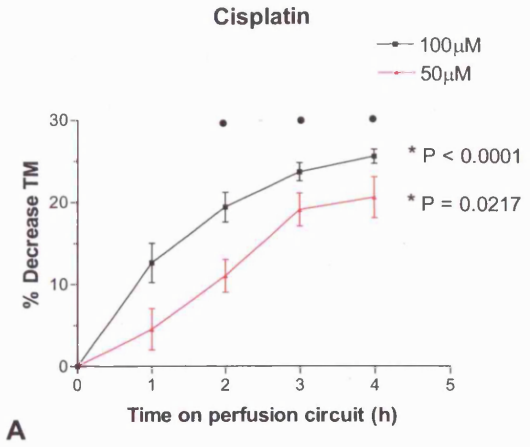

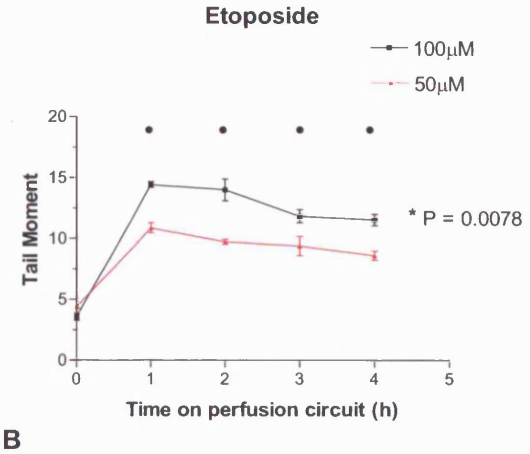

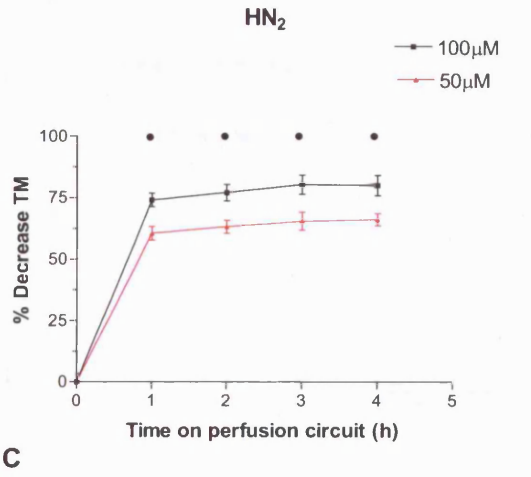

Figure 8.7. Effect of cytotoxic drugs on tumour DNA with time as assessed by the comet assay. Values are the mean (±SEM) of 2 (**A.** 50 μM), 4 (**B.** 50 & 100 μM; **C.** 50 μM), 5 (C, 100 μM) & 8 (**A.** 100 μM) measurements. (*), statistically significant with one-way ANOVA with post test for linear trend; (•), $P < 0.05$ between 50 μM & 100 μM using the one-tailed unpaired t-test.

HN_2, nitrogen mustard.

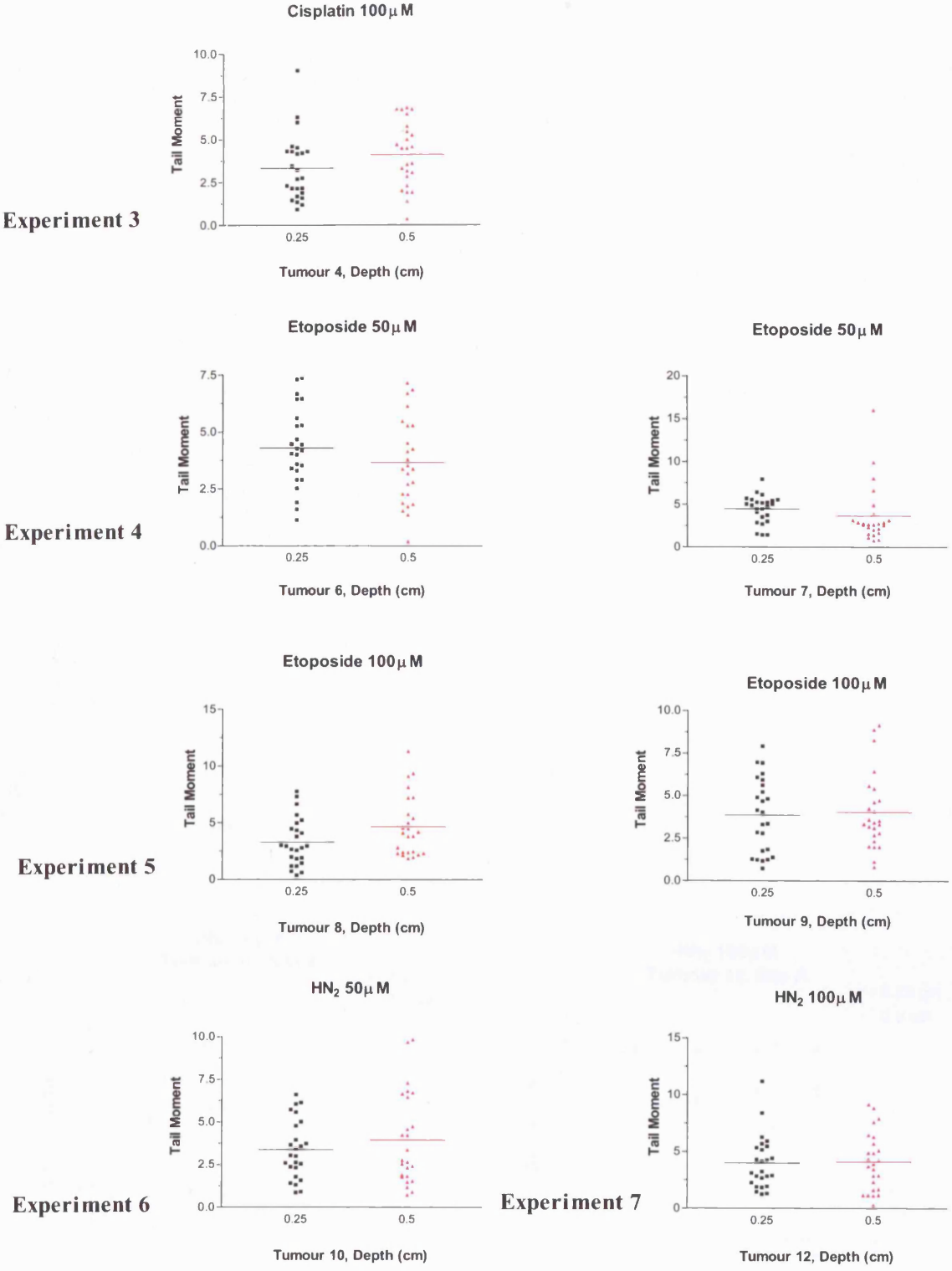

Figure 8.8. Tail Moment of intrahepatic human xenografts in nude rat livers at different depths prior to perfusion with cytotoxic drugs (Time = 0 h) as assessed by the comet assay. Twenty five individual cells from each sample are represented. There were no statistically significant differences between samples using the two-tailed unpaired t-test.

HN_2, nitrogen mustard.

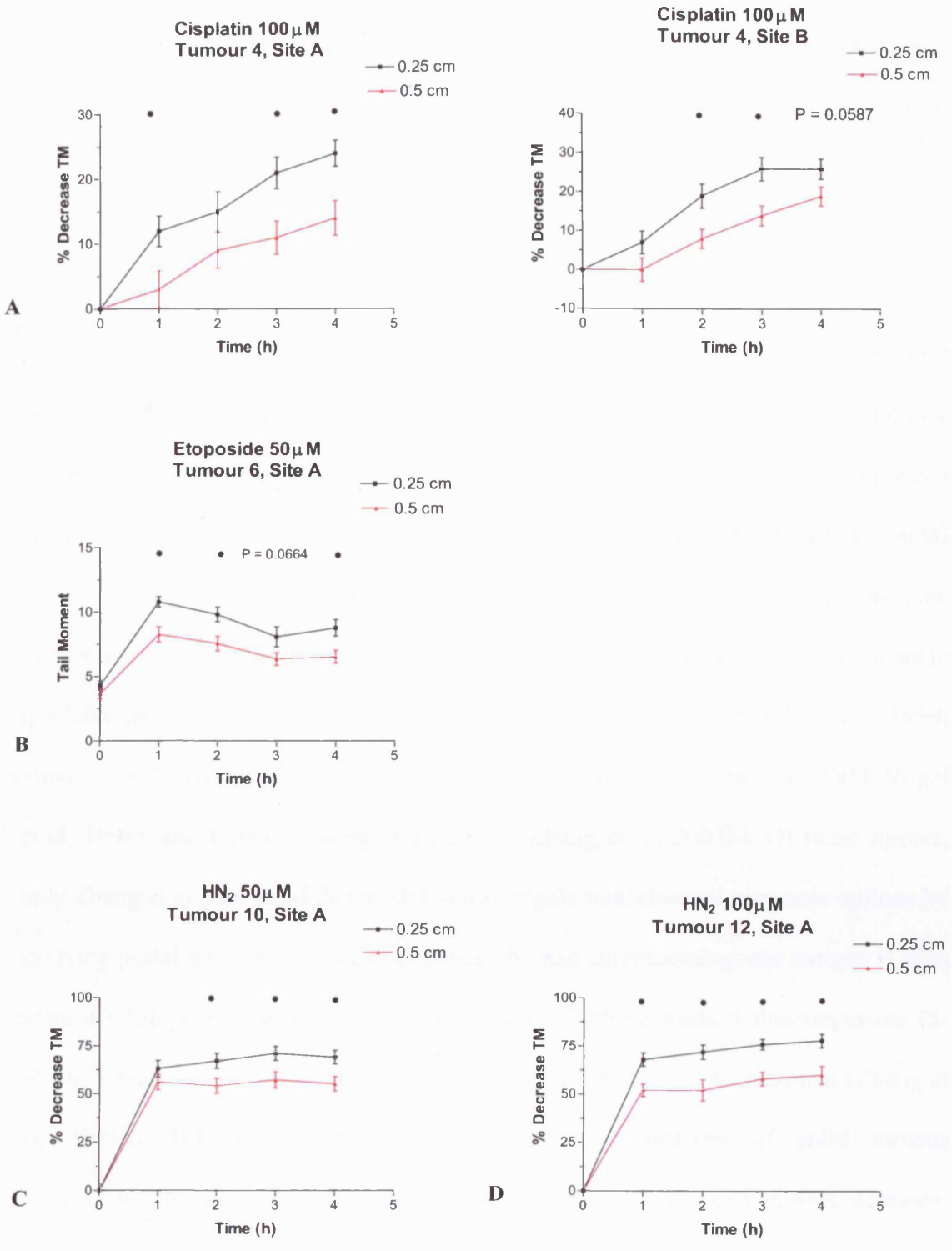

Figure 8.9. Percentage decrease of Tail Moment or Tail Moment of the same tumour and site but different depths during perfusion with cytotoxic drugs as assessed by the comet assay.

• $P < 0.05$, two-tailed unpaired t-test

8.3 Discussion

Using a closed recycling system, intrahepatic xenografts of human CRC in the nude rat have been perfused for 4 h using the IDPRL system and treated with chemotherapeutic agents allowing quantification and localisation of drug induced DNA damage.

Liver metastases of CRC remains a challenging problem associated with poor prognosis. It is generally accepted that the host microenvironment influences tumour biology with discrepancies noted in the efficacy of systemic treatments between ectopic and orthotopic tumours (Fidler, 1995), thus an appropriate experimental model based on orthotopic liver xenografts of human CRC may help to find new therapeutic options. Intrahepatic xenograft tumour models for human CRC in nude rats have previously been reported for the cell lines LS174T (Stein and Berger, 1999; Sundin, 1993; Sundin et al, 1993), HT-29 (Ashraf et al, 1997; Shen et al, 2000; Vogel et al, 1998), and LOVO (Zhang et al, 2003a; Zhang et al; 2003b). Of these studies, only Zhang et al have used this model to investigate new chemotherapeutic options by studying portal venous infusion of enhanced human carcinoembryonic antigen (CEA) promoter for yeast cytosine deaminase (yCD), which converts 5-fluorocytosine (5-FC) to 5-fluorouracil (5-FU), and subsequent intraperitoneal 5-FC treatment (Zhang et al, 2003b). In the current study, by direct implantation of solid tumour intrahepatically, successful generation of xenografts was achieved in 88% of cases. This compares favourably with previous studies, which report successful colonisation in only 50-60% of nude rats following injection of cells either directly into the liver (Stein and Berger, 1999; Zhang et al, 2003a; Zhang et al, 2003b), or via mesenteric, splenic or portal veins. Tumour growth in this study was found to be extremely

variable over 45 days as reflected by a median volume of 269.5 with a range of 22.5-1152 mm^3. The reason for this is unclear. All tumours were originally generated subcutaneously in nude mice, all had 2 mm^3 of macroscopically similar tissue implanted, and all tumours were generated for 45 days. Similar observations have been noted with other models, for example LS174T cells showed an exponential but somewhat irregular growth in the liver of nude rats within the observation period of 6 weeks (Stein and Berger, 1999).

Unlike the PV, the HA in the rat cannot be cannulated directly due to its small size and strong adhesion to the PV. Therefore, an indirect approach is employed for the cannulation of the HA. The major discriminatory feature among the various published methods for the IDPRL is the level of cannulation. In most cases, the rat liver is perfused by cannulation of the coeliac artery (Ahmad et al, 1984; Pang et al, 1988; Reichen, 1988), or aorta (Gardemann et al, 1987; Gascon-Barre et al, 1988; Kassissia et al, 1994). Although cannulation of the HA via the gastroduodenal artery (GDA) is a more direct method, in pharmokinetic studies, this method is restricted to larger animals such as the rabbit (Alexander et al, 1992), cat and dog (Lautt et al, 1993), mainly due to the larger size of the vessel. However, the rat has been used successfully as an animal model for the study of regional delivery of chemotherapeutic agents, such as mitomycin C and 5-FU (de Brauw et al, 1991; Hemingway et al, 1991; Marinelli et al, 1990), via the GDA. Among the methods of cannulation of the HA, despite the longer operation time, aortic cannulation was found to be the most suitable method in this study largely due to the relative ease of introducing a cannula. As most authors do not report the problems associated with the surgical procedure, it is difficult to make a comparison with the literature. One study,

however, specifically examining the 3 surgical procedures for HA perfusion, reported a low success rate of this method (30-40%) mainly due to extensive leaking, including leakage from the surface of the liver (Sahin and Rowland, 1998).

The rate at which substances can diffuse across the hepatic arterial and portal venous vasculatures has been shown to be modulated by the magnitude of the arterioportal pressure gradient (Browse et al, 1995). Thus constancy of both perfusion pressure and flow rate during an experiment is a prerequisite to approximate physiological conditions and maintain uniformity between experiments (Gores et al, 1986; Ross, 1972). Perfusion at lower pressures may result in nonhomogenous perfusate distribution within the liver, whilst the use of high perfusion pressures can result in an enlargement of sinusoidal fenestrations (Fraser et al, 1980) and barotrauma of the liver. The flow rates of 0.3 ml/min/g liver (HA) and 1.5 ml/min/g liver (PV) resulted in physiological perfusion pressures. Although it is appreciated that *in vivo* two thirds of the blood supply normally comes from the PV and one third from the HA, attempts to increase the HA flow during perfusion led to unacceptably high HA perfusion pressures.

The oxygen-carrying capacity of the perfusate was increased by the addition of erythrocytes, the haematocrit value of 20% is reported to be the ideal combination of blood and perfusate for the optimum oxygen-carrying capacity at physiological pressures (Riedel et al, 1983). Because human red blood cells are readily available from blood banks, previous investigators have employed them for isolated liver studies (Burczynski et al, 1996; Ellis et al, 1996; Rothbarth et al, 2002). Because of higher oxygen-carrying capacity higher flow rates were not required. Oxygen

consumption in the control liver gradually decreased throughout the perfusion (Figure 8.5.F) consistent with a decline in the viability of erythrocytes. Throughout the perfusion of both the control and livers treated with cytotoxics ALT levels rose, this may have been a reflection of loss of viability of the livers but could also be explained by haemolysis of red cells (Mischinger et al, 1992).

Although a number reports exist describing *in situ* perfusion of cytotoxics via the HA and PV of rat livers bearing rat CRC cell lines (Hemingway et al, 1991; Marinelli et al, 1990; Radnell et al, 1990), only one report to our knowledge describes an IDPRL model with a rat CRC cell line (Rothbarth et al, 2002). There are no reports to date of an IDPRL model with human CRC being perfused with cytotoxics.

Experiments using the IDPRL with a human CRC xenograft have confirmed the ability of the comet assay to detect DNA damage in FNA biopsies, demonstrating a similar time course of DNA damage relative to chemotherapy administration to *in vitro* cells and a similar relationship between dose of either ICLs or ds breaks. Two features are of note: firstly with etoposide, maximal ds breaks reflected by TM occur at 1 h after which the TM decreases. This response curve reflects the sum of a number of factors: damage induction by the circulating drug, pharmacological clearance of the etoposide, and repair of the drug induced ds breaks. The maximal damage at 1 h correlates with *in vivo* data in human WIDR carcinomas xenografted in nude mice treated with etoposide (Huang et al, 1998), whilst perfusion of the control liver in this section failed to demonstrate any significant increase in DNA damage after perfusion over a 4 h period. With the perfused rat liver model using 20% rat blood, 90% of drug clearance can be accounted for by the direct biliary clearance of etoposide or

conjugation to glucuronide with a drug half-life of 44 min (Hande et al, 1988). Thus the decrease in TM observed here would appear to be the result of DNA repair. Secondly, although there were no significant differences in DNA damage prior to perfusion with chemotherapeutic agents, a number of tumours displayed differences once cytotoxics had been added to the perfusate. Autopsy studies of liver metastases have demonstrated a decrease in the number of tumour vessels in their centre (Lin et al, 1984). Generally, small molecules with a molecular weight (MW) < 1000 show a more rapid diffusion into tissues than large molecules, such as antibodies or viral vectors. Under conditions of extensive intracellular binding and a low plasma membrane transport rate, penetration from the periphery to the centre of such drugs, such as cisplatin, etoposide and HN_2 (MWs 300, 588.6 and 192.5 respectively), can be slowed down considerably. The slow penetration of the small molecule drug doxorubicin has been shown in patients, resulting in gradients in clinical biopsies of solid tumours (Lankelma et al, 1999). Cells in the centre of tumour islets, which are the most remote from the microvessels, are exposed to lower drug concentrations in the surrounding extracellular fluid compared to the cells in the periphery. It could be argued that when the gradient reverses during drug clearance from the blood, the drug concentration in the cells at the periphery might become lower when compared to cells at the center.

This investigation was performed on only one tumour cell line and with a limited number of tumours. Studies on other CRC or HCC cell lines with larger variations in blood supply and drug sensitivities may lead to different results. Thus, this section of the study should primarily be regarded as a presentation of a methodological approach

for investigating intra- and intertumoural heterogeneities in drug induced DNA damage.

CHAPTER IX

RESPONSE TO CHEMOTHERAPY IN HCC AND CRC METASTASES IN THE ISOLATED PERFUSED HUMAN LIVER

IX. RESPONSE TO CHEMOTHERAPY IN HCC AND CRC METASTASES IN THE ISOLATED PERFUSED HUMAN LIVER

9.1 Introduction

The efficacy of chemotherapy in CRC and HCC has been approached to date using firstly *in vitro* cell culture studies (Chapters III-VI), which do not take into account the microenvironment of malignant cells, and secondly xenograft models in severe combined immunodeficient mice (Chapter VII), which do not behave like naturally occurring tumours in humans. In addition the isolated dual-perfused rat liver (IDPRL) has been used to assess the spatial and temporal pattern of chemotherapy related cancer DNA damage (Chapter VIII).

Normothermic extracorporeal perfusion of porcine livers has previously been used to optimise organ preservation protocols (St Peter et al, 2002). Butler et al have shown that the porcine liver can be perfused for up to 72 h (Butler et al, 2002), and Schon et al have demonstrated that livers preperfused before transplantation functioned well even if damaged by 1 h of warm ischaemia (Schon et al, 1993). Human cirrhotic and normal livers have also been perfused in isolation to study hepatic microcirculation and drug elimination (Villeneuve et al, 1990; Villeneuve et al, 1996a; Villeneuve et al, 1996b), and to study augmentation of portal blood flow to improve liver function (Cardoso et al, 1994).

Isolated *in situ* liver perfusion has been used to deliver the chemotherapeutic agent melphalan to patients with CRC hepatic metastases to examine its conjugation with glutathione (GSH) (Vahrmeijer et al, 1996). Similarly, isolated *in situ* lung perfusion

with doxorubicin to patients with pulmonary sarcoma metastases has been used to study *MDR1* gene expression (Abolhoda et al, 1999). A major limitation of conventional clinical studies has been the time lag between administration of chemotherapeutic agents and the determination of *MDR1* status. Using the isolated lung perfusion model the immediate molecular events occurring in tumours *in situ* in response to acute drug exposure could be accurately assessed.

In the current section of this study, liver specimens obtained from patients undergoing hemihepatectomy for liver tumours were perfused *ex vivo* with an oxygenated modified Krebs bicarbonate buffer solution containing 20% (vol./vol.) pre-washed human red blood cells (RBC) at 37°C for up to six hours, in order to investigate the short term effects of chemotherapeutic agents used in the treatment of liver cancer. As many chemotherapeutic agents produce DNA damage, the comet assay was used to detect DNA double-strand breaks and crosslinks (Fairbairn et al, 1995; Hartley et al, 1999). As only a few thousand cells are required for this assay, samples can be taken by fine needle aspiration (FNA) biopsies from a variety of sites within tumour nodules and can be repeated during the perfusion period (Olive et al, 1993).

9.2 Materials and methods

9.2.1 Patients and Tissue procurement

Eight patients undergoing hepatic resection for either HCC or CRC metastases were selected. The Royal Free Hospital (RFH) ethics committee approved the study, patients completed fully informed consent for the use of resected specimens in research.

9.2.2 Liver Perfusion Technique

At operation, the relevant hepatic duct, hepatic artery (HA) and branch of the portal vein (PV) were divided between ligatures. The relevant hepatic vein was also divided and the lobe removed to be immediately placed on ice. The branch of the PV was cannulated with polyvinylchloride tubing (Medtronic, Watford, UK) with an internal diameter of ¼ inch, intravenous cannulae (Beckton Dickinson Infusion Therapy, Helsingborg, Sweden) were used for the branch of the HA (14 GA, 2 mm) and the hepatic duct (16 GA, 1.7 mm). The liver was flushed with 1 L of ice cold University of Wisconsin (UW) solution (Viaspan®; Du Pont, Stevenage, UK), used widely for cold liver graft preservation (Kalayoglu et al, 1989), through the PV and HA branches. The effluent was then discarded. The specimen was immediately transported on ice to the experimental laboratory. The liver was weighed, and to prevent oozing from the resection surface was coated with Op Site spray (Smith and Nephew Medical Limited, Hull, England, UK).

The liver was placed on a purpose-built Perspex tray and connected to the liver perfusion apparatus in a closed recirculating system consisting of independent roller pumps (Watson-Marlow Limited, Falmouth, Cornwall, England, UK) for the PV and HA using polyvinylchloride tubing (Medtronic, Watford, UK) with an internal diameter of ¼ and 3/16 inches. The instantaneous flow rates were measured by 6 and 8 mm tubular flow probes connected to a Transonic Medical Flowmeter system (HT207, Transonic Medical System, NY, USA). Serial intraluminal pressure measurements were made by a Millar Mikro-tip catheter transducer (Millar Instruments, Houston, TX, USA) introduced via a Y-connection port. Microcirculatory perfusate flow of the tumours was measured using laser doppler

flowmetry (LDF) (DRT4, Moor Instruments Limited, Axminister, UK). All outputs were fed into a commercial analogue-to-digital data acquisition recording system (ADC/MacLab, AD Instrument, Hastings, UK). The perfusion fluid was collected from the hepatic veins and returned to the reservoir by gravity. Circulating perfusate was oxygenated through a Maxima hollow-fibre oxygenator (Johnson & Johnson Cardiovascular, Division of McNeilab, Anaheim, CA, USA) with a mixture of 95% oxygen and 5% carbon dioxide. The pH, pO_2 and pCO_2 of the circulating perfusate were monitored at regular time intervals with an automatic blood gas, electrolyte and haematocrit analyser (BG Electrolytes System, Instrumentation Laboratory, Lexington, MA, USA), and corrections made accordingly to ensure constant physiological values. The temperature was kept constant at 37°C by keeping the reservoir within a heated water bath (Figure 9.1). The perfusate consisted of 1.5 L Krebs bicarbonate buffer (pH 7.4) containing 20% (vol./vol.) prewashed human Type O RBC's (obtained from Blood Transfusion Services), 20 gm/L BSA, 2 gm/L alpha 1-acid glycoprotein, 2.1 mmol/L calcium, and 5.5 mmol/L glucose (Villeneuve et al. 1990). The perfusate was supplemented with 7000 units of heparin. Liver viability was assessed by gross liver appearance, measuring HA and PV pressures, measuring alanine aminotransferase (ALT) levels of the perfusate using a standard clinical biochemistry autoanalyser (autoanalyser Hitachi 747 Autoanalyser, Boehringer Mannheim, Germany), and bile production (measured directly with a calibrated collection vessel).

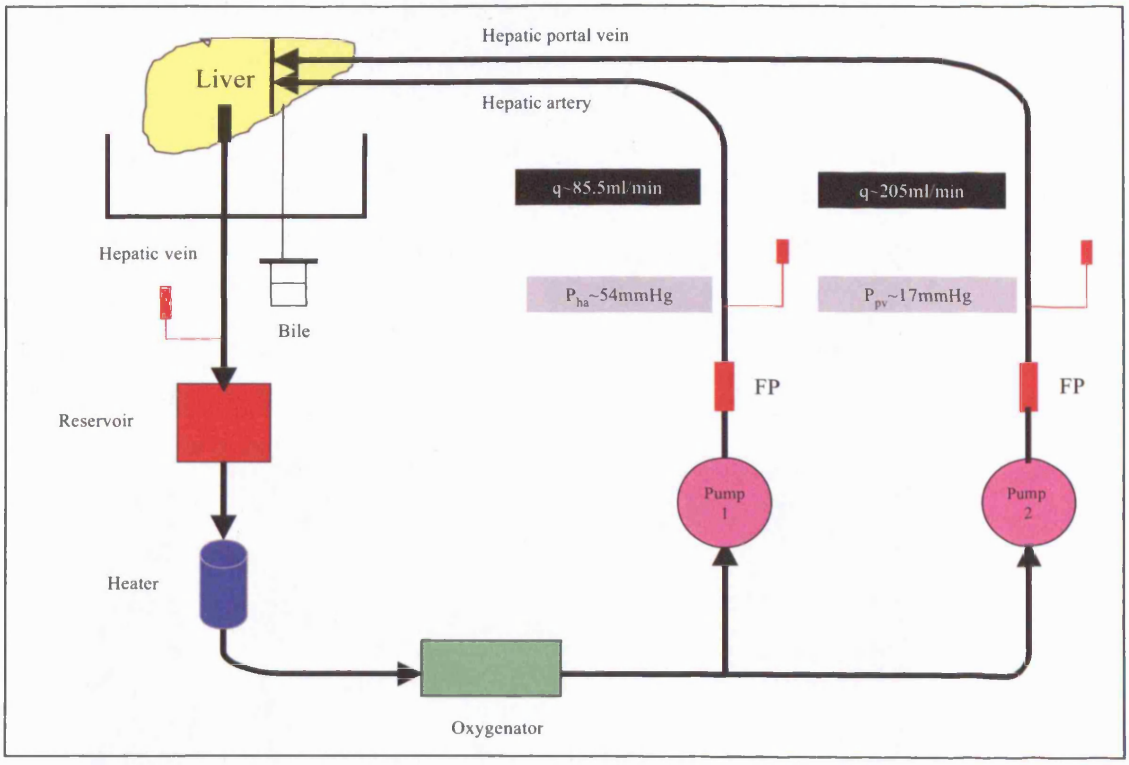

Figure 9.1. Extracorporeal perfusion circuit. FP, flow probe; P, pressure; q, flow; ivc, inferior vena cava; ha, hepatic artery; pv, portal vein.

At the end of each experiment the liver was perfused with 10% formalin and the specimen taken for histological examination. Sections were stained with haemotoxylin and eosin (H & E), and examined by light microscopy by an experienced histopathologist. Figure 9.2 demonstrates a typical perfused hemiliver.

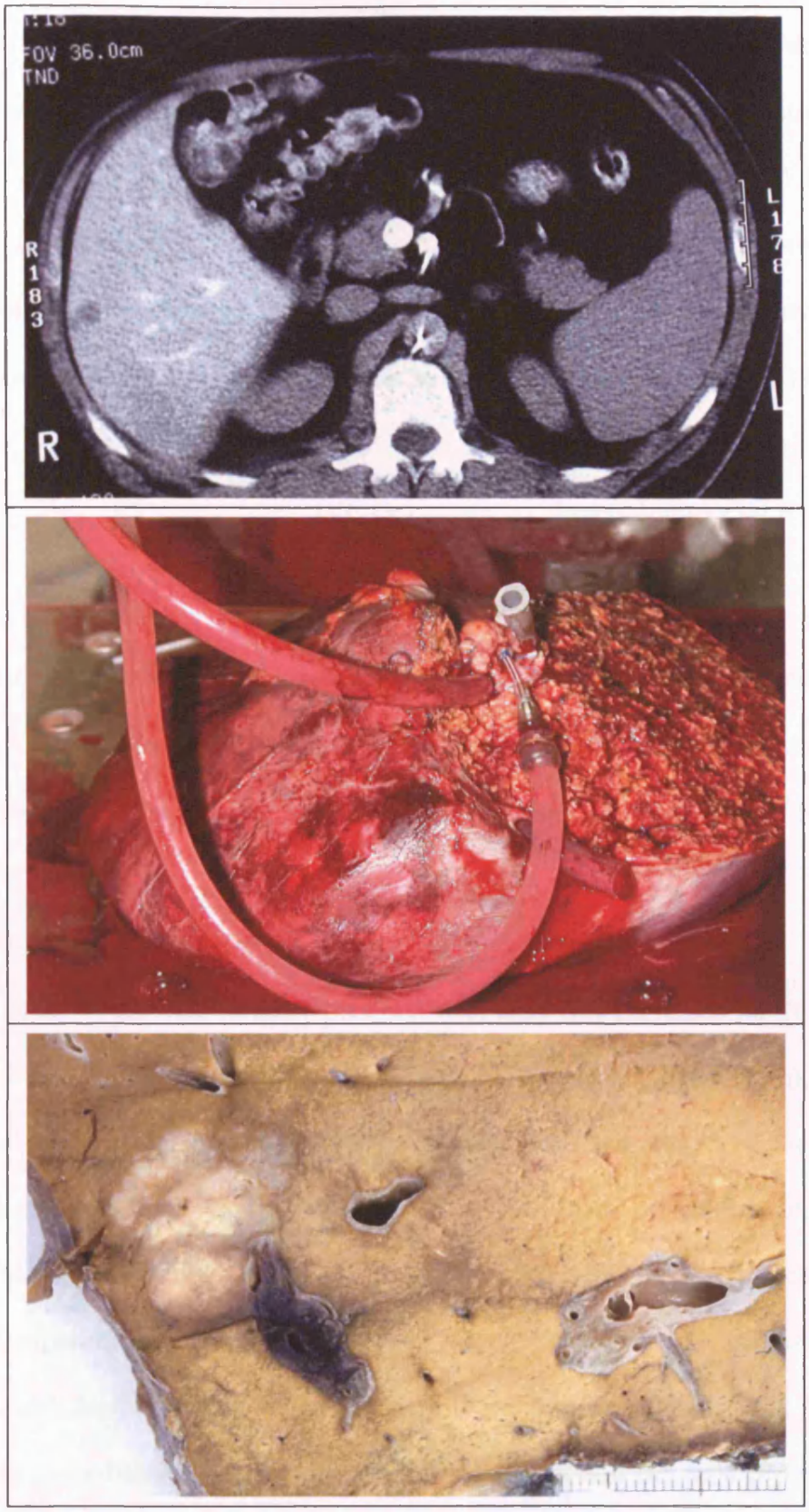

Figure 9.2. Control perfused hemiliver. **A.** Pre-operative CTScan demonstrating CRC metastases in segment VI. **B.** Hemiliver being perfused on perfusion apparatus. **C.** Macroscopic histological specimen demonstrating CRC metastases.

9.2.3 Analysis of spatial and temporal tumour drug induced DNA damage

One of the hemilivers was perfused with drug free perfusate as a control. As well as observing gross liver appearance, post perfusion histology, HA and PV pressures, ALT levels of the perfusate and bile production; FNA biopsies of tumour and wedge biopsies of normal liver were taken hourly to examine DNA integrity, and oxygen consumption (μM/min/g of liver) was calculated by (Mischinger et al, 1992):

$$\frac{\text{PV } O_2 \text{ content} - \text{IVC } O_2 \text{ content}}{100 \times \text{W (liver)}} \times \text{flow (ml/min)} \times 44.6$$

The normal liver wedge biopsies were reduced to a single cell suspension by finely mincing and filtering through a 30 μm nylon mesh, and then along with the procured FNA's frozen immediately in 1 ml RPMI, 10% foetal calf serum and 10% DMSO at –80°C.

The other livers were initially perfused with drug free perfusate for 20 min to allow stabilisation. Prior to initiation of cytotoxic perfusion (i.e. Time = 0 h), tumour FNA biopsies were obtained. The cytotoxic agent was then added to the recirculating perfusate. Three cytotoxics were used in total; cisplatin, etoposide, and mechlorethamine hydrochloride (nitrogen mustard [HN_2]), a single agent was used in each experiment. Tumour FNA biopsies were taken at 60 min intervals at accessible sites and depths depending on the size of the tumour studied. FNA biopsies were frozen immediately in 1 ml RPMI, 10% foetal calf serum and 10% DMSO at –80°C.

All samples were analysed using the comet assay (for details see Chapter II, Section 2.9). For the samples treated with alkylating agents one group was irradiated with 10

Gy using an X-ray source (dose rate 2.35 Gy/min) and the other group remained unirradiated. For the samples treated with etoposide this step was omitted and thus only one group analysed.

Statistical analysis

Results were expressed as mean ±SEM or SD. Statistical analysis of differences in perfusion characteristics with time were calculated using the two-tailed paired t-test. Comparison between percentage decrease in tail moment (TM) or TM with time and dose of each chemotherapeutic agent was calculated by one-way analysis of variance (ANOVA) followed by a post test for linear trend or the one-tailed unpaired t-test. Intra- and intertumour variability in percentage decrease in TM or TM with depth and site was calculated with either the unpaired t-test or one-way ANOVA followed by the Bonferroni multiple t-test when three or more groups were compared. Statistical significance was defined at $P < 0.05$.

Results

Table 9.1 summarises the clinicopathological characteristics of the 8 patients. Seven patients had moderately differentiated CRC metastases and had received between 4 and 6 cycles of pre-operative systemic chemotherapy with 5-FU and folinic acid. Two of those with CRC metastases presented with synchronous tumours, those with metachronous tumours had a mean disease free interval of 28.2 months (± SD 18.1). One patient had an HCC and had not received any pre-operative chemotherapy. A total of 13 tumours (12 CRC, 1 HCC) of median size 30 (range 20-85) mm were perfused in 8 hemilivers (1 left and 7 right).

Table 9.2 summarises the perfusion characteristics. Median perfusion time was 5 (range 4-6) h and median total perfusion flow 300 (range 110-420) ml/min, the HA contributing 35% (85.5 [range 35-190] ml/min) and PV 65% (205 [range 65-250] ml/min). Median microcirculatory perfusate flow of surface accessible tumours was 187 (range 155-207) flux units indicating perfusion and exposure to cytotoxic agents.

Figure 9.3 summarises the viability parameters of the hemiliver perfused with drug free perfusate as a control. It maintained a normal gross appearance, remaining homogenous in colour without evidence of white spots caused by air emboli or red spots due to nonhomogenous perfusion. Histological examination demonstrated minimal to no necrosis and preserved tissue structures of both tumour and normal liver. Microcirculatory perfusate flow and oxygen consumption values tended to decrease, whilst PV pressure, bile production and ALT levels of the perfusate tended to increase with time. Hepatic arterial pressures initially decreased then increased to values similar to those observed at the onset of perfusion. All values were solitary during a single experiment, thus statistical significance could not be calculated. The TMs of the control tumour and wedge biopsies of normal liver remained stable within the experiment with no statistically significant differences in values between 1 and 4 h ($P = 0.34$ and 0.1145 respectively) (Appendix 9.1).

Pt	Sex	Age (yr)	Hepatect -omy	Diagnosis	No.tumours/size (mm)	Tumour No.	Previous Chemotherapy	Liver metastases	Cytotoxic perfused
1	F	53	Right	CRC Mod. Diff.	2x (52 x 48 x 65) (31x 24 x 30)	1 & 2	5-FU/folinic acid	Synchronous	Cisplatin 23.3μM
2	M	51	Right	CRC Mod. Diff.	2x (20 x 20) (25 x 25)	3 & 4	5-FU/folinic acid	Synchronous	Cisplatin 50μM
3	M	64	Right	CRC Mod. Diff.	2x (42 x 37 x 32) (80 x 72 x 55)	5 & 6	5-FU/folinic acid	Metachronous	Cisplatin 100μM
4	M	58	Right	CRC Mod. Diff.	1x (85 x 75 x 75)	7	5-FU/folinic acid	Metachronous	Etoposide 50μM
5	M	55	Right	HCC	1x (80 x 75 x 50)	8	Nil	N/A	Etoposide 100μM
6	M	56	Right	CRC Mod. Diff.	1x (30 x 25 x 25)	9	5-FU/folinic acid	Metachronous	HN_2 50μM
7	M	57	Left	CRC Mod. Diff.	3x (24 x 24) (30 x 15) (25 x 25)	10, 11 & 12	5-FU/folinic acid	Metachronous	HN_2 100μM
8	M	51	Right	CRC Mod. Diff.	1x (25 x 23)	13	5-FU/folinic acid	Metachronous	Control

CRC, colorectal cancer; Mod. Diff., moderately differentiated adenocarcinoma; HN_2, nitrogen mustard.

Table 9.1. Patient clinicopathological characteristics.

Characteristics	Median	Range
Liver specimen weight (g)	749	678-1899
Duration of perfusion (h)	5	4-6
Total hepatic flow (ml/min)	300	110-420
Hepatic artery flow (ml/min)	85.5	35-190
Portal vein flow (ml/min)	205	65-250
Hepatic artery pressure (mmHg)	55	40-81
Portal vein pressure (mmHg)	17	9-24
Bile production (ml/hr)	4	3-6
ALT (IU/L)	250	71-464
Microcirculatory perfusate flow (flux)	187	155-207

ALT, alanine aminotransferase.

Table 9.2. Isolated Perfused Hemilivers: Perfusion Characteristics (n=8)

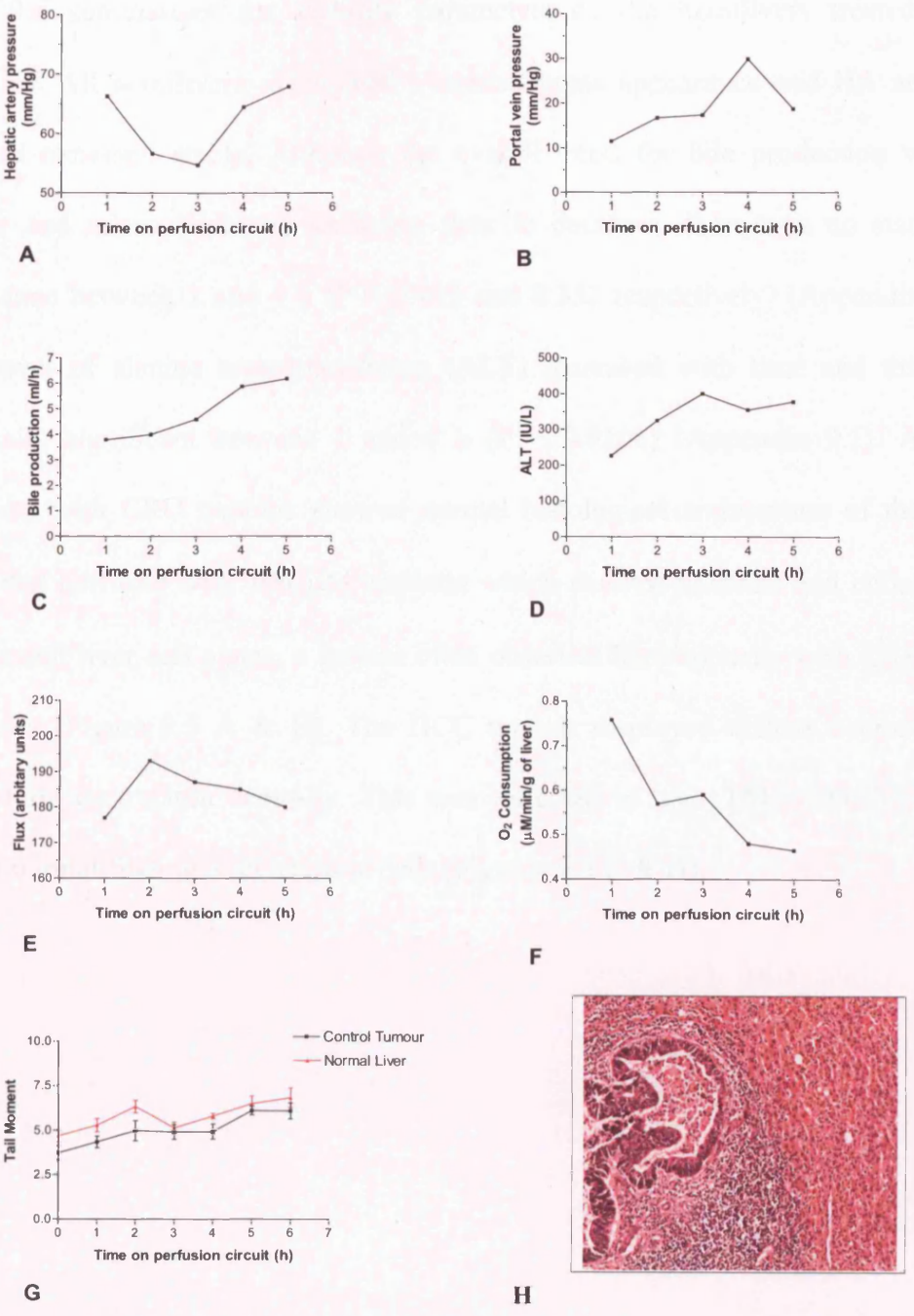

Figure 9.3. Viability parameters of the control liver and tumour whilst on the perfusion circuit. **A.** HA pressure, **B.** PV pressure, **C.** bile production, **D.** ALT levels of the perfusate, **E.** microcirculatory perfusate flow, **F.** O_2 consumption and **G.** TM as assessed by the comet assay of the control tumour and normal liver (values are a single measurement except **G.** where values are the mean ±SEM of 25 measurements and $P > 0.05$ between 1 and 4 h using the two-tailed paired t-test). **H.** Histology of control liver following 5 h of perfusion showing the infiltrative edge of the moderately differentiated CRC in the control hemiliver. There is some fibrosis and a moderate surrounding chronic inflammatory cell infiltrate with minimal to no necrosis and preserved tissue structure (high power view, x 10 objective lens).

Figure 9.4 summarises the viability parameters of the hemilivers treated with cytotoxics. All hemilivers maintained a normal gross appearance and HA and PV pressures remained stable. Although the overall trend for bile production was to increase and microcirculatory perfusate flow to decrease, there was no statistical significance between 1 and 4 h (P = 0.489 and 0.332 respectively) (Appendix 9.1). Mean level of alanine aminotransferase (ALT) increased with time and this was statistically significant between 1 and 4 h (P = 0.0108) (Appendix 9.1). All the hemilivers with CRC tumours showed normal histological architecture of the liver except that perfused with 100 μM cisplatin which showed necrosis and collapse of peritumoural liver cell plates, a feature often observed histologically with CRC liver metastases (Figure 9.5 A & B). The HCC tumour displayed diffuse necrosis and architectural destruction centrally. This was reflected in high TMs with the comet assay, a normal finding with necrotic cells (Figures 9.5 C & D).

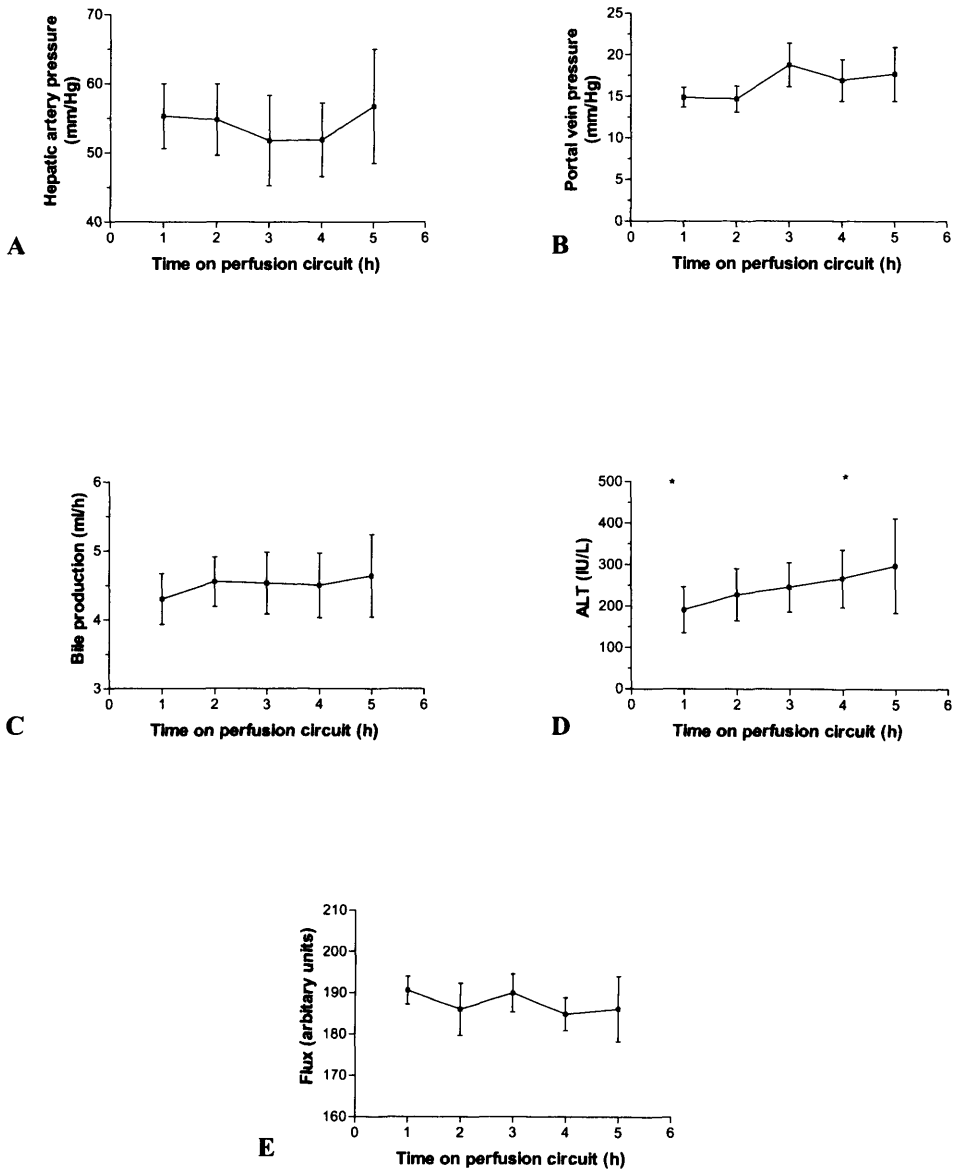

Figure 9.4. Viability of livers treated with chemotherapeutic agents whilst on the perfusion circuit was confirmed by stable **A.** hepatic artery and **B.** portal vein pressures, **C.** bile production, and **E.** microcirculatory perfusate flow (values are the mean [±SEM] of 7 [1-4 h] & 5 [5 h] individual experiments). $P > 0.05$ between 1 and 4 h using the two-tailed paired t-test. **D.** Mean ALT levels of the perfusate increased significantly between 1 and 4 h using the paired t-test (* $P = 0.0108$).

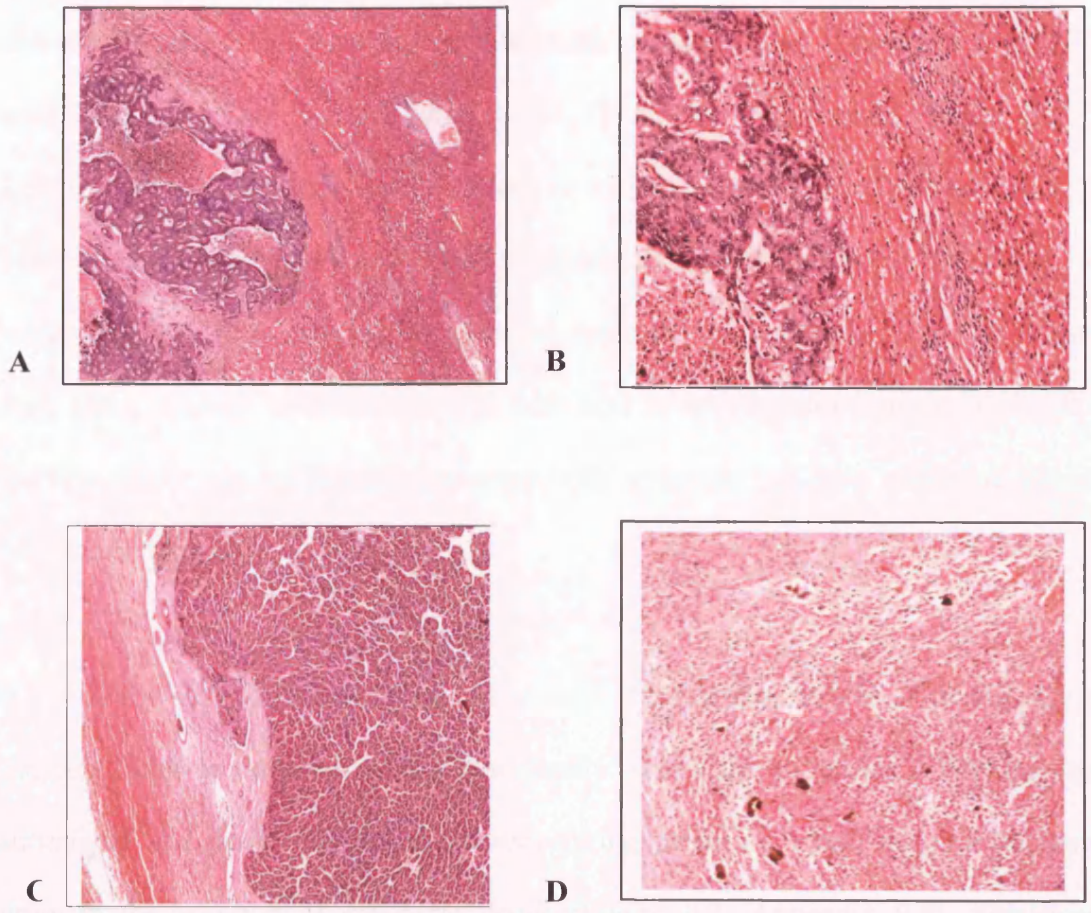

Figure 9.5. Abnormal histological findings post perfusion with cytotoxics. **A. & B.** Low and high power views (x 2.5 & x 10 objective lens) following 5 h of perfusion of the moderately differentiated CRC perfused with 100 μM cisplatin. Although the tumour remains well preserved there is extensive necrosis and collapse of the surrounding liver cell plates. **C. & D.** Low and high power views (x 2.5 & x 10 objective lens) following 5 h of perfusion of the HCC perfused with 100 μM etoposide. Superficially the HCC remained well-preserved (**C.**). There is both trabecular and microacinar architecture with an infiltrative edge and vascular invasion. At deeper levels (**D.**) the HCC tumour mass was necrotic with ghost outlines of trabecular structure and bile pigment.

Greater DNA damage was observed as the chemotherapeutic dose increased. This was statistically significant from 3 h onwards with cisplatin, at all timepoints except 3 h with etoposide and only 1 and 2 h with HN_2 (Figure 9.6, Appendices 9.5, 9.6 & 9.7). Differences were observed in the timing of maximal DNA damage of tumour cells between drugs during perfusion. Both etoposide and HN_2 had maximal effects at 1 h, whilst cisplatin demonstrated a gradual increase in DNA damage over 5 h (Figure 9.6). DNA damage increased linearly with time at all cisplatin concentrations ($P < 0.0001$). There was no linear relationship with etoposide and HN_2 with time (Figure 9.6, Appendix 9.8).

All tumours were large enough to take samples at different depths. The majority of tumours failed to demonstrate any statistically significant difference in TM between superficial and deep portions of tumours during perfusion with drug free perfusate prior to the addition of cytotoxic drugs (Figure 9.7, Appendix 9.9). Significant differences, however, were noted between 0.5 and 2 cm in Tumour 6 ($P < 0.05$), 1 and 4 cm in Tumour 7 ($P < 0.05$), and between 0.5 and 1.5, 2 and 3 cm in the Tumour 8 ($P < 0.05$, < 0.001 and < 0.001 respectively (Figure 9.7, Appendix 9.9). In these tumours central necrosis was observed on histological examination at deeper portions of the tumours.

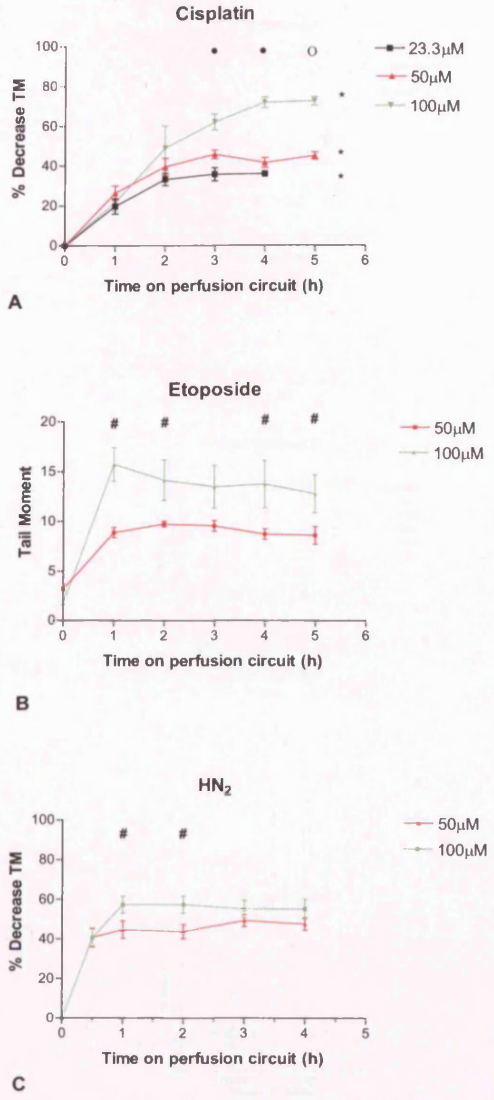

Figure 9.6. Effect of cytotoxic drugs on tumour DNA with time as assessed by the comet assay. Values are the mean (±SEM) of 6 (A. & B.) and 12 measurements (C.) at 0.5 & 1 cm.

* $P < 0.001$, linear trend with time with 23.3, 50 & 100 μM cisplatin (one-way ANOVA with post test for linear trend).

• $P < 0.001$, linear trend with concentration with 23.3, 50 & 100 μM cisplatin (one-way ANOVA with post test for linear trend).

o $P < 0.001$, between 50 & 100 μM cisplatin (one-tailed unpaired t-test).

# $P < 0.05$, between 50 & 100 μM etoposide and HN_2 (one-tailed unpaired t-test).

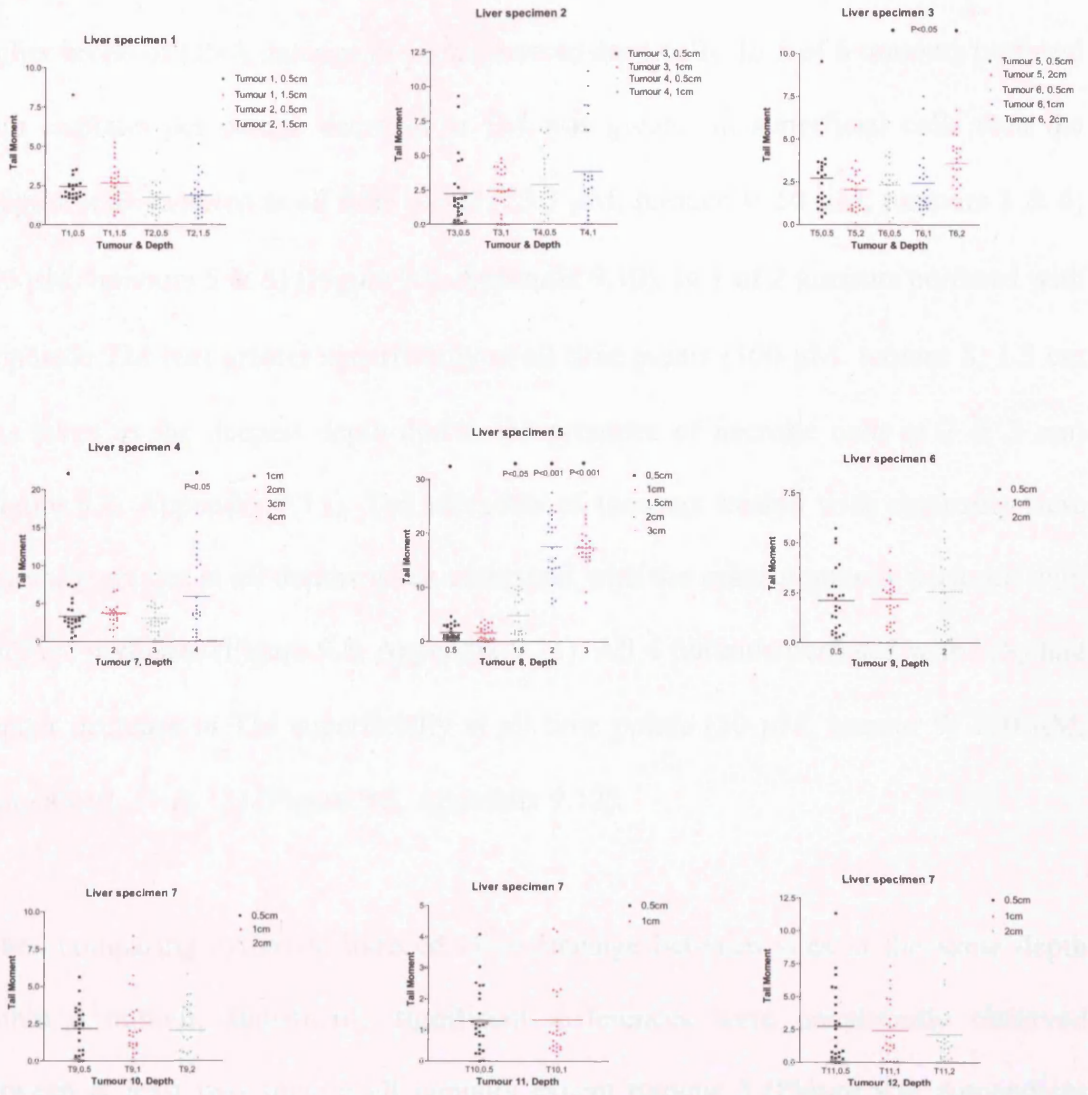

Figure 9.7. Tail moment of tumour samples at different depths prior to perfusion with cytoxic drugs (Time = 0 h) as assessed by the comet assay.

* two-tailed unpaired t-test.

• one-way ANOVA followed by the Bonferroni multiple t-test.

Once perfusion with cytotoxic drugs was commenced, superficial cells generally had higher levels of DNA damage in comparison to deep cells. In 5 of 6 tumours perfused with cisplatin percentage decrease in TM was greater in superficial cells than the deepest cells sampled at all time points (23.3 μM, tumour 1; 50 μM, tumours 3 & 4; 100 μM, tumours 5 & 6) (Figure 9.8, Appendix 9.10). In 1 of 2 tumours perfused with etoposide TM was greater superficially at all time points (100 μM, tumour 8; 1.5 cm was taken as the deepest depth due to the presence of necrotic cells at 2 & 3 cm) (Figure 9.8, Appendix 9.11). Tail moments of tumours treated with etoposide were generally greater at all depths when compared with the control tumour perfused with drug fee perfusate (Figure 9.8, Appendix 9.11). All 4 tumours perfused with HN_2 had greater decrease in TM superficially at all time points (50 μM, tumour 9; 100 μM, tumours 10, 11 & 12) (Figure 9.8, Appendix 9.12).

When comparing cytotoxic induced DNA damage between sites at the same depth within a tumour, statistically significant differences were consistently observed between at least two sites in all tumours except tumour 3 (Figure 9.9, Appendices 9.13, 9.14 & 9.15). Similar variability was also noted between tumours within the same hemiliver at the same depth. Statistically significant differences were noted between tumours 1 and 2 when perfused with 23.3 μM cisplatin, tumours 3 & 4 when perfused with 50 μM cisplatin, and tumours 10, 11 and 12 when perfused with 50 μM HN_2 (Figure 9.10, Appendices 9.16 & 9.17).

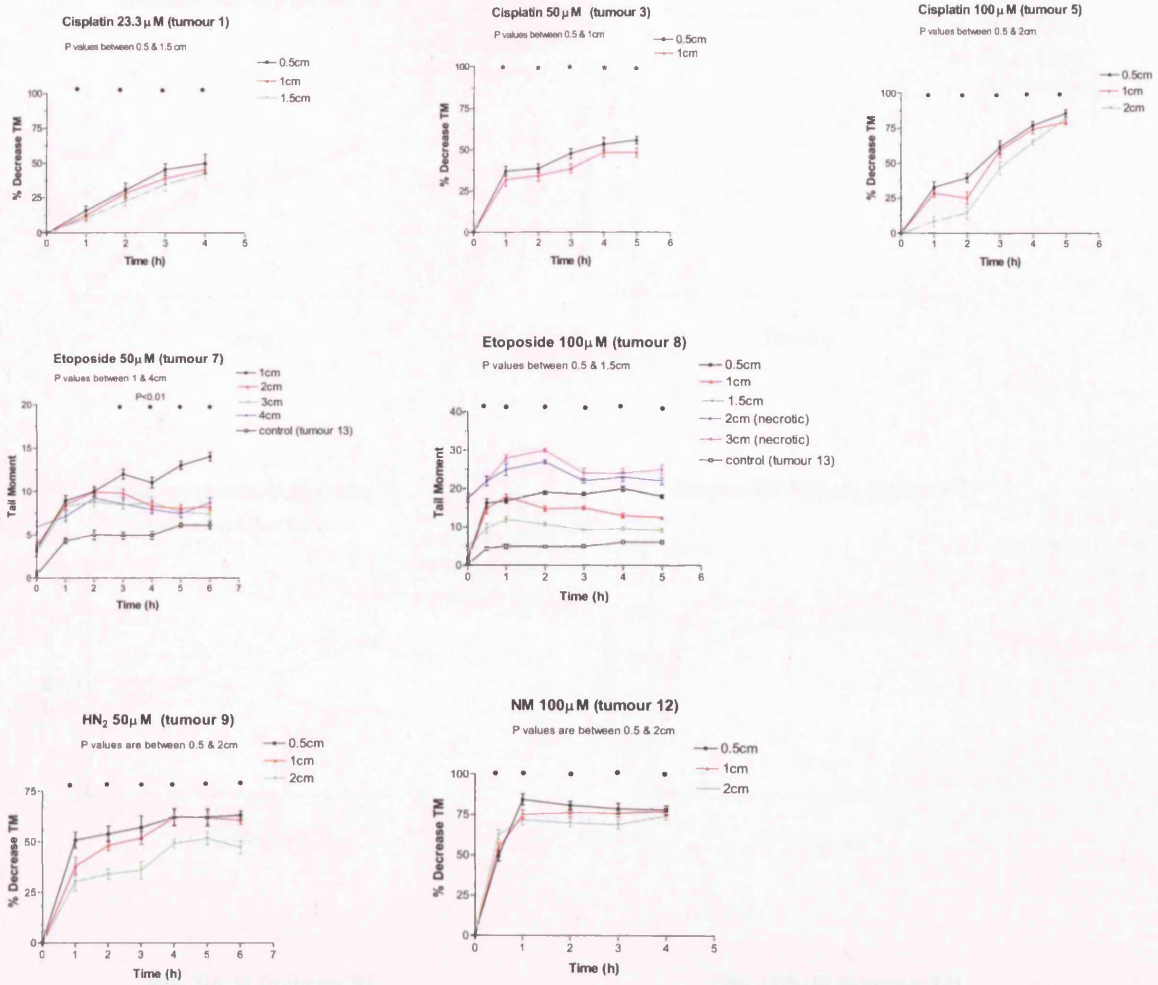

Figure 9.8. Examples of percentage decrease in Tail Moment/Tail Moment of the same tumour and site but different depths during perfusion with cytotoxic drugs as assessed by the comet assay. All values are from site A of the relevant tumours.

P values are between the most superficial and deepest tumour cells sampled.

• $P < 0.001$ (unless otherwise stated), one-way ANOVA followed by the Bonferroni multiple t-test

* $P < 0.0001$, two-tailed unpaired t-test.

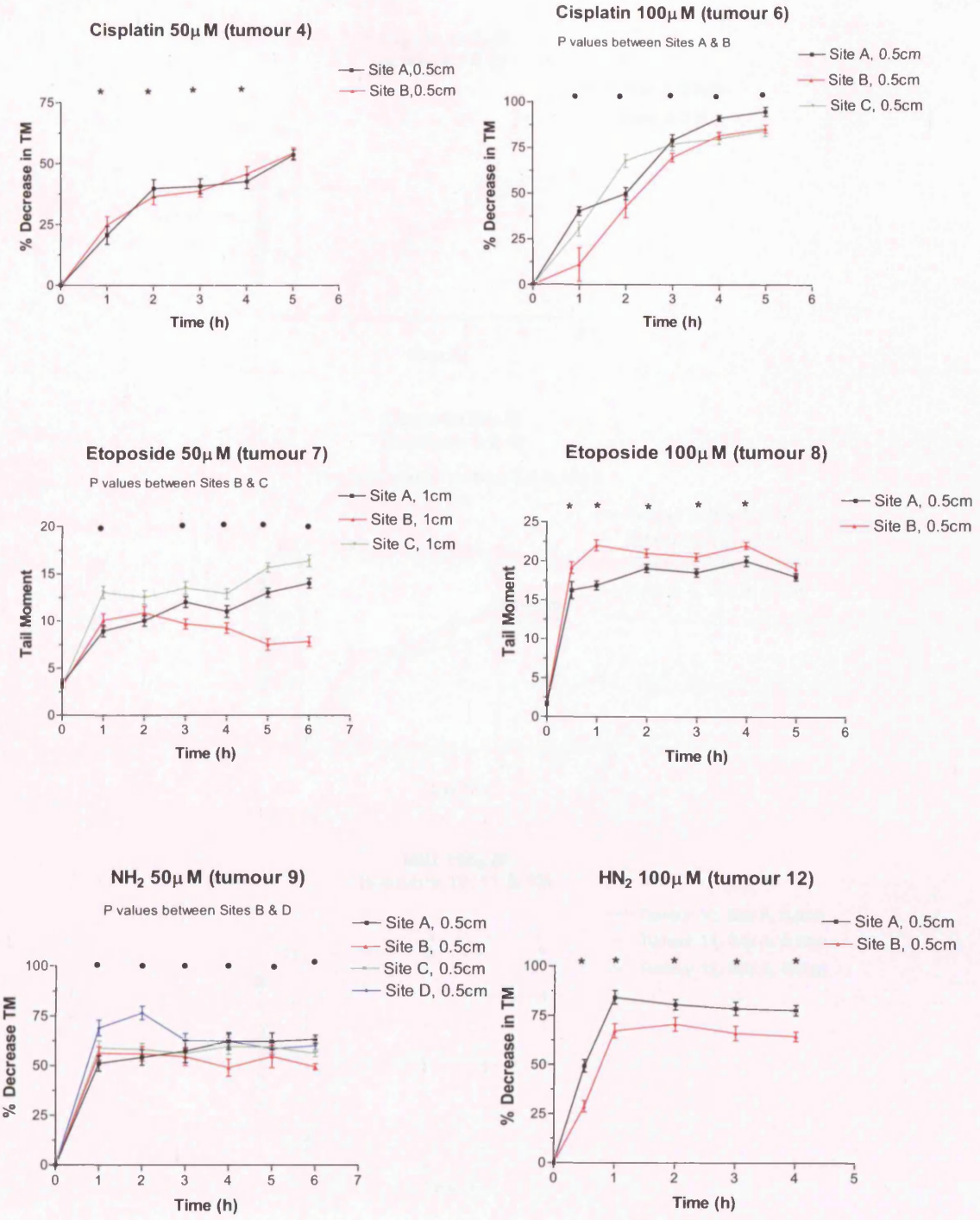

Figure 9.9. Examples of differences in percentage decrease in Tail Moment/ Tail Moment at the most superficial depth but different sites in the same tumour during perfusion with cytoxic drugs as assessed by the comet assay.

• $P < 0.05$, One-way ANOVA followed by the Bonferroni multiple t-test

* $P < 0.05$, two-tailed unpaired t-test.

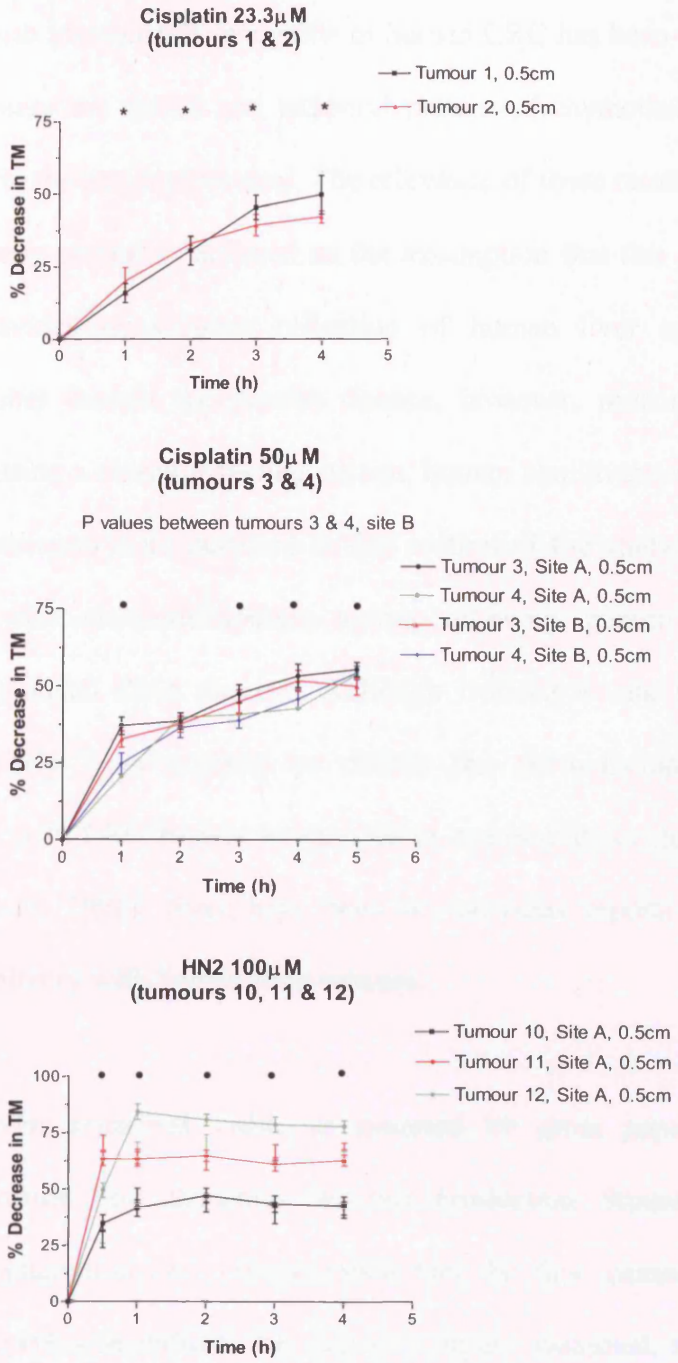

Figure 9.10. Examples of intertumour variation in percentage decrease in Tail Moment at the most superficial depth during perfusion with the same cytoxic drug as assessed by the comet assay.

• $P < 0.01$, One-way ANOVA followed by the Bonferroni multiple t-test.

* $P < 0.05$, two-tailed unpaired t-test.

9.3 Discussion

The IDPRL system with intrahepatic xenografts of human CRC has been shown to be a valuable tool to assess the spatial and temporal pattern of chemotherapy related cancer DNA damage in the previous chapter. The relevance of these results to clinical studies on chemotherapy responses is based on the assumption that this animal liver xenograft model provides an accurate reflection of human liver cancers. The comparability of animal models and human disease, however, remains uncertain (Perez, 1983). Thus, using a closed recycling system, human hemilivers with primary and secondary liver tumours were perfused in this section of the study for up to 6 hours and treated with chemotherapeutic agents allowing quantification and localisation of drug induced DNA damage. Although isolated *in situ* human liver perfusion has previously been reported to deliver the chemotherapeutic agent melphalan to patients with CRC hepatic metastases to examine its conjugation with GSH (Vahrmeijer et al, 1996), there have been no previous reports of *ex vivo* perfusion and drug delivery with human liver cancers.

The perfused hemilivers remained viable as assessed by gross appearance and histology, stable perfusion flow dynamics and bile production. Studies on organ preservation for transplantation have demonstrated that the flow characteristics of porcine livers during perfusion indicate the degree of injury sustained, in particular total hepatic and portal flow has been shown to inversely correlate with warm ischaemia time (Valero et al, 1998). Liver haemodynamic changes following liver resection have not been clearly defined. Rabinovici and Wiener demonstrated that liver blood flow per gram of liver increases immediately after partial hepatectomy *in vivo* and remains above preoperative levels for 24 h in the rat (Rabinovici and Wiener,

1963). It is appreciated that the HA perfusion pressures in this section of the study are lower than physiological values, this can be explained by the absence of sympathetic innervation. Previous studies have demonstrated that the addition of noradrenaline can restore perfusion pressures in IDPRLs to physiological levels (Yang et al, 1999). Bile production is a sensitive parameter of liver function. It requires an intact architecture of the liver sinusoid and hepatocyte (Jamieson et al, 1988; Sumimoto et al, 1988), and several dedicated metabolising steps which are energy dependent requiring adenosine-triphosphate (ATP). During ischaemia, the cellular ATP levels decrease, leading to reduced bile flow allowing the extent of hepatic injury to be assessed (Kamiike et al, 1985). The progressive rise in ALT in the perfusate during this study suggests hepatocyte injury. Using the isolated rat liver perfusion model, acid phosphatase, ALT, and aspartate aminotransferase (AST) were noted to correlate inversely with liver function during perfusion (Smrekova et al, 2000). In a further study high levels of AST, ALT, and lactate dehydrogenase in the effluent of cold-stored human liver grafts all predicted non-function (Lange et al, 1996). The perfused hemiliver will have undergone injury prior to removal during ligation of the hepatic vessels and hepatic resection (warm ischaemia); during transport from theatre to the laboratory (cold storage ischaemia); during ischaemic rewarming (warm ischaemia) and at reperfusion. However, this combined ischaemic injury is unlikely to have produced significant functional impairment. Perfusion of isolated porcine livers at 37°C for 3 h has demonstrated that basic liver function can be regained on a perfusion circuit after 75 min of circulatory arrest (Schon et al, 1993), and that 1 h of warm ischaemia followed by 24 h of normothermic perfusion can preserve liver function (St Peter et al, 2002).

The comet assay has been shown to be suitable for measuring DNA damage in cells obtained from FNA biopsies of treated tumours (Olive et al, 1993). Problems were anticipated as the result of constraints of sample size and mechanical damage to DNA on obtaining samples. However, adequate numbers of cells were obtained to perform the comet assay and minimal DNA damage was seen as reflected by the low mean TMs of tumour and normal liver throughout perfusion of the control hemiliver (Figure 9.3.G), and in tumours prior to perfusion with cytotoxics (Figure 9.7). There are inherent limitations to the use of the comet assay in this system. Only drugs that produce measurable quantities of DNA damage within 6 hours can be assessed, and such assessement can only be made in accessible tumours. In clinical practice, single drug administration is seldom used, this should not be a problem providing that DNA damage is produced by the combination chemotherapy.

The comet assays of the isolated perfused liver cancers demonstrated that DNA damage increased linearly with time at all cisplatin concentrations with peak levels being observed at 4-5 h at the end of each experiment. This correlates well with the previous *in vitro* and *in vivo* data obtained in this study and previous reports on the timing of DNA damage with cisplatin administration (Zwelling et al, 1978). Cell proliferation is an important determinant for cytotoxicity of cisplatin, with cells in active cell cycle being more susceptible to damage by cisplatin than quiescent cells in G_0 phase (Shalinsky et al, 1996). The assumed presence of proliferation thus provides further evidence of viability of the hemilivers whilst on the perfusion circuit.

In contrast, both etoposide, which produces double stranded breaks by interacting with DNA and the enzyme topoisomerase-II in proliferating cells (Huang et al, 1998),

and HN_2, an alkylating agent which forms a variety of adducts in both quiescent and proliferating cells (Webley et al, 2001), had maximal effects within an hour with no linear trend with time. Again this correlates well with the previous *in vitro* and *in vivo* data obtained in this study and previous reports on the timing of DNA damage with etoposide and HN_2 administration (Barret et al, 2000; Ross et al, 1978). Only two concentrations of these drugs were used, however, and these were physiologically high. Repeating the experiments with lower doses may have revealed a linear trend with time.

The majority of tumours demonstrated no statistically significant difference in TM between the most superficial and deepest depths studied prior to perfusion with cytotoxic drugs. Once perfusion with cytotoxics was commenced, however, tumours demonstrated more DNA damage at superficial levels, suggesting DNA damage is related to tumour vascularity and delivery of chemotherapeutic drugs rather than tumour biology. This correlates with autopsy studies of liver metastases which demonstrate a decrease in the number of tumour vessels in the centre of metastases (Lin et al, 1984), and the associated microenvironmental changes that are the result of inefficient vascular function (Sutherland, 1988). Considerable heterogeneity of DNA damage was found following perfusion at the same depth but different sites within the same tumour and between different tumours in the same hemiliver. This may reflect heterogeneity of drug delivery and distribution, tumour microenvironment or the multitude of molecular mechanisms that have been associated with intrinsic drug resistance. These observations underscore drug delivery as an important component of drug resistance.

The availability of resected human liver specimens offers an opportunity to study the heterogeneity of drug and DNA interaction secondary to differences in delivery and microenvironment, and the subsequent identification of populations of resistant tumour cells which can lead to treatment failure. A variety of short term *ex vivo* drug sensitivity tests have previously been developed to study cellular drug resistance in order to predict individual outcome in various neoplastic diseases. The avoidance of cell lines ensures relevance. These *ex vivo* assays, however, use tumour cell suspensions that cannot mimic the complexities of drug delivery, metabolism and excretion found clinically, thus affecting their ability to predict individual treatment outcome. As the perfusion model used in this section of the study involves solid tumours and permits easy exposure of the liver to different concentrations of test substances with repeated sampling, it may allow more precise prediction of outcome following chemotherapy. In addition, the concept of dynamic and transient changes in genetic expression in drug resistance is emerging as an important area for investigation. Despite perfusion time limitations, this model potentially allows the dynamic and transient changes in genetic expression involved in drug resistance, hypoxia, cell growth and apoptosis to be evaluated, contributing to a more detailed molecular understanding of acute gene regulation in response to chemotherapy. These issues are discussed in more detail in Chapter X.

CHAPTER X

CONCLUSIONS AND FUTURE DIRECTIONS

X. CONCLUSIONS AND FUTURE DIRECTIONS

Using FACScan analysis the expression of P-gp, MRP1 and LRP, along with the function of P-gp when present was studied in the chosen panel of HCC and CRC cell lines. The lack of functional P-gp when present, and the observation that there was no correlation of the presence of MRP1 and LRP with chemosensitivity, suggested these transport proteins had a limited role in resistance to these chemotherapy agents. It is likely that additional drug mechanisms contribute to resistance of these tumours. Candidates include other members of the MDR P-gp family which have recently been characterised. For example, MDR3, a phospholipid flippase, and a bile salt export pump, called sister of P-glycoprotein (SPGP), are expressed in hepatocytes under physiological conditions and play an important role in bile formation and excretion of various toxic substances, including drugs and their metabolites (Borst and Elferink, 2002) . MDR3 and SPGP expression has been demonstrated in human HCC, although they were expressed at low levels with a large variation between individual tumours (Zollner et al, 2005).

The current work has only examined expression of the founding member of the MRP family, MRP1. Recent work, however, has shown *MRP1* mRNA expression to be at least 10-fold lower than *MRP2* or *MRP3* mRNA expression in human HCC (Nies et al, 2001). Because of the similar substrate specificities of MRP1 and MRP2 (Konig et al, 1999), it has been suggested that MRP2 also confers drug resistance. This suggestion is supported by transfection of *MRP2* antisense RNA into HepG2 cells, which decreases MRP2 protein expression and increases sensitivity to cisplatin (Koike et al, 1997). MDR conferred by MRP2 has also been demonstrated in cells

expressing recombinant MRP2 (Cui et al, 1999). Similarly, resistance to etoposide and methotrexate conferred by MRP3 has been demonstrated after expression of recombinant MRP3 in human embryonic kidney 293 cells (Zeng et al, 1999). In addition, although this study suggests that GSH is an important component of MRP1-mediated MDR and drug transport, we have not specifically examined MRP1 function. Recently described is the 5-carboxyfluorescein diacetate (CFDA)/5-carboxyfluorescein (5-CF) efflux assay which has been used to study the functional activity of MRP (Lee and Piquette-Miller, 2001). In this assay, the nonfluorescent 5-CFDA passively diffuses into cells where it is converted to the fluorescent anion 5-CF by intracellular esterases. 5-CF effluxes from cells by the MRP family of transporters, and is not a substrate of P-gp. The identification of specific inhibitors of MRP-mediated transport function has been sought since the characterisation of the family. The most important inhibitors reported so far are analogues of cysteinyl leukotrienes, such as the leukotriene C_4 (LTC_4) analogue MK571. This analogue has so far been shown to inhibit MRP1 transport and to a lesser extent MRP2 transport (Buchler et al, 1996), MRP2 efflux function has also been shown to be reversibly inhibited by sulfinpyrazone and cyclosporin A (Morrow et al, 2000). Further studies to determine both the expression of the other members of the P-gp and MRP families, and the function of the MRP family would provide more understanding of intrinsic tumour drug resistance.

Rather than attempting to inhibit the function of MDR resistance efflux transporters, there has been recent interest in modulating their expression. Suppression of mRNA and protein expression of P-gp has been observed with subtoxic doses of the DNA cross-linking agents Mitomycin C and cisplatin (Ihnat et al, 1997). The pro-

inflammatory cytokines interleukin-6 (IL-6), interleukin-1β (IL-1β), and tumour necrosis factor-alpha (TNF-α), also cause significant down regulation in the expression and activity of MRP1, MRP3, and P-gp in the HCC cell lines HepG2 and HuH 7 (Lee and Piquette-Miller, 2003). These results merit further investigation and suggest the basis for novel clinical cancer chemotherapy regimens aimed at drug resistant tumours, where the MDR phenotype is modulated prior to treatment with cytotoxic agents.

In contrast to MDR secondary to increased drug export via P-gps and MRPs, insufficient drug uptake may also contribute to chemoresistance of HCC and CRC. Organic anion transporting proteins (OATPs) such as OATP2/SCL21A6 play an important role in drug absorption and regulation (Hagenbuch and Meier, 2003), increased expression of OATP2/SCL21A6 would thus lead to increased drug uptake into neoplastic cells. Hepatic uptake systems may represent an attractive target for chemotherapeutic agents of HCC and CRC metastases. Cisplatin covalently bound to bile acids have been proposed as a novel approach to provide specific drug targeting to the liver to overcome insufficient uptake into HCCs (Briz et al; 2002; Dominguez et al, 2001). The uptake of drugs bound to bile acids as carrier molecules would depend on preserved expression of the Na+/taurocholate co-transporter (NTCP/SLC10A1) and OATP2/SCL21A6 (Kullak-Ublick et al, 1997). Residual bile acid uptake has been shown to be detectable in HCC cells but at low levels in comparison to normal hepatocytes (Kullak-Ublick et al, 1996), this would favour the distribution of compound drugs to normal rather than malignant hepatocytes. However, there are only limited data on the expression of NTCP and

OATP2/SCL21A6 in HCCs, thus further studies are required to establish whether they would be a useful chemotherapeutic target.

The formation and excision of cisplatin DNA ICLs in the chosen human HCC and CRC cell lines were determined at the level of the overall genome by the comet assay, and related to platinum chemosensitivity. Resistant cell lines demonstrated quantitatively fewer ICLs than sensitive cell lines, and an increased capacity to repair those that were formed. The mechanism used by cells to repair ICLs is not clearly understood. As shown for classical nucleotide excision repair (NER), the ERCC1/XPF complex may interact with XPA to facilitate the repair of ICL. The mechanism may involve cooperation between NER and recombination, but outside of the classical context of NER. The fact that several types of DNA damage are recognised and repaired by NER has led to the search for inhibitors of this mechanism. XPA and ERCC1/XPF are potential targets, as these proteins are often found to be overexpressed in tumour cells resistant to cisplatin (Dabholkar et al, 1994; States and Reed, 1996). Furthermore, it has been suggested that the incision step, which involves XPA and ERCC1/XPF, is the rate-limiting step of NER (Barret et al, 1996). Thus, any inhibition of XPA or ERCC1/XPF should have the most efficient impact on NER.

To date the targeted inhibition of XPA by transfection with antisense XPA RNA has been shown to decrease *XPA* mRNA levels and sensitise human lung adenocarcinoma cells to cisplatin (Wu et al, 2003), and inhibition of NER by anti-XPA monoclonal antibodies has been achieved (Saijo et al, 2004). Detailed mechanistic studies, however, need to be performed to confirm any definite validity for this approach.

The fact that the final step of NER is DNA resynthesis has resulted in attempts to inhibit NER with antimetabolic drugs. For example, DNA polymerase inhibitors, such as aphidicolin (a selective inhibitor of DNA polymerase α and δ) and cytarabine have been tested in combination with several chemotherapeutic agents. While some of these combinations may prove to be clinically useful, such inhibitors cannot be considered true repair inhibitors. They are likely to affect DNA synthesis as well as DNA repair, and thus may affect normal cells as well as tumour cells. Similarly there has been considerable interest in modulating the sensitivity to bifunctional chemotherapeutic agents through activation or inactivation of various signal transduction cascades. Of the interactions studied to date, activation of the protein kinase C (Isonishi et al, 1994), EGF (Nishikawa et al, 1992), and HER-2/neu (Pietras et al, 1994) signal transduction pathways has been reported to decrease the repair of cisplatin-DNA adducts. However, the effects of these signal transduction pathways on DNA repair are relatively modest and are insufficient, by themselves, to explain the enhancement of cisplatin toxicity. Thus, while modulation of some signal transduction pathways may be useful for increasing tumour sensitivity to bifunctional chemotherapeutic agents, it appears that alteration of repair activity makes only a minor contribution to these interactions. Finally, replicative bypass appears to make a substantial contribution to the tolerance of unrepaired DNA adducts. Once the enzymatic mechanisms of replicative bypass are known in more detail, it should be possible to design inhibitors of replicative bypass that, along with more selective repair inhibitors, could increase the efficacy cisplatin.

The current study has successfully developed both murine and rat intrahepatic xenograft models of human HCC and CRC to study the topographic distribution of

chemotherapeutic agents within tumours. Although the malignant cells grew as solid tumours within a microenvironment similar to that seen clinically, tumour engraftment could not reliably be monitored. In addition, the animals had to be sacrificed after treatment in order to obtain samples. A model in which the human tumours contain a quantifiable marker permitting serial noninvasive monitoring of tumour burden would be an advantage. PLC/PRF/5 cells, which contain an integrated hepatitis B virus genome, secrete large amounts of HBsAg when growing as murine hepatic xenografts. HBsAg accumulates in the mouse's circulation and progressively increases over time. Tumour burden, as determined by wet weight, is proportional to serum HBsAg titre, and thus provides a noninvasive method for serially quantifying tumour burden at initiation of therapy and during chemotherapy (Leveille-Webster and Arias, 1996). HBsAg is an ideal circulating marker as it is rapidly secreted by tumour cells, is nonpathogenic, has a short half-life, and can be quantified by a highly sensitive reproducible RIA (Gupta et al, 1991). Similarly, nude mice with intrahepatically implanted human HCCs, have had their tumour size successfully evaluated with B-ultrasound from 2 to 9 weeks after implantation (Gao et al, 2004). A combination of these two procedures may enable FNAs to be taken from tumours in mice and rats, prior to chemotherapy to act as their own control, and sequentially thereafter, to avoid sacrificing the animals. Another consideration is that both the murine and rat intrahepatic xenograft models were originally derived from cell lines, therefore they do not necessarily reflect the original structure and biological behaviour of human tissue. Orthotopic implantation using intact human tissue obtained surgically has been described (Hoffman, 1994), adopting this technique with human HCC and CRC could further increase the relevance of these models.

This study has examined the topographic distribution of cisplatin DNA-adducts within tumours, and the potential mechanisms for drug heterogeneities, using the comet assay and by using different immunohistochemical stainings on parallel tissue sections. Immunohistochemical analysis by manual counting, however, is laborious and limited in scope. A sophisticated multi-step immunofluorescent staining and computer-controlled microscope scanning method has been developed, allowing simultaneous quanitative analysis of architectural patterns of proliferation, vascularisation, blood perfusion and oxygenation (Bussink et al, 1999). This allows quantitation of spatial relationships between these parameters in a tumour model, but does not provide temporal dynamics. Although useful for functional imaging, positron emission tomography, nuclear magnetic resonance, and ultrasound currently do not have the desired spatial resolution required to monitor events at a cellular level. Nuclear magnetic resonance microscopy can provide high-resolution structural information, and limited functional imaging. The only noninvasive method currently available that provides both is *in vivo* microscopy. This approach has been used to provide data on red blood cell velocity, vessel diameter, density, permeability, and leucocyte-endothelial interactions human CRC hepatic xenografts of mice (Fukumura et al, 1997). A major limitation of this method is that the imaging is surface weighted (< 40μm). With the availability of multiphoton microscopy and novel probes, it now possible to image deeper in tissue (< 40μm) without significant loss of spatial resolution. It is also possible to adapt some of these techniques to a clinical setting. Until technology for deeper imaging is developed, these techniques should provide useful insight into mechanisms that contribute to heterogeneous distribution of drugs in tumours.

Using a closed recycling system, intrahepatic xenografts of human CRC in nude rats and human hemilivers with primary and secondary liver tumours, were perfused via the HA and PV, and treated with chemotherapeutic agents allowing quantification of drug induced DNA damage. Tumours show heterogeneity of genotype and phenotype, and such heterogeneity in HCC and CRC tumours almost certainly affects response to cytotoxic agents. Since the early 1980s a variety of short term *ex vivo* drug sensitivity tests have been developed to study cellular drug resistance in order to predict individual outcome in various neoplastic diseases. These tests aim to mimic the situation within the tumour accurately enough to examine issues of dose response, sequence and timing. The avoidance of cell lines ensures relevance, and the sensitivity of some of these methods allows large numbers of chemotherapeutic permutations to be tested with a small amount of material. The colorimetric methyl-thiazol-terazolium (MTT) assay has the advantage of its suitability for automation (Sargent and Taylor, 1989), but contamination of more than 30% of non-neoplastic cells may interfere with proper interpretation (Kaspers et al, 1994). The differential staining cytotoxicity (DiSC) assay is a dye exclusion test that is based on morphological differentiation between living and dead tumour and non-tumour cells by light microscopy (Bird et al, 1986), which enables more reliable detection of contamination by non-neoplastic cells. However, assessment of cell kill is labour intensive and subject to individual interpretation. Although recent technical advances have led to the introduction of the adenosine triphosphate-tumour chemosensitivity assay (ATP-TCA), which has relatively high evaluability rates with solid tumours (Andreotti et al, 1995), cellular assays have largely been ignored due to their overall low evaluabilty rates and technical problems, in particular infection. In addition, these *ex vivo* assays use tumour cell suspensions, which cannot mimic the complexities of drug delivery,

metabolism and excretion found clinically, thus affecting their ability to predict individual treatment outcome. As both perfusion models used in this study involve solid tumours and permit easy exposure of the liver to different concentrations of test substances with repeated sampling, they may allow more precise prediction of outcome following chemotherapy.

The concept of dynamic and transient changes in genetic expression in drug resistance is emerging as an important area for investigation. The overexpression of genes associated with the development and maintenance of drug resistance phenotypes has been attributed to the selection and subsequent clonal expansion of pre-existing drug resistant cells. Although several drugs, by virtue of their mutagenic properties, have been suggested to increase the frequency with which these subpopulations arise, the possibility that chemotherapeutics may actually induce drug-resistant variants has remained largely unexplored. A number of studies indicate that the expression of the *MDR1* gene can be rapidly and transiently induced in cultured cell lines (Hu et al, 1995; Tomida et al, 1995), and *in vivo* in human metastatic lung sarcoma (Abolhoda et al, 1999), when exposed to a variety of chemotherapeutic agents. Several genes are thought to be activated under hypoxic conditions, such as vascular endothelial growth factor (VEGF) (Levy et al, 1996), erythropoietin (Jelkmann and Hellwig-Burgel, 2001), and glycolytic enzymes (Hanahan and Folkman, 1996), which are transcriptionally regulated by hypoxia inducible factor 1α (HIF-1α). As an important factor in tumourigenesis and angiogenesis, HIF-1α overexpression is associated with an increased mortality and treatment failure in various cancers (Unruh et al, 2003). In addition, HIF-1α can regulate the *MDR1* gene (Comerford et al, 2002), and blocking the activity of HIF-1α can enhance the therapeutic efficacy of cancer immunotherapy

(Sun et al, 2001). A number of drugs have been developed with the aim of counteracting genetic changes leading to cancer. Several oncogenes make cell surface receptors through which growth factors exert their effects, these receptors can be targeted by antibodies and small-molecule drugs in order to block their activity. Other drugs seek to block oncogene products that transmit growth stimulatory signals inside cells, such as the protein produced by the *ras* oncogene. Most cancers have inactivating mutations in one or more of tumour-suppressor genes, these normally act to control cell growth. For example, the tumour suppressor *p*16 normally holds up cell division by blocking the activity of cyclin-dependent kinase 4 (CDK4), one of several enzymes called CDKs that propel cells through the cell cycle. A small-molecule inhibitor of CDK4 would replace the function of *p*16 restoring cell growth control. Other mutations of oncogenes and tumour-suppressor genes impair apoptosis, or programmed cell death, which serves to remove cells whose DNA has been damaged. These mutations not only allow damaged cells to avoid death, but also make cancer cells resistant to many chemotherapeutic drugs that work by triggering apoptosis. Efforts to repair apoptosis have included gene therapy to replace mutated *p*53 with normal copies of *p*53, a tumour-suppressor gene that plays a role in apoptosis and is defective in approximately 50% of human cancers. The function of the oncogene *bc*l-2, an inhibitor of apoptosis, can also be impaired with antisense nucleotides designed to prevent the protein from being made. Despite perfusion time limitations, both models used in this study will potentially allow the dynamic and transient changes in genetic expression involved in drug resistance, hypoxia, cell growth and apoptosis to be evaluated, contributing to a more detailed molecular understanding of acute gene regulation.

In conclusion, eventually it may be possible to exploit and manipulate tumour environments to produce preferential effects of therapeutic agents on tumours. It may also be possible to treat tumours with combined therapy modalities that are effective against specifically characterised subpopulations and heterogeneous environments, and to control or stabilise the heterogeneity in favourable directions, for example, differentiation or expression of antigens or receptors that can then be treated with specific agents.

References

Anonymous (1992a) Expectancy or primary chemotherapy in patients with advanced asymptomatic colorectal cancer: a randomized trial. Nordic Gastrointestinal Tumor Adjuvant Therapy Group. *J Clin Oncol* **10**, 904-911.

Anonymous (1992b) Modulation of fluorouracil by leucovorin in patients with advanced colorectal cancer: evidence in terms of response rate. Advanced Colorectal Cancer Meta-Analysis Project. *J Clin Oncol* **10**, 896-903.

Anonymous (1994) Predictive factors for long term prognosis after partial hepatectomy for patients with hepatocellular carcinoma in Japan. The Liver Cancer Study Group of Japan. *Cancer* **74**, 2772-2780.

Anonymous (1995a) Efficacy of adjuvant fluorouracil and folinic acid in colon cancer. International Multicentre Pooled Analysis of Colon Cancer Trials (IMPACT) investigators. *Lancet* **345**, 939-944.

Anonymous (1995b) Phase III randomized study of two fluorouracil combinations with either interferon alfa-2a or leucovorin for advanced colorectal cancer. Corfu-A Study Group. *J Clin Oncol* **13**, 921-928.

Anonymous (1995c) A comparison of lipiodol chemoembolization and conservative treatment for unresectable hepatocellular carcinoma. Groupe d'Etude et de Traitement du Carcinome Hepatocellulaire. *N Engl J Med* **332**, 1256-1261.

Anonymous (1996) Reappraisal of hepatic arterial infusion in the treatment of nonresectable liver metastases from colorectal cancer. Meta-Analysis Group in Cancer. *J Natl Cancer Inst* **88**, 252-258.

Anonymous (1998a) Efficacy of intravenous continuous infusion of fluorouracil compared with bolus administration in advanced colorectal cancer. Meta-analysis Group In Cancer. *J Clin Oncol* **16**, 301-308.

Anonymous (1998b) Tamoxifen in treatment of hepatocellular carcinoma: a randomised controlled trial. CLIP Group (Cancer of the Liver Italian Programme). *Lancet* **352**, 17-20.

Abolhoda, A., Wilson, A.E., Ross, H., Danenberg, P.V., Burt, M. and Scotto, K.W. (1999) Rapid activation of MDR1 gene expression in human metastatic sarcoma after in vivo exposure to doxorubicin. *Clin Cancer Res* **5**, 3352-3356.

Abrams, R.A., Cardinale, R.M., Enger, C., Haulk, T.L., Hurwitz, H., Osterman, F. and Sitzmann, J.V (1997). Influence of prognostic groupings and treatment results in the management of unresectable hepatoma: experience with Cisplatinum-based chemoradiotherapy in 76 patients. *Int J Radiat Oncol Biol Phys* **39**, 1077-1085.

Ackerman, N.B. (1974) The blood supply of experimental liver metastases. IV. Changes in vascularity with increasing tumor growth. *Surgery* **75**, 589-596.

Adam, R., Akpinar, E., Johann, M., Kunstlinger, F., Majno, P. and Bismuth, H. (1997) Place of cryosurgery in the treatment of malignant liver tumors. *Ann Surg* **225**, 39-8.

Adam, R., Avisar, E., Ariche, A., Giachetti, S., Azoulay, D., Castaing, D., Kunstlinger, F., Levi, F. and Bismuth, F. (2001) Five-year survival following hepatic resection after neoadjuvant therapy for nonresectable colorectal. *Ann Surg Oncol* **8**, 347-353.

Adson, M.A. and van Heerden, J.A. (1980) Major hepatic resections for metastatic colorectal cancer. *Ann Surg* **191**, 576-583.

Adson, M.A., van Heerden, J.A., Adson, M.H., Wagner, J.S. and Ilstrup, D.M. (1984) Resection of hepatic metastases from colorectal cancer. *Arch Surg* **119**, 647-651.

Ahmad, A.B., Bennett, P.N. and Rowland, M. (1984) Influence of route of hepatic administration on drug availability. *J Pharmacol Exp Ther* **230**, 718-725.

Alapetite, C., Wacheter, T., Sage, E. and Moustacchi, E. (1996) Use of the alkaline comet assay to detect DNA repair deficiencies in human fibroblasts exposed to UVC, UVB, UVA and gamma-rays. *Int J Radiat Biol* **69**, 359-369.

Alberts, S.R., Horvath, W.L., Sternfeld, W.C., Goldberg, R.M., Mahoney, M.R., Dakhil, S.R., Levitt, R., Rowland, K., Nair, S., Sargent, D.J. and Donohue, J.H. (2005) Oxaliplatin, Fluorouracil, and Leucovorin for Patients With Unresectable Liver-Only Metastases From Colorectal Cancer: A North Central Cancer Treatment Group Phase II Study. *J Clin Oncol* **23**, 9243-9249.

Alexander, B., Mathie, R.T., Ralevic, V. and Burnstock, G. (1992) An isolated dual-perfused rabbit liver preparation for the study of hepatic blood flow regulation. *J Pharmacol Toxicol Methods* **27**, 17-22.

Allen-Mersh, T.G., Earlam, S., Fordy, C., Abrams, K. and Houghton, J. (1994) Quality of life and survival with continuous hepatic-artery floxuridine infusion for colorectal liver metastases. *Lancet* **344**, 1255-1260.

Andreotti, P.E., Cree, I.A., Kurbacher, C.M., Hartmann, D.M., Linder, D., Harel, G., Gleiberman, I., Caruso, P.A., Ricks, S.H. and Untch, M. (1995) Chemosensitivity testing of human tumors using a microplate adenosine triphosphate luminescence assay: clinical correlation for cisplatin resistance of ovarian carcinoma. *Cancer Res* **55**, 5276-5282.

Andrews, P.A., Murphy, M.P. and Howell, S.B. (1985) Differential potentiation of alkylating and platinating agent cytotoxicity in human ovarian carcinoma cells by glutathione depletion. *Cancer Res* **45**, 6250-6253.

Andrews, P.A., Velury, S., Mann, S.C. and Howell, S.B. (1988) cis-Diamminedichloroplatinum(II) accumulation in sensitive and resistant human ovarian carcinoma cells. *Cancer Res* **48**, 68-73.

Andrews, P.A. and Howell, S.B. (1990) Cellular pharmacology of cisplatin: perspectives on mechanisms of acquired resistance. *Cancer Cells* **2**, 35-43.

Arrick, B.A. and Nathan, C.F. (1984) Glutathione metabolism as a determinant of therapeutic efficacy: a review. *Cancer Res* **44**, 4224-4232.

Ashraf, S., Loizidou, M., Crowe, R., Turmaine, M., Taylor, I. and Burnstock, G. (1997) Blood vessels in liver metastases from both sarcoma and carcinoma lack perivascular innervation and smooth muscle cells. *Clin Exp Metastasis* **15**, 484-498.

Auckland k and Nicalaynes G (1981) Interstitial fluid volume: local regulatory mechanisms. *Physiol Rev* **61**, 556-643.

Bader, P., Fuchs, J., Wenderoth, M., von Schweinitz, D., Niethammer, D. and Beck, J.F. (1998) Altered expression of resistance associated genes in hepatoblastoma xenografts incorporated into mice following treatment with adriamycin or cisplatin. *Anticancer Res* **18**, 3127-3132.

Bailly, J.D., Muller, C., Jaffrezou, J.P., Demur, C., Gassar, G., Bordier, C. and Laurent, G. (1995) Lack of correlation between expression and function of P-glycoprotein in acute myeloid leukemia cell lines. *Leukemia* **9**, 799-807.

Ballantyne, G.H. and Quin, J. (1993) Surgical treatment of liver metastases in patients with colorectal cancer. *Cancer* **71**, 4252-4266.

Barnes, K.M., Dickstein, B., Cutler, G.B.J., Fojo, T. and Bates, S.E. (1996) Steroid treatment, accumulation, and antagonism of P-glycoprotein in multidrug-resistant cells. *Biochemistry* **35**, 4820-4827.

Barret, J.M., Calsou, P., Laurent, G. and Salles, B. (1996) DNA repair activity in protein extracts of fresh human malignant lymphoid cells. *Mol Pharmacol* **49**, 766-771.

Barret, J.M. and Hill, B.T. (1998) DNA repair mechanisms associated with cellular resistance to antitumor drugs: potential novel targets. *Anticancer Drugs* **9**, 105-123.

Barret, J.M., Hill, B.T. and Olive, P.L. (2000) Characterization of DNA-strand breakage induced in V79 cells by F 11782, a catalytic inhibitor of topoisomerases. *Br J Cancer* **83**, 1740-1746.

Bates, S.E., Currier, S.J., Alvarez, M. and Fojo, A.T. (1992) Modulation of P-glycoprotein phosphorylation and drug transport by sodium butyrate. *Biochemistry* **31**, 6366-6372.

Baxter, L.T., Zhu, H., Mackensen, D.G., Butler, W.F. and Jain, R.K. (1995) Biodistribution of monoclonal antibodies: scale-up from mouse to human using a physiologically based pharmacokinetic model. *Cancer Res* **55**, 4611-4622.

Beaumont, P.O., Moore, M.J., Ahmad, K., Payne, M.M., Lee, C. and Riddick, D.S. (1998) Role of glutathione S-transferases in the resistance of human colon cancer cell lines to doxorubicin. *Cancer Res* **58**, 947-955.

Beck, W.T. (1990) Mechanisms of multidrug resistance in human tumor cells. The roles of P-glycoprotein, DNA topoisomerase II, and other factors. *Cancer Treat Rev* **17 Suppl A**, 11-20.

Beesley RP (1987) Hepatitis B virus. The major etiology of HCC. In: Fortner JC and Rhodes JE, (Eds.) *Accomplishment in cancer research*, pp. 80-106. Philadelphia: JP Lippincott.

Behrens, B.C., Hamilton, T.C., Masuda, H., Grotzinger, K.R., Whang-Peng, J., Louie, K.G., Knutsen, T., McKoy, W.M., Young, R.C. and Ozols, R.F. (1987) Characterization of a cis-diamminedichloroplatinum(II)-resistant human ovarian cancer cell line and its use in evaluation of platinum analogues. *Cancer Res* **47**, 414-418.

Bellamy, W.T. (1992) Prediction of response to drug therapy of cancer. A review of in vitro assays. *Drugs* **44**, 690-708.

Bengmark, S. and Hafstrom, L. (1969) The natural history of primary and secondary malignant tumors of the liver. I. The prognosis for patients with hepatic metastases from colonic and rectal carcinoma by laparotomy. *Cancer* **23**, 198-202.

Bengtsson, G., Carlsson, G., Hafstrom, L. and Jonsson, P.E. (1981) Natural history of patients with untreated liver metastases from colorectal cancer. *Am J Surg* **141**, 586-589.

Bhattacharya, S., Dhillon, A.P., Rees, J., Savage, K., Saada, J., Burroughs, A., Rolles, K. and Davidson, B. (1997) Small hepatocellular carcinomas in cirrhotic explant livers: identification by macroscopic examination and lipiodol localization. *Hepatology* **25**, 613-618.

Bird, M.C., Bosanquet, A.G., Forskitt, S. and Gilby, E.D. (1986) Semi-micro adaptation of a 4-day differential staining cytotoxicity (DiSC) assay for determining the in-vitro chemosensitivity of haematological malignancies. *Leuk Res* **10**, 445-449.

Bismuth, H., Adam, R., Levi, F., Farabos, C., Waechter, F., Castaing, D., Majno, P. and Engerran, L. (1996) Resection of nonresectable liver metastases from colorectal cancer after neoadjuvant chemotherapy. *Ann Surg* **224**, 509-520.

Bismuth, H., Majno, P.E. and Adam, R. (1999) Liver transplantation for hepatocellular carcinoma. *Semin Liver Dis* **19**, 311-322.

Blasiak, J., Kowalik, J., Malecka-Panas, E., Drzewoski, J. and Wojewodzka, M. (2000) DNA damage and repair in human lymphocytes exposed to three anticancer platinum drugs. *Teratog Carcinog Mutagen* **20**, 119-131.

Boesch, D., Gaveriaux, C., Jachez, B., Pourtier-Manzanedo, A., Bollinger, P. and Loor, F. (1991) In vivo circumvention of P-glycoprotein-mediated multidrug resistance of tumor cells with SDZ PSC 833. *Cancer Res* **51**, 4226-4233.

Borst, P. and Elferink, R.O. (2002) Mammalian ABC transporters in health and disease. *Annu Rev Biochem* **71**, 537-592.

Bosman, F.T., Havenith, M. and Cleutjens, J.P. (1985) Basement membranes in cancer. *Ultrastruct Pathol* **8**, 291-304.

Brechot, C., Pourcel, C., Louise, A., Rain, B. and Tiollais, P. (1980) Presence of integrated hepatitis B virus DNA sequences in cellular DNA of human hepatocellular carcinoma. *Nature* **286**, 533-535.

Brennan M, Taley R and San Diego E (1964) Critical analysis of 594 cancer patients treated with 5-FU. In: Platner A, (Ed.) *Proceedings of the International Symposium on Chemotherapy of Cancer*, pp. 118-119. New York: Elsevier.

Bresailer RS and Kim Ys (1993) Malignant neoplasms of the large bowel. In: Sleirenger MH and Fordtran JS, (Eds.) *Gastrointestinal Disease*, pp. 1447-1493. Philadelphia: WB Saunders.

Briz, O., Serrano, M.A., Rebollo, N., Hagenbuch, B., Meier, P.J., Koepsell, H. and Marin, J.J. (2002) Carriers involved in targeting the cytostatic bile acid-cisplatin derivatives cis-diammine-chloro-cholylglycinate-platinum(II) and cis-diammine-bisursodeoxycholate-platinum(II) toward liver cells. *Mol Pharmacol* **61**, 853-860.

Bronner, C.E., Baker, S.M., Morrison, P.T., Warren, G., Smith, L.G., Lescoe, M.K., Kane, M., Earabino, C., Lipford, J. and Lindblom, A. (1994) Mutation in the DNA mismatch repair gene homologue hMLH1 is associated with hereditary non-polyposis colon cancer. *Nature* **368**, 258-261.

Brown, M.R., Kohn, E.C. and Hutter, R.V. (2000) The new millennium: applying novel technology to the study of the cancer cell in situ. *Cancer* **88**, 2-5.

Browse, D.J., Benjamin, I.S. and Alexander, B. (1995) The transhepatic response to noradrenaline in the rabbit liver: the influence of arterioportal pressure gradient. *J Pharm Pharmacol* **47**, 317-323.

Bruix, J., Castells, A., Bosch, J., Feu, F., Fuster, J., Garcia-Pagan, J.C., Visa, J., Bru, C. and Rodes, J. (1996) Surgical resection of hepatocellular carcinoma in cirrhotic patients: prognostic value of preoperative portal pressure. *Gastroenterology* **111**, 1018-1022.

Buchler, M., Konig, J., Brom, M., Kartenbeck, J., Spring, H., Horie, T. and Keppler, D. (1996) cDNA cloning of the hepatocyte canalicular isoform of the multidrug resistance protein, cMrp, reveals a novel conjugate export pump deficient in hyperbilirubinemic mutant rats. *J Biol Chem* **271**, 15091-15098.

Burczynski, F.J., Luxon, B.A. and Weisiger, R.A. (1996) Intrahepatic blood flow distribution in the perfused rat liver: effect of hepatic artery perfusion. *Am J Physiol* **271**, G561-G567

Bussink, J., Kaanders, J.H., Rijken, P.F., Peters, J.P., Hodgkiss, R.J., Marres, H.A. and van der Kogel, A.J. (1999) Vascular architecture and microenvironmental parameters in human squamous cell carcinoma xenografts: effects of carbogen and nicotinamide. *Radiother Oncol* **50**, 173-184.

Butler, A.J., Rees, M.A., Wight, D.G., Casey, N.D., Alexander, G., White, D.J. and Friend, P.J. (2002) Successful extracorporeal porcine liver perfusion for 72 hr. *Transplantation* **73**, 1212-1218.

Cady, B., Stone, M.D., McDermott, W.V.J., Jenkins, R.L., Bothe, A.J., Lavin, P.T., Lovett, E.J. and Steele, G.D.J. (1992) Technical and biological factors in disease-free survival after hepatic resection for colorectal cancer metastases. *Arch Surg* **127**, 561-568.

Cady, B., Jenkins, R.L., Steele, G.D.J., Lewis, W.D., Stone, M.D., McDermott, W.V., Jessup, J.M., Bothe, A., Lalor, P., Lovett, E.J., Lavin, P. and Linehan, D.C. (1998) Surgical margin in hepatic resection for colorectal metastasis: a critical and improvable determinant of outcome. *Ann Surg* **227**, 566-571.

Cardoso, J.E., Gautreau, C., Jeyaraj, P.R., Patrzalek, D., Cherruau, B., Vaubourdolle, M., Legendre, C., Wroblewski, T. and Houssin, D. (1994) Augmentation of portal blood flow improves function of human cirrhotic liver. *Hepatology* **19**, 375-380.

Casciari, J.J., Sotirchos, S.V. and Sutherland, R.M. (1992) Variations in tumor cell growth rates and metabolism with oxygen concentration, glucose concentration, and extracellular pH. *J Cell Physiol* **151**, 386-394.

Castells, A., Bruix, J., Bru, C., Fuster, J., Vilana, R., Navasa, M., Ayuso, C., Boix, L., Visa, J. and Rodes, J. (1993) Treatment of small hepatocellular carcinoma in cirrhotic patients: a cohort study comparing surgical resection and percutaneous ethanol injection. *Hepatology* **18**, 1121-1126.

Cawkwell L and Quirke P (1996) The molecular biology and genetics of colorectal cancer. In: Williams NS, (Ed.) *Colorectal Cancer*, pp. 1-1. London: Churchill Livingstone.

Chaney, S.G. and Sancar, A. (1996) DNA repair: enzymatic mechanisms and relevance to drug response. *J Natl Cancer Inst* **88**, 1346-1360.

Chaplin, D.J. and Acker, B. (1987) The effect of hydralazine on the tumor cytotoxicity of the hypoxic cell cytotoxin RSU-1069: evidence for therapeutic gain. *Int J Radiat Oncol Biol Phys* **13**, 579-585.

Chaplin, D.J., Olive, P.L. and Durand, R.E. (1987) Intermittent blood flow in a murine tumor: radiobiological effects. *Cancer Res* **47**, 597-601.

Chauvier, D., Morjani, H. and Manfait, M. (2002a) Homocamptothecin-daunorubicin association overcomes multidrug-resistance in breast cancer MCF7 cells. *Breast Cancer Res Treat* **73**, 113-125.

Chauvier, D., Kegelaer, G., Morjani, H. and Manfait, M. (2002b) Reversal of multidrug resistance-associated protein-mediated daunorubicin resistance by camptothecin. *J Pharm Sci* **91**, 1765-1775.

Chen G, Hutler K.J. and Zeller W.J. (1992) Further characterisation of acquired resistance to cisplatin in a rat ovarian tumour cell line. *In J Oncol* **1**, 135-140.

Chen, M.F., Hwang, T.L., Jeng, L.B., Wang, C.S., Jan, Y.Y. and Chen, S.C. (1994) Postoperative recurrence of hepatocellular carcinoma. Two hundred five consecutive patients who underwent hepatic resection in 15 years. *Arch Surg* **129**, 738-742.

Chen, Y.N., Mickley, L.A., Schwartz, A.M., Acton, E.M., Hwang, J.L. and Fojo, A.T. (1990) Characterization of adriamycin-resistant human breast cancer cells which display overexpression of a novel resistance-related membrane protein. *J Biol Chem* **265**, 10073-10080.

Chou, Y.Y., Cheng, A.L. and Hsu, H.C. (1997) Expression of P-glycoprotein and p53 in advanced hepatocellular carcinoma treated by single agent chemotherapy: clinical correlation. *J Gastroenterol Hepatol* **12**, 569-575.

Chu, E., Zinn, S., Boarman, D. and Allegra, C.J. (1990) Interaction of gamma interferon and 5-fluorouracil in the H630 human colon carcinoma cell line. *Cancer Res* **50**, 5834-5840.

Chugani, D.C., Rome, L.H. and Kedersha, N.L. (1993) Evidence that vault ribonucleoprotein particles localize to the nuclear pore complex. *J Cell Sci* **106**, 23-29.

Chung, Y.H., Song, I.H., Song, B.C., Lee, G.C., Koh, M.S., Yoon, H.K., Lee, Y.S., Sung, K.B. and Suh, D.J. (2000) Combined therapy consisting of intraarterial cisplatin infusion and systemic interferon-alpha for hepatocellular carcinoma patients with major portal vein thrombosis or distant metastasis. *Cancer* **88**, 1986-1991.

Cleaver, J.E., Charles, W.C., McDowell, M.L., Sadinski, W.J. and Mitchell, D.L. (1995) Overexpression of the XPA repair gene increases resistance to ultraviolet radiation in human cells by selective repair of DNA damage. *Cancer Res* **55**, 6152-6160.

Cobourn, C.S., Makowka, L., Langer, B., Taylor, B.R. and Falk, R.E. (1987) Examination of patient selection and outcome for hepatic resection for metastatic disease. *Surg Gynecol Obstet* **165**, 239-246.

Cohen AM, Minsky BD and Schilisky RL (1993) Colon Cancer. In: DeVita VT, Hellman S and Rosenberg SA, (Eds.) *Cancer: principles and practice of oncology*, 4th edn. pp. 929-977. Philadelphia: Lipincott.

Cole, S.P., Sparks, K.E., Fraser, K., Loe, D.W., Grant, C.E., Wilson, G.M. and Deeley, R.G. (1994) Pharmacological characterization of multidrug resistant MRP-transfected human tumor cells. *Cancer Res* **54**, 5902-5910.

Cole S.P and Tannock I (2004) Drug resistance. In: Tannock I.F., Hill R.P., Bristow R and Harrington L, (Eds.) *The Basic Science of Oncology*, 4th edn. New York: McGraw-Hill.

Colleoni, M., Gaion, F., Liessi, G., Mastropasqua, G., Nelli, P. and Manente, P. (1994) Medical treatment of hepatocellular carcinoma: any progress? *Tumori* **80**, 315-326.

Collins, A.R. (1993) Mutant rodent cell lines sensitive to ultraviolet light, ionizing radiation and cross-linking agents: a comprehensive survey of genetic and biochemical characteristics. *Mutat Res* **293**, 99-118.

Colvin M and Chabner B.A (1990) Alkylating Agents. In: Chabner B.A and Collins J.M, (Eds.) *Cancer Chemotherapy*, pp. 276-313. Philadelphia: JB Lippincott Co.

Comerford, K.M., Wallace, T.J., Karhausen, J., Louis, N.A., Montalto, M.C. and Colgan, S.P. (2002) Hypoxia-inducible factor-1-dependent regulation of the multidrug resistance (MDR1) gene. *Cancer Res* **62**, 3387-3394.

Comper, W.D. and Laurent, T.C. (1978) Physiological function of connective tissue polysaccharides. *Physiol Rev* **58**, 255-315.

Crews, K.A., Kuhn, J.A., McCarty, T.M., Fisher, T.L., Goldstein, R.M. and Preskitt, J.T. (1997) Cryosurgical ablation of hepatic tumors. *Am J Surg* **174**, 614-617.

Cui, Y., Konig, J., Buchholz, J.K., Spring, H., Leier, I. and Keppler, D. (1999) Drug resistance and ATP-dependent conjugate transport mediated by the apical multidrug resistance protein, MRP2, permanently expressed in human and canine cells. *Mol Pharmacol* **55**, 929-937.

Cunningham, D., Zalcberg, J.R., Rath, U., Oliver, I., van Cutsem, E., Svensson, C., Seitz, J.F., Harper, P., Kerr, D. and Perez-Manga, G. (1996) Final results of a randomised trial comparing 'Tomudex' (raltitrexed) with 5-fluorouracil plus leucovorin in advanced colorectal cancer. "Tomudex" Colorectal Cancer Study Group. *Ann Oncol* **7**, 961-965.

Cunningham, D., Pyrhonen, S., James, R.D., Punt, C.J., Hickish, T.F., Heikkila, R., Johannesen, T.B., Starkhammar, H., Topham, C.A., Awad, L., Jacques, C. and Herait, P. (1998) Randomised trial of irinotecan plus supportive care versus supportive care alone after fluorouracil failure for patients with metastatic colorectal cancer. *Lancet* **352**, 1413-1418.

Curley, S.A., Roh, M.S., Chase, J.L. and Hohn, D.C. (1993) Adjuvant hepatic arterial infusion chemotherapy after curative resection of colorectal liver metastases. *Am J Surg* **166**, 743-746.

Dabholkar, M., Vionnet, J., Bostick-Bruton, F., Yu, J.J. and Reed, E. (1994) Messenger RNA levels of XPAC and ERCC1 in ovarian cancer tissue correlate with response to platinum-based chemotherapy. *J Clin Invest* **94**, 703-708.

Danks, M.K., Warmoth, M.R., Friche, E., Granzen, B., Bugg, B.Y., Harker, W.G., Zwelling, L.A., Futscher, B.W., Suttle, D.P. and Beck, W.T. (1993) Single-strand conformational polymorphism analysis of the M(r) 170,000 isozyme of DNA topoisomerase II in human tumor cells. *Cancer Res* **53**, 1373-1379.

de Brauw, L.M., Marinelli, A., van, d., V, Hermans, J., Tjaden, U.R., Erkelens, C. and de Bruijn, E.A. (1991) Pharmacological evaluation of experimental isolated liver perfusion and hepatic artery infusion with 5-fluorouracil. *Cancer Res* **51**, 1694-1700.

de Gramont, A., Vignoud, J. and Tournigand, C. (1995) Oxaliplatin with high dose folinic acid and 5-Fluorouracil 48 hour infusion in pre-treated metastatic colorectal cancer. *Abstract Book 8th European Cancer Conference (ECCO), Paris* 716 (Abstract)

de Gramont, A., Bosset, J.F., Milan, C., Rougier, P., Bouche, O., Etienne, P.L., Morvan, F., Louvet, C., Guillot, T., Francois, E. and Bedenne, L. (1997a) Randomized trial comparing monthly low-dose leucovorin and fluorouracil bolus with bimonthly high-dose leucovorin and fluorouracil bolus plus continuous infusion for advanced colorectal cancer: a French intergroup study. *J Clin Oncol* **15**, 808-815.

de Gramont, A., Vignoud, J., Tournigand, C., Louvet, C., Andre, T., Varette, C., Raymond, E., Moreau, S., Le Bail, N. and Krulik, M. (1997b) Oxaliplatin with high-dose leucovorin and 5-fluorouracil 48-hour continuous infusion in pretreated metastatic colorectal cancer. *Eur J Cancer* **33**, 214-219.

Dellian, M., Yuan, F., Trubetskoy, V.S., Torchilin, V.P. and Jain, R.K. (2000) Vascular permeability in a human tumour xenograft: molecular charge dependence. *Br J Cancer* **82**, 1513-1518.

Deurloo, M.J., Kop, W., van Tellingen, O., Bartelink, H. and Begg, A.C. (1991) Intratumoural administration of cisplatin in slow-release devices: II. Pharmacokinetics and intratumoural distribution. *Cancer Chemother Pharmacol* **27**, 347-353.

Diaz-Rubio E, Zaniboni A and Gastiabuni J (1996) Phase II multicentric trial of Oxaliplatin (L-OHP) as first line chemotherapy in metastatic colorectal cancer. *Proc Am Soc Clin Oncol* **15**, 207

Dilley, A.V., Dy, D.Y., Warlters, A., Copeland, S., Gillies, A.E., Morris, R.W., Gibb, D.B., Cook, T.A. and Morris, D.L. (1993) Laboratory and animal model evaluation of the Cryotech LCS 2000 in hepatic cryotherapy. *Cryobiology* **30**, 74-85.

Doci, R., Bignami, P., Bozzetti, F., Bonfanti, G., Audisio, R., Colombo, M. and Gennari, L. (1988) Intrahepatic chemotherapy for unresectable hepatocellular carcinoma. *Cancer* **61**, 1983-1987.

Dominguez, M.F., Macias, R.I., Izco-Basurko, I., de La Fuente, A., Pascual, M.J., Criado, J.M., Monte, M.J., Yajeya, J. and Marin, J.J. (2001) Low in vivo toxicity of a novel cisplatin-ursodeoxycholic derivative (Bamet-UD2) with enhanced cytostatic activity versus liver tumors. *J Pharmacol Exp Ther* **297**, 1106-1112.

Donato, N., Dario, C., Giovanni, S., Virgilio, B., Paolo, D.P., Roberto, L., Gianfranco, P., Mario, L., Daniela, P. and Angelo, T. (1994) Retrospective study on adjuvant chemotherapy after surgical resection of colorectal cancer metastatic to the liver. *Eur J Surg Oncol* **20**, 454-460.

Dong, Z., Radinsky, R., Fan, D., Tsan, R., Bucana, C.D., Wilmanns, C. and Fidler, I.J. (1994) Organ-specific modulation of steady-state mdr gene expression and drug resistance in murine colon cancer cells. *J Natl Cancer Inst* **86**, 913-920.

Donnelly, E.T., Kelley, M. and Rockwell, S. (2004) Effects of RSR13 and oxygen on the cytotoxicity of cisplatin and carboplatin to EMT6 mouse mammary tumor cells in vitro and in vivo. *Cancer Chemother Pharmacol* **53**, 43-50.

Douple, E.B. and Richmond, R.C. (1979) Radiosensitization of hypoxic tumor cells by cis- and trans-dichlorodiammineplatinum (II). *Int J Radiat Oncol Biol Phys* **5**, 1369-1372.

Doyle, L.A., Yang, W., Abruzzo, L.V., Krogmann, T., Gao, Y., Rishi, A.K. and Ross, D.D. (1998) A multidrug resistance transporter from human MCF-7 breast cancer cells *Proc Natl Acad Sci USA* **95**, 15665-15670.

Duckett, D.R., Drummond, J.T., Murchie, A.I., Reardon, J.T., Sancar, A., Lilley, D.M. and Modrich, P. (1996) Human MutSalpha recognizes damaged DNA base pairs containing O6-methylguanine, O4-methylthymine, or the cisplatin-d(GpG) adduct. *Proc Natl Acad Sci USA* **93**, 6443-6447.

Dworkin, M.J. and Allen-Mersh, T.G. (1991) Regional infusion chemotherapy for colorectal hepatic metastases--where is it going? *Cancer Treat Rev* **18**, 213-224.

Eagle H. and Foley, G.E. (1956) The cytotoxic action of carcinolytic agents in tissue culture. *Am J Med* **21**, 739-749.

Eastman, A. and Schulte, N. (1988) Enhanced DNA repair as a mechanism of resistance to cis-diamminedichloroplatinum(II). *Biochemistry* **27**, 4730-4734.

Ebara, M., Ohto, M., Shinagawa, T., Sugiura, N., Kimura, K., Matsutani, S., Morita, M., Saisho, H., Tsuchiya, Y. and Okuda, K. (1986) Natural history of minute hepatocellular carcinoma smaller than three centimeters complicating cirrhosis. A study in 22 patients. *Gastroenterology* **90**, 289-298.

El-Serag, H.B. and Mason, A.C. (1999) Rising incidence of hepatocellular carcinoma in the United States. *N Engl J Med* **340**, 745-750.

Elias, D., Lasser, P., Rougier, P., Ducreux, M., Bognel, C. and Roche, A. (1995) Frequency, technical aspects, results, and indications of major hepatectomy after prolonged intra-arterial hepatic chemotherapy for initially unresectable hepatic tumors. *J Am Coll Surg* **180**, 213-219.

Ellis, A.G., Crinis, N.A. and Webster, L.K. (1996) Inhibition of etoposide elimination in the isolated perfused rat liver by Cremophor EL and Tween 80. *Cancer Chemother Pharmacol* **38**, 81-87.

Ensminger, W.D. and Gyves, J.W. (1983) Regional chemotherapy of neoplastic diseases. *Pharmacol Ther* **21**, 277-293.

Esteve J, Kricker A, Ferlay J and Parkis DM Lyons and International Agency for Research on Cancer, (Eds.) (1993) Facts and figures of cancer in the European Community.

Fairbairn, D.W., Olive, P.L. and O'Neill, K.L. (1995) The comet assay: a comprehensive review. *Mutat Res* **339**, 37-59.

Falcone, A., Allegrini, G., Masi, G., Lencioni, M., Pfanner, E., Brunetti, I., Danesi, R., Bocci, G., Del Tacca, M. and Conte, P. (2001) 5-fluorouracil administered as a 48-hour chronomodulated infusion in combination with leucovorin and cisplatin: a randomized phase II study in metastatic colorectal cancer. *Oncology* **61**, 28-35.

Falkson, G., Moertel, C.G., Lavin, P., Pretorius, F.J. and Carbone, P.P. (1978) Chemotherapy studies in primary liver cancer: a prospective randomized clinical trial. *Cancer* **42**, 2149-2156.

Falkson, G., Ryan, L.M., Johnson, L.A., Simson, I.W., Coetzer, B.J., Carbone, P.P., Creech, R.H. and Schutt, A.J. (1987) A random phase II study of mitoxantrone and cisplatin in patients with hepatocellular carcinoma. An ECOG study. *Cancer* **60**, 2141-2145.

Farinati, F., De Maria, N., Fornasiero, A., Salvagnini, M., Fagiuoli, S., Chiaramonte, M. and Naccarato, R. (1992) Prospective controlled trial with antiestrogen drug tamoxifen in patients with unresectable hepatocellular carcinoma. *Dig Dis Sci* **37**, 659-662.

Farmer, D.G., Rosove, M.H., Shaked, A. and Busuttil, R.W. (1994) Current treatment modalities for hepatocellular carcinoma. *Ann Surg* **219**, 236-247.

Fidler, I.J., Wilmanns, C., Staroselsky, A., Radinsky, R., Dong, Z. and Fan, D. (1994) Modulation of tumor cell response to chemotherapy by the organ environment. *Cancer Metastasis Rev* **13**, 209-222.

Fidler, I.J. (1995) Modulation of the organ microenvironment for treatment of cancer metastasis. *J Natl Cancer Inst* **87**, 1588-1592.

Finan, P.J., Marshall, R.J., Cooper, E.H. and Giles, G.R. (1985) Factors affecting survival in patients presenting with synchronous hepatic metastases from colorectal cancer: a clinical and computer analysis. *Br J Surg* **72**, 373-377.

Fink, D., Nebel, S., Aebi, S., Zheng, H., Cenni, B., Nehme, A., Christen, R.D. and Howell, S.B. (1996) The role of DNA mismatch repair in platinum drug resistance. *Cancer Res* **56**, 4881-4886.

Fishel, R., Lescoe, M.K., Rao, M.R., Copeland, N.G., Jenkins, N.A., Garber, J., Kane, M. and Kolodner, R. (1993) The human mutator gene homolog MSH2 and its association with hereditary nonpolyposis colon cancer. *Cell* **75**, 1027-1038.

Fong, Y., Cohen, A.M., Fortner, J.G., Enker, W.E., Turnbull, A.D., Coit, D.G., Marrero, A.M., Prasad, M., Blumgart, L.H. and Brennan, M.F. (1997) Liver resection for colorectal metastases. *J Clin Oncol* **15**, 938-946.

Fong, Y., Fortner, J., Sun, R.L., Brennan, M.F. and Blumgart, L.H. (1999) Clinical score for predicting recurrence after hepatic resection for metastatic colorectal cancer: analysis of 1001 consecutive cases. *Ann Surg* **230**, 309-318.

Ford, J.M. and Hait, W.N. (1990) Pharmacology of drugs that alter multidrug resistance in cancer. *Pharmacol Rev* **42**, 155-199.

Fossum, S., Smith, M.E., Bell, E.B. and Ford, W.L. (1980) The architecture of rat lymph nodes. III. The lymph nodes and lymph-borne cells of the congenitally athymic nude rat (rnu). *Scand J Immunol* **12**, 421-432.

Foster, G.R., Goldin, R.D., Main, J., Murray-Lyon, I., Hargreaves, S. and Thomas, H.C. (1997) Management of chronic hepatitis C: clinical audit of biopsy based management algorithm. *BMJ* **315**, 453-458.

Fram, R.J., Woda, B.A., Wilson, J.M. and Robichaud, N. (1990) Characterization of acquired resistance to cis-diamminedichloroplatinum (II) in BE human colon carcinoma cells. *Cancer Res* **50**, 72-77.

Francini, G., Petrioli, R., Lorenzini, L., Mancini, S., Armenio, S., Tanzini, G., Marsili, S., Aquino, A., Marzocca, G. and Civitelli, S. (1994) Folinic acid and 5-fluorouracil as adjuvant chemotherapy in colon cancer. *Gastroenterology* **106**, 899-906.

Fraser, R., Bowler, L.M., Day, W.A., Dobbs, B., Johnson, H.D. and Lee, D. (1980) High perfusion pressure damages the sieving ability of sinusoidal endothelium in rat livers. *Br J Exp Pathol* **61**, 222-228.

Fraval, H.N., Rawlings, C.J. and Roberts, J.J. (1978) Increased sensitivity of UV-repair-deficient human cells to DNA bound platinum products which unlike thymine dimers are not recognized by an endonuclease extracted from Micrococcus luteus. *Mutat Res* **51**, 121-132.

Freireich, E.J., Gehan, E.A., Rall, D.P., Schmidt, L.H. and Skipper, H.E. (1966) Quantitative comparison of toxicity of anticancer agents in mouse, rat, hamster, dog, monkey, and man. *Cancer Chemother Rep* **50**, 219-244.

Fukumura, D., Yuan, F., Monsky, W.L., Chen, Y. and Jain, R.K. (1997) Effect of host microenvironment on the microcirculation of human colon adenocarcinoma. *Am J Pathol* **151**, 679-688.

Futscher, B.W., Abbaszadegan, M.R., Domann, F. and Dalton, W.S. (1994) Analysis of MRP mRNA in mitoxantrone-selected, multidrug-resistant human tumor cells. *Biochem Pharmacol* **47**, 1601-1606.

Gao, Y.S., Chen, X.P., Li, K.Y. and Wu, Z.D. (2004) Nude mice model of human hepatocellular carcinoma via orthotopic implantation of histologically intact tissue. *World J Gastroenterol* **10**, 3107-3111.

Gardemann, A., Strulik, H. and Jungermann, K. (1987) Nervous control of glycogenolysis and blood flow in arterially and portally perfused liver. *Am J Physiol* **253**, E238-E245

Garufi C, Brienza S and Bensmain MA (1995) Addition of Oxaliplatin to chronomodulated 5-Fluorouracil and folinic acid for reversal of acquired chemoresistance in patients with advanced colorectal cancer. *Proc Am Soc Clin Oncol* **14**, 446

Gascon-Barre, M., Huet, P.M., St-Onge-Brault, G., Brault, A. and Kassissia, I. (1988) Liver extraction of vitamin D3 is independent of its hepatic venous or arterial route of delivery. Studies in isolated-perfused rat liver preparations. *J Pharmacol Exp Ther* **245**, 975-981.

Gayowski, T.J., Iwatsuki, S., Madariaga, J.R., Selby, R., Todo, S., Irish, W. and Starzl, T.E. (1994) Experience in hepatic resection for metastatic colorectal cancer: analysis of clinical and pathologic risk factors. *Surgery* **116**, 703-710.

Gerweck, L.E. and Seetharaman, K. (1996) Cellular pH gradient in tumor versus normal tissue: potential exploitation for the treatment of cancer. *Cancer Res* **56**, 1194-1198.

Giachetti S, Zidani R and Perpoint B (1997) Phase III trial of 5-fluorouracil, folinic acid, with or without oxaliplatin in previously untreated patients with metastatic colorectal cancer. *Proc Am Soc Clin Oncol* **16**, 229a (Abstract)

Giacchetti, S., Brienza S and Focan C (1998) Contribution of second line oxaliplatin-chronomodulated 5-fluorouracil, folinic acid and surgery to survival in metastatic colorectal cancer patients. *Proc Am Soc Clin Oncol* **16**, 273a (Abstract)

Giacchetti, S., Itzhaki, M., Gruia, G., Adam, R., Zidani, R., Kunstlinger, F., Brienza, S., Alafaci, E., Bertheault-Cvitkovic, F., Jasmin, C., Reynes, M., Bismuth, H., Misset, J.L. and Levi, F. (1999) Long-term survival of patients with unresectable colorectal cancer liver metastases following infusional chemotherapy with 5-fluorouracil, leucovorin, oxaliplatin and surgery. *Ann Oncol* **10**, 663-669.

Giovanella, B.C., Stehlin, J.S., Wall, M.E., Wani, M.C., Nicholas, A.W., Liu, L.F., Silber, R. and Potmesil, M. (1989) DNA topoisomerase I--targeted chemotherapy of human colon cancer in xenografts. *Science* **246**, 1046-1048.

Gordon, N.L., Dawson, A.A., Bennett, B., Innes, G., Eremin, O. and Jones, P.F. (1993) Outcome in colorectal adenocarcinoma: two seven-year studies of a population. *BMJ* **307**, 707-710.

Gores, G.J., Kost, L.J. and LaRusso, N.F. (1986) The isolated perfused rat liver: conceptual and practical considerations. *Hepatology* **6**, 511-517.

Goto, S., Yoshida, K., Morikawa, T., Urata, Y., Suzuki, K. and Kondo, T. (1995) Augmentation of transport for cisplatin-glutathione adduct in cisplatin-resistant cancer cells. *Cancer Res* **55**, 4297-4301.

Gottesman, M.M. and Pastan, I. (1993) Biochemistry of multidrug resistance mediated by the multidrug transporter. *Annu Rev Biochem* **62**, 385-427.

Gottesman, M.M., Pastan, I. and Ambudkar, S.V. (1996) P-glycoprotein and multidrug resistance. *Curr Opin Genet Dev* **6**, 610-617.

Grady, W., Rajput, A., Myeroff, L. and Markowitz, S. (1997) What's new with RII? *Gastroenterology* **112**, 297-302.

Grant, C.E., Valdimarsson, G., Hipfner, D.R., Almquist, K.C., Cole, S.P. and Deeley, R.G. (1994) Overexpression of multidrug resistance-associated protein (MRP) increases resistance to natural product drugs. *Cancer Res* **54**, 357-361.

Grau, C. and Overgaard, J. (1988) Effect of cancer chemotherapy on the hypoxic fraction of a solid tumor measured using a local tumor control assay. *Radiother Oncol* **13**, 301-309.

Greco, F.A., Figlin, R., York, M., Einhorn, L., Schilsky, R., Marshall, E.M., Buys, S.S., Froimtchuk, M.J., Schuller, J., Schuchter, L., Buyse, M., Ritter, L., Man, A. and Yap, A.K. (1996) Phase III randomized study to compare interferon alfa-2a in combination with fluorouracil versus fluorouracil alone in patients with advanced colorectal cancer. *J Clin Oncol* **14**, 2674-2681.

Green, J.A., Vistica, D.T., Young, R.C., Hamilton, T.C., Rogan, A.M. and Ozols, R.F. (1984) Potentiation of melphalan cytotoxicity in human ovarian cancer cell lines by glutathione depletion. *Cancer Res* **44**, 5427-5431.

Griffith, K.D., Sugarbaker, P.H. and Chang, A.E. (1990) Repeat hepatic resections for colorectal metastases. *Surgery* **107**, 101-104.

Guerci, A., Merlin, J.L., Missoum, N., Feldmann, L., Marchal, S., Witz, F., Rose, C. and Guerci, O. (1995) Predictive value for treatment outcome in acute myeloid leukemia of cellular daunorubicin accumulation and P-glycoprotein expression simultaneously determined by flow cytometry. *Blood* **85**, 2147-2153.

Gugenheim, J., Baldini, E., Casaccia, M., Ouzan, D., Saint-Paul, M.C. and Mouiel, J. (1997) Hepatic resection and transplantation for hepatocellular carcinoma in patients with cirrhosis. *Gastroenterol Clin Biol* **21**, 590-595.

Gupta, S., Aragona, E., Vemuru, R.P., Bhargava, K.K., Burk, R.D. and Chowdhury, J.R. (1991) Permanent engraftment and function of hepatocytes delivered to the liver: implications for gene therapy and liver repopulation. *Hepatology* **14**, 144-149.

Gura, T. (1997) Systems for identifying new drugs are often faulty. *Science* **278**, 1041-1042.

Hagenbuch, B. and Meier, P.J. (2003) The superfamily of organic anion transporting polypeptides. *Biochim Biophys Acta* **1609**, 1-18.

Hanahan, D. and Folkman, J. (1996) Patterns and emerging mechanisms of the angiogenic switch during tumorigenesis. *Cell* **86**, 353-364.

Hande, K., Anthony, L., Hamilton, R., Bennett, R., Sweetman, B. and Branch, R. (1988) Identification of etoposide glucuronide as a major metabolite of etoposide in the rat and rabbit. *Cancer Res* **48**, 1829-1834.

Haratake, J. and Scheuer, P.J. (1990) An immunohistochemical and ultrastructural study of the sinusoids of hepatocellular carcinoma. *Cancer* **65**, 1985-1993.

Hart, S.M., Ganeshaguru, K., Scheper, R.J., Prentice, H.G., Hoffbrand, A.V. and Mehta, A.B. (1997) Expression of the human major vault protein LRP in acute myeloid leukemia. *Exp Hematol* **25**, 1227-1232.

Hartley, J.M., Spanswick, V.J., Gander, M., Giacomini, G., Whelan, J., Souhami, R.L. and Hartley, J.A. (1999a) Measurement of DNA cross-linking in patients on ifosfamide therapy using the single cell gel electrophoresis (comet) assay. *Clin Cancer Res* **5**, 507-512.

Hasan, F., Jeffers, L.J., De Medina, M., Reddy, K.R., Parker, T., Schiff, E.R., Houghton, M., Choo, Q.L. and Kuo, G. (1990) Hepatitis C-associated hepatocellular carcinoma. *Hepatology* **12**, 589-591.

Havlik, R., Jiao, L.R., Nicholls, J., Jensen, S.L. and Habib, N.A. (2002) Gene therapy for liver metastases. *Semin Oncol* **29**, 202-208.

Heiger-Bernays, W.J., Essigmann, J.M. and Lippard, S.J. (1990) Effect of the antitumor drug cis-diamminedichloroplatinum(II) and related platinum complexes on eukaryotic DNA replication. *Biochemistry* **29**, 8461-8466.

Heijn, M., Roberge, S. and Jain, R.K. (1999) Cellular membrane permeability of anthracyclines does not correlate with their delivery in a tissue-isolated tumor. *Cancer Res* **59**, 4458-4463.

Helmlinger, G., Yuan, F., Dellian, M. and Jain, R.K. (1997) Interstitial pH and pO2 gradients in solid tumors in vivo: high-resolution measurements reveal a lack of correlation. *Nat Med* **3**, 177-182.

Hemingway, D.M., Cooke, T.G., Chang, D., Grime, S.J. and Jenkins, S.A. (1991) The effects of intra-arterial vasoconstrictors on the distribution of a radiolabelled low molecular weight marker in an experimental model of liver tumour. *Br J Cancer* **63**, 495-498.

Hobbs, S.K., Monsky, W.L., Yuan, F., Roberts, W.G., Griffith, L., Torchilin, V.P. and Jain, R.K. (1998) Regulation of transport pathways in tumor vessels: role of tumor type and microenvironment. *Proc Natl Acad Sci USA* **95**, 4607-4612.

Hochster, H.S., Green, M.D., Speyer, J., Fazzini, E., Blum, R. and Muggia, F.M. (1985) 4'Epidoxorubicin (epirubicin): activity in hepatocellular carcinoma. *J Clin Oncol* **3**, 1535-1540.

Hockel, M., Knoop, C., Schlenger, K., Vorndran, B., Baussmann, E., Mitze, M., Knapstein, P.G. and Vaupel, P. (1993) Intratumoral pO_2 predicts survival in advanced cancer of the uterine cervix. *Radiother Oncol* **26**, 45-50.

Hodgkiss, R.J., Jones, G., Long, A., Parrick, J., Smith, K.A., Stratford, M.R. and Wilson, G.D. (1991) Flow cytometric evaluation of hypoxic cells in solid experimental tumours using fluorescence immunodetection. *Br J Cancer* **63**, 119-125.

Hoffman, R.M. (1994) Orthotopic is orthodox: why are orthotopic-transplant metastatic models different from all other models? *J Cell Biochem* **56**, 1-3.

Holm, A., Bradley, E. and Aldrete, J.S. (1989) Hepatic resection of metastasis from colorectal carcinoma. Morbidity, mortality, and pattern of recurrence. *Ann Surg* **209**, 428-434.

Honjo, I., Suzuki, T., Ozawa, K., Takasan, H. and Kitamura, O. (1975) Ligation of a branch of the portal vein for carcinoma of the liver. *Am J Surg* **130**, 296-302.

Houghton, J.A., Adkins, D.A., Rahman, A. and Houghton, P.J. (1991) Interaction between 5-fluorouracil, [6RS] leucovorin, and recombinant human interferon-alpha 2a in cultured colon adenocarcinoma cells. *Cancer Commun* **3**, 225-231.

Hoy, C.A., Thompson, L.H., Mooney, C.L. and Salazar, E.P. (1985) Defective DNA cross-link removal in Chinese hamster cell mutants hypersensitive to bifunctional alkylating agents. *Cancer Res* **45**, 1737-1743.

Hu, X.F., Slater, A., Wall, D.M., Kantharidis, P., Parkin, J.D., Cowman, A. and Zalcberg, J.R. (1995) Rapid up-regulation of mdr1 expression by anthracyclines in a classical multidrug-resistant cell line. *Br J Cancer* **71**, 931-936.

Huang, P., Olive, P.L. and Durand, R.E. (1998) Use of the comet assay for assessment of drug resistance and its modulation in vivo. *Br J Cancer* **77**, 412-416.

Hughes, K.S., Simon, R., Songhorabodi, S., Adson, M.A., Ilstrup, D.M., Fortner, J.G., Maclean, B.J., Foster, J.H., Daly, J.M. and Fitzherbert, D. (1986) Resection of the liver for colorectal carcinoma metastases: a multi-institutional study of patterns of recurrence. *Surgery* **100**, 278-284.

Hughes, K., Scheele, J. and Sugarbaker, P.H. (1989) Surgery for colorectal cancer metastatic to the liver. Optimizing the results of treatment. *Surg Clin North Am* **69**, 339-359.

Huylesk, Scheele J, and Sugarbaker PH. (1989) Surgery for colorectal cancer metastatic to the liver. Surgical Clinics of North America **69**, 339-359.

Ihnat, M.A., Lariviere, J.P., Warren, A.J., La Ronde, N., Blaxall, J.R., Pierre, K.M., Turpie, B.W. and Hamilton, J.W. (1997) Suppression of P-glycoprotein expression and multidrug resistance by DNA cross-linking agents. *Clin Cancer Res* **3**, 1339-1346.

Ikeda, K., Saitoh, S., Koida, I., Tsubota, A., Arase, Y., Chayama, K. and Kumada, H. (1993) Diagnosis and follow-up of small hepatocellular carcinoma with selective intraarterial digital subtraction angiography. *Hepatology* **17**, 1003-1007.

Iliakis, G. (1991) The role of DNA double strand breaks in ionizing radiation-induced killing of eukaryotic cells. *Bioessays* **13**, 641-648.

Ishikawa, T. (1992) The ATP-dependent glutathione S-conjugate export pump. *Trends Biochem Sci* **17**, 463-468.

Ishikawa, T. and Ali-Osman, F. (1993) Glutathione-associated cis-diamminedichloroplatinum(II) metabolism and ATP-dependent efflux from leukemia cells. Molecular characterization of glutathione-platinum complex and its biological significance. *J Biol Chem* **268**, 20116-20125.

Ishikawa, T., Bao, J.J., Yamane, Y., Akimaru, K., Frindrich, K., Wright, C.D. and Kuo, M.T. (1996) Coordinated induction of MRP/GS-X pump and gamma-glutamylcysteine synthetase by heavy metals in human leukemia cells. *J Biol Chem* **271**, 14981-14988.

Isobe, H., Sakai, H., Imari, Y., Ikeda, M., Shiomichi, S. and Nawata, H. (1994) Intratumor ethanol injection therapy for solitary minute hepatocellular carcinoma. A study of 37 patients. *J Clin Gastroenterol* **18**, 122-126.

Isonishi, S., Hom, D.K., Eastman, A. and Howell, S.B. (1994) Enhancement of sensitivity to platinum(II)-containing drugs by 12-O-tetradecanoyl-phorbol-13-acetate in a human ovarian carcinoma cell line. *Br J Cancer* **69**, 217-221.

Isshiki, K., Nakao, A., Ito, M., Hamaguchi, M. and Takagi, H. (1993) P-glycoprotein expression in hepatocellular carcinoma. *J Surg Oncol* **52**, 21-25.

Itsubo, M. and Toda, G. (1996) Immunohistochemical study of expression of p-glycoprotein and mutant p53 protein in hepatocellular carcinoma from the viewpoint of modulation of transcriptional activity of MDR1 gene. *International Hepatology Communications* **5**, 317-325.

Iwatsuki, S. and Starzl, T.E. (1988) Personal experience with 411 hepatic resections. *Ann Surg* **208**, 421-434.

Izquierdo, M.A., van der Zee, A.G., Vermorken, J.B., van, Belien, J.A., Giaccone, G., Scheffer, G.L., Flens, M.J., Pinedo, H.M. and Kenemans, P. (1995) Drug resistance-associated marker Lrp for prediction of response to chemotherapy and prognoses in advanced ovarian carcinoma. *J Natl Cancer Inst* **87**, 1230-1237.

Izquierdo, M.A., Shoemaker, R.H., Flens, M.J., Scheffer, G.L., Wu, L., Prather, T.R. and Scheper, R.J. (1996) Overlapping phenotypes of multidrug resistance among panels of human cancer-cell lines. *Int J Cancer* **65**, 230-237.

Jahde, E., Glusenkamp, K.H., Klunder, I., Hulser, D.F., Tietze, L.F. and Rajewsky, M.F. (1989) Hydrogen ion-mediated enhancement of cytotoxicity of bis-chloroethylating drugs in rat mammary carcinoma cells in vitro. *Cancer* **49**, 2965-2972.

Jain, R.K. (1996) Delivery of molecular medicine to solid tumors. *Science* **271**, 1079-1080. Jain, R.K., Safabakhsh, N., Sckell, A., Chen, Y., Jiang, P., Benjamin, L., Yuan, F. and Keshet, E. (1998a) Endothelial cell death, angiogenesis, and microvascular function after castration in an androgen-dependent tumor: role of vascular endothelial growth factor. *Proc Natl Acad Sci USA* **95**, 10820-10825.

Jain, R.K., Safabakhsh, N., Sckell, A., Chen, Y., Jiang, P., Benjamin, L., Yuan, F. and Keshet, E. (1998) Endothelial cell death, angiogenesis, and microvascular function after castration in an androgen-dependent tumor: role of vascular endothelial growth factor. *Proc Natl Acad Sci USA* **95**, 10820-10825.

Jain, R.K. (1998) The next frontier of molecular medicine: delivery of therapeutics. *Nat Med* **4**, 655-657.

Jain, R.K. (1999) Understanding barriers to drug delivery: high resolution in vivo imaging is key. *Clin Cancer Res* **5**, 1605-1606.

Jamieson, N.V., Sundberg, R., Lindell, S., Southard, J.H. and Belzer, F.O. (1988) A comparison of cold storage solutions for hepatic preservation using the isolated perfused rabbit liver. *Cryobiology* **25**, 300-310.

Jelkmann, W. and Hellwig-Burgel, T. (2001) Biology of erythropoietin. *Adv Exp Med Biol* **502**, 169-187.

Johnson, S.W., Perez, R.P., Godwin, A.K., Yeung, A.T., Handel, L.M., Ozols, R.F. and Hamilton, T.C. (1994a) Role of platinum-DNA adduct formation and removal in cisplatin resistance in human ovarian cancer cell lines. *Biochem Pharmacol* **47**, 689-697.

Johnson, S.W., Swiggard, P.A., Handel, L.M., Brennan, J.M., Godwin, A.K., Ozols, R.F. and Hamilton, T.C. (1994b) Relationship between platinum-DNA adduct formation and removal and cisplatin cytotoxicity in cisplatin-sensitive and -resistant human ovarian cancer cells. *Cancer Res* **54**, 5911-5916.

Johnsson, A. and Cavallin-Stahl, E. (1996) A topographic study on the distribution of cisplatin in xenografted tumors on nude mice. *Anticancer Drugs* **7**, 70-77.

Kaklamani, E., Trichopoulos, D., Tzonou, A., Zavitsanos, X., Koumantaki, Y., Hatzakis, A., Hsieh, C.C. and Hatziyannis, S. (1991) Hepatitis B and C viruses and their interaction in the origin of hepatocellular carcinoma. *JAMA* **265**, 1974-1976.

Kalayoglu, M., Stratta, R.J., Sollinger, H.W., Hoffmann, R.M., D'Alessandro, A.M., Pirsch, J.D. and Belzer, F.O. (1989) Clinical results in liver transplantation using UW solution for extended preservation. *Transplant Proc* **21**, 1342-1343.

Kamada, N., Calne, R.Y., Wight, D.G. and Lines, J.G. (1980) Orthotopic rat liver transplantation after long-term preservation by continuous perfusion with fluorocarbon emulsion. *Transplantation* **30**, 43-48.

Kamiike, W., Nakahara, M., Nakao, K., Koseki, M., Nishida, T., Kawashima, Y., Watanabe, F. and Tagawa, K. (1985) Correlation between cellular ATP level and bile excretion in the rat liver. *Transplantation* **39**, 50-55.

Kardinal, C.G., Moertel, C.G., Wieand, H.S., Schutt, A.J., O'Connell, M.J., Wright, K., Wiesenfeld, M., Tschetter, L.K. and Krook, J.E. (1993) Combined doxorubicin and alpha-interferon therapy of advanced hepatocellular carcinoma. *Cancer* **71**, 2187-2190.

Kasahara, K., Fujiwara, Y., Nishio, K., Ohmori, T., Sugimoto, Y., Komiya, K., Matsuda, T. and Saijo, N. (1991) Metallothionein content correlates with the sensitivity of human small cell lung cancer cell lines to cisplatin. *Cancer Res* **51**, 3237-3242.

Kaspers, G.J., Veerman, A.J., Pieters, R., Broekema, G.J., Huismans, D.R., Kazemier, K.M., Loonen, A.H., Rottier, M.A., van Zantwijk, C.H. and Hahlen, K. (1994) Mononuclear cells contaminating acute lymphoblastic leukaemic samples tested for cellular drug resistance using the methyl-thiazol-tetrazolium assay. *Br J Cancer* **70**, 1047-1052.

Kassissia, I., Brault, A. and Huet, P.M. (1994) Hepatic artery and portal vein vascularization of normal and cirrhotic rat liver. *Hepatology* **19**, 1189-1197.

Kaufmen D and Chabner B.A. (1996) Clinical strategies for cancer treatment: the role of drugs. In: Chabner B.A. and Longo D.L., (Eds.) *Cancer Chemotherapy and Biotherapy*, 2nd edn. Philadelphia: Lippincott-Raven Publishers.

Kelland, L.R., Mistry, P., Abel, G., Freidlos, F., Loh, S.Y., Roberts, J.J. and Harrap, K.R. (1992a) Establishment and characterization of an in vitro model of acquired resistance to cisplatin in a human testicular nonseminomatous germ cell line. *Cancer Res* **52**, 1710-1716.

Kelland, L.R., Jones, M., Abel, G., Valenti, M., Gwynne, J. and Harrap, K.R. (1992b) Human ovarian-carcinoma cell lines and companion xenografts: a disease-oriented approach to new platinum anticancer drug discovery. *Cancer Chemother Pharmacol* **30**, 43-50.

Kemeny, N., Cohen, A., Bertino, J.R., Sigurdson, E.R., Botet, J. and Oderman, P. (1990) Continuous intrahepatic infusion of floxuridine and leucovorin through an implantable pump for the treatment of hepatic metastases from colorectal carcinoma. *Cancer* **65**, 2446-2450.

Kemeny, N., Adak S, Lipsitz S, Gray B and MacDonald J (1999a) Results of the Intergroup (Eastern Cooperative Oncology Group (ECOG) and Southwest Oncology Group (SWOG) prospective randomised study of surgery alone versus continuous hepatic artery infusion of FUDR and continuous systemic infusion of 5-FU after hepatic resection for colorectal liver metastases. *Am Soc Clin Oncol* **35**, A1012.

Kemeny, N., Huang, Y., Cohen, A.M., Shi, W., Conti, J.A., Brennan, M.F., Bertino, J.R., Turnbull, A.D., Sullivan, D., Stockman, J., Blumgart, L.H. and Fong, Y. (1999b) Hepatic arterial infusion of chemotherapy after resection of hepatic metastases from colorectal cancer. *N Engl J Med* **341**, 2039-2048.

Kemler, R. (1993) From cadherins to catenins: cytoplasmic protein interactions and regulation of cell adhesion. *Trends Genet* **9**, 317-321.

Kerr D (1997) Clinical efficacy of 'Tomudex' (Raltitrexed) in advanced colorectal cancer. *Anticancer Drugs* **S11-15** (Abstract).

Kickhoefer, V.A., Rajavel, K.S., Scheffer, G.L., Dalton, W.S., Scheper, R.J. and Rome, L.H. (1998) Vaults are up-regulated in multidrug-resistant cancer cell lines. *J Biol Chem* **273**, 8971-8974.

Kiehntopf, M., Brach, M.A., Licht, T., Petschauer, S., Karawajew, L., Kirschning, C. and Herrmann, F. (1994) Ribozyme-mediated cleavage of the MDR-1 transcript restores chemosensitivity in previously resistant cancer cells. *EMBO J* **13**, 4645-4652.

Kijosawa K, Sodeyuma T and Tanaka E (1990) Interrelationship of blood transfusion, non-A, non-B hepatitis and HCC: analysis by detection of antibody to hepatitis C virus. *Hepatology* **12**, 641-675.

Kim, D.K., Watson, R.C., Pahnke, L.D. and Fortner, J.G. (1977) Tumor vascularity as a prognostic factor for hepatic tumors. *Ann Surg* **185**, 31-34.

Kinami, Y., Takashima, S., Tanaka, T., Arizuka, S., Ashida, Y. and Miyazaki, I. (1985) Intra-arterial continuous infusion in patients with advanced and recurrent cancer of the digestive system. *Gan To Kagaku Ryoho* **12**, 1990-1998.

Kita, K., Itoshima, T. and Tsuji, T. (1991) Observation of microvascular casts of human hepatocellular carcinoma by scanning electron microscopy. *Gastroenterol Jpn* **26**, 319-328.

Kobayashi, H., Man, S., Graham, C.H., Kapitain, S.J., Teicher, B.A. and Kerbel, R.S. (1993) Acquired multicellular-mediated resistance to alkylating agents in cancer. *Proc Natl Acad Sci USA* **90**, 3294-3298.

Kohne, C.H., Schoffski, P., Wilke, H., Kaufer, C., Andreesen, R., Ohl, U., Klaasen, U., Westerhausen, M., Hiddemann, W., Schott, G., Harstick, A., Bade, J., Horster, A., Schubert, U., Hecker, H., Dorken, B. and Schmoll, H.J. (1998) Effective biomodulation by leucovorin of high-dose infusion fluorouracil given as a weekly 24-hour infusion: results of a randomized trial in patients with advanced colorectal cancer. *J Clin Oncol* **16**, 418-426.

Koike, K., Abe, T., Hisano, T., Kubo, T., Wada, M., Kohno, K. and Kuwano, M. (1996) Overexpression of multidrug resistance protein gene in human cancer cell lines selected for drug resistance to epipodophyllotoxins. *Jpn J Cancer Res* **87**, 765-772.

Koike, K., Kawabe, T., Tanaka, T., Toh, S., Uchiumi, T., Wada, M., Akiyama, S., Ono, M. and Kuwano, M. (1997) A canalicular multispecific organic anion transporter (cMOAT) antisense cDNA enhances drug sensitivity in human hepatic cancer cells. *Cancer Res* **57**, 5475-5479.

Konig, J., Nies, A.T., Cui, Y., Leier, I. and Keppler, D. (1999) Conjugate export pumps of the multidrug resistance protein (MRP) family: localization, substrate specificity, and MRP2-mediated drug resistance. *Biochim Biophys Acta* **1461**, 377-394.

Korbelik, M. and Skov, K.A. (1989) Inactivation of hypoxic cells by cisplatin and radiation at clinically relevant doses. *Radiat Res* **119**, 145-156.

Kotzampassi, K., Eleftheriadis, E. and Aletras, H. (1992) Experimental and clinical evaluation of capsular and parenchymal total liver perfusion. Liver microcirculation. *HPB Surg* **6**, 99-104.

Kramer, R., Weber, T.K., Morse, B., Arceci, R., Staniunas, R., Steele, G.J. and Summerhayes, I.C. (1993) Constitutive expression of multidrug resistance in human colorectal tumours and cell lines. *Br J Cancer* **67**, 959-968.

Kristjansen, P.E., Roberge, S., Lee, I. and Jain, R.K. (1994) Tissue-isolated human tumor xenografts in athymic nude mice. *Microvasc Res* **48**, 389-402.

Kristjansen, P.E., Brown, T.J., Shipley, L.A. and Jain, R.K. (1996) Intratumor pharmacokinetics, flow resistance, and metabolism during gemcitabine infusion in ex vivo perfused human small cell lung cancer. *Clin Cancer Res* **2**, 359-367.

Kullak-Ublick, G.A., Beuers, U. and Paumgartner, G. (1996) Molecular and functional characterization of bile acid transport in human hepatoblastoma HepG2 cells. *Hepatology* **23**, 1053-1060.

Kullak-Ublick, G.A., Glasa, J., Boker, C., Oswald, M., Grutzner, U., Hagenbuch, B., Stieger, B., Meier, P.J., Beuers, U., Kramer, W., Wess, G. and Paumgartner, G. (1997) Chlorambucil-taurocholate is transported by bile acid carriers expressed in human hepatocellular carcinomas. *Gastroenterology* **113**, 1295-1305.

Kunzelmann, K., Slotki, I.N., Klein, P., Koslowsky, T., Ausiello, D.A., Greger, R. and Cabantchik, Z.I. (1994) Effects of P-glycoprotein expression on cyclic AMP and volume-activated ion fluxes and conductances in HT-29 colon adenocarcinoma cells. *J Cell Physiol* **161**, 393-406.

Kuppen, P.J., Schuitemaker, H., van't Veer, L.J., de Bruijn, E.A., van Oosterom, A.T. and Schrier, P.I. (1988) cis-diamminedichloroplatinum(II)-resistant sublines derived from two human ovarian tumor cell lines. *Cancer Res* **48**, 3355-3359.

Labianca, R., Cascinu, S., Frontini, L., Barni, S., Fiorentini, G., Comella, G., Zaniboni, A., Gottardi, O., Arnoldi, E., Oliani, C., Duro, M., Pavanato, G., Martignoni, G., Raina, A., Piazza, E., Dallavalle, G., Valsecchi, R., Pancera, G. and Luporini, G. (1997) High-versus low-dose levo-leucovorin as a modulator of 5-fluorouracil in advanced colorectal cancer: a 'GISCAD' phase III study. Italian Group for the Study of Digestive Tract Cancer. *Ann Oncol* **8**, 169-174.

Lai, C.L., Lau, J.Y., Wu, P.C., Ngan, H., Chung, H.T., Mitchell, S.J., Corbett, T.J., Chow, A.W. and Lin, H.J. (1993) Recombinant interferon-alpha in inoperable hepatocellular carcinoma: a randomized controlled trial. *Hepatology* **17**, 389-394.

Lai, G.M., Ozols, R.F., Smyth, J.F., Young, R.C. and Hamilton, T.C. (1988) Enhanced DNA repair and resistance to cisplatin in human ovarian cancer. *Biochem Pharmacol* **37**, 4597-4600.

Lai, G.M., Chen, Y.N., Mickley, L.A., Fojo, A.T. and Bates, S.E. (1991) P-glycoprotein expression and schedule dependence of adriamycin cytotoxicity in human colon carcinoma cell lines. *Int J Cancer* **49**, 696-703.

Lalloo, A.K., Luo, F.R., Guo, A., Paranjpe, P.V., Lee, S.H., Vyas, V., Rubin, E. and Sinko, P.J. (2004) Membrane transport of camptothecin: facilitation by human P-glycoprotein (ABCB1) and multidrug resistance protein 2 (ABCC2). *BMC Med* **2**, 16

Lange, R., Erhard, J., Rauen, U., de Groot, H. and Eigler, F.W. (1996) Determination of hepatocellular enzymes in effluent of human liver grafts for preoperative evaluation of transplant quality. *Transplantation* **62**, 1255-1259.

Lankelma, J., Dekker, H., Luque, F.R., Luykx, S., Hoekman, K., van, d., V, van Diest, P.J. and Pinedo, H.M. (1999) Doxorubicin gradients in human breast cancer. *Clin Cancer Res* **5**, 1703-1707.

Larminat, F. and Bohr, V.A. (1994) Role of the human ERCC-1 gene in gene-specific repair of cisplatin-induced DNA damage. *Nucleic Acids Res* **22**, 3005-3010.

Laska, D.A., Houchins, J.O., Pratt, S.E., Horn, J., Xia, X., Hanssen, B.R., Williams, D.C., Dantzig, A.H. and Lindstrom, T. (2002) Characterization and application of a vinblastine-selected CACO-2 cell line for evaluation of p-glycoprotein. *In Vitro Cell Dev Biol Anim* **38**, 401-410.

Lautier, D., Canitrot, Y., Deeley, R.G. and Cole, S.P. (1996) Multidrug resistance mediated by the multidrug resistance protein (MRP) gene. *Biochem Pharmacol* **52**, 967-977.

Lautt, W.W., Schafer, J. and Legare, D.J. (1993) Hepatic blood flow distribution: consideration of gravity, liver surface, and norepinephrine on regional heterogeneity. *Can J Physiol Pharmacol* **71**, 128-135.

Lawley, P.D. and Phillips, D.H. (1996) DNA adducts from chemotherapeutic agents. *Mutat Res* **355**, 13-40.

Lee, F.I. (1966) Cirrhosis and hepatoma in alcoholics. *Gut* **7**, 77-85.

Lee, G. and Piquette-Miller, M. (2001) Influence of IL-6 on MDR and MRP-mediated multidrug resistance in human hepatoma cells. *Can J Physiol Pharmacol* **79**, 876-884.

Lee, G. and Piquette-Miller, M. (2003) Cytokines alter the expression and activity of the multidrug resistance transporters in human hepatoma cell lines; analysis using RT-PCR and cDNA microarrays. *J Pharm Sci* **92**, 2152-2163.

Lee, K., Belinsky, M.G., Bell, D.W., Testa, J.R. and Kruh, G.D. (1998) Isolation of MOAT-B, a widely expressed multidrug resistance-associated protein/canalicular multispecific organic anion transporter-related transporter. *Cancer Res* **58**, 2741-2747.

Leith, C.P., Chen, I.M., Kopecky, K.J., Appelbaum, F.R., Head, D.R., Godwin, J.E., Weick, J.K. and Willman, C.L. (1995) Correlation of multidrug resistance (MDR1) protein expression with functional dye/drug efflux in acute myeloid leukemia by multiparameter flow cytometry: identification of discordant MDR-/efflux+ and MDR1+/efflux- cases. *Blood* **86**, 2329-2342.

Leith, C.P., Kopecky, K.J., Chen, I.M., Eijdems, L., Slovak, M.L., McConnell, T.S., Head, D.R., Weick, J., Grever, M.R., Appelbaum, F.R. and Willman, C.L. (1999) Frequency and clinical significance of the expression of the multidrug resistance proteins MDR1/P-glycoprotein, MRP1, and LRP in acute myeloid leukemia: a Southwest Oncology Group Study. *Blood* **94**, 1086-1099.

Less, J.R., Posner, M.C., Skalak, T.C., Wolmark, N. and Jain, R.K. (1997) Geometric resistance and microvascular network architecture of human colorectal carcinoma. *Microcirculation* **4**, 25-33.

Leung, T.W., Patt, Y.Z., Lau, W.Y., Ho, S.K., Yu, S.C., Chan, A.T., Mok, T.S., Yeo, W., Liew, C.T., Leung, N.W., Tang, A.M. and Johnson, P.J. (1999) Complete pathological remission is possible with systemic combination chemotherapy for inoperable hepatocellular carcinoma. *Clin Cancer Res* **5**, 1676-1681.

Leunig, M., Yuan, F., Menger, M.D., Boucher, Y., Goetz, A.E., Messmer, K. and Jain, R.K. (1992) Angiogenesis, microvascular architecture, microhemodynamics, and interstitial fluid pressure during early growth of human adenocarcinoma LS174T in SCID mice. *Cancer Res* **52**, 6553-6560.

Leveille-Webster, C.R. and Arias, I.A. (1996) Establishment and serial quantification of intrahepatic xenografts of human hepatocellular carcinoma in severe combined immunodeficiency mice, and development of therapeutic strategies to overcome multidrug resistance. *Clin Cancer Res* **2**, 695-706.

Levi, F., Perpoint, B., Garufi, C., Focan, C., Chollet, P., Depres-Brummer, P., Zidani, R., Brienza, S., Itzhaki, M. and Iacobelli, S. (1993) Oxaliplatin activity against metastatic colorectal cancer. A phase II study of 5-day continuous venous infusion at circadian rhythm modulated rate. *Eur J Cancer* **29A**, 1280-1284.

Levi, F., Zidani, R. and Misset, J.L. (1997) Randomised multicentre trial of chronotherapy with oxaliplatin, fluorouracil, and folinic acid in metastatic colorectal cancer. International Organization for Cancer Chronotherapy. *Lancet* **350**, 681-686.

Levy, A.P., Levy, N.S. and Goldberg, M.A. (1996) Post-transcriptional regulation of vascular endothelial growth factor by hypoxia. *J Biol Chem* **271**, 2746-2753.

Li, Q., Yu, J.J., Mu, C., Yunmbam, M.K., Slavsky, D., Cross, C.L., Bostick-Bruton, F. and Reed, E. (2000) Association between the level of ERCC-1 expression and the repair of cisplatin-induced DNA damage in human ovarian cancer cells. *Anticancer Res* **20**, 645-652.

Liaw, Y.F., Tai, D.I., Chu, C.M., Lin, D.Y., Sheen, I.S., Chen, T.J. and Pao, C.C. (1986) Early detection of hepatocellular carcinoma in patients with chronic type B hepatitis. A prospective study. *Gastroenterology* **90**, 263-267.

Lin, G., Lunderquist, A., Hagerstrand, I. and Boijsen, E. (1984) Postmortem examination of the blood supply and vascular pattern of small liver metastases in man. *Surgery* **96**, 517-526.

Lin, H.L., Liu, T.Y., Lui, W.Y. and Chi, C.W. (1999) Up-regulation of multidrug resistance transporter expression by berberine in human and murine hepatoma cells. *Cancer* **85**, 1937-1942.

Livraghi, T., Bolondi, L., Buscarini, L., Cottone, M., Mazziotti, A., Morabito, A. and Torzilli, G. (1995) No treatment, resection and ethanol injection in hepatocellular carcinoma: a retrospective analysis of survival in 391 patients with cirrhosis. Italian Cooperative HCC Study Group. *J Hepatol* **22**, 522-526.

Llovet, J.M., Bruix, J., Fuster, J., Castells, A., Garcia-Valdecasas, J.C., Grande, L., Franca, A., Bru, C., Navasa, M., Ayuso, M.C., Sole, M., Real, M.I., Vilana, R., Rimola, A., Visa, J. and Rodes, J. (1998) Liver transplantation for small hepatocellular carcinoma: the tumor-node-metastasis classification does not have prognostic power. *Hepatology* **27**, 1572-1577.

Llovet, J.M., Bustamante, J., Castells, A., Vilana, R., Ayuso, M.C., Sala, M., Bru, C., Rodes, J. and Bruix, J. (1999a) Natural history of untreated nonsurgical hepatocellular carcinoma: rationale for the design and evaluation of therapeutic trials. *Hepatology* **29**, 62-67.

Llovet, J.M., Fuster, J. and Bruix, J. (1999b) Intention-to-treat analysis of surgical treatment for early hepatocellular carcinoma: resection versus transplantation. *Hepatology* **30**, 1434-1440.

Loe, D.W., Almquist, K.C., Cole, S.P. and Deeley, R.G. (1996a) ATP-dependent 17 beta-estradiol 17-(beta-D-glucuronide) transport by multidrug resistance protein (MRP). Inhibition by cholestatic steroids. *J Biol Chem* **271**, 9683-9689.

Loe, D.W., Almquist, K.C., Deeley, R.G. and Cole, S.P. (1996b) Multidrug resistance protein (MRP)-mediated transport of leukotriene C4 and chemotherapeutic agents in membrane vesicles. Demonstration of glutathione-dependent vincristine transport. *J Biol Chem* **271**, 9675-9682.

Loe, D.W., Deeley, R.G. and Cole, S.P. (1998) Characterization of vincristine transport by the M(r) 190,000 multidrug resistance protein (MRP): evidence for cotransport with reduced glutathione. *Cancer Res* **58**, 5130-5136.

Lorenz, M., Muller, H.H., Schramm, H., Gassel, H.J., Rau, H.G., Ridwelski, K., Hauss, J., Stieger, R., Jauch, K.W., Bechstein, W.O. and Encke, A. (1998) Randomized trial of surgery versus surgery followed by adjuvant hepatic arterial infusion with 5-fluorouracil and folinic acid for liver metastases of colorectal cancer. German Cooperative on Liver Metastases (Arbeitsgruppe Lebermetastasen). *Ann Surg* **228**, 756-762.

Luo, F.R., Paranjpe, P.V., Guo, A., Rubin, E. and Sinko, P. (2002) Intestinal transport of irinotecan in Caco-2 cells and MDCK II cells overexpressing efflux transporters Pgp, cMOAT, and MRP1. *Drug Metab Dispos* **30**, 763-770.

Ma, L., Hoeijmakers, J.H. and van der Eb, A.J. (1995) Mammalian nucleotide excision repair. *Biochim Biophys Acta* **1242**, 137-163.

Machover, D., Diaz-Rubio, E., de Gramont, A., Schilf, A., Gastiaburu, J.J., Brienza, S., Itzhaki, M., Metzger, G., N'Daw, D., Vignoud, J., Abad, A., Francois, E., Gamelin, E., Marty, M., Sastre, J., Seitz, J.F. and Ychou, M. (1996) Two consecutive phase II studies of oxaliplatin (L-OHP) for treatment of patients with advanced colorectal carcinoma who were resistant to previous treatment with fluoropyrimidines. *Ann Oncol* **7**, 95-98.

Malinge, J.M., Giraud-Panis, M.J. and Leng, M. (1999) Interstrand cross-links of cisplatin induce striking distortions in DNA. *J Inorg Biochem* **77**, 23-29.

Mamenta, E.L., Poma, E.E., Kaufmann, W.K., Delmastro, D.A., Grady, H.L. and Chaney, S.G. (1994) Enhanced replicative bypass of platinum-DNA adducts in cisplatin-resistant human ovarian carcinoma cell lines. *Cancer Res* **54**, 3500-3505.

Marinelli, A., van, d., V, Kuppen, P.J., Franken, H.C., Souverijn, J.H. and Eggermont, A.M. (1990) A comparative study of isolated liver perfusion versus hepatic artery infusion with mitomycin C in rats. *Br J Cancer* **62**, 891-896.

Martin EW, Minton JP and Carey LC (1993) CEA directed second-look surgery in asymptomatic patients after primary resection of colorectal cancer. *Ann Surg* **202**, 310-317.

Martinez-Hernandez, A. and Martinez, J. (1991) The role of capillarization in hepatic failure: studies in carbon tetrachloride-induced cirrhosis. *Hepatology* **14**, 864-874.

Martinez, C.F., Tomas, A., Donoso, L., Enriquez, J., Guarner, C., Balanzo, J., Martinez, N.A. and Vilardell, F. (1994) Controlled trial of tamoxifen in patients with advanced hepatocellular carcinoma. *J Hepatol* **20**, 702-706.

Marucci, L., Varticovski, L. and Arias, I.M. (1997) Effect of a xanthine analog on human hepatocellular carcinoma cells (Alexander) in culture and in xenografts in SCID mice. *Hepatology* **26**, 1195-1202.

Masuda, H., Ozols, R.F., Lai, G.M., Fojo, A., Rothenberg, M. and Hamilton, T.C. (1988) Increased DNA repair as a mechanism of acquired resistance to cis-diamminedichloroplatinum (II) in human ovarian cancer cell lines. *Cancer Res* **48**, 5713-5716.

Masuda, H., Tanaka, T., Matsuda, H. and Kusaba, I. (1990) Increased removal of DNA-bound platinum in a human ovarian cancer cell line resistant to cis-diamminedichloroplatinum(II). *Cancer Res* **50**, 1863-1866.

Mathurin, P., Rixe, O., Carbonell, N., Bernard, B., Cluzel, P., Bellin, M.F., Khayat, D., Opolon, P. and Poynard, T. (1998) Review article: Overview of medical treatments in unresectable hepatocellular carcinoma--an impossible meta-analysis? *Aliment Pharmacol Ther* **12**, 111-126.

Matsui, O., Kadoya, M., Kameyama, T., Yoshikawa, J., Takashima, T., Nakanuma, Y., Unoura, M., Kobayashi, K., Izumi, R. and Ida, M. (1991) Benign and malignant nodules in cirrhotic livers: distinction based on blood supply. *Radiology* **178**, 493-497.

Matsunaga, T., Shirasawa, H., Hishiki, T., Enomoto, H., Kouchi, K., Ohtsuka, Y., Iwai, J., Yoshida, H., Tanabe, M., Kobayashi, S., Asano, T., Etoh, T., Nishi, Y. and Ohnuma, N. (1988) Expression of MRP and cMOAT in childhood neuroblastomas and malignant liver tumors and its relevance to clinical behavior. *Jpn J Cancer Res* **89**, 1276-1283.

McEntee, G.P., Batts, K.A., Katzmann, J.A., Ilstrup, D.M. and Nagorney, D.M. (1992) Relationship of nuclear DNA content to clinical and pathologic findings in patients with primary hepatic malignancy. *Surgery* **111**, 376-379.

Meijer, C., Mulder, N.H., Timmer-Bosscha, H., Sluiter, W.J., Meersma, G.J. and de Vries, E.G. (1992) Relationship of cellular glutathione to the cytotoxicity and resistance of seven platinum compounds. *Cancer Res* **52**, 6885-6889.

Meijer, D.K., Keulemans, K. and Mulder, G.J. (1981) Isolated perfused rat liver technique. *Methods Enzymol* **77**, 81-94.

Meijer, G.A., Schroeijers, A.B., Flens, M.J., Meuwissen, S.G., van, d., V, Baak, J.P. and Scheper, R.J. (1999) Increased expression of multidrug resistance related proteins Pgp, MRP1, and LRP/MVP occurs early in colorectal carcinogenesis. *J Clin Pathol* **52**, 450-454.

Mellstedt, H., Frodin, J.E., Masucci, G., Ragnhammar, P., Fagerberg, J., Hjelm, A.L., Shetye, J., Wersall, P. and Osterborg, A. (1991) The therapeutic use of monoclonal antibodies in colorectal carcinoma. *Semin Oncol* **18**, 462-477.

Melvik, J.E. and Pettersen, E.O. (1988) Oxygen- and temperature-dependent cytotoxic and radiosensitizing effects of cis-dichlorodiammineplatinum(II) on human NHIK 3025 cells in vitro. *Radiat Res* **114**, 489-499.

Metzger, R., Leichman, C.G., Danenberg, K.D., Danenberg, P.V., Lenz, H.J., Hayashi, K., Groshen, S., Salonga, D., Cohen, H., Laine, L., Crookes, P., Silberman, H., Baranda, J., Konda, B. and Leichman, L. (1998) ERCC1 mRNA levels complement thymidylate synthase mRNA levels in predicting response and survival for gastric cancer patients receiving combination cisplatin and fluorouracil chemotherapy. *J Clin Oncol* **16**, 309-316.

Miller LL (1972) History of Isolated Liver Perfusion and Some Still Unsolved Problems. In: Bartosek I, Guaitani A and Miller LL, (Eds.) *Isolated Liver Perfusion and its Applications*, pp. 1-9. New York: Raven Press.

Mischinger, H.J., Walsh, T.R., Liu, T., Rao, P.N., Rubin, R., Nakamura, K., Todo, S. and Starzl, T.E. (1992) An improved technique for isolated perfusion of rat livers and an evaluation of perfusates. *J Surg Res* **53**, 158-165.

Modrich, P. (1994) Mismatch repair, genetic stability, and cancer. *Science* **266**, 1959-1960.

Moertel CA and Reitemeyar RJ (1969) *Advanced GI Cancer: clinical management and chemotherapy*, New York: Springer Verlay.

Moertel, C.G., Fleming, T.R., Macdonald, J.S., Haller, D.G., Laurie, J.A., Tangen, C.M., Ungerleider, J.S., Emerson, W.A., Tormey, D.C. and Glick, J.H. (1995)

Fluorouracil plus levamisole as effective adjuvant therapy after resection of stage III colon carcinoma: a final report. *Ann Intern Med* **122**, 321-326.

Morrison, P.F., Bungay, P.M., Hsiao, J.K., Ball, B.A., Mefford, I.N. and Dedrick, R.L. (1991) Quantitative microdialysis: analysis of transients and application to pharmacokinetics in brain. *J Neurochem* **57**, 103-119.

Morrow, C.S., Smitherman, P.K. and Townsend, A.J. (2000) Role of multidrug-resistance protein 2 in glutathione S-transferase P1-1-mediated resistance to 4-nitroquinoline 1-oxide toxicities in HepG2 cells. *Mol Carcinog* **29**, 170-178.

Nagase, H., Miyoshi, Y., Horii, A., Aoki, T., Ogawa, M., Utsunomiya, J., Baba, S., Sasazuki, T. and Nakamura, Y. (1992) Correlation between the location of germ-line mutations in the APC gene and the number of colorectal polyps in familial adenomatous polyposis patients. *Cancer Res* **52**, 4055-4057.

Nagasue, N., Yukaya, H., Ogawa, Y., Sasaki, Y., Chang, Y.C. and Niimi, K. (1986) Clinical experience with 118 hepatic resections for hepatocellular carcinoma. *Surgery* **99**, 694-701.

Nagorney, D.M., van Heerden, J.A., Ilstrup, D.M. and Adson, M.A. (1989) Primary hepatic malignancy: surgical management and determinants of survival. *Surgery* **106**, 740-748.

Nakamura, S., Yokoi, Y., Suzuki, S., Baba, S. and Muro, H. (1992) Results of extensive surgery for liver metastases in colorectal carcinoma. *Br J Surg* **79**, 35-38.

Nerenstone, S.R., Ihde, D.C. and Friedman, M.A. (1988) Clinical trials in primary hepatocellular carcinoma: current status and future directions. *Cancer Treat Rev* **15**, 1-31.

Netti, P.A., Berk, D.A., Swartz, M.A., Grodzinsky, A.J. and Jain, R.K. (2000) Role of extracellular matrix assembly in interstitial transport in solid tumors. *Cancer Res* **60**, 2497-2503.

Ng, I.O., Liu, C.L., Fan, S.T. and Ng, M. (2000) Expression of P-glycoprotein in hepatocellular carcinoma. A determinant of chemotherapy response. *Am J Clin Pathol* **113**, 355-363.

Nicolaides, N.C., Papadopoulos, N., Liu, B., Wei, Y.F., Carter, K.C., Ruben, S.M., Rosen, C.A., Haseltine, W.A., Fleischmann, R.D. and Fraser, C.M. (1994) Mutations of two PMS homologues in hereditary nonpolyposis colon cancer. *Nature* **371**, 75-80.

Niederhuber, J.E. and Ensminger, W.D. (1983) Surgical considerations in the management of hepatic neoplasia. *Semin Oncol* **10**, 135-147.

Nies, A.T., Konig, J., Pfannschmidt, M., Klar, E., Hofmann, W.J. and Keppler, D. (2001) Expression of the multidrug resistance proteins MRP2 and MRP3 in human hepatocellular carcinoma. *Int J Cancer* **94**, 492-499.

Nishikawa, K., Rosenblum, M.G., Newman, R.A., Pandita, T.K., Hittelman, W.N. and Donato, N.J. (1992) Resistance of human cervical carcinoma cells to tumor necrosis factor correlates with their increased sensitivity to cisplatin: evidence of a role for DNA repair and epidermal growth factor receptor. *Cancer Res* **52**, 4758-4765.

Nolsoe, C.P., Torp-Pedersen, S., Burcharth, F., Horn, T., Pedersen, S., Christensen, N.E., Olldag, E.S., Andersen, P.H., Karstrup, S. and Lorentzen, T. (1993) Interstitial hyperthermia of colorectal liver metastases with a US-guided Nd-YAG laser with a diffuser tip: a pilot clinical study. *Radiology* **187**, 333-337.

Nonami, T., Takeuchi, Y., Yasui, M., Kurokawa, T., Taniguch, K., Harada, A., Nakao, A. and Takagi, H. (1997) Regional adjuvant chemotherapy after partial hepatectomy for metastatic colorectal carcinoma. *Semin Oncol* **24**, S6-S6.

Okuda, K., Nakashima, T., Sakamoto, K., Ikari, T., Hidaka, H., Kubo, Y., Sakuma, K., Motoike, Y., Okuda, H. and Obata, H. (1982) Hepatocellular carcinoma arising in noncirrhotic and highly cirrhotic livers: a comparative study of histopathology and frequency of hepatitis B markers. *Cancer* **49**, 450-455.

Okuda, K. (1992) Hepatocellular carcinoma: recent progress. *Hepatology* **15**, 948-963.

Okuda, K., Tanaka, M., Shibata, J., Ando, E., Ogata, T., Kinoshita, H., Eriguchi, N., Aoyagi, S. and Tanikawa, K. (1999) Hepatic arterial infusion chemotherapy with continuous low dose administration of cisplatin and 5-fluorouracil for multiple recurrence of hepatocellular carcinoma after surgical treatment. *Oncol Rep* **6**, 587-591.

Olive, P.L., Banath, J.P. and Durand, R.E. (1990) Heterogeneity in radiation-induced DNA damage and repair in tumor and normal cells measured using the "comet" assay. *Radiat Res* **122**, 86-94.

Olive, P.L. and Banath, J.P. (1992) Growth fraction measured using the comet assay. *Cell Prolif* **25**, 447-457.

Olive, P.L., Durand, R.E., Le Riche, J., Olivotto, I.A. and Jackson, S.M. (1993) Gel electrophoresis of individual cells to quantify hypoxic fraction in human breast cancers. *Cancer Res* **53**, 733-736.

Olive, P.L., Vikse, C.M. and Banath, J.P. (1996) Use of the comet assay to identify cells sensitive to tirapazamine in multicell spheroids and tumors in mice. *Cancer Res* **56**, 4460-4463.

Olive, P.L., Banath, J.P. and Durand, R.E. (1997) Detection of subpopulations resistant to DNA-damaging agents in spheroids and murine tumours. *Mutat Res* **375**, 157-165.

Olschwang, S., Tiret, A., Laurent-Puig, P., Muleris, M., Parc, R. and Thomas, G. (1993) Restriction of ocular fundus lesions to a specific subgroup of APC mutations in adenomatous polyposis coli patients. *Cell* **75**, 959-968.

Onohara, S., Kobayashi, H., Itoh, Y. and Shinohara, S. (1988) Intra-arterial cis-platinum infusion with sodium thiosulfate protection and angiotensin II induced hypertension for treatment of hepatocellular carcinoma. *Acta Radiol* **29**, 197-202.

Osmak, M. (1992) Collateral resistance or sensitivity of human larynx carcinoma HEp2 cells resistant to cis-dichlorodiammineplatinum (II) or vincristine sulfate. *Neoplasma* **39**, 197-202.

Ostling, O. and Johanson, K.J. (1984) Microelectrophoretic study of radiation-induced DNA damages in individual mammalian cells. *Biochem Biophys Res Commun* **123**, 291-298.

Ouchi, K., Matsubara, S., Fukuhara, K., Tominaga, T. and Matsuno, S. (1993) Recurrence of hepatocellular carcinoma in the liver remnant after hepatic resection. *Am J Surg* **166**, 270-273.

Ozols, R.F., Louie, K.G., Plowman, J., Behrens, B.C., Fine, R.L., Dykes, D. and Hamilton, T.C. (1987) Enhanced melphalan cytotoxicity in human ovarian cancer in vitro and in tumor-bearing nude mice by buthionine sulfoximine depletion of glutathione. *Biochem Pharmacol* **36**, 147-153.

Page, J.D., Husain, I., Sancar, A. and Chaney, S.G. (1990) Effect of the diaminocyclohexane carrier ligand on platinum adduct formation, repair, and lethality. *Biochemistry* **29**, 1016-1024.

Palmer, M., Petrelli, N.J. and Herrera, L. (1989) No treatment option for liver metastases from colorectal adenocarcinoma. *Dis Colon Rectum* **32**, 698-701.

Pang, K.S., Cherry, W.F., Accaputo, J., Schwab, A.J. and Goresky, C.A. (1988) Combined hepatic arterial-portal venous and hepatic arterial-hepatic venous perfusions to probe the abundance of drug metabolizing activities: perihepatic venous O-deethylation activity for phenacetin and periportal sulfation activity for acetaminophen in the once-through rat liver preparation. *J Pharmacol Exp Ther* **247**, 690-700.

Paraskevopoulos, J.A. (1994) Management options for primary hepatocellular carcinoma. An overview. *Acta Oncol* **33**, 895-900.

Park, J.G., Lee, S.K., Hong, I.G., Kim, H.S., Lim, K.H., Choe, K.J., Kim, W.H., Kim, Y.I., Tsuruo, T. and Gottesman, M.M. (1994) MDR1 gene expression: its effect on drug resistance to doxorubicin in human hepatocellular carcinoma cell lines. *J Natl Cancer Inst* **86**, 700-705.

Parker, R.J., Eastman, A., Bostick-Bruton, F. and Reed, E. (1991) Acquired cisplatin resistance in human ovarian cancer cells is associated with enhanced repair of cisplatin-DNA lesions and reduced drug accumulation. *J Clin Invest* **87**, 772-777.

Patt, Y.Z., Yoffe, B., Charnsangavej, C., Pazdur, R., Fischer, H., Cleary, K., Roh, M., Smith, R., Noonan, C.A. and Levin, B. (1993) Low serum alpha-fetoprotein level in patients with hepatocellular carcinoma as a predictor of response to 5-FU and interferon-alpha-2b. *Cancer* **72**, 2574-2582.

Patt, Y.Z., Charnsangavej, C., Yoffe, B., Smith, R., Lawrence, D., Chuang, V., Carrasco, H., Roh, M., Chase, J. and Fischer, H. (1994) Hepatic arterial infusion of floxuridine, leucovorin, doxorubicin, and cisplatin for hepatocellular carcinoma: effects of hepatitis B and C viral infection on drug toxicity and patient survival. *J Clin Oncol* **12**, 1204-1211.

Pavone, P., Marsili, L., Petroni, G.A., Cardone, G., Cisternino, S., Di Girolamo, M. and Passariello, R. (1992) Arteriography in diagnosing hepatocellular carcinoma. *Ital J Gastroenterol* **24**, 92-94.

Pegg, D.E., Foreman, J. and Rolles, K. (1984) Metabolism during preservation and viability of ischemically injured canine kidneys. *Transplantation* **38**, 78-81.

Pelletier, G., Roche, A., Ink, O., Anciaux, M.L., Derhy, S., Rougier, P., Lenoir, C., Attali, P. and Etienne, J.P. (1990) A randomized trial of hepatic arterial chemoembolization in patients with unresectable hepatocellular carcinoma. *J Hepatol* **11**, 181-184.

Perez, T.R. (1983) Is cirrhosis of the liver experimentally produced by CCl4 and adequate model of human cirrhosis? *Hepatology* **3**, 112-120.

Perrin, D., van Hille, B. and Hill, B.T. (1998) Differential sensitivities of recombinant human topoisomerase IIalpha and beta to various classes of topoisomerase II-interacting agents. *Biochem Pharmacol* **56**, 503-507.

Peters, W.H. and Roelofs, H.M. (1992) Biochemical characterization of resistance to mitoxantrone and adriamycin in Caco-2 human colon adenocarcinoma cells: a possible role for glutathione S-transferases. *Cancer Res* **52**, 1886-1890.

Petrelli, N.J. and Mittelman, A. (1984) An analysis of chemotherapy for colorectal carcinoma. *J Surg Oncol* **25**, 201-206.

Pietras, R.J., Fendly, B.M., Chazin, V.R., Pegram, M.D., Howell, S.B. and Slamon, D.J. (1994) Antibody to HER-2/neu receptor blocks DNA repair after cisplatin in human breast and ovarian cancer cells. *Oncogene* **9**, 1829-1838.

Pinto, A.L. and Lippard, S.J. (1985) Sequence-dependent termination of in vitro DNA synthesis by cis- and trans-diamminedichloroplatinum (II). *Proc Natl Acad Sci USA* **82**, 4616-4619.

Potapova, O., Haghighi, A., Bost, F., Liu, C., Birrer, M.J., Gjerset, R. and Mercola, D. (1997) The Jun kinase/stress-activated protein kinase pathway functions to regulate DNA repair and inhibition of the pathway sensitizes tumor cells to cisplatin. *J Biol Chem* **272**, 14041-14044.

Price, T.J., Ross, P.J., Hickish, T., Tait, D., Norman, A.R., Ford, H.E., Middleton, G., Sumpter, K., Hill, M., Oates, J. and Cunningham, D. (2004) Phase III study of mitomycin-C with protracted venous infusion or circadian-timed infusion of 5-fluorouracil in advanced colorectal carcinoma. *Clin Colorectal Cancer* **3**, 235-242.

Priebe, W., Krawczyk, M., Kuo, M.T., Yamane, Y., Savaraj, N. and Ishikawa, T. (1998) Doxorubicin- and daunorubicin-glutathione conjugates, but not unconjugated drugs, competitively inhibit leukotriene C4 transport mediated by MRP/GS-X pump. *Biochem Biophys Res Commun* **247**, 859-863.

Pries, J.M., Staples, A.B. and Hanson, R.F. (1981) The effect of hepatic blood flow on taurocholate extraction by the isolated perfused rat liver. *J Lab Clin Med* **97**, 412-417.

Priestman T.J (1989) *Cancer Chemotherapy: An Introduction*, 3rd edn. London: Springer Verlag.

Prokipcak, R.D., Raouf, A. and Lee, C. (1999) The AU-rich 3' untranslated region of human MDR1 mRNA is an inefficient mRNA destabilizer. *Biochem Biophys Res Commun* **261**, 627-634.

Rabinovici, N. and Wiener, E. (1963) Hemodynamic changes in the hepatectomized liver of the rat and their relationship to regeneration. *J Surg Res* **3**, 3-8.

Radnell, M., Jeppsson, B. and Bengmark, S. (1990) A technique for isolated liver perfusion in the rat with survival and results of cytotoxic drug perfusion on liver tumor growth. *J Surg Res* **49**, 394-399.

Ravikumar, T.S., Kane, R., Cady, B., Jenkins, R., Clouse, M. and Steele, G.J. (1991a) A 5-year study of cryosurgery in the treatment of liver tumors. *Arch Surg* **126**, 1520-1523.

Ravikumar, T.S., Steele, G.J., Kane, R. and King, V. (1991b) Experimental and clinical observations on hepatic cryosurgery for colorectal metastases. *Cancer Res* **51**, 6323-6327.

Reed E and Kohn K.W (1990) Platinum Analogues. In: Chabner B.A and Collins J.M, (Eds.) *Cancer Chemotherapy:Principles and Practice*, pp. 465-490. Philadelphia: JB Lippincott Co.

Reichen, J. (1988) Role of the hepatic artery in canalicular bile formation by the perfused rat liver. A multiple indicator dilution study. *J Clin Invest* **81**, 1462-1469.

Repat Hepatic Resection Registry (1994) Repeat liver resections from colorectal metastasis. In: Sugarbaker PH, (Ed.) *Cancer Treatment and Research*, pp. 185-196. Boston, Massachusetts: Kluwer Academic.

Richmond, R.C., Stafford, J.H., Ryan, T.P., Mahtani, H.K., Memoli, V.A., Taylor, J.H. and Coughlin, C.T. (1992) Platinum levels and clinical responses of tumours treated by cisplatin with and without concurrent hyperthermia: a case study. *Int J Hyperthermia* **8**, 147-156.

Riedel, G.L., Scholle, J.L., Shepherd, A.P. and Ward, W.F. (1983) Effects of hematocrit on oxygenation of the isolated perfused rat liver. *Am J Physiol* **245**, G769-G774

Riethmuller, G., Holz, E., Schlimok, G., Schmiegel, W., Raab, R., Hoffken, K., Gruber, R., Funke, I., Pichlmaier, H., Hirche, H., Buggisch, P., Witte, J. and Pichlmayr, R. (1998) Monoclonal antibody therapy for resected Dukes' C colorectal

cancer: seven-year outcome of a multicenter randomized trial. *J Clin Oncol* **16**, 1788-1794.

Rodgers, M.S. and McCall, J.L. (2000) Surgery for colorectal liver metastases with hepatic lymph node involvement: a systematic review. *Br J Surg* **87**, 1142-1155.

Roelofsen, H., Vos, T.A., Schippers, I.J., Kuipers, F., Koning, H., Moshage, H., Jansen, P.L. and Muller, M. (1997) Increased levels of the multidrug resistance protein in lateral membranes of proliferating hepatocyte-derived cells. *Gastroenterology* **112**, 511-521.

Rogan, A.M., Hamilton, T.C., Young, R.C., Klecker, R.W.J. and Ozols, R.F. (1984) Reversal of adriamycin resistance by verapamil in human ovarian cancer. *Science* **224**, 994-996.

Rogler, C.E., Sherman, M., Su, C.Y., Shafritz, D.A., Summers, J., Shows, T.B., Henderson, A. and Kew, M. (1985) Deletion in chromosome 11p associated with a hepatitis B integration site in hepatocellular carcinoma. *Science* **230**, 319-322.

Ronnov-Jessen, L., Petersen, O.W. and Bissell, M.J. (1996) Cellular changes involved in conversion of normal to malignant breast: importance of the stromal reaction. *Physiol Rev* **76**, 69-125.

Rosen, C.B., Nagorney, D.M., Taswell, H.F., Helgeson, S.L., Ilstrup, D.M., van Heerden, J.A. and Adson, M.A. (1992) Perioperative blood transfusion and determinants of survival after liver resection for metastatic colorectal carcinoma. *Ann Surg* **216**, 493-504.

Ross BD (1972) *Perfusion Techniques in Biochemistry. A Laboratory Manual in the Use of Isolated Perfused Organs in Biochemical Experimentation*, Oxford: Clarendon Press.

Ross, D.D. (2000) Novel mechanisms of drug resistance in leukemia. *Leukemia* **14**, 467-473.

Ross, P., Norman, A., Cunningham, D., Webb, A., Iveson, T., Padhani, A., Prendiville, J., Watson, M., Massey, A., Popescu, R. and Oates, J. (1997) A prospective randomised trial of protracted venous infusion 5-fluorouracil with or without mitomycin C in advanced colorectal cancer. *Ann Oncol* **8**, 995-1001.

Ross, W.E., Ewig, R.A. and Kohn, K.W. (1978) Differences between melphalan and nitrogen mustard in the formation and removal of DNA cross-links. *Cancer Res* **38**, 1502-1506.

Rossi, S., Di Stasi, M., Buscarini, E., Quaretti, P., Garbagnati, F., Squassante, L., Paties, C.T., Silverman, D.E. and Buscarini, L. (1996) Percutaneous RF interstitial thermal ablation in the treatment of hepatic cancer. *AJR Am J Roentgenol* **167**, 759-768.

Rothbarth, J., Sparidans, R.W., Beijnen, J.H., Schultze-Kool, L.J., Putter, H., van, d., V and Mulder, G.J. (2002) Reduced liver uptake of arterially infused melphalan during retrograde rat liver perfusion with unaffected liver tumor uptake. *J Pharmacol Exp Ther* **303**, 736-740.

Rougier, P., Laplanche, A., Huguier, M., Hay, J.M., Ollivier, J.M., Escat, J., Salmon, R., Julien, M., Roullet, A.J. and Gallot, D. (1992) Hepatic arterial infusion of floxuridine in patients with liver metastases from colorectal carcinoma: long-term results of a prospective randomized trial. *J Clin Oncol* **10**, 1112-1118.

Ruers, T.J., Joosten, J., Jager, G.J. and Wobbes, T. (2001) Long-term results of treating hepatic colorectal metastases with cryosurgery. *Br J Surg* **88**, 844-849.

Rustgi, V.K. (1987) Epidemiology of hepatocellular carcinoma. *Gastroenterol Clin North Am* **16**, 545-551.

Ryder, S.D., Rizzi, P.M., Metivier, E., Karani, J. and Williams, R. (1996) Chemoembolisation with lipiodol and doxorubicin: applicability in British patients with hepatocellular carcinoma. *Gut* **38**, 125-128.

Sahin, S. and Rowland, M. (1998) Development of an optimal method for the dual perfusion of the isolated rat liver. *J Pharmacol Toxicol Methods* **39**, 35-43.

Saijo, M., Matsuda, T., Kuraoka, I. and Tanaka, K. (2004) Inhibition of nucleotide excision repair by anti-XPA monoclonal antibodies which interfere with binding to RPA, ERCC1, and TFIIH. *Biochem Biophys Res Commun* **321**, 815-822.

Saitoh, S., Ikeda, K., Koida, I., Tsubota, A., Arase, Y., Chayama, K. and Kumada, H. (1994) Small hepatocellular carcinoma: evaluation of portal blood flow with CT during arterial portography performed with balloon occlusion of the hepatic artery. *Radiology* **193**, 67-70.

Samdani, A., Vijapurkar, U., Grimm, M.A., Spier, C.S., Grogan, T.M., Glinsmann-Gibson, B.J. and List, A.F. (1996) Cytogenetics and P-glycoprotein (PGP) are independent predictors of treatment outcome in acute myeloid leukemia (AML). *Leuk Res* **20**, 175-180.

Sancar, A. (1996) DNA excision repair. *Annu Rev Biochem* **65**, 43-81.

Sargent, J.M. and Taylor, C.G. (1989) Appraisal of the MTT assay as a rapid test of chemosensitivity in acute myeloid leukaemia. *Br J Cancer* **60**, 206-210.

Scheele, J., Stangl, R. and Altendorf-Hofmann, A. (1990) Hepatic metastases from colorectal carcinoma: impact of surgical resection on the natural history. *Br J Surg* **77**, 1241-1246.

Scheele, J., Stang, R., Altendorf-Hofmann, A. and Paul, M. (1995) Resection of colorectal liver metastases. *World J Surg* **19**, 59-71.

Scheffer, G.L., Wijngaard, P.L., Flens, M.J., Izquierdo, M.A., Slovak, M.L., Pinedo, H.M., Meijer, C.J., Clevers, H.C. and Scheper, R.J. (1995) The drug resistance-related protein LRP is the human major vault protein. *Nat Med* **1**, 578-582.

Scheithauer, W., Rosen, H., Kornek, G.V., Sebesta, C. and Depisch, D. (1993) Randomised comparison of combination chemotherapy plus supportive care with supportive care alone in patients with metastatic colorectal cancer. *BMJ* **306**, 752-755.

Scheper, R.J., Broxterman, H.J., Scheffer, G.L., Kaaijk, P., Dalton, W.S., van Heijningen, T.H., van Kalken, C.K., Slovak, M.L. and de Vries, E.G. (1993) Overexpression of a M(r) 110,000 vesicular protein in non-P-glycoprotein-mediated multidrug resistance. *Cancer Res* **53**, 1475-1479.

Schlesselman, J.J. (1995) Net effect of oral contraceptive use on the risk of cancer in women in the United States. *Obstet Gynecol* **85**, 793-801.

Schneider, E., Yamazaki, H., Sinha, B.K. and Cowan, K.H. (1995) Buthionine sulphoximine-mediated sensitisation of etoposide-resistant human breast cancer MCF7 cells overexpressing the multidrug resistance-associated protein involves increased drug accumulation. *Br J Cancer* **71**, 738-743.

Schon, M.R., Hunt, C.J., Pegg, D.E. and Wight, D.G. (1993) The possibility of resuscitating livers after warm ischemic injury. *Transplantation* **56**, 24-31.

Sehested, M. and Hou-Jensen, K. (1981) Factor VII related antigen as an endothelial cell marker in benign and malignant diseases. *Virchows Arch A Pathol Anat Histol* **391**, 217-225.

Seifalian, A.M., Stansby, G.P., Hobbs, K.E., Hawkes, D.J. and Colchester, A.C. (1991) Measurement of liver blood flow: a review. *HPB Surg* **4**, 171-186.

Seifalian, A.M., Mallet, S.V., Rolles, K. and Davidson, B.R. (1997) Hepatic microcirculation during human orthotopic liver transplantation. *Br J Surg* **84**, 1391-1395.

Seifert, J.K., Junginger, T. and Morris, D.L. (1998) A collective review of the world literature on hepatic cryotherapy. *J R Coll Surg Edinb* **43**, 141-154.

Senent, L., Jarque, I., Martin, G., Sempere, A., Gonzalez-Garcia, Y., Gomis, F., Perez-Sirvent, M., De La Rubia, J. and Sanz, M.A. (1998) P-glycoprotein expression and prognostic value in acute myeloid leukemia. *Haematologica* **83**, 783-787.

Seymour, M.T., Slevin, M.L., Kerr, D.J., Cunningham, D., James, R.D., Ledermann, J.A., Perren, T.J., McAdam, W.A., Harper, P.G., Neoptolemos, J.P., Nicholson, M., Duffy, A.M., Stephens, R.J., Stenning, S.P. and Taylor, I. (1996) Randomized trial assessing the addition of interferon alpha-2a to fluorouracil and leucovorin in advanced colorectal cancer. Colorectal Cancer Working Party of the United Kingdom Medical Research Council. *J Clin Oncol* **14**, 2280-2288.

Shalinsky, D.R., Bischoff, E.D., Gregory, M.L., Lamph, W.W., Heyman, R.A., Hayes, J.S., Thomazy, V. and Davies, P.J. (1996) Enhanced antitumor efficacy of cisplatin in combination with ALRT1057 (9-cis retinoic acid) in human oral squamous carcinoma xenografts in nude mice. *Clin Cancer Res* **2**, 511-520.

Sharma, R., Adam, E. and Schumacher, U. (1997) The action of 5-fluorouracil on human HT29 colon cancer cells grown in SCID mice: mitosis, apoptosis and cell differentiation. *Br J Cancer* **76**, 1011-1016.

Shen, Y., Vogel, I. and Kalthoff, H. (2000) Comparative study of metastasis-associated characteristics of tumor cells with different metastatic capacities. *Zhonghua Zhong Liu Za Zhi* **22**, 201-204.

Shepherd, F.A., Evans, W.K., Blackstein, M.E., Fine, S., Heathcote, J., Langer, B., Taylor, B., Habal, F., Kutas, G. and Pritchard, K.I. (1987) Hepatic arterial infusion of mitoxantrone in the treatment of primary hepatocellular carcinoma. *J Clin Oncol* **5**, 635-640.

Sherlock S and Dooley J (1993) *Diseases of the Liver and Biliary System*, 9th edn. Oxford: Blackwell.

Shibata, T., Niinobu, T., Ogata, N. and Takami, M. (2000) Microwave coagulation therapy for multiple hepatic metastases from colorectal carcinoma. *Cancer* **89**, 276-284.

Shimizu, S., Eguchi, Y., Kamiike, W., Itoh, Y., Hasegawa, J., Yamabe, K., Otsuki, Y., Matsuda, H. and Tsujimoto, Y. (1996) Induction of apoptosis as well as necrosis by hypoxia and predominant prevention of apoptosis by Bcl-2 and Bcl-XL. *Cancer Res* **56**, 2161-2166.

Shweiki, D., Itin, A., Soffer, D. and Keshet, E. (1992) Vascular endothelial growth factor induced by hypoxia may mediate hypoxia-initiated angiogenesis. *Nature* **359**, 843-845.

Siddik, Z.H., Newell, D.R., Boxall, F.E. and Harrap, K.R. (1987) The comparative pharmacokinetics of carboplatin and cisplatin in mice and rats. *Biochem Pharmacol* **36**, 1925-1932.

Sigurdson, E.R., Ridge, J.A., Kemeny, N. and Daly, J.M. (1987) Tumor and liver drug uptake following hepatic artery and portal vein infusion. *J Clin Oncol* **5**, 1836-1840.

Sijbers, A.M., van der Spek, P.J., Odijk, H., van den Berg, J., van Duin, M., Westerveld, A., Jaspers, N.G., Bootsma, D. and Hoeijmakers, J.H. (1996) Mutational analysis of the human nucleotide excision repair gene ERCC1. *Nucleic Acids Res* **24**, 3370-3380.

Simonetti, R.G., Liberati, A., Angiolini, C. and Pagliaro, L. (1997) Treatment of hepatocellular carcinoma: a systematic review of randomized controlled trials. *Ann Oncol* **8**, 117-136.

Skarsgard, L.D., Skwarchuk, M.W., Vinczan, A., Kristl, J. and Chaplin, D.J. (1995) The cytotoxicity of melphalan and its relationship to pH, hypoxia and drug uptake. *Anticancer Res* **15**, 219-223.

Skehan, P., Storeng, R., Scudiero, D., Monks, A., McMahon, J., Vistica, D., Warren, J.T., Bokesch, H., Kenney, S. and Boyd, M.R. (1990) New colorimetric cytotoxicity assay for anticancer-drug screening. *J Natl Cancer Inst* **82**, 1107-1112.

Skov, K.A., Adomat, H., Farrell, N.P. and Matthews, J.B. (1998) Assessment of toxicity of bis-platinum complexes in hypoxic and aerobic cells. *Anticancer Drug Des* **13**, 207-220.

Smrekova, R., Vajdova, K., Kukan, M., Ulicna, O., Lutterova, M., Wsolova, L. and Horecky, J. (2000) A rapid, simple, and cost-effective method for screening liver preservation solutions in the rat. *Transplantation* **70**, 430-436.

Solbiati, L., Goldberg, S.N., Ierace, T., Livraghi, T., Meloni, F., Dellanoce, M., Sironi, S. and Gazelle, G.S. (1997) Hepatic metastases: percutaneous radio-frequency ablation with cooled-tip electrodes. *Radiology* **205**, 367-373.

Somfai-Relle, S., Suzukake, K., Vistica, B.P. and Vistica, D.T. (1984) Reduction in cellular glutathione by buthionine sulfoximine and sensitization of murine tumor cells resistant to L-phenylalanine mustard. *Biochem Pharmacol* **33**, 485-490.

Son, K., Kew, M. and Rabson, A.R. (1982) Depressed natural killer cell activity in patients with hepatocellular carcinoma. In vitro effects of interferon and levamisole. *Cancer* **50**, 2820-2825.

Spanswick, V.J., Hartley, J.M., Ward, T.H. and Hartley, J.A. (1999) *Cytotoxic Drug Resistance Mechanisms (Methods in Molecular Medicine)*, 28 edn. Totowa, NJ: Humana Press Inc.

St Peter, S.D., Imber, C.J., Lopez, I., Hughes, D. and Friend, P.J. (2002) Extended preservation of non-heart-beating donor livers with normothermic machine perfusion. *Br J Surg* **89**, 609-616.

Stangl, R., Altendorf-Hofmann, A., Charnley, R.M. and Scheele, J. (1994) Factors influencing the natural history of colorectal liver metastases. *Lancet* **343**, 1405-1410.

Starnes, H.F.J., Tewari, A., Flokas, K., Kosek, J.C., Brown, D., Van-Kessel, A.L. and Mondon, C.E. (1991) Effectiveness of a purified human hemoglobin as a blood substitute in the perfused rat liver. *Gastroenterology* **101**, 1345-1353.

States, J.C. and Reed, E. (1996) Enhanced XPA mRNA levels in cisplatin-resistant human ovarian cancer are not associated with XPA mutations or gene amplification. *Cancer Lett* **108**, 233-237.

Stein, T.N. and Berger, M.R. (1999) Quantification of liver metastases from LS174T human colorectal cancer cells in nude rats by PCR. *Anticancer Res* **19**, 3939-3945.

Stone, M.D., Cady, B., Jenkins, R.L., McDermott, W.V. and Steele, G.D.J. (1990) Surgical therapy for recurrent liver metastases from colorectal cancer. *Arch Surg* **125**, 718-721.

Stratford, I.J., Williamson, C. and Adams, G.E. (1980) Combination studies with misonidazole and a cis-platinum complex: cytotoxicity and radiosensitization in vitro. *Br J Cancer* **41**, 517-522.

Sumimoto, K., Inagaki, K., Yamada, K., Kawasaki, T. and Dohi, K. (1988) Reliable indices for the determination of viability of grafted liver immediately after orthotopic transplantation. Bile flow rate and cellular adenosine triphosphate level. *Transplantation* **46**, 506-509.

Sun, X., Kanwar, J.R., Leung, E., Lehnert, K., Wang, D. and Krissansen, G.W. (2001) Gene transfer of antisense hypoxia inducible factor-1 alpha enhances the therapeutic efficacy of cancer immunotherapy. *Gene Ther* **8**, 638-645.

Sundin, A. (1993) Radioimmunolocalization and quantification of liver metastases and subcutaneous tumours from a human colonic cancer xenografted in the nude rat. *Acta Radiol Suppl* **382**, 1-29.

Sundin, A., Ahlstrom, H., Carlsson, L., Graf, W., Glimelius, B. and Carlsson, J. (1993) Radioimmunolocalization of hepatic metastases and subcutaneous xenografts from a human colonic cancer in the nude rat. Aspects of tumour implantation site and mode of antibody administration. *Acta Oncol* **32**, 877-885.

Suo, Z., Lippard, S.J. and Johnson, K.A. (1999) Single d(GpG)/cis-diammineplatinum(II) adduct-induced inhibition of DNA polymerization. *Biochemistry* **38**, 715-726.

Sutherland, R.M. (1988) Cell and environment interactions in tumor microregions: the multicell spheroid model. *Science* **240**, 177-184.

Szymkowski, D.E., Yarema, K., Essigmann, J.M., Lippard, S.J. and Wood, R.D. (1992) An intrastrand d(GpG) platinum crosslink in duplex M13 DNA is refractory to repair by human cell extracts. *Proc Natl Acad Sci USA* **89**, 10772-10776.

Takahashi, Y., Ellis, L.M., Wilson, M.R., Bucana, C.D., Kitadai, Y. and Fidler, I.J. (1996) Progressive upregulation of metastasis-related genes in human colon cancer cells implanted into the cecum of nude mice. *Oncol Res* **8**, 163-169.

Takano, H., Kohno, K., Matsuo, K., Matsuda, T. and Kuwano, M. (1992) DNA topoisomerase-targeting antitumor agents and drug resistance. *Anticancer Drugs* **3**, 323-330.

Takata, M., Sasaki, M.S., Sonoda, E., Morrison, C., Hashimoto, M., Utsumi, H., Yamaguchi-Iwai, Y., Shinohara, A. and Takeda, S. (1998) Homologous recombination and non-homologous end-joining pathways of DNA double-strand break repair have overlapping roles in the maintenance of chromosomal integrity in vertebrate cells. *EMBO J* **17**, 5497-5508.

Takayasu, K., Shima, Y., Muramatsu, Y., Goto, H., Moriyama, N., Yamada, T., Makuuchi, M., Yamasaki, S., Hasegawa, H. and Okazaki, N. (1986) Angiography of small hepatocellular carcinomas: analysis of 105 resected tumors. *AJR Am J Roentgenol* **147**, 525-529.

Takeuchi, A., Kaneko, S., Matsushita, E., Urabe, T., Shimoda, A. and Kobayashi, K. (1999) Interferon-alpha modulates resistance to cisplatin in three human hepatoma cell lines. *J Gastroenterol* **34**, 351-358.

Tanaka, S., Kitamra, T., Fujita, M., Kasugai, H., Inoue, A. and Ishiguro, S. (1992) Small hepatocellular carcinoma: differentiation from adenomatous hyperplastic nodule with color Doppler flow imaging. *Radiology* **182**, 161-165.

Taniguchi, H., Daidoh, T., Shioaki, Y. and Takahashi, T. (1993) Blood supply and drug delivery to primary and secondary human liver cancers studied with in vivo bromodeoxyuridine labeling. *Cancer* **71**, 50-55.

Taylor, I., Bennett, R. and Sherriff, S. (1978) The blood supply of colorectal liver metastases. *Br J Cancer* **38**, 749-756.

Teicher, B.A., Lazo, J.S. and Sartorelli, A.C. (1981) Classification of antineoplastic agents by their selective toxicities toward oxygenated and hypoxic tumor cells. *Cancer Res* **41**, 73-81.

Teicher, B.A., Holden, S.A., Herman, T.S., Sotomayor, E.A., Khandekar, V., Rosbe, K.W., Brann, T.W., Korbut, T.T. and Frei, E. (1991) Characteristics of five human tumor cell lines and sublines resistant to cis-diamminedichloroplatinum(II). *Int J Cancer* **47**, 252-260.

Tew, K.D. (1994) Glutathione-associated enzymes in anticancer drug resistance. *Cancer Res* **54**, 4313-4320.

Thompson, L.H. (1996) Evidence that mammalian cells possess homologous recombinational repair pathways. *Mutat Res* **363**, 77-88.

Tomida, A., Naito, M. and Tsuruo, T. (1995) Acute induction of adriamycin-resistance in human colon carcinoma HT-29 cells exposed to a sublethal dose of adriamycin. *Jpn J Cancer Res* **86**, 224-232.

Tong, A.W., Su, D., Mues, G., Tillery, G.W., Goldstein, R., Klintmalm, G. and Stone, M.J. (1996) Chemosensitization of human hepatocellular carcinoma cells with cyclosporin A in post-liver transplant patient plasma. *Clin Cancer Res* **2**, 531-539.

Tong, M.J., Sun, S.C., Schaeffer, B.T., Chang, N.K., Lo, K.J. and Peters, R.L. (1971) Hepatitis-associated antigen and hepatocellular carcinoma in Taiwan. *Ann Intern Med* **75**, 687-691.

Trotter, M.J., Chaplin, D.J., Durand, R.E. and Olive, P.L. (1989) The use of fluorescent probes to identify regions of transient perfusion in murine tumors. *Int J Radiat Oncol Biol Phys* **16**, 931-934.

Tsuji, A., Morita, S., Horimi, T., Takasaki, M., Takahashi, I. and Shirasaka, T. (2000) Combination chemotherapy of continuous 5-FU infusion and low-dose cisplatin infusion for the treatment of advanced and recurrent gastric and colorectal adenocarcinomas. *Gan To Kagaku Ryoho* **27 Suppl 2**, 528-534.

Ueno, K., Miyazono, N., Inoue, H., Nishida, H., Kanetsuki, I. and Nakajo, M. (2000) Transcatheter arterial chemoembolization therapy using iodized oil for patients with unresectable hepatocellular carcinoma: evaluation of three kinds of regimens and analysis of prognostic factors. *Cancer* **88**, 1574-1581.

Unruh, A., Ressel, A., Mohamed, H.G., Johnson, R.S., Nadrowitz, R., Richter, E., Katschinski, D.M. and Wenger, R.H. (2003) The hypoxia-inducible factor-1 alpha is a negative factor for tumor therapy. *Oncogene* **22**, 3213-3220.

Vahrmeijer, A.L., Snel, C.A., Steenvoorden, D.P., Beijnen, J.H., Pang, K.S., Schutrups, J., Tirona, R., Keizer, H.J., van Dierendonck, J.H., van, d., V and Mulder, G.J. (1996) Lack of glutathione conjugation of melphalan in the isolated in situ liver perfusion in humans. *Cancer Res* **56**, 4709-4714.

Vaisman, A., Varchenko, M., Umar, A., Kunkel, T.A., Risinger, J.I., Barrett, J.C., Hamilton, T.C. and Chaney, S.G. (1998) The role of hMLH1, hMSH3, and hMSH6 defects in cisplatin and oxaliplatin resistance: correlation with replicative bypass of platinum-DNA adducts. *Cancer Res* **58**, 3579-3585.

Valero, R., Garcia-Valdecasas, J.C., Tabet, J., Taura, P., Rull, R., Beltran, J., Garcia, F., Gonzalez, F.X., Lopez-Boado, M.A., Cabrer, C. and Visa, J. (1998) Hepatic blood flow and oxygen extraction ratio during normothermic recirculation and total body cooling as viability predictors in non-heart-beating donor pigs. *Transplantation* **66**, 170-176.

Vaupel, P., Kallinowski, F. and Okunieff, P. (1989) Blood flow, oxygen and nutrient supply, and metabolic microenvironment of human tumors: a review. *Cancer Res* **49**, 6449-6465.

Verdi, C.J., Ahmann, F.R., Schifman, R.B., Elvick, A.L., Ahmann, M.E. and Marx, P.C. (1993) Comparative evaluation of serum CA 195 and carcinoembryonic antigen in metastatic carcinoma. *Cancer* **71**, 3625-3632.

Versantvoort, C.H., Broxterman, H.J., Bagrij, T., Scheper, R.J. and Twentyman, P.R. (1995) Regulation by glutathione of drug transport in multidrug-resistant human lung tumour cell lines overexpressing multidrug resistance-associated protein. *Br J Cancer* **72**, 82-89.

Villeneuve, J.P., Huet, P.M., Gariepy, L., Fenyves, D., Willems, B., Cote, J., Lapointe, R. and Marleau, D. (1990) Isolated perfused cirrhotic human liver obtained from liver transplant patients: a feasibility study. *Hepatology* **12**, 257-263.

Villeneuve, J.P., Dagenais, M., Huet, P.M., Roy, A., Lapointe, R. and Marleau, D. (1996a) The hepatic microcirculation in the isolated perfused human liver. *Hepatology* **23**, 24-31.

Villeneuve, J.P., Dagenais, M., Huet, P.M., Lapointe, R., Roy, A. and Marleau, D. (1996b) Clearance by the liver in cirrhosis. III. Propranolol uptake by the isolated perfused human liver. *Can J Physiol Pharmacol* **74**, 1327-1332.

Vock, E.H., Lutz, W.K., Hormes, P., Hoffmann, H.D. and Vamvakas, S. (1998) Discrimination between genotoxicity and cytotoxicity in the induction of DNA double-strand breaks in cells treated with etoposide, melphalan, cisplatin, potassium cyanide, Triton X-100, and gamma-irradiation. *Mutat Res* **413**, 83-94.

Vogel, I., Shen, Y., Soeth, E., Juhl, H., Kremer, B., Kalthoff, H. and Henne-Bruns, D. (1998) A human carcinoma model in athymic rats reflecting solid and disseminated colorectal metastases. *Langenbecks Arch Surg* **383**, 466-473.

Vogel, V.G. and McPherson, R.S. (1989) Dietary epidemiology of colon cancer. *Hematol Oncol Clin North Am* **3**, 35-63.

Vogelstein, B., Fearon, E.R., Hamilton, S.R., Kern, S.E., Preisinger, A.C., Leppert, M., Nakamura, Y., White, R., Smits, A.M. and Bos, J.L. (1988) Genetic alterations during colorectal-tumor development. *N Engl J Med* **319**, 525-532.

Von Hoff, D.D. (1990) He's not going to talk about in vitro predictive assays again, is he? *J Natl Cancer Inst* **82**, 96-101.

Vos, J.G., Berkvens, J.M. and Kruijt, B.C. (1980) The athymic nude rat. I. Morphology of lymphoid and endocrine organs. *Clin Immunol Immunopathol* **15**, 213-228.

Vredenburg, M.R., Ojima, I., Veith, J., Pera, P., Kee, K., Cabral, F., Sharma, A., Kanter, P., Greco, W.R. and Bernacki, R.J. (2001) Effects of orally active taxanes on P-glycoprotein modulation and colon and breast carcinoma drug resistance. *J Natl Cancer Inst* **93**, 1234-1245.

Wadler, S. and Schwartz, E.L. (1990) Antineoplastic activity of the combination of interferon and cytotoxic agents against experimental and human malignancies: a review. *Cancer Res* **50**, 3473-3486.

Wadler, S. (1991) The role of immunotherapy in colorectal cancer. *Semin Oncol* **18**, 27-38.

Wands, J.R. and Blum, H.E. (1991) Primary hepatocellular carcinoma. *N Engl J Med* **325**, 729-731.

Wang, L.Q., Persson, B.G., Stenram, U. and Bengmark, S. (1994) Influence of portal branch ligation on the outcome of repeat dearterializations of an experimental liver tumor in the rat. *J Surg Oncol* **55**, 229-234.

Weaver, M.L., Ashton, J.G. and Zemel, R. (1998) Treatment of colorectal liver metastases by cryotherapy. *Semin Surg Oncol* **14**, 163-170.

Webley, S.D., Francis, R.J., Pedley, R.B., Sharma, S.K., Begent, R.H., Hartley, J.A. and Hochhauser, D. (2001) Measurement of the critical DNA lesions produced by antibody-directed enzyme prodrug therapy (ADEPT) in vitro, in vivo and in clinical material. *Br J Cancer* **84**, 1671-1676.

Weichselbaum, R.R., Dahlberg, W., Beckett, M., Karrison, T., Miller, D., Clark, J. and Ervin, T.J. (1986) Radiation-resistant and repair-proficient human tumor cells may be associated with radiotherapy failure in head- and neck-cancer patients. *Proc Natl Acad Sci USA* **83**, 2684-2688.

Weinstein, R.S., Jakate, S.M., Dominguez, J.M., Lebovitz, M.D., Koukoulis, G.K., Kuszak, J.R., Klusens, L.F., Grogan, T.M., Saclarides, T.J. and Roninson, I.B. (1991) Relationship of the expression of the multidrug resistance gene product (P-glycoprotein) in human colon carcinoma to local tumor aggressiveness and lymph node metastasis. *Cancer Res* **51**, 2720-2726.

Wheatley, A.M., Almond, N.E., Stuart, E.T. and Zhao, D. (1993) Interpretation of the laser Doppler flow signal from the liver of the rat. *Microvasc Res* **45**, 290-301.

Wike-Hooley, J.L., Haveman, J. and Reinhold, H.S. (1984) The relevance of tumour pH to the treatment of malignant disease. *Radiother Oncol* **2**, 343-366.

Wong, W.S., Patel, S.C., Cruz, F.S., Gala, K.V. and Turner, A.F. (1998) Cryosurgery as a treatment for advanced stage hepatocellular carcinoma: results, complications, and alcohol ablation. *Cancer* **82**, 1268-1278.

Wood, P., Burgess, R., MacGregor, A. and Yin, J.A. (1994) P-glycoprotein expression on acute myeloid leukaemia blast cells at diagnosis predicts response to chemotherapy and survival. *Br J Haematol* **87**, 509-514.

Wood, R.D. (1995) Proteins that participate in nucleotide excision repair of DNA in mammalian cells. *Philos Trans R Soc Lond B Biol Sci* **347**, 69-74.

Wood, R.D. (1996) DNA repair in eukaryotes. *Annu Rev Biochem* **65**, 135-167.

Wu, X., Fan, W., Xu, S. and Zhou, Y. (2003) Sensitization to the cytotoxicity of cisplatin by transfection with nucleotide excision repair gene xeroderma pigmentosun group A antisense RNA in human lung adenocarcinoma cells. *Clin Cancer Res* **9**, 5874-5879.

Yamada, M., O'Regan, E., Brown, R. and Karran, P. (1997) Selective recognition of a cisplatin-DNA adduct by human mismatch repair proteins. *Nucleic Acids Res* **25**, 491-496.

Yamauchi, M., Nakahara, M., Maezawa, Y., Satoh, S., Nishikawa, F., Ohata, M., Mizuhara, Y., Hirakawa, J., Nakajima, H. and Fujisawa, K. (1993) Prevalence of hepatocellular carcinoma in patients with alcoholic cirrhosis and prior exposure to hepatitis C. *Am J Gastroenterol* **88**, 39-43.

Yang, W., Benjamin, I.S. and Alexander, B. (1999) Localisation of hepatic vascular resistance sites in the isolated dual-perfused rat liver. *Eur J Pharmacol* **364**, 13-21.

Yeh, F.S., Yu, M.C., Mo, C.C., Luo, S., Tong, M.J. and Henderson, B.E. (1989) Hepatitis B virus, aflatoxins, and hepatocellular carcinoma in southern Guangxi, China. *Cancer Res* **49**, 2506-2509.

Yuan, F., Leunig, M., Huang, S.K., Berk, D.A., Papahadjopoulos, D. and Jain, R.K. (1994) Microvascular permeability and interstitial penetration of sterically stabilized (stealth) liposomes in a human tumor xenograft. *Cancer Res* **54**, 3352-3356.

Yuan, F., Dellian, M., Fukumura, D., Leunig, M., Berk, D.A., Torchilin, V.P. and Jain, R.K. (1995) Vascular permeability in a human tumor xenograft: molecular size dependence and cutoff size. *Cancer Res* **55**, 3752-3756.

Yuan, F., Chen, Y., Dellian, M., Safabakhsh, N., Ferrara, N. and Jain, R.K. (1996) Time-dependent vascular regression and permeability changes in established human tumor xenografts induced by an anti-vascular endothelial growth factor/vascular permeability factor antibody. *Proc Natl Acad Sci USA* **93**, 14765-14770.

Zaniboni, A., Simoncini, E., Marpicati, P. and Marini, G. (1988) Phase II study of 5-fluorouracil (5-FU) and high dose folinic acid (HDFA) in hepatocellular carcinoma. *Br J Cancer* **57**, 319

Zeng, H., Bain, L.J., Belinsky, M.G. and Kruh, G.D. (1999) Expression of multidrug resistance protein-3 (multispecific organic anion transporter-D) in human embryonic kidney 293 cells confers resistance to anticancer agents. *Cancer Res* **59**, 5964-5967.

Zhang, M., Li, S., Li, J., Ensminger, W.D. and Lawrence, T.S. (2003a) Ionizing radiation increases adenovirus uptake and improves transgene expression in intrahepatic colon cancer xenografts. *Mol Ther* **8**, 21-28.

Zhang, M., Li, S., Nyati, M.K., DeRemer, S., Parsels, J., Rehemtulla, A., Ensminger, W.D. and Lawrence, T.S. (2003b) Regional delivery and selective expression of a high-activity yeast cytosine deaminase in an intrahepatic colon cancer model. *Cancer Res* **63**, 658-663.

Zhen, W., Link, C.J.J., O'Connor, P.M., Reed, E., Parker, R., Howell, S.B. and Bohr, V.A. (1992) Increased gene-specific repair of cisplatin interstrand cross-links in cisplatin-resistant human ovarian cancer cell lines. *Mol Cell Biol* **12**, 3689-3698.

Zibari, G.B., Riche, A., Zizzi, H.C., McMillan, R.W., Aultman, D.F., Boykin, K.N., Gonzalez, E., Nandy, I., Dies, D.F., Gholson, C.F., Holcombe, R.F. and McDonald, J.C. (1998) Surgical and nonsurgical management of primary and metastatic liver tumors. *Am Surg* **64**, 211-220.

Zollner, G., Wagner, M., Fickert, P., Silbert, D., Fuchsbichler, A., Zatloukal, K., Denk, H. and Trauner, M. (2005) Hepatobiliary transporter expression in human hepatocellular carcinoma. *Liver Int* **25**, 367-379.

Zwelling, L.A., Kohn, K.W., Ross, W.E., Ewig, R.A. and Anderson, T. (1978) Kinetics of formation and disappearance of a DNA cross-linking effect in mouse leukemia L1210 cells treated with cis- and trans-diamminedichloroplatinum(II). *Cancer Res* **38**, 1762-1768.

Appendix 2.1: Reagents and solutions

Amersham, Life Sciences, UK: Rainbow coloured protein molecular weight markers, ECL western blot detection reagents, nitro-cellulose membrane and Nova blot electrode papers.

An Der Grub, Kaumberg, Austria: Permeabilisation reagents A (fixation medium) and B (permeabilisation medium).

Collaborative Biochemical Products, Becton Dickson, Bedford (MA), USA: Matrigel.

Bio-rad Laboratories Ltd, UK: Biorad Protein Assay Reagent.

Dr R Hodgkiss, Gray Laboratory Cancer Research Trust, Middlesex, UK: 7-(4'-(2-nitroimidazol-1-yl)-theophylline (NITP).

Fuji PhotoFilm Ltd (UK): Fuji Film Super RX, Medical X-Ray film.

Novartis Pharma, Basel, Switzerland: cyclosporin D analogue PSC833.

Novex, Groningen, the Netherlands: Nu-PAGE: LDS sample buffer, sample reducing reagent (10x), sample buffer (4x), antioxidant and transfer buffer (20x).

Pharmacia & Upjohn, London, England: Gelfoam.

Sigma-Aldrich, UK: The protein binding dye, sulfohodamine B (SRB); the fluorescent substrate 3,3'-diethyloxacarbocyanine (DiOC2); the western blot reagents aprotinin, phenylmethylsulfonyl fluoride (PMSF), β mercapto-ethanol and Ponceau's reagent; D L-buthionine-(S,R)-sulfoxamine (BSO); agarose, types IA and VII; propidium iodide; Hoechst 33342 and the calcium channel blocker verapamil (vpm).

Appendix 2.2: Drugs

David Bull Laboratories, Warwick, UK: Cisplatin (*cis*-dichlorodiammine platinum (II)), vincristine and 5-Fluorouracil (5-FU)

Glaxo Wellcome, Middlesex, UK: Melphalan.

Bristol-Myers Pharmaceuticals, Dublin, Ireland: Etoposide.

Sigma-Aldrich, UK: Mechlorethamine (Nitrogen Mustard).

Appendix 3.1: Data for SRB Growth Assay

Table 1: Absorbance measurements at 540 nm for HCC & CRC cell lines
(arbitary units)

Time/h	Hep G2	SkHep -1	C3A	PLC/P RF/5	Hep3B	WIDR	CAC O2	HT29	SW620
24	0.067	0.662	0.353	0.992	0.819	0.362	0.431	0.555	0.389
	0.069	0.676	0.349	1.023	0.843	0.37	0.462	0.511	0.376
	0.08	0.683	0.344	0.96	0.836	0.335	0.464	0.583	0.346
	0.079	0.689	0.373	0.998	0.829	0.353	0.489	0.584	0.384
48	0.269	1.662	0.926	1.742	1.203	0.964	0.699	1.179	0.524
	0.246	1.602	0.93	1.871	1.371	0.908	0.747	1.07	0.568
	0.233	1.543	0.927	2.014	1.29	0.928	0.689	1.06	0.552
	0.244	1.574	0.953	1.807	1.09	0.899	0.766	1.114	0.548
72	0.551	2.915	1.512	2.447	1.835	1.464	1.133	2.175	0.686
	0.536	2.89	1.428	2.496	1.771	1.447	1.108	2.112	0.721
	0.523	2.859	1.358	2.407	1.696	1.322	1.296	2.172	0.754
	0.492	2.84	1.388	2.351	1.315	1.209	1.215	2.168	0.739
96	1.082	2.858	1.453	3.037	2.451	1.623	1.766	2.782	1.169
	1.118	2.875	1.957	3.034	2.512	1.812	1.784	2.796	1.175
	1.182	3.086	1.6	3.052	2.279	1.848	2.128	2.718	1.171
	1.064	2.96	1.689	3.024	2.163	1.842	2.02	2.767	1.149
120	1.812	2.91	2.243	2.81	2.934	2.351	2.503	2.77	2.124
	1.786	2.927	2.392	3.014	2.82	2.389	2.515	2.886	2.112
	1.625	3.137	2.326	3.057	2.826	2.393	2.66	3.013	2.123
	1.673	3.013	2.265	2.861	2.856	2.345	2.695	2.856	2.156

Table 2: Mean Absorbance Values at 540 nm (arbitary units)

Time/h	Hep G2	SkHep -1	C3A	PLC/P RF/5	Hep3B	WIDR	CAC O2	HT29	SW620
24	0.073	0.677	0.354	0.993	0.832	0.355	0.461	0.558	0.373
48	0.248	1.595	0.934	1.858	1.238	0.924	0.725	1.105	0.548
72	0.525	2.876	1.421	2.425	1.654	1.36	1.188	2.156	0.725
96	1.111	2.944	1.674	3.036	2.351	1.781	1.924	2.765	1.166
120	1.724	2.996	2.306	2.935	2.859	2.369	2.593	2.881	2.128

Table 3: Standard deviation of data

Time/h	Hep G2	SkHep -1	C3A	PLC/P RF/5	Hep3B	WIDR	CAC O2	HT29	SW620
24	0.007	0.016	0.013	0.026	0.01	0.015	0.024	0.034	0.019
48	0.015	0.0506	0.013	0.116	0.12	0.029	0.037	0.054	0.018
72	0.025	0.0331	0.067	0.061	0.233	0.119	0.085	0.03	0.029
96	0.052	0.104	0.211	0.012	0.159	0.106	0.178	0.034	0.0116
120	0.081	0.103	0.067	0.0118	0.052	0.025	0.098	0.1	0.018

Appendix 3.2: Data for SRB Inoculation Densities

Table 1: Mean absorbance measurements at 540 nm for HCC cell lines

(arbitary units). (±Standard Deviation)

Cell Line	Inoculation Density	24 h	48 h	72 h	96 h	120 h
HepG2	$5x10^3$	-	-	-	-	-
	$1x10^4$	0.074 (0.006)	0.248 (0.015)	0.525 (0.025)	1.112 (0.052)	1.724 (0.089)
	$2x10^4$	0.163 (0.011)	0.517 (0.009)	1.156 (0.133)	2.192 (0.022)	2.421 (0.024)
	$4x10^4$	0.310 (0.02)	0.941 (0.02)	2.059 (0.055)	2.546 (0.071)	2.422 (0.121)
	$5x10^4$	0.601 (0.041)	1.729 (0.045)	2.542 (0.043)	2.742 (0.05)	2.607 (0.045)
SKHep -1	$5x10^3$	0.466 (0.024)	1.057 (0.048)	2.427 (0.135)	2.886 (0.071)	2.941 (0.087)
	$1x10^4$	0.671 (0.025)	1.602 (0.039)	2.856 (0.029)	2.887 (0.129)	3.048 (0.173)
	$2x10^4$	1.378 (0.052)	2.331 (0.075)	3.115 (0.163)	3.136 (0.136)	3.09 (0.156)
	$4x10^4$	2.375 (0.031)	2.480 (0.089)	3.326 (0.162)	3.345 (0.16)	3.049 (0.039)
	$5x10^4$	2.485 (0.0144)	2.513 (0.04)	3.475 (0.261)	3.297 (0.033)	3.073 (0.066)
C3A	$5x10^3$	0.146 (0.005)	0.390 (0.009)	0.682 (0.01)	1.063 (0.047)	1.407 (0.048)
	$1x10^4$	0.354 (0.013)	0.934 (0.013)	1.421 (0.067)	1.674 (0.211)	2.306 (0.066)
	$2x10^4$	0.593 (0.021)	1.735 (0.025)	2.221 (0.02)	2.495 (0.02)	2.649 (0.117)
	$4x10^4$	1.212 (0.05)	2.319 (0.025)	2.521 (0.047)	2.664 (0.052)	2.86 (0.098)
	$5x10^4$	1.256 (0.049)	2.359 (0.055)	2.427 (0.086)	2.779 (0.104)	2.66 (0.049)
PLC/P RF/5	$5x10^3$	0.541 (0.01)	0.971 (0.091)	1.793 (0.058)	2.650 (0.0133)	2.741 (0.036)
	$1x10^4$	0.993 (0.026)	1.858 (0.116)	2.425 (0.061)	3.036 (0.011)	2.935 (0.118)
	$2x10^4$	1.842 (0.019)	2.438 (0.042)	2.632 (0.031)	3.085 (0.035)	2.971 (0.084)
	$4x10^4$	2.596 (0.046)	2.706 (0.099)	2.717 (0.063)	2.991 (0.063)	2.5402 (0.144)
	$5x10^4$	2.654 (0.04)	2.644 (0.089)	2.472 (0.031)	2.651 (0.099)	2.058 (0.173)
Hep3B	$5x10^3$	0.343 (0.027)	0.656 (0.133)	0.695 (0.107)	2.351 (0.159)	2.412 (0.145)
	$1x10^4$	0.832 (0.01)	1.238 (0.12)	1.654 (0.233)	1.497 (0.175)	2.859 (0.052)
	$2x10^4$	1.695 (0.1)	2.336 (0.154)	2.599 (0.112)	2.858 (0.155)	2.982 (0.087)
	$4x10^4$	2.636 (0.036)	2.573 (0.077)	3.089 (0.205)	3.145 (0.163)	2.914 0.141)
	$5x10^4$	2.342 (0.29)	2.643 (0.115)	2.935 (0.033)	2.988 (0.032)	2.305 (0.313)

Table 2: Absorbance measurements at 540 nm for CRC cell lines

(arbitary units) (±Standard Deviation)

Cell Line	Inoculation Density	24 h	48 h	72 h	96 h	120 h
WIDR	$5x10^3$	0.140 (0.024)	0.382 (0.012)	0.696 (0.01)	1.113 (0.054)	1.368 (0.057)
	$1x10^4$	0.355 (0.015)	0.924 (0.029)	1.360 (0.119)	1.781 (0.106)	2.369 (0.025)
	$2x10^4$	0.580 (0.032)	1.669 (0.039)	2.172 (0.028)	2.500 (0.062)	2.771 (0.055)
	$4x10^4$	1.302 (0.013)	2.345 (0.041)	2.469 (0.048)	2.736 (0.098)	3.072 (0.082)
	$5x10^4$	1.265 (0.093)	2.359 (0.023)	2.435 (0.027)	2.812 (0.037)	2.774 (0.141)
CACO2	$5x10^3$	0.317 (0.013)	0.496 (0.021)	0.802 (0.006)	1.312 (0.106)	2.162 (0.195)
	$1x10^4$	0.462 (0.023)	0.725 (0.037)	1.188 (0.085)	1.924 (0.178)	2.593 (0.098)
	$2x10^4$	0.901 (0.06)	1.361 (0.082)	2.382 (0.136)	2.676 (0.077)	2.815 (0.016)
	$4x10^4$	1.832 (0.084)	2.202 (0.06)	2.948 (0.092)	2.891 (0.095)	2.932 (0.098)
	$5x10^4$	2.099 (0.039)	2.314 (0.053)	2.881 (0.102)	2.862 (0.079)	2.949 (0.097)
HT29	$5x10^3$	0.226 (0.026)	0.521 (0.01)	1.165 (0.066)	2.034 (0.12)	2.196 (0.107)
	$1x10^4$	0.558 (0.034)	1.106 (0.054)	2.156 (0.029)	2.765 (0.04)	2.881 (0.1)
	$2x10^4$	1.302 (0.345)	1.919 (0.036)	2.861 (0.03)	3.090 (0.087)	3.089 (0.117)
	$4x10^4$	2.250 (0.055)	2.508 (0.036)	3.333 (0.04)	3.441 (0.263)	3.126 (0.1)
	$5x10^4$	2.313 (0.081)	2.538 (0.051)	3.335 (0.2)	3.437 (0.176)	3.181 (0.152)
SW620	$5x10^3$	0.222 (0.073)	0.285 (0.027)	0.394 (0.02)	0.573 (0.03)	1.153 (0.06)
	$1x10^4$	0.373 (0.019)	0.548 (0.018)	0.725 (0.029)	1.166 (0.012)	2.128 (0.018)
	$2x10^4$	0.752 (0.022)	1.051 (0.056)	1.532 (0.06)	2.225 (0.054)	2.525 (0.105)
	$4x10^4$	1.587 (0.161)	2.032 (0.047)	2.397 (0.105)	2.522 (0.043)	2.608 (0.095)
	$5x10^4$	1.845 (0.04)	2.221 (0.077)	2.533 (0.111)	2.752 (0.047)	2.824 (0.068)

Appendix 3.3: Data for SRB HCC Chemosensitivity Assays

Survival as percentage of control (±SEM)

Table 1: Cisplatin

Cisplatin (μM)	Hep3 B		Cisplatin (μM)	PLC/P RF/5		Cisplatin (μM)	C3A		Cisplatin (μM)	HepG2	SkHep-1
0.01	100.0 (0.7)		**0.01**	100.0 (0.98)		**0.01**	100.0 (1.17)		**0.01**	100 (1.59)	100.0 (1.87)
0.15	91.9 (0.85)		**0.045**	92.5 (1.22)		**0.045**	96.81 (1.06)		**1**	93.2 (1.05)	92.3 (2.42)
0.19	96.3 (0.86)		**0.137**	94.29 (0.72)		**0.137**	95.9 (1.06)		**4**	92.3 (2.32)	90.7 (2.85)
0.76	95.34 (0.59)		**0.411**	95.23 (1.34)		**0.38**	82.81 (3.75)		**7**	84.3 (3.96)	84.6 (2.69)
1.56	95.09 (0.47)		**1.234**	93.88 (0.81)		**1.2**	62.48 (3.60)		**10**	86.0 (4.02)	89.7 (0.77)
3.12	90.77 (0.57)		**3.7**	94.7 (1.29)		**3.7**	40.18 (2.18)		**40**	14.3 (3.53)	2.2 (0.25)
6.25	72.28 (1.26)		**11.1**	91.04 (1.57)		**11.1**	21.32 (1.13)		**70**	3.9 (0.11)	2.7 (0.308)
12.5	11.27 (0.53)		**33.3**	62.05 (3.08)		**33.3**	8.84 (0.50)		**100**	5.1 (0.31)	6.2 (0.215)
25.0	5.23 (0.27)		**40**	3.8 (0.3)		**100**	8.85 (0.26)				
50.0	4.2 (0.31)		**100**	4.29 (0.7)							
100	2.8 (0.21)										

Table 2: Etoposide

Etoposide (μM)	Hep3 B		Etoposide (μM)	PLC/P RF/5		Etoposide (μM)	C3A		Etoposide (μM)	HepG2	SkHep-1
0.01	100.0 (2.66)		**0.01**	100.0 (1.047)		**0.01**	100.0 (1.43)		**0.01**	100.0 (1.64)	100.0 (2.49)
0.45	93.7 (1.66)		**0.2**	94.91 (2.42)		**0.2**	98.26 (0.92)		**1**	86.6 (1.18)	77.3 (1.53)
0.8	96.6 (0.50)		**0.5**	98.0 (0.935)		**0.45**	98.46 (0.99)		**5**	79.9 (1.96)	51.7 (2.087)
1.7	92.7 (0.74)		**1.7**	93.78 (1.27)		**1.37**	83.8 (2.69)		**10**	73.2 (1.82)	47.8 (2.15)
3.45	84.1 (1.05)		**5.0**	91.85 (1.26)		**4.1**	64.92 (2.57)		**50**	49.3 (2.009)	18.6 (3.04)
6.9	61.7 (0.72)		**13.8**	82.95 (1.839)		**12.3**	53.7 (3.52)		**100**	44.2 (2.02)	11.1 (2.46)
13.8	29.4 (1.31)		**40.0**	62.94 (1.99)		**37.0**	41.18 (1.37)		**500**	6.6 (1.73)	0.6 (0.158)
27.7	13.9 (0.59)		**166.0**	48.02 (2.02)		**111.0**	44.1 (2.05)				
55.5	10.59 (0.43)		**400.0**	3.98 (3.98)		**333.0**	9.29 (1.19)				
166.0	9.47 (0.99)										
333.0	1.56 (0.13)										

Table 3: 5-FU

5-FU (μM)	Hep3B	PLC/P RF/5	C3A		5-FU (μM)	HepG2	SkHep -1
0.01	100.0 (3.20)	100.0 (2.36)	100.0 (1.73)		**0.01**	100.0 (2.22)	100.0 (1.99)
0.05	102.1 (0.91)	93.11 (3.40)	104.6 (0.62)		**1.0**	91.1 (1.109)	88.4 (0.98)
0.152	100.1 (1.77)	97.09 (2.18)	105.5 (0.71)		**5.0**	88.0 (1.68)	90.8 (1.54)
0.45	94.85 (1.14)	96.37 (2.31)	105.2 (0.50)		**10.0**	82.0 (1.126)	68.6 (1.16)
1.37	87.1 (1.80)	95.21 (1.65)	102.5 (1.83)		**50.0**	71.6 (1.55)	56.5 (1.92)
4.1	76.4 (2.34)	91.41 (2.247)	66.69 (1.49)		**100.0**	68.6 (1.18)	50.3 (2.08)
12.3	72.44 (1.70)	80.9 (3.36)	39.66 (1.99)		**500.0**	69.3 (1.85)	17.4 (1.54)
37.0	64.5 (2.17)	69.48 (2.18)	29.94 (1.06)		**1000.0**	65.8 (1.94)	4.7 (0.55)
111.0	38.09 (1.46)	57.68 (1.57)	31.56 (1.09)				
333.0	14.48 (0.55)	34.91 (1.40)	18.93 (0.62)				
1000.0	11.07 (0.48)	21.7 (0.683)	7.56 (0.40)				

Table 4: Melphalan

Melphalan (μM)	Hep3B	PLC/P RF/5	C3A	HepG2	SkHep-1
0.01	100.0 (0.82)	100.0 (4.050)	100.0 (2.82)	100.0 (3.65)	100.0 (1.55)
1	95.6 (0.455)	108.5 (0.530)	99.3 (2.31)	90.2 (6.8)	95.5 (0.37)
4	98.45 (0.88)	110.62 (1.12)	78.66 (2.78)	94.3 (4.53)	92.5 (1.086)
7	97.37 (1.03)	112.87 (2.2)	72.5 (3.84)	88.0 (5.38)	90.9 (1.011)
10	95.77 (0.508)	110.0 (2.15)	67.3 (2.63)	89.0 (4.52)	91.1 (0.72)
40	82.2 (0.52)	95.39 (1.64)	47.4 (1.54)	51.1 (8.81)	47.8 (3.68)
70	21.86 (0.74)	78.89 (1.68)	28.5 (1.68)	22.5 (6.18)	12.9 (1.06)
100	4.847 (0.23)	67.32 (2.1)	26.7 (2.09)	11.9 (2.95)	4.4 (1.41)
400	1.47 (0.066)	3.07 (0.15)	13.23 (0.84)	4.0 (1.08)	0.4 (0.052)
700	1.48 (0.103)	2.15 (0.09)	2.83 (0.14)	0.7 (0.07)	0.3 (0.046)
1000	1.52 (0.138)	1.77 (0.13)	1.66 (0.23)	0.8 (0.17)	0

Appendix 3.4: Data for SRB CRC Chemosensitivity Assays

Survival as percentage of control (±SEM)

Table 1: Cisplatin

Cisplatin (μM)	SW620		Cisplatin (μM)	CACO2	HT-29		Cisplatin (μM)	WIDR
0.01	100.0 (0.92)		**0.01**	100.0 (2.72)	100.0 (3.78)		**0.01**	100.0 (0.56)
0.15	99.92 (0.75		**1**	92.8 (2.18)	76.2 (2.19)		**0.45**	97.0 (1.04)
0.45	101.8 (2.68)		**4**	85.4 (4.56)	65.2 (2.3)		**1.37**	93.99 (0.10)
1.37	103.6 (2.33)		**7**	68.2 (1.17)	48.6 (3.39)		**4.11**	90.93 (0.97)
4.11	101.3 (2.04)		**10**	58.1 (5.15)	43.9 (3.15)		**12**	57.16 (0.68)
12.00	96.47 (2.21)		**40**	21.7 (2.82)	4.6 (0.677)		**37**	13.67 (1.04)
37.00	58.95 (1.77)		**70**	19.4 (1.23)	2.7 (0.23)		**111**	3.97 (1.50)
111.00	23.77 (2.33)		**100**	19.9 (0.29)	1.5 (15.4)			
333.00	15.23 (0.70)							

Table 2: Etoposide

Etoposide (μM)	SW620		Etoposide (μM)	HT-29		Etoposide (μM)	WIDR		Etoposide (μM)	CACO2
0.01	100.0 (1.11)		**0.01**	100.0 (3.01)		**0.1**	100.0 (0.151)		**0.1**	100.0 (8.009)
1.6	93.28 (0.92)		**0.7**	86.0 (2.71)		**0.7**	86.69 (1.096)		**10**	75.1 (6.99)
3.3	85.07 (2.09)		**1**	89.8 (1.31)		**1.6**	87.61 (0.79)		**40**	31.4 (0.98)
6.60	72.17 (2.31)		**4**	57.7 (9.18)		**3.30**	78.13 (0.121)		**70.00**	25.1 (1.53)
13.20	58.59 (2.39)		**7**	37.4 (10.9)		**6.60**	55.28 (0.9)		**100**	27.8 (1.41)
26.40	52.07 (1.64)		**10**	35.3 (10.2)		**13.20**	23.22 (1.15)		**400**	6.6 (2.25)
52.80	44.03 (2.07)		**40**	7.5 (2.39)		**26.40**	7.92 (0.39)			
105.60	32.68 (1.89)		**70**	11.0 (3.36)		**52.80**	6.83 (0.2)			
211.00	2.7 (0.17)		**100**	11.8 (3.76)		**105.60**	7.017 (0.25)			
422.00	3.18 (0.172)		**500**	0.6 (1.3)						

Table 3: 5-FU

5-FU (μM)	SW620	WIDR		5-FU (μM)	HT-29	CACO2
0.1	100.0 (8.5)	100.0 (1.4)		**0.1**	100.0 (2.87)	100.0 (2.8)
0.15	95.62 (8.8)	96.8 (0.204)		**1.0**	75.1 (2.007)	89.0 (3.03)
0.45	91.68 (7.56)	92.3 (2.68)		**5.0**	75.8 (2.82)	87.2 (1.43)
1.37	93.69 (7.02)	88.4 (0.95)		**10.0**	68.0 (2.066)	84.4 (1.7)
4.10	92.7 (7.077)	83.5 (1.23)		**50.0**	59.0 (3.46)	83.3 (2.11)
12.30	91.9 (8.07)	76.9 (1.45)		**100.0**	35.0 (4.35)	78.7 (1.488)
37.00	85.15 (7.99)	79.3 (2.22)		**500.0**	7.9 (0.85)	65.2 (1.46)
111.0	68.69 (6.327)	55.39 (1.22)		**1000.0**	5.2 (0.59)	25.4 (10.07)
333.0	42.67 (3.43)	40.11 (2.47)				
1000	30.56 (3.25)	22.9 (0.59)				
2000	27.77 (2.7)	5.6 (0.66)				

Table 4: Melphalan

Melphalan (μM)	WIDR	CACO2	HT-29	SW620
0.01	100.0 (0.49)	100.0 (1.76)	100.0 (1.937)	100.0 (3.65)
1	98.0 (1.115)	96.8 (1.11)	96.4 (1.011)	97.42 (6.8)
4	96.47 (2.5)	97.9 (1.26)	86.7 (2.84)	98.0 (4.53)
7	92.5 (0.68)	95.7 (1.89)	82.6 (3.89)	96.32 (5.38)
10	82.9 (1.65)	96.0 (1.62)	80.2 (3.79)	95.8 (4.52)
40	85.2 (2.9)	84.5 (1.81)	54.4 (3.59)	92.65 (8.81)
70	59.21 (2.107)	63.6 (4.98)	31.5 (1.39)	76.68 (6.18)
100	36.78 (0.17)	43.2 (6.55)	16.4 (2.8)	58.3 (2.95)
400	5.6 (0.39)	1.3 (0.19)	3.4 (0.29)	6.3 (1.08)
700	0.77 (1.4)	0.7 (0.067)	0.8 (0.07)	0.9 (0.07)
1000	2.0 (0.068)	0.8 (0.08)	0.8 (0.208)	1.2 (1.2)

Appendix 4.1: Data for SRB assays for P-gp reversal in selected P-gp positive HCC & CRC cell lines

Survival as percentage of control, ±SEM

Table 1: HCC

Etoposide (μM)	HepG2	HepG2 & vpl (6μM)		Vincristine (μM)	HepG2	HepG2 & vpl (6μM)
0.01	100.0 (1.64)	98.53 (3.29)		**0.01**	100.0 (3.6)	100.0 (2.22)
1.0	86.6 (1.18)	87.9 (2.97)		**0.1**	84.0 (4.7)	76.0 (3.4)
5.0	79.9 (1.96)	73.69 (3.5)		**0.4**	76.0 (2.9)	52.8 (4.22)
10.0	73.2 (1.82)	71.88 (1.66)		**1.0**	62.0 (3.33)	48.2 (6.0)
50.0	49.3 (2.01)	51.12 (2.65)		**4.0**	54.0 (6.3)	42.0 (4.33)
100.0	44.2 (2.02)	41.93 (3.26)		**10.0**	46.0 (2.78)	40.0 (4.0)
500.0	6.6 (1.73)	5.59 (3.07)		**40.0**	40.0 (5.9)	36.0 (2.77)
				100.0	36.0 (4.8)	32.0 (10.0)

Table 2: CRC

Etoposide (μM)	SW620	SW620& vpl (6μM)		Vincristine (μM)	SW620	SW620& vpl (6μM)
0.01	100.0 (2.99)	100.0 (2.68)		**0.01**	100.0 (1.57)	100.0 (1.14)
1.6	998.0 (1.9)	96.8 (3.3)		**0.046**	73.42 (0.94)	79.7 (1.69)
3.3	86.4 (1.59)	76.0 (6.4)		**0.137**	72.59 (2.12)	76.2 (1.71)
6.6	75.95 (3.39)	65.29 (1.03)		**0.411**	74.5 (1.54)	73.1 (2.69)
13.2	59.92 (1.147)	51.6 (1.11)		**1.23**	74.17 (2.16)	71.81 (2.82)
26.4	49.7 (1.104)	46.1 (2.88)		**3.7**	76.01 (2.9)	77.47 (2.33)
52.8	43.3 (5.28)	40.048 (3.12)		**11.1**	76.7 (3.57)	72.99 (1.59)
105.6	31.22 (1.13)	25.8 (1.24)		**33.3**	67.9 (2.04)	72.19 (4.5)
211.0	2.847 (0.13)	2.787 (0.12)		**100.0**	45.3 (1.04)	46.7 (1.29)
422.0	3.2 (0.134)	3.33 (0.12)		**225.0**	10.77 (0.43)	11.8 (0.5)

Appendix 5.1: Data for GSH assays in HCC & CRC cell lines

Table 1: HCC

Cell Lines	Total GSH I	Total GSH II	Total GSH III	Mean (nM/10^6 cells)	SEM
HepG2	2.1	9.7	9.6	7.13	2.51
SK-Hep-1	4.5	7.6	6.25	6.11	0.89
C3A	1.75	5.2	7.4	4.58	1.097
PLC/PRF/5	2.7	6.5	4.55	3.53	0.57
Hep3B	2.4	4.2	4.0	4.78	1.64

Cell Lines	+ BSO I	+ BSO II	+ BSO III	Mean (nM/10^6 cells)	SEM
HepG2	1.2	2.8	2.4	2.13	0.48
SK-Hep-1	2.4	4.8	1.25	2.81	1.04
C3A	1.8	3.7	1.1	3.0	0.87
PLC/PRF/5	2.8	4.6	1.6	2.15	0.92
Hep3B	1.25	4.0	1.2	2.2	0.77

Table 2: CRC

Cell Lines	Total GSH I	Total GSH II	Total GSH III	Mean (nM/10^6 cells)	SEM
WIDR	2.80	5.10	6.10	4.67	0.98
CACO2	1.80	11.25	6.50	6.52	2.73
HT-29	1.75	7.80	4.70	4.75	1.75
SW620	2.10	4.00	6.00	4.03	1.12

Cell Lines	+ BSO I	+ BSO II	+ BSO III	Mean (nM/10^6 cells)	SEM
WIDR	1.50	3.80	0.75	2.02	0.92
CACO2	2.30	4.40	4.10	3.6	0.65
HT-29	2.45	2.50	3.60	2.85	0.37
SW620	2.50	1.60	2.10	2.07	0.26

Appendix 5.2: Data for effect of BSO (50 μM) on IC_{50}s with cisplatin in HCC & CRC cell lines

Survival as percentage of control, ±SEM

Table 1a: Untreated HCC cells

Cisplatin (μM)	HepG2	SkHep -1		Cisplatin (μM)	Hep3B		Cisplatin (μM)	PLC/PRF/ 5		Cisplatin (μM)	C3A
0.01	100.0	100.0		**0.1**	100.0		**0.01**	100.0		**1.0**	100.0
4.0	98.89 (4.35)	90.48 (4.49)		**0.19**	100.43 (0.25)		**0.045**	92.50 (1.22)		**1.5**	84.48 (2.52)
6.0	94.47 (1.70)	89.38 (1.15)		**0.39**	101.58 (2.76)		**0.137**	94.29 (0.72)		**3.1**	76.22 (2.07)
8.0	94.04 (1.076)	88.53 (2.47)		**0.78**	99.86 (1.44)		**0.41**	95.23 (1.34)		**6.2**	55.79 (6.10)
10.0	92.91 (1.07)	87.61 (2.28)		**1.5**	98.94 (1.21)		**1.23**	93.88 (0.81)		**12.5**	28.97 (6.61)
20.0	78.25 (3.06)	63.15 (6.42)		**3.12**	100.38 (1.35)		**3.7**	94.70 (1.29)		**25.0**	22.74 (2.93)
30.0	24.95 (3.13)	32.33 (5.59)		**6.3**	97.5 (2.98)		**11.1**	91.04 (1.57)		**50.0**	20.81 (6.39)
40.0	20.87 (2.29)	21.27 (9.75)		**12.5**	76.83 (4.06)		**33.3**	62.05 (3.08)		**100.0**	20.53 (7.20)
60.0	16.28 (1.98)	9.40 (3.45)		**25.0**	15.89 (9.43)		**40.0**	3.80 (0.30)			
80.0	24.0 (2.07)	6.96 (2.51)		**50.0**	17.56 (6.94)		**100.0**	4.29 (0.42)			
100.0	23.06 (2.56)	6.56 (3.06)		**100.0**	6.85 (3.48)						

Table 1b: HCC cells treated with BSO (50 μM)

	HepG2	SkHep -1			Hep3B			PLC/PRF/ 5			C3A
Cisplatin (μM)	**+ BSO**	**+ BSO**		**Cisplatin (μM)**	**+ BSO**		**Cisplatin (μM)**	**+ BSO**		**Cisplatin (μM)**	
0.01	100.0	100.0		**0.10**	100.0		**0.01**	100.0		**1.0**	100.0
4.0	96.20 (2.47)	89.23 (3.21)		**0.19**	98.40 (3.34)		**0.045**	90.03 (3.65)		**1.5**	93.38 (5.38)
6.0	95.84 (1.70)	87.52 (2.18)		**0.39**	93.06 (3.78)		**0.137**	91.98 (2.58)		**3.1**	78.77 (3.59)
8.0	93.07 (1.05)	87.03 (1.95)		**0.78**	92.49 (0.95)		**0.411**	88.58 (0.84)		**6.2**	55.28 (2.20)
10.0	88.89 (1.36)	84.37 (1.45)		**1.5**	90.40 (3.14)		**1.234**	89.54 (0.99)		**12.5**	24.13 (4.16)
20.0	29.98 (7.96)	38.94 (6.66)		**3.12**	82.20 (6.33)		**3.7**	87.36 (3.51)		**25.0**	12.65 (4.91)
30.0	21.05 (9.0)	16.43 (8.14)		**6.3**	73.23 (2.15)		**11.10**	79.36 (2.40)		**50.0**	9.91 (2.76)
40.0	25.7 (9.68)	12.62 (3.92)		**12.5**	18.92 (6.98)		**33.30**	35.55 (2.00)		**100.0**	8.15 (2.98)
60.0	15.93 (0.64)	5.62 (1.6)		**25.0**	15.32 (5.73)		**40.0**	1.55 (1.75)			
80.0	8.85 (2.23)	6.10 (2.54)		**50.0**	9.94 (1.52)		**100.0**	1.55 (3.90)			
100.0	5.12 (0.39)	8.21 (3.22)		**100.0**	15.77 (0.36)						

Table 2a: Untreated CRC cells

Cisplatin (μM)	CAC02	HT-29		Cisplatin (μM)	SW620		Cisplatin (μM)	WIDR
0	100.0	100.0		**0.10**	100.0		**0.10**	100.0
1.5	99.32 (5.91)	91.48 (0.85)		**0.15**	99.92 (0.75)		**0.45**	97.00 (5.70)
3.1	95.27 (9.14)	90.90 (3.28)		**0.45**	101.88 (2.68)		**1.37**	93.99 (3.99)
6.2	76.38 (6.47)	75.09 (2.66)		**1.37**	103.61 (2.33)		**4.11**	90.93 (5.70)
12.5	47.57 (0.41)	24.65 (1.72)		**4.11**	101.32 (2.043)		**12.0**	57.16 (2.90)
25.0	25.82 (7.59)	1.30 (4.08)		**12.0**	96.47 (2.21)		**37.0**	13.67 (8.60)
50.0	16.33 (8.28)	3.10 (2.58)		**37.0**	58.95 (1.77)		**111.0**	3.97 (2.43)
100.0	13.67 (7.25)	6.80 (1.69)		**111.0**	23.77 (2.33)			
200.0	14.71 (6.14)	5.30 (1.08)		**333.0**	15.23 (0.70)			

Table 2b: HCC cells treated with BSO (50 μM)

Cisplatin (μM)	CAC02	HT-29		Cisplatin (μM)	SW620		Cisplatin (μM)	WIDR
	+ BSO	**+ BSO**			**+ BSO**			**+ BSO**
0.1	100.0	100.00		**0.10**	100.0 (3.20)		**0.1**	100.0 (3.50)
1.5	92.78 (2.18)	101.47 (0.84)		**0.15**	93.50 (4.70)		**0.45**	98.99 (7.32)
3.1	96.77 (4.12)	102.58 (5.08)		**0.45**	99.59 (6.0)		**1.37**	96.74 (2.80)
6.2	80.72 (0.96)	75.23 (2.26)		**1.37**	92.56 (2.77)		**4.11**	79.60 (5.80)
12.5	42.14 (9.03)	14.87 (3.47)		**4.11**	90.40 (4.78)		**12.0**	41.70 (1.89)
25.0	23.0 (1.27)	4.611 (2.41)		**12.0**	69.04 (5.20)		**37.0**	7.95 (4.90)
50.0	16.09 (2.61)	5.098 (4.56)		**37.0**	38.49 (3.80)		**111.0**	2.50 (4.20)
100.0	14.34 (3.57)	6.57 (0.46)		**111.0**	13.70 (3.11)			
200.0	16.73 (8.09)	10.65 (1.26)		**333.0**	9.11 (1.60)			

Appendix 6.1: Data for IC_{50}s after 1 h exposure to cisplatin in HCC & CRC cell lines

Survival as percentage of control, ±SEM

Table 1a: HCC cells

Cisplatin (μM)	HepG2	SkHep-1	C3A	PLC/PR F/5	Hep3B
0.01	100.0 (0.58)	100.0 (2.38)	100.0 (1.28)	100.0 (3.64)	100.0 (1.02)
0.045	99.21 (2.43)	100.0 (2.33)	76.97 (3.11)	100.0 (3.0)	100.0 (1.7)
0.137	98.30 (2.88)	99.45 (3.85)	68.30 (4.24)	98.34 (2.38)	97.61 (1.69)
0.411	99.30 (3.02)	97.78 (1.70)	66.02 (4.23)	96.91 (4.62)	87.50 (4.23)
1.23	98.86 (3.40)	97.0 (2.27)	68.10 (3.85)	92.53 (2.28)	81.0 (2.47)
3.7	101.65 (3.30)	88.80 (4.37)	71.07 (5.35)	86.39 (2.10)	74.59 (1.47)
11.1	81.12 (4.66)	91.66 (2.11)	50.19 (2.83)	92.22 (2.23)	64.45 (2.88)
33.3	75.30 (9.98)	77.28 (2.37)	42.16 (1.44)	81.37 (2.87)	44.0 (3.47)
60.0	63.70 (3.32)	67.70 (4.32)	34.6 (3.5)	74.9 (2.19)	41.63 (1.66)
80.0	67.70 (3.66)	65.39 (2.56)	29.11 (4.62)	65.0 (3.7)	37.43 (5.35)
100.0	37.30 (4.17)	42.0 (1.17)	22.50 (1.52)	45.83 (2.36)	19.66 (2.17)

Table 1b: CRC cells

Cisplatin (μM)	SW620		Cisplatin (μM)	HT-29
0.01	100.0 (1.77)		**0.01**	100.0 (4.5)
0.15	99.82 (4.37)		**1.0**	96.23 (3.19)
0.45	103.2 (6.30)		**4.0**	95.45 (3.6)
1.37	104.54 (3.50)		**7.0**	88.71 (5.21)
4.11	100.47 (2.06)		**10.0**	73.90 (6.0)
12.0	98.33 (3.90)		**40.0**	54.60 (5.4)
37.0	82.70 (2.77)		**70.0**	32.70 (3.88)
111.0	53.84 (3.30)		**100.0**	31.50 (3.49)
333.0	41.20 (1.24)			

Appendix 6.2: Data for Comet Assays after 1 h exposure to cisplatin in HCC & CRC cell lines

Interstrand Cross Links represented as % decrease in Tail Moment ±SEM

Table 1a: HCC cells

Cell Line	Time (h)	Cisplatin (μM)			
		10	25	45	100
HepG2	6	4.0 ± 5.7	22.4 ± 4.7	13.6 ± 6.7	47.12 ± 2.3
	12	17.1 ± 3.2	27.47 ± 3.5	40.3 ± 4.3	68.0 ± 3.4
	18	0.0 ± 5.3	16.3 ± 6.5	36.9 ± 2.8	76.6 ± 2.3
	24	0.0 ± 5.0	0.0 ± 6.4	17.3 ± 2.1	58.2 ± 4.0
	48	0.0 ± 1.33	2.0 ± 3.6	15.4 ± 3.88	49.1 ± 1.77
	72	0.0 ± 12.4	0.0 ± 1.22	10.0 ± 5.4	33.8 ± 3.4
SkHep-1	6	28.66 ± 3.8	37.3 ± 1.2	48.9 ± 2.4	58.8 ± 4.7
	12	38.0 ± 7.0	33.0 ± 4.3	51.65 ± 3.4	72.0 ± 4.6
	18	13.5 ± 4.5	19.0 ± 4.3	43.47 ± 5.0	59.89 ± 3.99
	24	9.8 ± 3.22	0.0 ± 5.9	19.0 ± 6.7	49.3 ± 7.4
	48	0.0 ± 4.98	0.0 ± 6.55	19.1 ± 2.44	49.9 ± 3.9
	72	0.0 ± 9.0	0.0 ± 12.4	11.22 ± 3.2	24.05 ± 2.3
C3A	6	25.11 ± 3.8	32.6 ± 1.2	59.9 ± 2.4	67.2 ± 4.7
	12	39.66 ± 7.0	59.0 ± 4.3	64.33 ± 3.4	89.46 ± 4.6
	18	42.8 ± 4.5	65.31 ± 4.3	69.08 ± 5.0	91.2 ± 3.99
	24	35.9 ± 3.22	42.1 ± 5.9	62.45 ± 6.7	82.0 ± 7.4
	48	32.3 ± 4.98	33.8 ± 6.55	32.58 ± 2.44	92.87 ± 3.9
	72	30.0 ± 11.0	35.0 ± 12.0	39.0 ± 3.2	86.72 ± 2.3
PLC/PRF/ 5	6	0.0 ± 0.0	0.56 ± 3.0	9.88 ± 2.38	19.2 ± 4.62
	12	15.93 ± 2.28	19.23 ± 2.1	25.0 ± 2.23	56.0 ± 2.55
	24	23.58 ± 4.9	29.7 ± 2.94	35.5 ± 1.86	59.18 ± 2.17
	48	8.1 ± 3.192	29.0 ± 1.42	32.2 ± 2.36	38.56 ± 2.1
	72	9.48 ± 4.3	18.53 ± 3.5	27.11 ± 5.8	35.68 ± 3.77
Hep3B	6	20.6 ± 5.7	37.7 ± 4.7	47.6 ± 6.77	67.5 ± 2.3
	12	29.2± 3.2	34.4 ± 3.5	60.1 ± 4.3	84.8 ± 3.4
	18	18.0 ± 6.0	29.0 ± 6.5	57.3 ± 9.8	82.0 ± 2.3
	24	10.0 ± 5.0	23.5 ± 6.4	40.0 ± 2.1	84.0 ± 4.0
	48	12.0 ± 4.6	14.1 ± 6.9	42.0 ± 3.88	88.42 ± 1.77
	72	9.0 ± 15.0	6.0 ± 3.2	41.0 ± 5.4	84.6 ± 3.4

Table 1b: CRC cells

Cell Line	Time (h)	Cisplatin (μM)			
		10	25	45	100
HT-29	6	7.0 ± 5.31	7.6 ± 4.58	19.7 ± 5.06	49.7 ± 7.8
	12	16.0 ± 4.3	25.8 ± 4.15	47.2 ± 4.2	63.11 ± 4.32
	24	12.0 ± 3.1	19.0 ± 2.98	35.0 ± 3.99	65.1 ± 1.4
	48	10.21 ± 2.32	16.5 ± 3.26	33.21 ± 3.7	62.35 ± 4.6
	72	5.88 ± 3.87	9.76 ± 4.12	27.78 ± 3.7	58.35 ± 4.82
SW620	6	0.0 ± 0.0	3.0 ± 2.33	13.3 ± 2.41	33.0 ± 2.1
	12	12.1 ± 2.73	21.1 ± 2.6	27.0 ± 3.0	60.33 ± 3.54
	24	4.58 ± 2.75	11.0 ± 2.12	21.36 ± 2.01	58.64 ± 3.24
	48	1.4 ± 3.55	10.2 ± 2.8	16.0 ± 1.85	63.77 ± 2.95
	72	1.1 ± 5.9	8.2 ± 2.58	13.0 ± 3.06	45.71 ± 2.73

Appendix 7.1: Raw data for formation of ICLs in *in-vivo* intrahepatic CRC and HCC xenografts of nude mice

A: Percentage decrease of Tail Moment of SW620 cells treated with 4 mg/kg (i.v.) cisplatin as assessed by the comet assay

Values are the mean of 25 measurements
(*Two-tailed unpaired t-test, n=12)

Time (h)	Site & Depth (cm)		Mouse & Tumour Number						
			Mouse 1		Mouse 2		Mouse 3		P
			T1	T2	T1	T2	T1	T2	
6	A	0.25	25.0	18.0	17.0	27.0	23.0	10.0	
		0.5	22.0	19.0	9.0	8.0	29.0	12.0	
	B	0.25	15.0	31.0	10.0	8.0	27.0	15.0	
		0.5	17.0	22.0	11.0	18.0	18.0	15.0	
	*Total	0.25 *vs* 0.5							P=0.451
12	A	0.25	50.0	52.0	33.0	46.0	58.0	17.0	
		0.5	38.0	46.0	24.0	29.0	52.0	16.0	
	B	0.25	42.0	45.0	39.0	52.0	43.0	29.0	
		0.5	19.0	35.0	31.0	16.0	37.0	21.0	
	*Total	0.25 *vs* 0.5							P= 0.02
24	A	0.25	48.0	24.0	36.0	29.0	42.0	32.0	
		0.5	22.0	28.0	32.0	24.0	29.0	27.0	
	B	0.25	38.0	33.0	56.0	38.0	41.0	29.0	
		0.5	18.0	32.0	41.0	26.0	32.0	19.0	
	*Total	0.25 *vs* 0.5							P= 0.0057
48	A	0.25	16.0	12.0	33.0	21.0	31.0	23.0	
		0.5	26.0	32.0	26.0	31.0	19.0	27.0	
	B	0.25	24.0	19.0	18.0	29.0	15.0	26.0	
		0.5	24.0	27.0	28.0	18.0	24.0	27.0	
	*Total	0.25 *vs* 0.5							P= 0.1347
72	A	0.25	6.0	12.0	8.0	23.0	9.0	12.0	
		0.5	20.0	14.0	16.0	18.0	22.0	18.0	
	B	0.25	15.0	21.0	10.0	16.0	16.0	9.0	
		0.5	18.0	17.0	19.0	12.0	26.0	21.0	
	*Total	0.25 *vs* 0.5							P= 0.0086

B: Percentage decrease of Tail Moment of C3A cells treated with 4 mg/kg (iv) cisplatin as assessed by the comet assay

Values are the mean of 25 measurements
(*Two-tailed unpaired t-test, n=12)

Time (h)	Site & Depth (cm)		Mouse & Tumour Number						
			Mouse 1		Mouse 2		Mouse 3		P
			T1	T2	T1	T2	T1	T2	
6	A	0.25	42.0	56.0	62.0	33.0	48.0	29.0	
		0.5	37.0	55.0	42.0	38.0	52.0	32.0	
	B	0.25	49.0	52.0	48.0	39.0	45.0	18.0	
		0.5	42.0	47.0	49.0	31.0	56.0	25.0	
	*Total	0.25 *vs* 0.5							P= 0.7859
12	A	0.25	67.0	78.0	66.0	55.0	57.0	48.0	
		0.5	59.0	63.0	52.0	49.0	49.0	35.0	
	B	0.25	72.0	69.0	58.0	62.0	58.0	69.0	
		0.5	61.0	48.0	55.0	52.0	35.0	53.0	
	*Total	0.25 *vs* 0.5							P= 0.002
24	A	0.25	75.0	78.0	67.0	35.0	56.0	62.0	
		0.5	53.0	73.0	49.0	38.0	42.0	49.0	
	B	0.25	69.0	82.0	58.0	42.0	59.0	54.0	
		0.5	61.0	76.0	52.0	36.0	50.0	46.0	
	*Total	0.25 *vs* 0.5							P= 0.0983
48	A	0.25	55.0	56.0	67.0	47.0	38.0	48.0	
		0.5	48.0	56.0	57.0	38.0	42.0	50.0	
	B	0.25	49.0	59.0	63.0	56.0	32.0	52.0	
		0.5	41.0	48.0	65.0	48.0	35.0	42.0	
	*Total	0.25 *vs* 0.5							P= 0.2665
72	A	0.25	32.0	48.0	52.0	39.0	17.0	37.0	
		0.5	39.0	19.0	29.0	38.0	36.0	35.0	
	B	0.25	27.0	33.0	36.0	32.0	26.0	41.0	
		0.5	52.0	36.0	34.0	43.0	42.0	39.0	
	*Total	0.25 *vs* 0.5							P= 0.6149

Appendix 7.2: Comparison of percentage decrease in Tail Moment at different depths, sites and between tumours, with 4 mg/kg cisplatin (i.v.) on intrahepatic human xenografts in nude mice at 12 h as assessed by the comet assay

A: Depth (Two-tailed unpaired t-test) (n=25, except * n=12)

Xenograft	Site	Depth (cm)	Mouse & Tumour Number						
			Mouse 1		Mouse 2		Mouse 3		
			T1	T2	T1	T2	T1	T2	Total
SW620	A	0.25 *vs* 0.5	P = 0.043	P = 0.303	P = 0.029	P = 0.015	P = 0.20	P = 0.869	
	B	0.25 *vs* 0.5	P = 0.003	P = 0.048	P = 0.056	P<0.0001	P = 0.487	P = 0.069	
	*A & B	0.25 *vs* 0.5							P =0.02
C3A	A	0.25 *vs* 0.5	P = 0.166	P = 0.01	P = 0.073	P = 0.067	P = 0.233	P = 0.001	
	B	0.25 *vs* 0.5	P = 0.154	P = 0.013	P = 0.694	P = 0.075	P<0.0001	P = 0.002	
	*A & B	0.25 *vs* 0.5							P=0.002

B: Site (Two-tailed unpaired t-test) (n=25)

Xenograft	Depth (cm)	Site	Mouse & Tumour Number					
			Mouse 1		Mouse 2		Mouse 3	
			T1	T2	T1	T2	T1	T2
SW620	0.25	A *vs* B	P = 0.355	P = 0.167	P = 0.134	P = 0.383	P = 0.085	P = 0.048
C3A	0.25	A *vs* B	P = 0.396	P = 0.272	P = 0.332	P = 0.031	P = 0.86	P<0.0001

C: Intertumour (One-way ANOVA followed by the Bonferroni multiple t-test) (n=25)

Xenograft	Depth (cm)	Tumour Number & Site	Mouse Number		
			Mouse 1	Mouse 2	Mouse 3
SW620	0.25	T1 A *vs* T2 A	P > 0.05	P > 0.05	P < 0.001
		T1 A *vs* T2 B	P > 0.05	P < 0.01	P < 0.001
		T1 B *vs* T2 A	P > 0.05	P > 0.05	P < 0.01
		T1 B *vs* T2 A	P > 0.05	P > 0.05	P > 0.05
C3A	0.25	T1 A *vs* T2 A	P > 0.05	P > 0.05	P < 0.001
		T1 A *vs* T2 B	P > 0.05	P < 0.01	P < 0.001
		T1 B *vs* T2 A	P > 0.05	P > 0.05	P < 0.01
		T1 B *vs* T2 A	P > 0.05	P > 0.05	P > 0.05

Appendix 7.3: Raw data for proliferation in *in-vivo* intrahepatic CRC and HCC xenografts of nude mice

A: Labelling Index (LI, %) of SW620 intrahepatic xenografts treated with 4 mg/kg (i.v.) of cisplatin at 12 h, as measured with the monoclonal antibody MIB-1 against Ki-67

LI assessed in 10 high power fields (each high powered field consisted of 50-100 cells)

Xenograft	Depth (cm)	Mouse & Tumour Number					
		Mouse 1		Mouse 2		Mouse 3	
		T1	T2	T1	T2	T1	T2
SW620	0.25	14.7	17.8	14.8	11.2	8.4	13.4
		11.2	17.9	11.2	14.2	10.5	14.3
		12.6	12.7	12.4	7.4	12.6	9.1
		10.6	18.5	15.0	8.3	9.9	14.2
		14.3	12.8	13.5	13.3	11.8	12.6
		8.6	9.6	12.1	12.8	11.5	9.2
		8.2	12.9	7.9	13.0	9.8	14.4
		13.6	14.9	9.6	16.0	15.2	8.8
		15.8	12.9	13.2	14.2	14.4	11.1
		12.7	7.8	14.3	11.7	12.3	12.2
	0.5	11.6	10.3	7.4	9.2	7.5	7.8
		8.4	6.7	9.6	13.6	11.7	10.2
		6.1	4.7	5.9	8.4	11.0	6.7
		12.4	12.1	12.7	6.9	12.6	9.2
		9.1	8.2	8.6	14.3	15.0	12.7
		7.3	8.7	9.6	12.9	7.8	9.7
		8.7	5.6	5.8	6.7	11.6	9.3
		9.8	8.9	12.0	4.9	12.8	10.8
		9.1	5.1	12.3	10.2	6.7	13.5
		9.8	10.6	9.7	7.9	5.6	15.2

B: Labelling Index (LI, %) of C3A intrahepatic xenografts treated with 4 mg/kg (i.v.) of cisplatin at 12 h, as measured with the monoclonal antibody MIB-1 against Ki-67

LI assessed in 10 high power fields (each high powered field consisted of 50-100 cells)

Xenograft	Depth (cm)	Mouse & Tumour Number					
		Mouse 1		Mouse 2		Mouse 3	
		T1	T2	T1	T2	T1	T2
C3A	0.25	13.2	15.4	12.8	12.8	17.4	21.3
		24.8	16.5	17.2	15.3	21.2	13.5
		12.1	17.2	22.3	14.8	16.3	16.7
		14.0	18.0	18.6	19.6	12.8	15.8
		14.2	15.7	20.5	29.8	16.0	19.3
		25.0	16.8	12.7	12.6	19.1	25.3
		7.8	17.2	11.5	9.3	21.9	17.5
		19.2	16.8	18.3	22.9	15.1	18.6
		17.9	18.2	12.3	17.8	11.0	12.8
		15.3	13.5	16.3	16.9	18.4	19.4
	0.5	6.1	12.3	12.6	7.2	17.8	9.3
		17.4	12.8	13.2	15.7	11.1	15.9
		16.7	15.3	14.3	12.7	16.1	14.4
		7.6	22.8	9.4	10.0	12.8	15.9
		21.3	18.6	8.4	9.5	7.1	12.3
		16.5	12.3	13.7	18.5	19.9	9.7
		7.4	13.2	16.2	16.5	15.2	16.0
		17.5	15.8	9.7	15.0	7.7	12.2
		9.8	13.3	8.4	7.0	18.4	13.8
		18.0	15.0	9.2	19.6	15.5	6.9

Appendix 7.4: Raw data for hypoxia in *in-vivo* intrahepatic CRC and HCC xenografts of nude mice

A: Labelling Index (LI, %) of SW620 intrahepatic xenografts treated with 4 mg/kg (i.v.) of cisplatin at 12 h, as measured with polyclonal rabbit anti-serum against theophylline (covalently linked to the hypoxic probe NITP)

LI assessed in 10 high power fields (each high powered field consisted of 50-100 cells)

Xenograft	Depth (cm)	Mouse & Tumour Number					
		Mouse 1		Mouse 2		Mouse 3	
		T1	T2	T1	T2	T1	T2
SW620	0.25	6.8	13.0	6.8	2.8	0.3	7.8
		27.3	6.9	17.3	9.7	4.7	9.2
		4.2	4.0	3.2	3.8	9.7	7.6
		7.3	1.3	8.1	6.7	7.8	8.3
		13.8	6.1	9.3	5.5	2.4	5.6
		17.7	4.2	3.4	6.8	3.6	11.8
		10.8	9.8	6.1	9.8	4.7	2.4
		11.8	11.2	5.1	6.7	16.2	8.6
		3.5	2.4	5.4	10.9	11.9	7.3
		4.2	6.9	7.6	3.6	6.6	1.9
	0.5	16.7	14.2	12.8	17.5	12.6	3.7
		2.4	18.3	13.8	7.2	8.8	7.6
		11.8	12.6	8.1	8.6	7.9	8.6
		18.3	7.8	4.3	6.3	8.3	6.5
		19.3	2.8	15.0	10.6	9.4	8.4
		17.8	17.4	11.6	9.8	7.8	12.1
		15.4	12.8	9.2	15.6	3.9	11.9
		9.6	6.4	7.8	11.3	8.2	15.6
		7.3	6.3	12.9	7.4	7.4	7.9
		11.8	9.9	4.6	8.7	9.8	8.7

B: Labelling Index (LI, %) of C3A intrahepatic xenografts treated 4 mg/kg (i.v.) of cisplatin at 12 h, as measured with polyclonal rabbit anti-serum against theophylline (covalently linked to the hypoxic probe NITP)

LI assessed in 10 high power fields (each high powered field consisted of 50-100 cells)

Xenograft	Depth (cm)	Mouse & Tumour Number					
		Mouse 1		Mouse 2		Mouse 3	
		T1	T2	T1	T2	T1	T2
C3A	0.25	7.7	5.8	3.6	8.3	7.4	1.7
		17.3	6.7	9.6	7.9	5.3	5.8
		6.7	3.6	8.7	16.8	5.6	7.9
		10.6	13.4	6.3	4.3	6.3	8.4
		7.9	11.8	5.8	7.8	6.6	7.8
		3.8	6.6	9.3	3.8	8.5	6.3
		9.7	3.8	13.4	4.3	16.4	6.7
		11.7	4.9	4.8	6.9	11.5	8.3
		0.3	14.8	2.8	12.7	2.8	10.8
		7.8	8.7	5.8	11.3	3.9	7.2
	0.5	12.2	4.2	12.3	13.7	11.5	16.8
		13.0	5.1	15.8	13.5	3.6	23.9
		14.5	6.7	9.8	15.3	6.9	6.5
		5.3	7.4	7.9	8.7	9.7	8.0
		8.4	15.8	18.6	8.6	15.3	6.7
		17.2	18.8	15.8	15.8	9.8	16.7
		21.3	13.8	7.6	7.3	7.8	12.9
		2.8	14.1	16.6	19.8	12.2	3.6
		6.7	9.8	19.8	17.8	9.7	14.8
		13.3	7.9	5.9	3.6	19.4	12.1

Appendix 7.5: Raw data for vascularity in *in-vivo* intrahepatic CRC and HCC xenografts of nude mice

Vascular density (VD) (= number of vascular structures/mm^2) of SW620 & C3A intrahepatic xenografts treated with 4 mg/kg (i.v.) of cisplatin at 12 h, as measured with mouse monoclonal anti-human von Willebrand factor

VD assessed in 10 high power fields (each high powered field consisted of 50-100 cells)

Xenograft	Depth (cm)	Mouse & Tumour Number					
		Mouse 1		Mouse 2		Mouse 3	
		T1	T2	T1	T2	T1	T2
SW620	0.25	29.0	17.0	14.0	32.0	29.0	28.0
		18.0	28.0	27.0	36.0	19.0	22.0
		25.0	38.0	24.0	37.0	35.0	33.0
		17.0	27.0	9.0	21.0	22.0	27.0
		21.0	22.0	34.0	29.0	17.0	25.0
		33.0	37.0	11.0	28.0	38.0	36.0
		18.0	29.0	29.0	33.0	15.0	29.0
		7.0	18.0	36.0	26.0	40.0	21.0
		38.0	30.0	40.0	30.0	25.0	28.0
		17.0	35.0	19.0	25.0	28.0	19.0
	0.5	18.0	16.0	27.0	23.0	27.0	23.0
		22.0	23.0	19.0	16.0	34.0	21.0
		21.0	31.0	24.0	28.0	31.0	25.0
		15.0	11.0	18.0	26.0	23.0	32.0
		26.0	17.0	22.0	24.0	20.0	13.0
		14.0	27.0	18.0	8.0	27.0	23.0
		8.0	25.0	26.0	14.0	28.0	16.0
		25.0	6.0	25.0	17.0	17.0	22.0
		19.0	21.0	12.0	22.0	21.0	28.0
		21.0	21.0	20.0	28.0	28.0	31.0

Xenograft	Depth (cm)	Mouse & Tumour Number					
		Mouse 1		Mouse 2		Mouse 3	
		T1	T2	T1	T2	T1	T2
C3A	0.25	32.0	22.0	40.0	17.0	28.0	36.0
		36.0	28.0	31.0	26.0	33.0	35.0
		29.0	39.0	35.0	28.0	36.0	32.0
		24.0	36.0	28.0	25.0	29.0	28.0
		17.0	33.0	33.0	31.0	32.0	26.0
		36.0	29.0	29.0	36.0	26.0	28.0
		39.0	17.0	27.0	26.0	15.0	30.0
		18.0	32.0	23.0	18.0	28.0	16.0
		29.0	26.0	33.0	29.0	28.0	28.0
		21.0	13.0	27.0	16.0	32.0	32.0
	0.5	19.0	24.0	19.0	20.0	30.0	17.0
		24.0	27.0	28.0	22.0	27.0	26.0
		22.0	31.0	31.0	24.0	29.0	27.0
		29.0	26.0	16.0	29.0	18.0	23.0
		13.0	12.0	25.0	17.0	32.0	20.0
		24.0	8.0	24.0	16.0	15.0	13.0
		14.0	19.0	12.0	24.0	17.0	24.0
		17.0	22.0	11.0	19.0	26.0	9.0
		25.0	20.0	21.0	21.0	23.0	16.0
		19.0	22.0	16.0	9.0	19.0	20.0

Appendix 7.6: Raw data for expression of P-gp in *in-vivo* intrahepatic CRC and HCC xenografts of nude mice

Expression of P-gp (LI, %) in SW620 & C3A intrahepatic xenografts treated with 4 mg/kg (i.v.) of cisplatin at 12 h, as measured with mouse monoclonal anti-human P-gp antibody

LI assessed in 10 high power fields (each high powered field consisted of 50-100 cells)

Xenograft	Depth (cm)	Mouse & Tumour Number					
		Mouse 1		Mouse 2		Mouse 3	
		T1	T2	T1	T2	T1	T2
SW620	0.25	10.0	5.0	7.5	21.4	7.77	6.6
		11.2	18.0	9.8	14.6	12.6	27.0
		25.0	26.0	15.0	4.5	10.0	13.0
		16.0	17.4	18.7	19.8	5.8	23.9
		32.0	12.5	30.4	36.0	19.0	14.45
		9.0	28.8	23.9	17.0	16.0	23.01
		17.0	13.2	18.7	13.6	26.6	12.38
		28.0	19.8	7.9	22.0	18.5	14.81
		8.9	14.9	24.0	8.2	19.8	33.1
		19.6	27.0	17.6	21.3	10.0	9.40
	0.5	4.6	18.6	11.2	16.2	15.3	7.6
		13.2	16.3	6.4	8.4	9.0	11.2
		15.0	9.8	3.0	9.2	4.3	5.0
		16.59	20.5	22.39	15.0	13.91	12.8
		10.77	13.43	9.05	18.42	23.8	9.9
		19.22	17.8	10.72	9.8	11.9	15.67
		25.62	14.55	17.3	14.19	14.6	21.03
		15.0	10.9	14.08	25.6	18.2	13.6
		18.33	11.61	22.9	12.9	7.67	16.9
		20.3	22.39	10.2	17.11	8.7	18.3

Xenograft	Depth (cm)	Mouse & Tumour Number					
		Mouse 1		Mouse 2		Mouse 3	
		T1	T2	T1	T2	T1	T2
C3A	0.25	5.0	18.2	6.7	9.6	18.7	26.0
		29.2	11.3	16.5	7.3	17.2	13.3
		14.6	9.8	22.1	15.2	6.3	15.0
		12.4	14.54	16.03	16.5	12.8	11.07
		8.8	9.74	6.96	23.6	16.2	13.0
		13.3	6.5	11.6	16.8	19.6	15.69
		12.2	9.2	9.9	9.5	9.5	19.81
		13.9	15.3	13.85	14.6	17.3	14.23
		8.7	10.67	15.6	17.4	7.8	23.23
		16.3	8.35	13.7	7.6	21.5	6.38
	0.5	8.5	16.5	13.5	24.6	25.0	5.6
		6.4	13.2	10.3	19.6	16.7	9.7
		9.5	11.5	19.0	14.5	15.0	16.0
		10.82	13.41	11.05	13.76	14.16	9.14
		11.33	13.3	11.14	9.43	6.82	13.22
		9.05	19.02	10.46	15.83	17.91	14.18
		8.023	12.8	9.97	11.68	13.26	18.33
		13.01	18.57	14.99	6.98	13.16	16.86
		12.38	7.65	17.33	16.7	9.80	15.0
		9.08	8.49	11.65	13.6	7.6	6.79

Appendix 7.7: Proliferation statistics of xenografts of nude mice

(SD = standard deviation; CD = coefficient of variation) (n = 10 fields)
Unpaired t-test (two-tailed) (n = 10), *(n = 60), #(n = 6)

Xenograft	Depth (cm)		Mouse & Tumour Number (n = 10)						
			Mouse 1		Mouse 2		Mouse 3		Total
			T1	T2	T1	T2	T1	T2	
SW620	0.25	Mean	12.23	13.78	12.4	12.21	11.64	11.93	
		SD	2.55	3.55	2.3	2.67	2.11	2.25	
		CV (%)	20.85	25.78	18.55	21.87	18.09	18.85	
	0.5	Mean	9.23	8.09	9.36	9.5	10.23	10.51	
		SD	1.85	2.51	2.49	3.19	3.107	2.62	
		CV (%)	20.06	31.07	26.67	33.57	30.37	24.89	
	0.25 *vs* 0.5	Unpaired t-test	P=0.0075	P=0.0006	P=0.011	P=0.0541	P=0.2502	P=0.2094	*P<0.0001
C3A	0.25	Mean	16.35	16.53	16.25	17.18	16.92	18.02	
		SD	5.468	1.38	3.771	5.867	3.446	3.686	
		CV (%)	33.44	8.35	23.2	34.15	20.36	20.45	
	0.5	Mean	13.83	15.14	11.51	13.17	14.16	12.64	
		SD	5.487	3.331	2.809	4.571	4.392	3.163	
		CV (%)	39.67	22.0	24.41	34.71	31.02	25.02	
	0.25 *vs* 0.5	Unpaired t-test	P=0.3172	P=0.2386	P=0.0051	P=0.1054	P=0.1353	P=0.0025	*P<0.0001
SW620 *vs* C3A	0.25	Unpaired t-test							#P<0.0001
	0.5	Unpaired t-test							#P<0.0001

Appendix 7.8: Hypoxia statistics of xenografts of nude mice

(SD = standard deviation; CD = coefficient of variation) (n = 10 fields)
Unpaired t-test (two-tailed) (n = 10), *(n = 60), #(n = 6)

Xenograft	Depth (cm)		Mouse & Tumour Number (n = 10)						
			Mouse 1		Mouse 2		Mouse 3		Total
			T1	T2	T1	T2	T1	T2	
SW620	0.25	Mean	10.74	6.58	7.23	6.63	6.79	7.05	
		SD	7.44	3.82	4.04	2.81	4.77	3.02	
		CV (%)	69.29	57.99	55.87	42.33	70.20	42.90	
	0.5	Mean	13.04	10.85	10.01	10.3	8.41	9.1	
		SD	5.47	5.08	3.79	3.66	2.18	3.33	
		CV (%)	41.97	46.79	37.82	35.56	25.89	36.56	
	0.25 *vs* 0.5	Unpaired t-test	P=0.441	P=0.048	P= 0.129	P= 0.022	P= 0.341	P= 0.166	*P=0.0007
C3A	0.25	Mean	8.35	8.01	7.01	8.41	7.43	7.09	
		SD	4.56	4.02	3.22	4.15	3.97	2.35	
		CV (%)	54.64	50.18	45.93	49.36	53.45	33.11	
	0.5	Mean	11.47	10.36	13.01	12.41	10.59	12.2	
		SD	5.68	4.953	4.97	5.15	4.42	6.15	
		CV (%)	49.51	47.81	38.22	41.47	41.72	50.37	
	0.25 *vs* 0.5	Unpaired t-test	P=0.192	P= 0.259	P= 0.089	P= 0.072	P= 0.109	P= 0.024	*P<0.0001
SW620 *vs* C3A	0.25	Unpaired t-test							#P=0.7677
	0.5	Unpaired t-test							#P=0.0152

Appendix 7.9: Vascularity statistics of xenografts of nude mice

(SD = standard deviation; CD = coefficient of variation) (n = 10 fields).
Unpaired t-test (two-tailed) (n = 10), *(n = 60), #(n = 6)

Xenograft	Depth (cm)		Mouse & Tumour Number (n =10)						
			Mouse 1		Mouse 2		Mouse 3		Total
			T1	T2	T1	T2	T1	T2	
SW620	0.25	Mean	22.3	28.1	24.3	29.7	26.8	26.8	
		SD	9.081	7.4	10.81	4.99	8.791	5.287	
		CV (%)	40.72	26.34	44.49	16.80	32.80	19.73	
	0.5	Mean	18.9	19.8	21.1	20.6	25.6	23.4	
		SD	5.425	7.51	4.606	6.620	5.254	6.022	
		CV (%)	28.71	37.93	21.83	32.14	20.52	25.74	
	0.25 *vs* 0.5	Unpaired t-test	P=0.323	P=0.0228	P=0.4005	P=0.0027	P=0.715	P=0.1964	*P=0.0004
C3A	0.25	Mean	28.1	27.5	30.6	25.2	28.7	29.1	
		SD	7.838	8.236	4.858	6.477	5.677	5.626	
		CV (%)	27.89	29.95	15.88	25.70	19.78	19.33	
	0.5	Mean	20.6	21.1	20.3	20.1	23.6	19.5	
		SD	5.103	6.887	6.701	5.425	6.041	5.798	
		CV (%)	24.77	32.64	33.01	26.99	25.60	29.73	
	0.25 *vs* 0.5	Unpaired t-test	P=0.0207	P=0.0757	P=0.001	P=0.0724	P=0.0675	P=0.0014	*P<0.0001
SW620 *vs* C3A	0.25	Unpaired t-test							#P=0.1645
	0.5	Unpaired t-test							#P=0.5269

Appendix 7.10: P-gp statistics of xenografts of nude mice

(SD = standard deviation; CD = coefficient of variation) (n = 10 fields)
Unpaired t-test (two-tailed) (n = 10), *(n = 60), #(n = 6)

Xenograft	Depth (cm)		Mouse & Tumour Number (n =10)						
			Mouse 1		Mouse 2		Mouse 3		Total
			T1	T2	T1	T2	T1	T2	
SW620	0.25	Mean	17.67	18.26	17.35	17.84	14.61	17.77	
		SD	8.337	7.427	7.528	8.664	6.481	8.509	
		CV (%)	47.18	40.67	43.39	48.57	44.37	47.90	
	0.5	Mean	15.86	15.59	12.72	14.68	12.74	13.20	
		SD	5.717	4.241	6.502	5.145	5.691	4.954	
		CV (%)	36.04	27.21	51.10	35.04	44.68	37.53	
	0.25 *vs* 0.5	Unpaired t-test	P=0.579	P=0.336	P=0.159	P=0.335	P=0.502	P=0.159	*P=0.0107
C3A	0.25	Mean	13.44	11.36	13.29	13.81	14.69	15.77	
		SD	6.463	3.579	4.703	5.214	5.274	5.808	
		CV (%)	48.09	31.51	35.38	37.76	35.90	36.83	
	0.5	Mean	9.809	13.44	12.94	14.67	13.94	12.48	
		SD	2.053	3.787	3.179	5.010	5.333	4.399	
		CV (%)	20.93	28.17	24.57	34.16	38.25	35.24	
	0.25 *vs* 0.5	Unpaired t-test	P=0.108	P=0.222	P=0.845	P=0.712	P=0.756	P=0.171	*P=0.3301
SW620 *vs* C3A	0.25	Unpaired t-test							#P=0.0038
	0.5	Unpaired t-test							#P=0.1578

Appendix 7.11: Volume correlations of xenografts of nude mice

Correlation's are calculated as Pearson's correlation coefficients (*r*) (Two-tailed)

SW620

Parameter	Depth (cm)		Mouse & Tumour Number							
			Mouse 1		Mouse 2		Mouse 3			
			T1	T2	T1	T2	T1	T2	Pearson *r*	P
VOLUME (mm^3)			1968.7	1687.5	1367.2	1366.9	381.15	486.0		
vs proliferation (LI%)	0.25	Mean	12.23	13.78	12.4	12.21	11.64	11.93	0.5311	P=0.2783
		SD	2.55	3.55	2.30	2.67	2.10	2.24	0.6263	P=0.1834
		CV	20.85	25.78	18.55	21.87	18.09	18.85	0.6320	P=0.1782
	0.5	Mean	9.23	8.09	9.35	9.49	10.23	10.51	-0.8167	P=0.0473
		SD	1.85	2.51	2.50	3.19	3.10	2.62	-0.6192	P=0.1899
		CV	20.06	31.07	26.67	33.57	30.37	24.89	-0.2290	P=0.6626
vs hypoxia (LI%)	0.25	Mean	10.74	6.58	7.23	6.63	6.79	7.05	0.5342	P= 0.275
		SD	7.44	3.82	4.04	2.81	4.76	3.02	0.4473	P=0.3737
		CV	69.29	57.99	55.87	42.33	70.20	42.9	0.1685	P=0.7496
	0.5	Mean	13.04	10.85	10.01	10.3	8.41	9.1	0.9167	P=0.0101
		SD	5.47	5.08	3.79	3.66	2.18	3.33	0.9172	P=0.01
		CV	41.97	46.79	37.82	35.56	25.89	36.56	0.7936	P=0.0595
vs vascularity (VD, no.mm^2)	0.25	Mean	22.3	28.1	24.3	29.7	26.8	26.8	-0.3202	P=0.536
		SD	9.081	7.4	10.81	4.99	8.791	5.287	0.2471	P=0.6369
		CV	40.72	26.34	44.49	16.8	32.80	19.73	0.3258	P= 0.528
	0.5	Mean	18.9	19.8	21.1	20.6	25.6	23.4	-0.9702	P=0.0013
		SD	5.425	7.51	4.606	6.62	5.254	6.022	0.2283	P= 0.663
		CV	28.71	37.93	21.83	32.14	20.52	25.74	0.6072	P= 0.201
vs adducts (% Decrease TM)	0.25	Mean	46.0	48.5	36.0	49.0	50.5	23.0	0.3770	P=0.4612
		SD	5.68	4.95	4.24	4.24	10.61	8.49	-0.8255	P=0.043
		CV	52.3	40.21	31.79	48.66	31.0	36.89	0.6822	P=0.1355
	0.5	Mean	28.5	40.5	27.5	22.5	44.5	18.5	-0.04241	P=0.9364
		SD	13.43	7.77	4.95	9.19	10.6	3.5	0.4102	P=0.4192
		CV	67.14	39.21	38.0	60.86	43.84	29.11	0.5943	P=0.2135
vascularity *vs* hypoxia	0.25								-0.8262	P=0.0427
	0.5								-0.8980	P= 0.015

C3A

Parameter	Depth (cm)		Mouse & Tumour Number							
			Mouse 1		Mouse 2		Mouse 3			
			T1	T2	T1	T2	T1	T2	Pearson *r*	P
VOLUME (mm^3)			1000.0	306.25	1968.8	1171.9	400.0	2679.7		
vs proliferation (LI%)	0.25	Mean	16.35	16.53	16.25	17.18	16.92	18.02	0.5190	P=0.2914
		SD	5.46	1.38	3.77	5.86	3.44	3.69	0.2477	P=0.6361
		CV	33.44	8.35	23.2	34.15	20.36	20.45	0.2053	P=0.6963
	0.5	Mean	13.83	15.14	11.51	13.17	14.16	12.64	-0.8283	P=0.0417
		SD	5.48	3.33	2.8	4.57	4.39	3.16	-0.4611	P=0.3574
		CV	39.67	22.0	24.41	34.71	31.02	25.0	-0.2296	P=0.6616
vs hypoxia (LI%)	0.25	Mean	8.35	8.01	7.01	8.41	7.43	7.09	-0.5747	P=0.2329
		SD	4.56	4.02	3.22	4.15	3.97	2.34	-0.8340	P=0.039
		CV	54.64	50.18	45.93	49.36	53.45	33.11	-0.8665	P=0.0255
	0.5	Mean	12.47	11.36	13.91	13.41	11.59	16.20	0.9783	P=0.0007
		SD	5.68	4.95	4.97	5.15	4.42	6.15	0.7038	P=0.1186
		CV	49.51	47.81	38.22	41.47	41.72	50.37	0.09047	P=0.8647
vs vascularity (VD, no.mm^2)	0.25	Mean	28.1	27.5	30.6	25.2	28.7	29.1	0.4214	P=0.4053
		SD	7.838	8.236	4.858	6.477	5.677	5.626	-0.6012	P= 0.207
		CV	27.89	29.95	15.88	25.70	19.78	19.33	-0.6112	P= 0.197
	0.5	Mean	20.6	21.1	20.3	20.1	23.6	19.5	-0.7203	P=0.1064
		SD	5.103	6.887	6.701	5.425	6.041	5.798	-0.1201	P= 0.82
		CV	24.77	32.64	33.01	26.99	25.60	29.73	0.2812	P= 0.589
vs adducts (% Decrease TM)	0.25	Mean	69.5	73.5	62.0	58.5	57.5	58.5	-0.4435	P=0.3784
		SD	3.53	6.36	5.66	4.95	0.70	14.84	0.7859	P=0.0639
		CV	25.09	28.66	29.12	28.46	21.23	45.38	0.8254	P=0.0430
	0.5	Mean	60.0	55.5	53.5	50.5	42.0	44.0	-0.2210	P=0.6740
		SD	1.41	2.12	10.60	9.89	2.12	12.7	0.877	P=0.0218
		CV	22.36	23.97	39.11	43.57	24.27	58.93	0.8832	P=0.0197
vascularity *vs* hypoxia	0.25								-0.8441	P= 0.035
	0.5								-0.7207	P= 0.106

Appendix 7.12: Adduct correlations of xenografts of nude mice

Correlation's are calculated as Pearson's correlation coefficients (*r*) (Two-tailed) (n=6)

SW620

Parameter	Depth (cm)	Mouse & Tumour Number							
		Mouse 1		Mouse 2		Mouse 3			
		T1	T2	T1	T2	T1	T2	Pearson *r*	P
ADDUCTS (% Decrease TM)	0.25	46.0	48.5	36.0	49.0	50.5	23.0		
	0.5	28.5	40.5	27.5	22.5	44.5	18.5		
vs proliferation (LI%)	0.25	12.23	13.78	12.4	12.21	11.64	11.93	-0.8630	P=0.0269
	0.5	9.23	8.09	9.359	9.499	10.23	10.51	0.07921	P=0.8814
	0.25&0.5							0.4442	P=0.1480
vs hypoxia (LI%)	0.25	10.74	6.58	7.23	6.63	6.79	7.05	0.05828	P=0.9127
	0.5	13.04	10.85	10.01	10.30	8.41	9.10	-0.1370	P=0.7958
	0.25&0.5							-0.3853	P=0.2162
vs vascularity (VD, no.mm^2)	0.25	22.3	28.1	24.3	29.7	26.8	26.8	-0.3446	P=0.5036
	0.5	18.9	19.8	21.1	20.6	25.6	23.4	0.03941	P= 0.941
	0.25&0.5							-0.1549	P=0.6308

C3A

Parameter	Depth (cm)	Mouse & Tumour Number							
		Mouse 1		Mouse 2		Mouse 3			
		T1	T2	T1	T2	T1	T2	Pearson *r*	P
ADDUCTS (% Decrease TM)	0.25	69.5	73.5	62.0	58.5	57.5	58.5		
	0.5	60.0	55.5	53.5	50.5	42.0	44.0		
vs proliferation (LI%)	0.25	16.35	16.53	16.25	17.18	16.92	18.02	-0.4183	P=0.4092
	0.5	13.83	15.14	11.51	13.17	14.16	12.64	0.6262	P=0.1835
	0.25&0.5							0.5857	P=0.0454
vs hypoxia (LI%)	0.25	8.35	8.01	7.01	8.41	7.43	7.09	0.4403	P=0.3823
	0.5	12.47	11.36	13.91	13.41	11.59	16.20	-0.3192	P=0.5375
	0.25&0.5							-0.6766	P=0.0157
vs vascularity (VD, no.mm^2)	0.25	28.1	27.5	30.6	25.2	28.7	29.1	-0.4110	P= 0.418
	0.5	20.6	21.1	20.3	20.1	23.6	19.5	-0.08972	P= 0.866
	0.25&0.5							-0.04169	P=0.8976

Appendix 8.1: Raw Data for *in-vitro* SW620 Comet Assays

Percentage decrease of Tail Moment of SW620 cells treated with cisplatin, HN_2 & chlorambucil as assessed by the comet assay.

Values are the mean (±SEM) of 3 experiments

***Tail Moment of SW620 cells treated with etoposide as assessed by the comet assay.**

Values are the mean (±SEM) of 3 experiments

Cytotoxic	Dose	Time (h)			
		1	2	3	4
Cisplatin	**50μM**	12.1 (±1.23)	15.4 (±0.72)	16.95 (±1.99)	17.3 (±4.03)
	100μM	22.3 (±2.51)	25.0 (±1.90)	28.0 (±2.77)	30.9 (±1.82)
***Etoposide**	**50μM**	10.13 (±1.02)	9.3 (±0.44)	9.34 (±0.52)	8.07 (±0.43)
	100μM	14.41(±1.04)	11.54 (±1.41)	10.38 (±0.82)	10.46 (±0.73)
HN_2	**50μM**	66.6 (±2.57)	75.0 (±2.46)	80.51 (±2.42)	79.83 (±1.9)
	100μM	84.6 (±3.7)	86.0 (±2.51)	91.59 (±1.55)	95.97 (±2.55)
Chlorambucil	**50μM**	11.0 (±2.53)	28.0 (±5.94)	36.0 (±3.59)	44.0 (±4.87)
	100μM	17.0 (±5.48)	42.0 (±5.46)	42.0 (±4.64)	52.3 (±3.95)

Appendix 8.2: Linear trend of increase in *in vitro* SW620 DNA damage with time as assessed by the comet assay

One-way ANOVA with post test for linear trend

Drug	Dose	Time (h)				P
		1	2	3	4	
Cisplatin	**50μM**	12.1 (±1.23)	15.4 (±0.727)	16.952 (±1.99)	17.3 (±4.03)	0.1427
	100μM	22.3 (±2.51)	25.0 (±1.90)	28.0 (±2.77)	30.9 (±1.82)	0.0226
***Etoposide**	**50μM**	10.14 (±1.024)	9.301 (±0.438)	9.341 (±0.52)	8.07 (±0.43)	0.0672
	100μM	14.41 (±1.045)	11.54 (±1.42)	10.38 (±0.82)	10.46 (±0.74)	0.0232
HN_2	**50μM**	66.6 (±2.57)	75.0 (±1.47)	80.51 (±2.42)	79.83 (±1.29)	0.0010
	100μM	84.6 (±3.7)	86.0 (±2.51)	91.59 (±1.55)	95.97 (±2.55)	0.0108
Chlorambucil	**50μM**	11.0 (±2.53)	28.0 (±5.94)	36.0 (±3.58)	44.0 (±4.87)	0.0006
	100μM	17.0 (±5.0)	42.0 (±5.0)	42.0 (±4.0)	52.3 (±3.0)	0.0006

Values are the mean ±SEM of % decrease in TM of 3 individual experiments

* Values are the mean ±SEM of TM of 3 individual experiments

Appendix 8.3: Linear trend of *in vitro* SW620 DNA damage with dose of cytotoxic as assessed by the comet assay

One-tailed unpaired t-test

Cisplatin

Time (h)	Cisplatin		P
	50μM	100μM	
1	12.1 (±1.23)	22.3 (±2.51)	0.0109
2	15.4 (±0.727)	25.0 (±1.90)	0.0046
3	16.952 (±1.99)	28.0 (±2.77)	0.0160
4	17.3 (±4.03)	30.9 (±1.82)	0.0185

Values are the mean ±SEM of % decrease in TM of 3 individual experiments

Etoposide

Time (h)	Etoposide		P
	50μM	100μM	
1	10.14 (±1.024)	14.41 (±1.045)	0.0215
2	9.301 (±0.438)	11.54 (±1.42)	0.1029
3	9.341 (±0.52)	10.38 (±0.82)	0.1710
4	8.07 (±0.43)	10.46 (±0.74)	0.0247

Values are the mean ±SEM of TM of 3 individual experiments

Nitrogen Mustard

Time (h)	HN_2		P
	50μM	100μM	
1	66.6 (±2.57)	84.6 (±3.7)	0.0081
2	75.0 (±1.47)	86.0 (±2.51)	0.0097
3	80.51 (±2.42)	91.59 (±1.55)	0.0091
4	79.83 (±1.29)	95.97 (±2.55)	0.0048

Values are the mean ±SEM of % decrease in TM of 3 individual experiments

Chlorambucil

Time (h)	Chlorambucil		P
	50μM	100μM	
1	11.0 (±2.53)	17.0 (±5.0)	0.1882
2	28.0 (±5.94)	42.0 (±5.0)	0.0788
3	36.0 (±3.58)	42.0 (±4.0)	0.1820
4	44.0 (±4.87)	52.3 (±3.0)	0.1283

Values are the mean ±SEM of % decrease in TM of 3 individual experiments

Appendix 8.4: Raw data for isolated dual-perfused rat liver xenografts (SW620)

Percentage decrease of Tail Moment of xenografts treated with cisplatin as assessed by the comet assay

Values are the mean (±SEM) of 25 measurements

Cytotoxic perfused	Tumour Number	Site & Depth (cm)	Time (h)			
			1	2	3	4
Cisplatin 50μM	1	A	2.0 (±3.99)	9.0 (±3.2)	17.0 (±2.73)	18 (±2.44)
		B	7.0 (±2.31)	13.0 (±2.81)	21.0 (±3.63)	23 (±2.57
Cisplatin 100μM	2	A	16.0 (±3.31)	21.0 (±3.3)	21.0 (±3.15)	25 (±3.5)
		B	9.0 (±3.63)	22.0 (±3.39)	26.0 (±2.71)	26 (±3.18)
	3	A	24.0 (±3.49)	26.0 (±3.08)	28.0 (±2.88)	29 (±2.99)
		B	20.0 (±4.0)	24.0 (±1.93)	25.0 (±4.0)	28 (±3.62)
	4	A, 0.25	12.0 (±2.36)	15.0 (±3.5)	21.0 (±2.45)	24 (±2.007)
		A, 0.5	3.0 (±2.84)	9.0 (±2.76)	11.0 (±2.55)	14 (±2.66)
		B, 0.25	7.0 (±2.93)	19.0 (±3.09)	26.0 (±2.98)	26 (±2.62)
		B, 0.5	0.0 (±2.98)	8.0 (±2.46)	14.0 (±2.56)	19 (±2.49)
	5	A	8.00 (±3.87)	18.00 (±3.39)	23.00 (±2.46)	25 (±3.07)
		B	5.00 (±6.10)	10.00 (±3.67)	19.00 (±3.18)	21 (±3.75)

Tail Moment of xenografts treated with etoposide as assessed by the comet assay

Values are the mean (±SEM) of 25 measurements

Cytotoxic perfused	Tumour Number	Site & Depth (cm)	Time (h)			
			1	2	3	4
Etoposide 50μM	6	A, 0.25	10.79 (±0.4)	9.81 (±0.56)	8.07 (±0.78)	8.77 (±0.64)
		A, 0.5	8.27 (±0.59)	7.56 (±0.57)	6.34 (±0.49)	6.52 (±0.5)
		B, 0.25	9.84 (±0.69)	9.22 (±0.75)	11.69 (±1.08)	7.77 (±0.69)
		B, 0.5	8.77 (±0.64)	8.65 (±0.70)	7.15 (±0.62)	7.23 (±0.39)
	7	A, 0.25	10.99 (±0.51)	10.17 (±0.65)	8.77 (±0.64)	8.37 (±0.56)
		A, 0.5	9.52 (±0.51)	8.15 (±0.59)	7.33 (±0.60)	7.33 (±0.92)
		B, 0.25	11.83 (±0.41)	9.7 (±0.74)	9.01 (±0.66)	9.53 (±0.68)
		B, 0.5	10.04 (±0.52)	8.75 (±0.62)	8.19 (±0.64)	8.09 (±0.48)
Etoposide 100μM	8	A, 0.25	15.12 (±0.65)	12.22 (±0.57)	10.99 (±0.63)	10.79 (±0.78)
		A, 0.5	10.63 (±0.87)	10.17 (±0.4)	9.18 (±0.9)	10.12 (±0.63)
		B, 0.25	14.26 (±0.84)	16.46 (±1.60)	10.85 (±0.54)	10.69 (±0.82)
		B, 0.5	11.41 (±0.65)	11.36 (±0.59)	9.38 (±0.43)	9.21 (±0.44)
	9	A, 0.25	14.12 (±0.67)	13.73 (±1.02)	12.36 (±0.53)	12.44 (±0.9)
		A, 0.5	12.58 (±0.53)	11.65 (±0.59)	10.79 (±0.78)	10.65 (±0.5)
		B, 0.25	14.23 (±0.75)	13.53 (±0.79)	13.11 (±1.08)	12.24 (±0.5)
		B, 0.5	12.04 (±0.58)	12.24 (±0.51)	10.79 (±0.78)	10.37 (±0.4)

Percentage decrease of Tail Moment of xenografts treated with nitrogen mustard as assessed by the comet assay

Values are the mean (±SEM) of 25 measurements

Cytotoxic perfused	Tumour Number	Site & Depth (cm)	Time (h)			
			1	2	3	4
HN_2 50μM	10	A, 0.25	63.0 (±4.37)	67.0 (±3.98)	71.0 (±3.63)	69 (±3.5)
		A, 0.5	56.0 (±3.85)	54.0 (±3.86)	57.0 (±4.13)	55 (±3.7)
		B, 0.25	60.0 (±4.0)	61.0 (±3.57)	62.0 (±4.27)	65 (±2.9)
		B, 0.5	50.0 (±5.5)	52.0 (±4.2)	54.0 (±3.6)	51 (±4.1)
	11	A	66.0 (±4.99)	68.0 (±4.51)	72.0 (±3.71)	71 (±2.97)
		B	53.0 (±3.74)	57.0 (±4.28)	57.0 (±4.52)	60 (±3.41)
HN_2 100μM	12	A, 0.25	68.0 (±3.42)	72.0 (±3.7)	76.0 (±2.7)	78 (±3.48)
		A, 0.5	52.0 (±3.25)	52.0 (±5.45)	58.0 (±3.49)	60 (±4.6)
		B, 0.25	67.0 (±3.35)	67.0 (±3.48)	68.0 (±4.36)	66 (±3.5)
		B, 0.5	58.0 (±3.79)	56.0 (±3.34)	59.0 (±2.8)	63 (±3.7)
	13	A	77.0 (±4.49)	78.0 (±4.88)	81.0 (±4.5)	79 (±4.34)
		B	72.0 (±4.21)	72.0 (±3.7)	71.0 (±3.9)	74 (±4.31)
	14	A	77.0 (±4.32)	84.0 (±3.87)	90.0 (±4.16)	88 (±2.67)
		B	78.0 (±4.75)	83.0 (±3.94)	85.0 (±4.06)	87 (±2.14)
	15	A	81.0 (±4.36)	84.0 (±4.13)	87.0 (±3.92)	89 (±2.18)

Appendix 8.5: Comparison of rat liver xenograft (SW620) DNA damage between doses of cytotoxic as assessed by the comet assay

One-tailed unpaired t-test

Cisplatin

Time (h)	Cisplatin		P
	50μM (n=2)	100μM (n=8)	
1	4.5 (±2.5)	12.63 (±2.39)	0.0746
2	11.00 (±2.0)	19.38 (±1.81)	0.0312
3	19.0 (±2.0)	23.63 (±1.10)	0.0468
4	20.5 (±2.5)	25.5 (±0.86)	0.0204

Values are the mean ±SEM of % decrease in TM of combined measurements at 0.25cm

Etoposide

Time (h)	Etoposide		P
	50 μM (n=4)	100 μM (n=4)	
1	10.86 (±0.41)	14.43 (±0.23)	0.0001
2	9.73 (±0.28)	12.99 (±0.37)	0.0019
3	8.38 (±0.3)	11.83 (±0.54)	0.0217
4	8.61 (±0.37)	11.54 (±0.46)	0.0013

Values are the mean ±SEM of TM of combined measurements at 0.25cm.

Nitrogen Mustard

Time (h)	HN_2		P
	50 μM (n=4)	100 μM (n=5)	
1	60.50 (±2.78)	74.29 (±2.75)	0.0057
2	63.25 (±2.59)	77.0 (±3.34)	0.0085
3	65.5 (±3.62)	80.4 (±3.93)	0.0148
4	66.25 (±2.42)	80.00 (±4.15)	0.0162

Values are the mean ±SEM of % decrease in TM of combined measurements at 0.25cm

Appendix 8.6: Linear trend of increase in rat liver xenograft (SW620) DNA damage with time as assessed by the comet assay

One-way ANOVA with post test for linear trend

Drug	Dose	Time (h)				P
		1	2	3	4	
Cisplatin	**50μM (n=2)**	4.5 (±2.5)	11.0 (±2.0)	19.0 (±2.0)	20.5 (±2.5)	0.0217
	100μM (n=8)	12.63 (±2.39)	19.38 (±1.81)	23.63 (±1.1)	25.5 (±0.86)	< 0.0001
***Etoposide**	**50μM (n=4)**	10.86 (±0.41)	9.73 (±0.28)	9.38 (±0.79)	8.61 (±0.37)	0.453
	100μM (n=4)	14.43 (±0.23)	13.99 (±0.89)	11.83 (±0.54)	11.54 (±0.46)	0.0078
HN_2	**50μM (n=4)**	60.5 (±2.78)	63.25 (±2.59)	65.5 (±3.62)	66.25 (±2.24)	0.5176
	100μM (n=5)	74.00 (±2.75)	77.14 (±3.34)	80.4 (±3.93)	80.0 (±4.15)	0.5715

Values are the mean ±SEM of % decrease in TM of combined measurements at 0.25cm

* Values are the mean ±SEM of TM of combined measurements at 0.25cm

Appendix 8.7: Tail moment of rat liver xenografts (SW620) at different depths prior to perfusion with cytoxic drugs (Time = 0 h) as assessed by the comet assay
Two-tailed unpaired t-test

Cytotoxic perfused	Tumour Number	Depth (cm)	TM (±SEM) (n=25)	P
Cisplatin 100μM	4	0.25 *vs* 0.5	3.33 (±0.38) *vs* 4.11 (±0.37)	0.1536
Etoposide 50μM	6	0.25 *vs* 0.5	4.29 (±0.34) *vs* 3.66 (±0.37)	0.2190
	7	0.25 *vs* 0.5	4.48 (±0.32) *vs* 3.66 (±0.67)	0.2754
Etoposide 100μM	8	0.25 *vs* 0.5	3.3 (±0.42) *vs* 4.65 (±0.54)	0.0530
	9	0.25 *vs* 0.5	3.86 (±0.43) *vs* 4.02 (±0.44)	0.7948
HN_2 50μM	10	0.25 *vs* 0.5	3.38 (±0.34) *vs* 3.94 (±0.55)	0.3893
HN_2 100μM	12	0.25 *vs* 0.5	4.0 (±0.47) *vs* 4.1 (±0.51)	0.8910

Appendix 8.8: Comparison of percentage decrease in Tail Moment and Tail Moment (*) at different depths of rat liver xenografts (SW620) during perfusion with cytotoxics as assessed by the comet assay

Two-tailed unpaired t-test (n=25)

Cytotoxic perfused	Tumour Number	Site	Depth (cm)	Time (h)			
				1	2	3	4
Cisplatin 100μM	4	A	0.25 *vs* 0.5	P = 0.0186	P = 0.1563	P = 0.0067	P<0.0001
		B	0.25 *vs* 0.5	P = 0.1004	P = 0.0076	P = 0.0037	P = 0.0587
***Etoposide 50μM**	6	A	0.25 *vs* 0.5	P = 0.0009	P = 0.0066	P = 0.0664	P = 0.0079
		B	0.25 *vs* 0.5	P = 0.243	P = 0.582	P = 0.0007	P = 0.4989
	7	A	0.25 *vs* 0.5	P = 0.0475	P = 0.0261	P = 0.1072	P = 0.3391
		B	0.25 *vs* 0.5	P = 0.0095	P = 0.0201	P = 0.3818	P = 0.09
***Etoposide 100μM**	8	A	0.25 *vs* 0.5	P = 0.0004	P = 0.0887	P = 0.1076	P = 0.5072
		B	0.25 *vs* 0.5	P = 0.0035	P = 0.9059	P = 0.0396	P = 0.1176
	9	A	0.25 *vs* 0.5	P = 0.0783	P = 0.0849	P = 0.1048	P = 0.0896
		B	0.25 *vs* 0.5	P = 0.0251	P = 0.1772	P = 0.0888	P = 0.0073
HN_2 50μM	10	A	0.25 *vs* 0.5	P = 0.2353	P = 0.0232	P = 0.0142	P = 0.0084
		B	0.25 *vs* 0.5	P = 0.1480	P = 0.1091	P = 0.1585	P = 0.0077
HN_2 100μM	12	A	0.25 *vs* 0.5	P = 0.0014	P = 0.0039	P = 0.0002	P = 0.0031
		B	0.25 *vs* 0.5	P = 0.0815	P = 0.0271	P = 0.0888	P = 0.5586

Appendix 8.9: Comparison of percentage decrease in Tail Moment and Tail Moment (*) at different sites in the same rat liver xenograft (SW620) during perfusion with cytotoxics as assessed by the comet assay

Two-tailed unpaired t-test (n=25)

Cytotoxic perfused	Tumour Number	Depth (cm)	Site	Time (h)			
				1	2	3	4
Cisplatin 50μM	1	0.25	A *vs* B	P = 0.2836	P = 0.3523	P = 0.3829	P = 0.1647
Cisplatin 100μM	2	0.25	A *vs* B	P = 0.1606	P = 0.8335	P = 0.2348	P = 0.8342
	3	0.25	A *vs* B	P = 0.4548	P = 0.5847	P = 0.5456	P = 0.8322
	4	0.25	A *vs* B	P = 0.1901	P = 0.3669	P = 0.2004	P = 0.5474
	5	0.25	A *vs* B	P = 0.6798	P = 0.1159	P = 0.3248	P = 0.4133
***Etoposide 50μM**	6	0.25	A *vs* B	P = 0.234	P = 0.5358	P = 0.0091	P = 0.2933
	7	0.25	A *vs* B	P = 0.2054	P = 0.6460	P = 0.7935	P = 0.1942
***Etoposide 100μM**	8	0.25	A *vs* B	P = 0.4221	P = 0.0162	P = 0.8684	P = 0.5072
	9	0.25	A *vs* B	P = 0.9088	P = 0.8776	P = 0.5364	P = 0.8500
HN_2 50μM	10	0.25	A *vs* B	P = 0.6149	P = 0.2673	P = 0.1149	P = 0.3832
	11	0.25	A *vs* B	P = 0.0424	P = 0.0832	P = 0.0135	P = 0.0188
HN_2 100μM	12	0.25	A *vs* B	P = 0.8354	P = 0.3299	P = 0.1253	P = 0.0192
	13	0.25	A *vs* B	P = 0.4206	P = 0.3321	P = 0.0996	P = 0.4177
	14	0.25	A *vs* B	P = 0.8769	P = 0.8571	P = 0.3940	P = 0.7714

Appendix 8.10: Comparison of percentage decrease in Tail Moment and Tail Moment (*) in different rat liver xenografts (SW620) in the same liver during perfusion with cytotoxics as assessed by the comet assay

One-way ANOVA followed by the Bonferroni multiple t-test

Cytotoxic perfused	Depth (cm)	Tumour Number & Site	Time (h)			
			1	2	3	4
Cisplatin 100μM	0.25	2A *vs* 3A	P > 0.05	P > 0.05	P > 0.05	P > 0.05
		2A *vs* 3B	P > 0.05	P > 0.05	P > 0.05	P > 0.05
		2B *vs* 3A	P < 0.05	P > 0.05	P > 0.05	P > 0.05
		2B *vs* 3B	P > 0.05	P > 0.05	P > 0.05	P > 0.05
	0.25	4A *vs* 5A	P > 0.05	P > 0.05	P > 0.05	P > 0.05
		4A *vs* 5B	P > 0.05	P > 0.05	P > 0.05	P > 0.05
		4B *vs* 5A	P > 0.05	P > 0.05	P > 0.05	P > 0.05
		4B *vs* 5B	P > 0.05	P > 0.05	P > 0.05	P > 0.05
Etoposide 50μM	0.25	6A *vs* 7A	P > 0.05	P > 0.05	P > 0.05	P > 0.05
		6A *vs* 7B	P > 0.05	P > 0.05	P > 0.05	P > 0.05
		6B *vs* 7A	P < 0.05	P > 0.05	P > 0.05	P > 0.05
		6B *vs* 7B	P > 0.01	P > 0.05	P > 0.05	P > 0.05
Etoposide 100μM	0.25	8A *vs* 9A	P > 0.05	P > 0.05	P > 0.05	P > 0.05
		8A *vs* 9B	P > 0.05	P > 0.05	P > 0.05	P > 0.05
		8B *vs* 9A	P > 0.05	P > 0.05	P > 0.05	P > 0.05
		8B *vs* 9B	P > 0.05	P > 0.05	P < 0.05	P > 0.05
HN_2 50μM	0.25	10A *vs* 11A	P > 0.05	P > 0.05	P > 0.05	P > 0.05
		10A *vs* 11B	P > 0.05	P > 0.05	P > 0.05	P > 0.05
		10B *vs* 11A	P > 0.05	P > 0.05	P > 0.05	P > 0.05
		10B *vs* 11B	P > 0.05	P > 0.05	P > 0.05	P > 0.05
HN_2 100μM	0.25	12A *vs* 13A	P > 0.05	P > 0.05	P > 0.05	P > 0.05
		12A *vs* 13B	P > 0.05	P > 0.05	P > 0.05	P > 0.05
		12B *vs* 13A	P > 0.05	P > 0.05	P > 0.05	P > 0.05
		12B *vs* 13B	P > 0.05	P > 0.05	P > 0.05	P > 0.05
	0.25	14A *vs* 15	P > 0.05	P > 0.05	P > 0.05	P > 0.05
		14B *vs* 15	P > 0.05	P > 0.05	P > 0.05	P > 0.05

Appendix 9.1: Viability parameters of human hemilivers whilst on perfusion circuit

Paired t-test (n=8, except * where n=4)

Viability Parameters	1 h Mean (± SEM)	4 h Mean (± SEM)	P
Portal Vein Pressure (mm/Hg)	14.88 (±1.19)	16.97 (±2.53)	0.265
Hepatic Artery Pressure (mm/Hg)	55.32 (±4.69)	51.91 (±5.35)	0.146
Bile Production (ml/h)	4.301 (±0.37)	4.5 (±0.47)	0.489
Microcirculatory Perfusate Flow (flux units)	190.6 (±3.44)	184.9 (±3.99)	0.332
ALT (IU/L)	191.0 (±55.68)	267.28 (±69.37)	0.0108
***TM of control tumour**	4.33 (±0.64)	4.915 (±0.84)	0.34
***TM of control normal liver**	5.273 (±0.365)	5.785 (±0.151)	0.1145

ALT, alanine aminotransferase.

Appendix 9.2: Raw data of % decrease of TM of human tumours treated with cisplatin as assessed by the comet assay

Values are the mean (±SD) of 6 measurements

Cytotoxic perfused	Tumour Number	Site & Depth (cm)	Time (h)				
			1	2	3	4	5
Cisplatin 23.3μM	1	A, 0.5	16.01 (±3.3)	30.6 (±5.01)	45.3 (±4.17)	49.6 (±6.58)	
		A, 1	12.3 (±3.19)	28.3 (±4.11)	38.86 (±4.29)	45.4 (±3.47)	
		A, 1.5	10.4 (±2.54)	22.7 (±3.30)	34.5 (±4.42)	42.4 (±3.99)	
	2	A, 0.5	20.0 (±4.80)	32.9 (±2.45)	39.2 (±3.68)	42.0 (±2.1)	
		A, 1	18.1 (±3.93)	29.85 (±2.63)	33.6 (±3.9)	36.0 (±1.99)	
		A, 1.5	17.4 (±4.22)	24.7 (±3.43)	30.2 (±4.19)	36.4 (±3.6)	
Cisplatin 50μM	3	A, 0.5	37.0 (±2.85)	38.6 (±2.66)	47.5 (±2.88)	53.3 (±3.85)	55.4 (±2.29)
		A, 1	31.8 (±3.61)	34.2 (±3.28)	38.4 (±2.84)	48.2 (±2.77)	48.1 (±2.69)
		B, 0.5	32.7 (±2.67)	37.6 (±2.71)	44.9 (±3.9)	51.7 (±3.43)	49.9 (±2.77)
		B, 1	29.0 (±3.43)	31.0 (±3.93)	41.1 (±2.8)	46.4 (±2.64)	41.6 (±2.23)
	4	A, 0.5	20.6 (±3.73)	39.8 (±3.59)	40.71 (±3.08)	42.7 (±2.86)	53.7 (±2.11)
		A, 1	13.4 (±3.169)	37.8 (±5.54)	38.4 (±2.98)	40.5 (±2.507)	44.1 (±1.63)
		B, 0.5	24.7 (±3.44)	36.4 (±3.26)	38.8 (±2.5)	45.8 (±2.96)	54.3 (±2.22)
		B, 1	23.26 (±3.69)	33.5 (±2.83)	35.4 (±3.56)	44.1 (±3.099)	46.1 (±2.41)
Cisplatin 100μM	5	A, 0.5	32.9 (±4.028)	39.7 (±3.277)	61.5 (±4.822)	77.1 (±2.83)	85.9 (±2.65)
		A, 1	28.6 (±2.722)	25.4 (±4.36)	59.24 (±4.92)	74.5 (±3.22)	79.53 (±1.7)
		A, 2	8.5 (±3.51)	14.7 (±4.23)	46.8 (±4.52)	65.2 (±2.03)	82.33 (±3.05)
		B, 0.5	26.9 (±4.3)	35.0 (±3.42)	67.0 (±4.62)	70.0 (±2.76)	78.28 (±1.85)
		B, 1	19.5 (±5.2)	27.4 (±4.05)	58.4 (±4.54)	64.7 (±2.04)	77.3 (±1.27)
		B, 2	11.5 (±2.87)	16.1 (±4.39)	54.5 (±3.56)	62.4 (±2.63)	73.7 (±3.24)
		C, 0.5	34.1 (±4.39)	46.0 (±2.309)	72.42 (±3.68)	86.0 (±2.45)	89.0 (±1.41)
		C, 1	30.9 (±3.933)	44.4 (±2.59)	63.7 (±3.77)	80.0 (±2.21)	86.55 (±2.17)
		C, 2	21.3 (±3.51)	27.6 (±3.26)	57.4 (±3.61)	68.0 (±2.31)	72.2 (±2.01)
	6	A, 0.5	40.2 (±2.37)	49.86 (±3.35)	79.05 (±3.15)	91.18 (±1.542)	94.87 (±2.468)
		A, 1	30.5 (±2.18)	34.7 (±4.6)	78.6 (±4.0)	93.45 (±2.8)	95.41 (±1.208)
		A, 2	8.8 (±3.31)	18.0 (±4.36)	74.7 (±3.91)	81.3 (±2.23)	87.75 (±2.21)
		B, 0.5	11.0 (±9.2)	42.5 (±5.8)	69.67 (±2.39)	81.62 (±1.98)	85.42 (±2.11)
		B, 1	9.0 (±3.87)	32.2 (±7.048)	62.8 (±2.98)	75.28 (±2.1)	78.9 (±2.4)
		B, 2	10.0 (±5.4)	25.5 (±6.107)	53.4 (±3.65)	57.5 (±2.599)	69.21 (±3.44)
		C, 0.5	30.5 (±3.94)	67.8 (±3.58)	77.0 (±3.42)	80.005 (±2.95)	84.5 (±3.044)
		C, 1	19.1 (±6.31)	57.8 (±3.23)	66.1 (±2.79)	74.0 (±1.71)	71.0 (±3.09)
		C, 2	11.2 (±4.04)	40.0 (±1.344)	61.6 (±3.19)	65.7 (±2.61)	71.2 (±2.69)

Appendix 9.3: Raw data of TM of human tumours treated with etoposide as assessed by the comet assay

Values are the mean (±SEM) of 25 measurements

Cytotoxic perfused	Tumour Number	Site & Depth (cm)	Time (h)					
			1	2	3	4	5	6
Etoposide 50μM	7	A, 1	8.93 (±0.61)	10.0 (±0.554)	12.0 (±0.579)	11.0 (±0.63)	13.0 (±0.478)	14.0 (±0.508)
		A, 2	8.5 (±0.601)	9.9 (±0.43)	9.76 (±0.46)	8.255 (±0.679)	8.0 (±0.459)	8.2 (±0.438)
		A, 3	8.27 (±0.535)	8.79 (±0.54)	8.44 (±0.457)	8.67 (±0.675)	7.62 (±0.463)	7.36 (±0.54)
		A, 4	7.12 (±0.59)	9.208 (±0.47)	8.539 (±0.58)	7.87 (±0.47)	7.41 (±0.45)	8.67 (±0.589)
		B, 1	10.039 (±0.695)	10.83 (±0.69)	9.67 (±0.514)	9.234 (±0.563)	7.5 (±0.606)	7.831 (±0.516)
		B, 2	10.52 (±0.648)	9.76 (±0.52)	8.94 (±0.552)	7.457 (±0.486)	8.23 (±0.43)	7.74 (±0.39)
		B, 3	10.229 (±0.48)	9.54 (±0.95)	7.88 (±0.53)	7.735 (±0.62)	8.06 (±0.466)	5.503 (±0.278)
		B, 4	9.12 (±0.59)	9.167 (±0.665)	6.72 (±0.691)	5.62 (±0.617)	6.41 (±0.714)	6.162 (±0.548)
		C, 1	13.01 (±0.657)	12.48 (±0.723)	13.48 (±0.679)	12.87 (±0.541)	15.66 (±0.484)	16.38 (±0.619)
		C, 2	12.417 (±0.610)	11.61 (±0.483)	11.651 (±0.56)	13.14 (±0.52)	13.018 (±0.434)	12.406 (±0.714)
		C, 3	9.55 (±0.55)	10.27 (±0.72)	8.708 (±0.48)	9.1 (±0.65)	8.536 (±0.517)	9.0198 (±0.639)
		C, 4	7.22 (±0.579)	9.66 (±0.708)	8.27 (±0.53)	7.77 (±0.399)	6.889 (±0.413)	8.4 (±0.623)
			0.5	1	2	3	4	5
Etoposide 100μM	8	A, 0.5	16.26 (±1.079)	16.86 (±0.57)	19.054 (±0.533)	18.5 (±0.534)	20.0 (±0.63)	18.0 (±0.469)
		A, 1	14.87 (±1.42)	17.914 (±0.657)	14.81 (±0.648)	15.0 (±0.457)	13.0 (±0.55)	12.5 (±0.396)
		A, 1.5	9.666 (±1.232)	12.009 (±0.72)	10.75 (±0.44)	9.247 (±0.39)	9.55 (±0.502)	9.17 (±0.487)
		A, 2	22.0 (±1.11)	25.0 (±1.47)	27.0 (±0.504)	22.0 (±0.512)	23.0 (±1.132)	22.0 (±0.927)
		B, 0.5	19.1 (±0.75)	22.0 (±0.707)	21.0 (±0.54)	20.5 (±0.5)	22.0 (±0.456)	19.0 (±0.79)
		B, 1	16.0 (±0.77)	15.0 (±0.549)	10.47 (±0.56)	9.68 (±0.46)	9.25 (±0.51)	9.12 (±0.54)
		B, 1.5	9.065 (±0.872)	10.68 (±0.46)	8.898 (±0.522)	8.17 (±0.44)	8.85 (±0.643)	9.0 (±0.58)
		B, 2	9.76 (±0.695)	10.99 (±0.51)	8.86 (±0.402)	11.34 (±1.1)	9.567 (±1.47)	8.86 (±1.2)

Appendix 9.4: Raw data of % decrease of TM of human tumours treated with HN_2 as assessed by the comet assay

Values are the mean (±SD) of 6 measurements

Cytotoxic perfused	Tumour Number	Site & Depth (cm)	Time (h)					
			1	2	3	4	5	6
HN_2 50μM	9	A, 0.5	51.0 (±3.89)	54.0 (±3.84)	57.2 (±5.71)	62.3 (±4.25)	62.2 (±4.27)	63.3 (±2.08)
		A, 1	38.0 (±4.27)	48.3 (±2.56)	52.0 (±3.18)	62.0 (±3.63)	62.1 (±3.36)	60.6 (±1.91)
		A, 2	30.4 (±4.42)	34.1 (±2.6)	36.1 (±4.33)	49.3 (±2.24)	51.8 (±3.31)	47.3 (±3.21)
		B, 0.5	56.0 (±3.36)	55.8 (±3.68)	54.4 (±4.34)	48.9 (±4.28)	54.5 (±5.51)	49.4 (±1.55)
		B, 1	36.7 (±2.52)	44.01 (±3.19)	40.3 (±4.91)	40.8 (±5.13)	45.1 (±2.65)	49.4 (±2.42)
		B, 2	23.1 (±2.96)	31.5 (±3.66)	30.0 (±3.61)	33.2 (±2.83)	35.41 (±4.84)	33.4 (±3.39)
		C, 0.5	58.6 (±3.75)	58.1 (±2.95)	56.0 (±2.19)	59.5 (±3.93)	59.3 (±2.96)	56.2 (±1.85)
		C, 1	44.9 (±3.86)	46.4 (±2.92)	44.0 (±5.67)	46.0 (±3.71)	47.6 (±3.38)	44.5 (±2.26)
		C, 2	26.3 (±5.01)	27.8 (±3.61)	31.3 (±3.71)	37.6 (±3.74)	30.2 (±2.35)	42.8 (±3.44)
		D, 0.5	68.8 (±3.96)	76.4 (±3.36)	62.61 (±3.53)	62.3 (±3.37)	58.43 (±3.1)	60.0 (±3.03)
		D, 1	36.0 (±5.66)	40.4 (±3.5)	35.0 (±3.47)	52.0 (±3.49)	41.4 (±3.02)	38.8 (±2.55)
		D, 2	20.0 (±4.76)	20.8 (±2.73)	27.0 (±3.75)	39.3 (±5.05)	34.83 (±3.27)	34.6 (±2.4)
			0.5	**1**	**2**	**3**	**4**	
HN_2 100μM	10	A, 0.5	34.8 (±3.66)	41.5 (±3.65)	47.1 (±3.19)	43.4 (±3.63)	42.6 (±3.99)	
		A, 1	19.0 (±3.86)	36.3 (±2.54)	38.6 (±2.94)	38.3 (±2.81)	31.4 (±4.0)	
		A, 2	18.3 (±3.48)	22.5 (±3.38)	32.3 (±3.44)	25.0 (±2.41)	25.9 (±3.45)	
		B, 0.5	27.8 (±3.91)	47.0 (±3.26)	42.0 (±2.187)	38.4 (±3.64)	40.8 (±3.63)	
		B, 1	21.9 (±3.8)	37.7 (±3.05)	35.0 (±2.41)	31.7 (±2.98)	23.7 (±2.13)	
		B, 2	18.2 (±4.25)	17.7 (±3.5)	25.0 (±5.19)	19.6 (±4.73)	18.9 (±2.96)	
	11	A, 0.5	63.4 (±3.041)	63.3 (±3.19)	64.8 (±2.49)	61.0 (±2.93)	62.8 (±2.387)	
		A, 1	49.85 (±3.56)	51.5 (±4.27)	54.6 (±2.81)	55.29 (±4.36)	56.9 (±1.41)	
		B, 0.5	70.5 (±3.35)	64.4 (±3.2)	61.6 (±3.2)	66.3 (±3.38)	69.1 (±1.4)	
		B, 1	42.6 (±3.8)	61.9 (±3.49)	62.0 (±3.12)	57.1 (±3.055)	59.78 (±2.31)	

Cytotoxic perfused	Tumour Number	Site & Depth (cm)	Time (h)				
			0.5	1	2	3	4
HN_2 100μM	12	A, 0.5	49.4 (±3.23)	84.3 (±3.45)	80.7 (±2.62)	78.7 (±3.32)	77.9 (±2.67)
		A, 1	54.2 (±3.35)	74.92 (±3.08)	76.2 (±2.52)	75.9 (±2.5)	76.9 (±2.49)
		A, 2	62.3 (±3.16)	71.9 (±3.316)	69.8 (±2.52)	68.9 (±2.65)	74.1 (±2.45)
		B, 0.5	28.8 (±2.91)	67.3 (±3.59)	70.7 (±3.46)	66.1 (±3.66)	64.5 (±2.43)
		B, 1	25.42 (±3.845)	58.0 (±3.68)	55.2 (±1.93)	52.0 (±5.36)	57.1 (±3.4)
		B, 2	19.1 (±2.86)	49.28 (±4.37)	43.1 (±3.219)	45.0 (±8.07)	40.0 (±3.6)

Appendix 9.5: Linear trend of human tumour DNA damage with concentration of cisplatin as assessed by the comet assay

One-way ANOVA with post test for linear trend; except * = one-tailed unpaired t-test

Time (h)	Cisplatin			P
	23.3μM (n=6)	50μM (n=6)	100μM (n=6)	
1	15.7 (±1.493)	26.7 (±3.587)	21.8 (±4.249)	0.214
2	28.17 (±1.561)	37.4 (±0.788	40.9 (±8.037)	0.0776
3	36.94 (±2.169)	41.45 (±1.578)	62.04 (±4.004)	< 0.0001
4	41.96 (±2.135)	47.03 (±2.044)	72.75 (±2.469)	< 0.0001
5	ND	50.91 (±1.777)	79.08 (±2.671)	< 0.0001*

Values are the mean ±SEM of % decrease in TM of combined measurements of 0.5 & 1 cm

ND, not done

Appendix 9.6: Linear trend of human tumour DNA damage with concentration of etoposide as assessed by the comet assay

One-tailed unpaired t-test

Time (h)	Etoposide		P
	50μM (n=6)	100μM (n=6)	
1	8.89 (±0.504)	15.74 (±1.685)	0.0015
2	9.74 (±0.286)	14.16 (±2.034)	0.0285
3	9.55 (±0.538)	13.52 (±2.139)	0.0515
4	8.75 (±0.516)	13.77 (±2.377)	0.0328
5	8.63 (±0.884)	12.79 (±1.886)	0.0365

Values are the mean ±SEM of TM of combined measurements of 0.5 & 1 cm.

Appendix 9.7: Linear trend of human tumour DNA damage with concentration of HN_2 as assessed by the comet assay

One-tailed unpaired t-test

Time (h)	HN_2		P
	50μM (n=12)	100μM (n=12)	
0.5	40.82 (±4.408)	40.64 (±4.884)	0.489
1	44.80 (±4.414)	57.34 (±4.318)	0.0273
2	43.83 (±3.524)	57.37 (±4.244)	0.0112
3	49.43 (±3.002)	55.35 (±4.377)	0.138
4	47.74 (±3.214)	55.29 (±4.981)	0.108

Values are the mean ±SEM of % decrease in TM of combined measurements of 0.5 & 1cm.

Appendix 9.8: Linear trend of increase in human tumour DNA damage with time as assessed by the comet assay

One-way ANOVA with post test for linear trend

Drug	Dose	Time (h)						P
		0.5	1	2	3	4	5	
Cisplatin (n=6)	23.3μM		15.7 (±1.493)	28.17 (±1.56)	36.94 (±2.169)	41.96 (±2.135)		< 0.0001
	50μM		26.7 (±3.588)	37.4 (±0.788)	41.45 (±1.578)	47.03 (±2.044)	50.92 (±1.776)	< 0.0001
	100μM		21.8 (±4.249)	40.9 (±8.037)	62.04 (±4.003)	72.75 (±2.469)	79.08 (±2.671)	< 0.0001
***Etoposide** (n=6)	50μM		8.89 (±0.505)	9.75 (±0.287)	9.56 (±0.538)	8.75 (±0.516)	8.63 (±0.884)	0.408
	100μM		15.74 (±1.685)	14.16 (±2.03)	13.51 (±2.139)	13.77 (±2.377)	12.79 (±1.886)	0.3392
HN_2 (n=12)	50μM	40.82 (±4.408)	44.80 (±4.414)	43.82 (±3.524)	49.43 (±3.002)	47.74 (±3.214)		0.1259
	100μM	40.64 (±4.884)	57.34 (±4.318)	57.37 (±4.244)	55.35 (±4.377)	55.29 (±4.982)		0.0642

Values are the mean ±SEM of % decrease in TM of combined measurements of 0.5 & 1 cm.

* Values are the mean ±SEM of TM of combined measurements of 0.5 & 1 cm.

Appendix 9.9: TM of human tumours at different depths prior to perfusion with cytoxic drugs (Time = 0 h) as assessed by the comet assay

One-way ANOVA followed by the Bonferroni multiple t-test; except * = two-tailed unpaired t-test

Cytotoxic perfused	Tumour Number	Depth (cm)	TM (±SEM) (n=25)	P
Cisplatin 23.3μM	1	0.5 *vs* 1.5	2.45 (±0.26) *vs* 2.64 (±0.25)	0.6044*
	2	0.5 *vs* 1.5	1.74 (±0.25) *vs* 1.89 (±0.22)	0.6535*
Cisplatin 50μM	3	0.5 *vs* 1	2.23 (±0.49) *vs* 2.41 (±0.31)	0.752*
	4	0.5 *vs* 1	2.85 (±0.412) *vs* 3.78 (±0.66)	0.237*
Cisplatin 100μM	5	0.5 *vs* 2	2.72 (±0.4) *vs* 2.048 (±0.25)	0.1629*
	6	0.5 *vs* 1	2.34 (±0.26) *vs* 2.447 (±0.36)	> 0.05
		0.5 *vs* 2	2.34 (±0.26) *vs* 3.59 (±0.3)	< 0.05
Etoposide 50μM	7	1 *vs* 2	3.34 (±0.38) *vs* 3.759 (±0.35)	> 0.05
		1 *vs* 3	3.34 (±0.38) *vs* 3.013 (±0.37)	> 0.05
		1 *vs* 4	3.34 (±0.38) *vs* 5.903 (±1.0)	< 0.05
Etoposide 100μM	8	0.5 *vs* 1	1.67 (±0.25) *vs* 1.63 (±0.26)	> 0.05
		0.5 *vs* 1.5	1.67 (±0.25) *vs* 4.82 (±0.76)	< 0.05
		0.5 *vs* 2	1.67 (±0.25) *vs* 17.54 (±1.19)	< 0.001
		0.5 *vs* 3	1.67 (±0.25) *vs* 17.33 (±0.76)	< 0.001
HN_2 50μM	9	0.5 *vs* 1	(±)*vs*(±)	> 0.05
		0.5 *vs* 2	(±)*vs*(±)	> 0.05
HN_2 100μM	10	0.5 *vs* 1	2.15 (±0.3) *vs* 2.56 (±0.44)	> 0.05
		0.5 *vs* 2	2.15 (±0.3) *vs* 2.05 (±0.35)	> 0.05
	11	0.5 *vs* 1	1.29 (±0.2) *vs* 1.33 (±0.23)	0.9102*
	12	0.5 *vs* 1	2.76 (±0.57) *vs* 2.43 (±0.42)	> 0.05
		0.5 *vs* 2	2.76 (±0.57) *vs* 2.13 (±0.39)	> 0.05

Appendix 9.10: Comparison of % decrease in TM of human tumours at different depths during perfusion with cisplatin as assessed by the comet assay

One-way ANOVA followed by the Bonferroni multiple t-test
except * = two-tailed unpaired t-test

Cytotoxic perfused	Tumour Number	Site	Depth (cm)	Time (h)				
				1	2	3	4	5
Cisplatin 23.3μM	1	A	0.5 *vs* 1	P<0.001	P >0.05	P<0.001	P<0.01	
			0.5 *vs* 1.5	P<0.001	P<0.001	P<0.001	P<0.001	
			1 *vs* 1.5	P >0.05	P<0.001	P<0.05	P >0.05	
	2	A	0.5 *vs* 1	P>0.05	P<0.001	P<0.001	P<0.001	
			0.5 *vs* 1.5	P>0.05	P<0.001	P<0.001	P<0.001	
			1 *vs* 1.5	P>0.05	P<0.001	P<0.05	P>0.05	
Cisplatin 50μM	3	*A	0.5 *vs* 1	P<0.0001	P<0.0001	P<0.0001	P<0.0001	P<0.0001
		*B	0.5 *vs* 1	P<0.0001	P<0.0001	P=0.0002	P=0.1941	P<0.0001
	4	*A	0.5 *vs* 1	P<0.0001	P=0.0391	P=0.0027	P=0.0009	P<0.0001
		*B	0.5 *vs* 1	P=0.0985	P=0.0003	P<0.0001	P=0.041	P<0.0001
Cisplatin 100μM	5	A	0.5 *vs* 1	P<0.001	P<0.001	P>0.05	P<0.01	P<0.001
			0.5 *vs* 2	P<0.001	P<0.001	P<0.001	P<0.001	P<0.001
			1 *vs* 2	P<0.001	P<0.001	P<0.001	P<0.001	P<0.001
		B	0.5 *vs* 1	P<0.001	P<0.001	P<0.001	P<0.001	P>0.05
			0.5 *vs* 2	P<0.001	P<0.001	P<0.001	P<0.001	P<0.001
			1 *vs* 2	P<0.001	P<0.001	P<0.001	P<0.01	P<0.001
		C	0.5 *vs* 1	P<0.05	P>0.05	P<0.001	P<0.001	P<0.001
			0.5 *vs* 2	P<0.001	P<0.001	P<0.001	P<0.001	P<0.001
			1 *vs* 2	P<0.001	P<0.001	P<0.001	P<0.001	P<0.001
	6	A	0.5 *vs* 1	P<0.001	P<0.001	P>0.05	P<0.01	P>0.05
			0.5 *vs* 2	P<0.001	P<0.001	P<0.001	P<0.001	P<0.001
			1 *vs* 2	P<0.001	P<0.001	P<0.01	P<0.001	P<0.001
		B	0.5 *vs* 1	P>0.05	P<0.001	P<0.001	P<0.001	P<0.001
			0.5 *vs* 2	P>0.05	P<0.001	P<0.001	P<0.001	P<0.001
			1 *vs* 2	P>0.05	P<0.01	P<0.001	P<0.001	P<0.001
		C	0.5 *vs* 1	P<0.001	P<0.001	P<0.001	P<0.001	P<0.001
			0.5 *vs* 2	P<0.001	P<0.001	P<0.001	P<0.001	P<0.001
			1 *vs* 2	P<0.001	P<0.001	P<0.001	P<0.001	P>0.05

Appendix 9.11: Comparison of TM at different depths of human tumours during perfusion with etoposide as assessed by the comet assay

One-way ANOVA followed by the Bonferroni multiple t-test

Cytotoxic perfused	Tumour Number	Site	Depth (cm)	Time (h)					
				1	2	3	4	5	6
Etoposide 50μM	7	A	1 *vs* 2	P>0.05	P>0.05	P<0.05	P<0.05	P<0.001	P<0.001
			1 *vs* 3	P>0.05	P>0.05	P<0.001	P>0.05	P<0.001	P<0.001
			1 *vs* 4	P>0.05	P>0.05	P<0.001	P<0.01	P<0.001	P<0.001
			1 *vs* Control	P<0.001	P<0.001	P<0.001	P<0.001	P<0.001	P<0.001
			2 *vs* 3	P>0.05	P>0.05	P>0.05	P>0.05	P>0.05	P>0.05
			2 *vs* 4	P>0.05	P>0.05	P>0.05	P>0.05	P>0.05	P>0.05
			2 *vs* Control	P<0.001	P<0.001	P<0.001	P<0.001	P<0.05	P<0.05
			3 *vs* 4	P>0.05	P>0.05	P>0.05	P>0.05	P>0.05	P>0.05
			3 *vs* Control	P<0.001	P<0.001	P<0.001	P<0.001	P>0.05	P>0.05
			4 *vs* Control	P<0.01	P<0.001	P<0.001	P<0.01	P>0.05	P<0.01
		B	1 *vs* 2	P>0.05	P>0.05	P>0.05	P>0.05	P>0.05	P>0.05
			1 *vs* 3	P>0.05	P>0.05	P>0.05	P>0.05	P>0.05	P<0.01
			1 *vs* 4	P>0.05	P>0.05	P<0.01	P<0.001	P>0.05	P>0.05
			1 *vs* Control	P<0.001	P<0.001	P<0.001	P<0.001	P>0.05	P>0.05
			2 *vs* 3	P>0.05	P>0.05	P>0.05	P>0.05	P>0.05	P<0.01
			2 *vs* 4	P>0.05	P>0.05	P<0.05	P>0.05	P>0.05	P>0.05
			2 *vs* Control	P<0.001	P<0.001	P<0.001	P<0.05	P<0.05	P>0.05
			3 *vs* 4	P>0.05	P>0.05	P>0.05	P>0.05	P>0.05	P>0.05
			3 *vs* Control	P<0.001	P<0.001	P<0.01	P<0.01	P>0.05	P>0.05
			4 *vs* Control	P<0.001	P<0.001	P>0.05	P>0.05	P>0.05	P>0.05
		C	1 *vs* 2	P>0.05	P>0.05	P>0.05	P>0.05	P<0.001	P<0.001
			1 *vs* 3	P<0.001	P>0.05	P<0.001	P<0.001	P<0.001	P<0.001
			1 *vs* 4	P<0.001	P<0.05	P<0.001	P<0.001	P<0.001	P<0.001
			1 *vs* Control	P<0.001	P<0.001	P<0.001	P<0.001	P<0.001	P<0.001
			2 *vs* 3	P<0.01	P>0.05	P<0.01	P<0.001	P<0.001	P<0.01
			2 *vs* 4	P<0.001	P>0.05	P<0.001	P<0.001	P<0.001	P<0.001
			2 *vs* Control	P<0.001	P<0.001	P<0.001	P<0.001	P<0.001	P<0.001
			3 *vs* 4	P<0.05	P>0.05	P>0.05	P>0.05	P>0.05	P>0.05
			3 *vs* Control	P<0.001	P<0.001	P<0.001	P<0.001	P<0.01	P<0.05
			4 *vs* Control	P<0.01	P<0.001	P<0.001	P<0.01	P>0.05	P>0.05
				0.5	**1**	**2**	**3**	**4**	**5**
Etoposide 100μM	8	A	0.5 *vs* 1	P>0.05	P>0.05	P<0.001	P<0.001	P<0.001	P<0.001
			0.5 *vs* 1.5	P<0.001	P<0.001	P<0.001	P<0.001	P<0.001	P<0.001
			0.5 *vs* Control	P<0.001	P<0.001	P<0.001	P<0.001	P<0.001	P<0.001
			1 *vs* 1.5	P<0.01	P<0.001	P<0.001	P<0.001	P<0.001	P<0.001
			1 *vs* Control	P<0.001	P<0.001	P<0.001	P<0.001	P<0.001	P<0.001
			1.5 *vs* Control	P< 0.01	P<0.001	P<0.001	P<0.001	P<0.001	P<0.001
		B	0.5 *vs* 1	P<0.05	P<0.001	P<0.001	P<0.001	P<0.001	P<0.001
			0.5 *vs* 1.5	P<0.001	P<0.001	P<0.001	P<0.001	P<0.001	P<0.001
			0.5 *vs* Control	P<0.001	P<0.001	P<0.001	P<0.001	P<0.001	P<0.001
			1 *vs* 1.5	P<0.001	P<0.001	P>0.05	P>0.05	P>0.05	P>0.05
			1 *vs* Control	P<0.001	P<0.001	P<0.001	P<0.001	P<0.001	P<0.01
			1.5 *vs* Control	P<0.001	P<0.001	P<0.001	P<0.001	P<0.001	P<0.01

Control, TMs of tumour of control liver perfused without cytotoxics

Appendix 9.12: Comparison of % decrease in TM of human tumours at different depths during perfusion with HN_2 as assessed by the comet assay

One-way ANOVA followed by the Bonferroni multiple t-test
except * = two-tailed unpaired t-test

Cytotoxic perfused	Tumour Number	Site	Depth (cm)	Time (h)					
				1	2	3	4	5	6
HN_2 50μM	9	A	0.5 *vs* 1	P < 0.001	P < 0.001	P < 0.001	P > 0.05	P > 0.05	P < 0.001
			0.5 *vs* 2	P < 0.001	P < 0.001	P < 0.001	P < 0.001	P < 0.001	P < 0.001
			1 *vs* 2	P < 0.001	P < 0.001	P < 0.001	P < 0.001	P < 0.001	P < 0.001
		B	0.5 *vs* 1	P < 0.001	P < 0.001	P < 0.001	P < 0.001	P < 0.001	P > 0.05
			0.5 *vs* 2	P < 0.001	P < 0.001	P < 0.001	P < 0.001	P < 0.001	P < 0.001
			1 *vs* 2	P < 0.001	P < 0.001	P < 0.001	P < 0.001	P < 0.001	P < 0.001
		C	0.5 *vs* 1	P < 0.001	P < 0.001	P < 0.001	P < 0.001	P < 0.001	P < 0.001
			0.5 *vs* 2	P < 0.001	P < 0.001	P < 0.001	P < 0.001	P < 0.001	P < 0.001
			1 *vs* 2	P < 0.001	P < 0.001	P < 0.001	P < 0.001	P < 0.001	P > 0.05
		D	0.5 *vs* 1	P < 0.001	P < 0.001	P < 0.001	P < 0.001	P < 0.001	P < 0.001
			0.5 *vs* 2	P < 0.001	P < 0.001	P < 0.001	P < 0.001	P < 0.001	P < 0.001
			1 *vs* 2	P < 0.001	P < 0.001	P < 0.001	P < 0.001	P < 0.001	P < 0.001
				0.5	**1**	**2**	**3**	**4**	
HN_2 100μM	10	A	0.5 *vs* 1	P < 0.001	P < 0.001	P < 0.001	P < 0.001	P < 0.001	
			0.5 *vs* 2	P < 0.001	P < 0.001	P < 0.001	P < 0.001	P < 0.001	
			1 *vs* 2	P > 0.05	P < 0.001	P < 0.001	P < 0.001	P < 0.001	
		B	0.5 *vs* 1	P < 0.001	P < 0.001	P < 0.001	P < 0.001	P < 0.001	
			0.5 *vs* 2	P < 0.001	P < 0.001	P < 0.001	P < 0.001	P < 0.001	
			1 *vs* 2	P < 0.01	P < 0.001	P < 0.001	P < 0.001	P < 0.001	
	11	*A	0.5 *vs* 1	P<0.0001	P<0.0001	P<0.0001	P<0.0001	P<0.0001	
		*B	0.5 *vs* 1	P<0.0001	P=0.0112	P=0.6565	P<0.0001	P<0.0001	
	12	A	0.5 *vs* 1	P < 0.001	P < 0.001	P < 0.001	P < 0.01	P > 0.05	
			0.5 *vs* 2	P < 0.001	P < 0.001	P < 0.001	P < 0.001	P < 0.001	
			1 *vs* 2	P < 0.001	P < 0.01	P < 0.001	P < 0.001	P < 0.001	
		B	0.5 *vs* 1	P < 0.01	P < 0.001	P < 0.001	P < 0.001	P < 0.001	
			0.5 *vs* 2	P < 0.001	P < 0.001	P < 0.001	P < 0.001	P < 0.001	
			1 *vs* 2	P < 0.001	P < 0.001	P < 0.001	P < 0.001	P < 0.001	

Appendix 9.13: Comparison of % decrease in TM at different sites in the same human tumour during perfusion with cisplatin as assessed by the comet assay

One-way ANOVA followed by the Bonferroni multiple t-test
except * = two-tailed unpaired t-test

Cytotoxic perfused	Tumour Number	Depth (cm)	Site	Time (h)				
				1	2	3	4	5
Cisplatin 50μM	3	*0.5	A*vs*B	P<0.0001	P=0.1942	P=0.01	P=0.1274	P<0.0001
		*1	A*vs*B	P=0.0071	P=0.003	P=0.0014	P=0.0228	P<0.0001
	4	*0.5	A*vs*B	P=0.0002	P=0.001	P=0.02	P=0.0005	P=0.3322
		*1	A*vs*B	P<0.0001	P=0.0012	P=0.0022	P<0.0001	P=0.0012
Cisplatin 100μM	5	0.5	A*vs*B	P>0.05	P>0.05	P>0.05	P<0.01	P<0.001
			A*vs*C	P>0.05	P<0.01	P<0.01	P<0.001	P>0.05
			B*vs*C	P<0.05	P<0.001	P>0.05	P<0.001	P<0.001
		1	A*vs*B	P<0.01	P>0.05	P>0.05	P<0.001	P>0.05
			A*vs*C	P>0.05	P<0.001	P>0.05	P<0.01	P<0.001
			B*vs*C	P<0.001	P<0.001	P>0.05	P<0.001	P<0.001
		2	A*vs*B	P>0.05	P>0.05	P<0.05	P>0.05	P<0.001
			A*vs*C	P<0.001	P<0.001	P<0.001	P>0.05	P<0.001
			B*vs*C	P<0.001	P<0.001	P>0.05	P<0.01	P>0.05
	6	0.5	A*vs*B	P<0.001	P<0.05	P<0.001	P<0.001	P<0.001
			A*vs*C	P<0.05	P<0.001	P>0.05	P<0.001	P<0.001
			B*vs*C	P<0.001	P<0.001	P<0.01	P>0.05	P>0.05
		1	A*vs*B	P<0.001	P>0.05	P<0.001	P<0.001	P<0.001
			A*vs*C	P<0.001	P>0.05	P<0.001	P<0.001	P<0.001
			B*vs*C	P>0.05	P<0.05	P>0.05	P<0.001	P<0.001
		2	A*vs*B	P>0.05	P<0.05	P<0.001	P<0.001	P<0.001
			A*vs*C	P>0.05	P<0.001	P<0.001	P<0.001	P<0.001
			B*vs*C	P>0.05	P<0.001	P<0.01	P<0.001	P>0.05

Appendix 9.14: Comparison of TM at different sites in the same human tumour during perfusion with etoposide as assessed by the comet assay

One-way ANOVA followed by the Bonferroni multiple t-test
except * = two-tailed unpaired t-test

Cytotoxic perfused	Tumour Number	Depth (cm)	Site	Time (h)					
				1	2	3	4	5	6
Etoposide 50μM	7	1	A*vs*B	P>0.05	P>0.05	P<0.05	P>0.05	P<0.001	P<0.001
			A*vs*C	P<0.001	P<0.05	P>0.05	P>0.05	P<0.01	P<0.01
			B*vs*C	P<0.01	P>0.05	P<0.001	P<0.001	P<0.001	P<0.001
		2	A*vs*B	P>0.05	P>0.05	P>0.05	P>0.05	P>0.05	P>0.05
			A*vs*C	P<0.001	P<0.05	P<0.05	P<0.001	P<0.001	P<0.001
			B*vs*C	P>0.05	P<0.05	P<0.01	P<0.001	P<0.001	P<0.001
		3	A*vs*B	P<0.05	P>0.05	P>0.05	P>0.05	P>0.05	P<0.05
			A*vs*C	P>0.05	P>0.05	P>0.05	P>0.05	P>0.05	P>0.05
			B*vs*C	P>0.05	P>0.05	P>0.05	P>0.05	P>0.05	P<0.001
		4	A*vs*B	P>0.05	P>0.05	P>0.05	P<0.01	P>0.05	P<0.05
			A*vs*C	P>0.05	P>0.05	P>0.05	P>0.05	P>0.05	P>0.05
			B*vs*C	P>0.05	P>0.05	P>0.05	P<0.05	P>0.05	P<0.05
				0.5	**1**	**2**	**3**	**4**	**5**
Etoposide 100μM	8	*0.5	A*vs*B	P=0.0327	P<0.0001	P=0.0135	P=0.0087	P=0.0133	P=0.2818
		*1	A*vs*B	P=0.4876	P=0.0014	P<0.0001	P<0.0001	P<0.0001	P<0.0001
		*1.5	A*vs*B	P=0.6923	P=0.1263	P=0.0092	P=0.0732	P=0.3951	P=0.8233

Appendix 9.15: Comparison of % decrease in TM at different sites in the same human tumour during perfusion with HN_2 as assessed by the comet assay

One-way ANOVA followed by the Bonferroni multiple t-test
except * = two-tailed unpaired t-test

Cytotoxic perfused	Tumour Number	Depth (cm)	Site	Time (h)					
				1	2	3	4	5	6
HN_2 50μM	9	0.5	AvsB	P<0.001	P>0.05	P>0.05	P<0.001	P<0.001	P<0.001
			AvsC	P<0.001	P<0.001	P>0.05	P>0.05	P>0.05	P<0.001
			AvsD	P<0.001	P<0.001	P<0.001	P>0.05	P<0.01	P<0.001
			BvsC	P>0.05	P>0.05	P>0.05	P<0.001	P<0.001	P<0.001
			BvsD	P<0.001	P<0.001	P<0.001	P<0.001	P<0.01	P<0.001
			CvsD	P<0.001	P<0.001	P<0.001	P>0.05	P>0.05	P<0.001
		1	AvsB	P>0.05	P<0.001	P<0.001	P<0.001	P<0.001	P<0.001
			AvsC	P<0.001	P>0.05	P<0.001	P<0.001	P<0.001	P<0.001
			AvsD	P>0.05	P<0.001	P<0.001	P<0.001	P<0.001	P<0.001
			BvsC	P<0.001	P<0.05	P<0.05	P<0.001	P<0.05	P<0.001
			BvsD	P>0.05	P<0.001	P<0.001	P<0.001	P<0.001	P<0.001
			CvsD	P<0.001	P<0.001	P<0.001	P<0.001	P<0.001	P<0.001
		2	AvsB	P<0.001	P<0.05	P<0.001	P<0.001	P<0.001	P<0.001
			AvsC	P<0.01	P<0.001	P<0.001	P<0.001	P<0.001	P<0.001
			AvsD	P<0.001	P<0.001	P<0.001	P<0.001	P<0.001	P<0.001
			BvsC	P>0.05	P<0.001	P>0.05	P<0.001	P<0.001	P<0.001
			BvsD	P>0.05	P<0.001	P<0.05	P<0.001	P>0.05	P>0.05
			CvsD	P<0.001	P<0.001	P<0.001	P>0.05	P<0.001	P<0.001
				0.5	1	2	3	4	
HN_2 100μM	10	*0.5	AvsB	P<0.0001	P<0.0001	P<0.0001	P<0.0001	P=0.1017	
		*1	AvsB	P=0.0101	P=0.0842	P<0.0001	P<0.0001	P<0.0001	
		*2	AvsB	P=0.9279	P<0.0001	P<0.0001	P<0.0001	P<0.0001	
	11	*0.5	AvsB	P<0.0001	P=0.2295	P=0.0003	P<0.0001	P<0.0001	
		*1	AvsB	P<0.0001	P<0.0001	P<0.0001	P=0.0956	P<0.0001	
	12	*0.5	AvsB	P<0.0001	P<0.0001	P<0.0001	P<0.0001	P<0.0001	
		*1	AvsB	P<0.0001	P<0.0001	P<0.0001	P<0.0001	P<0.0001	
		*2	AvsB	P<0.0001	P<0.0001	P<0.0001	P<0.0001	P<0.0001	

Appendix 9.16: Comparison of % decrease in TM in different human tumours in the same hemiliver during perfusion with cisplatin as assessed by the comet assay One-way ANOVA followed by the Bonferroni multiple t-test
except * = two-tailed unpaired t-test

Cytotoxic perfused	Depth (cm)	Tumour Number & Site	Time (h)				
			1	2	3	4	5
Cisplatin 23.3μM	0.5	*1 *vs* 2	P=0.0013	P=0.0446	P<0.0001	P<0.0001	
	1	*1 *vs* 2	P<0.0001	P=0.1188	P<0.0001	P<0.0001	
	1.5	*1 *vs* 2	P<0.0001	P=0.0409	P=0.0009	P<0.0001	
Cisplatin 50μM	0.5	3A *vs* 4A	P<0.001	P>0.05	P<0.001	P<0.001	P>0.05
		3A *vs* 4B	P<0.001	P>0.05	P<0.001	P<0.001	P>0.05
		3B *vs* 4A	P<0.001	P>0.05	P<0.001	P<0.001	P<0.001
		3B *vs* 4B	P<0.001	P>0.05	P<0.001	P<0.001	P<0.001
	1	3A *vs* 4A	P<0.001	P<0.05	P>0.05	P<0.001	P<0.001
		3A *vs* 4B	P<0.001	P>0.05	P<0.01	P<0.001	P<0.05
		3B *vs* 4A	P<0.001	P<0.001	P<0.05	P<0.001	P<0.01
		3B *vs* 4B	P<0.001	P>0.05	P<0.001	P<0.05	P<0.001
Cisplatin 100μM	0.5	*5ABC *vs* *6ABC*	P=0.6704	P=0.1823	P=0.1235	P=0.3204	P=0.4472
	1	*5ABC *vs* *6ABC*	P=0.3936	P=0.4169	P=0.1615	P=0.3666	P=0.9375
	1.5	*5ABC *vs* *6ABC*	P=0.3917	P=0.3351	P=0.2119	P=0.7001	P=0.9974

Appendix 9.17: Comparison of % decrease in TM in different human tumours in the same hemiliver during perfusion with HN_2 as assessed by the comet assay

One-way ANOVA followed by the Bonferroni multiple t-test

Cytotoxic perfused	Depth (cm)	Tumour Number & Site	Time (h)				
			0.5	1	2	3	4
HN_2 100μM	0.5	10A *vs* 11A	P < 0.001	P < 0.001	P < 0.001	P < 0.001	P < 0.001
		10A *vs* 11B	P < 0.001	P < 0.001	P < 0.001	P < 0.001	P < 0.001
		10A *vs* 12A	P < 0.001	P < 0.001	P < 0.001	P < 0.001	P < 0.001
		10A *vs* 12B	P < 0.001	P < 0.001	P < 0.001	P < 0.001	P < 0.001
		10B *vs* 11A	P < 0.001	P < 0.001	P < 0.001	P < 0.001	P < 0.001
		10B *vs* 11B	P < 0.001	P < 0.001	P < 0.001	P < 0.001	P < 0.001
		10B *vs* 12A	P < 0.001	P < 0.001	P < 0.001	P < 0.001	P < 0.001
		10B *vs* 12B	P > 0.05	P < 0.001	P < 0.001	P < 0.001	P < 0.001
		11A *vs* 12A	P < 0.001	P < 0.001	P < 0.001	P < 0.001	P < 0.001
		11A *vs* 12B	P < 0.001	P < 0.001	P < 0.001	P < 0.001	P > 0.05
		11B *vs* 12A	P < 0.001	P < 0.001	P < 0.001	P < 0.001	P < 0.001
		11B *vs* 12B	P < 0.001	P < 0.05	P < 0.001	P > 0.05	P < 0.001
	1	10A *vs* 11A	P < 0.001	P < 0.001	P < 0.001	P < 0.001	P < 0.001
		10A *vs* 11B	P < 0.001	P < 0.001	P < 0.001	P < 0.001	P < 0.001
		10A *vs* 12A	P < 0.001	P < 0.001	P < 0.001	P < 0.001	P < 0.001
		10A *vs* 12B	P < 0.001	P < 0.001	P < 0.001	P < 0.001	P < 0.001
		10B *vs* 11A	P < 0.001	P < 0.001	P < 0.001	P < 0.001	P < 0.001
		10B *vs* 11B	P < 0.001	P < 0.001	P < 0.001	P < 0.001	P < 0.001
		10B *vs* 12A	P < 0.001	P < 0.001	P < 0.001	P < 0.001	P < 0.001
		10B *vs* 12B	P < 0.05	P < 0.001	P < 0.001	P < 0.001	P < 0.001
		11A *vs* 12A	P < 0.001	P < 0.001	P < 0.001	P < 0.001	P < 0.001
		11A *vs* 12B	P < 0.001	P < 0.001	P > 0.05	P < 0.05	P > 0.05
		11B *vs* 12A	P < 0.001	P < 0.001	P < 0.001	P < 0.001	P < 0.001
		11B *vs* 12B	P < 0.001	P < 0.01	P < 0.001	P < 0.001	P < 0.05

Publications related to this work

Spalding DRC, Davidson B, Hochhauser D, Hartley J. (1999) Cisplatin sensitivity and DNA repair evaluated by Comet assay in hepatocellular and pancreatic tumour cell lines. *European J Surgical Oncol* **25**, 657.

Spalding DRC, Davidson B, Hochhauser D, Gordon M. (1999) Transport proteins in drug resistance of human hepatocellular carcinoma cell lines. *European J Surgical Oncol* **25**, 663

Sirivatanauksorn Y, **Spalding DRC,** Sarouei K, Ganeshaguru K, Davidson B. (2000) Expression of Multiple Drug Resistance in Human Pancreatic Cancer Cells. *Gut* 47, **(3):** A150

Spalding DRC, Hochhauser D, Hartley J, Davidson B. (2002) Heterogeneity of Response to Chemotherapy in Liver Tumours Evaluated by the Comet Assay in an Isolated Perfused Human Liver. *BJS* **89**, (1): 50.

Spalding DRC, Gordon M, Ganeshaguru K, Hochhauser D, Davidson B. (2002) Transport proteins and multi-drug resistance in human colorectal cell lines. *European J Surgical Oncol* **28**, (7): 772.

Spalding DRC, Davidson B. (2005) Analysis of Spatial and Temporal Cisplatin Induced DNA Damage and Repair of Intrahepatic Human Cancer Xenografts using the Comet Assay in Nude Mice. *European J Surgical Oncol* **31**, (9): 1063.

Spalding DRC, Fuller B, Davidson B. (2005) Response to chemotherapy in an isolated dual perfused rat liver containing human tumour. *European J Surgical Oncol* **31**, (9): 1079.